University of Stavanger

Faculty of Science and Technology

MASTER'S THESIS

Study program: Mechanical and Structural Engineering and Materials Science Specialization: Offshore Structures	Spring semester, 2012 **Open** / ~~Restricted access~~
Writer: Stig Madland	…… (Writer's signature)
Faculty supervisor: Ove Tobias Gudmestad External supervisor(s): Jan Vatsvåg (Global Maritime)	
Title of thesis: Dynamic Analysis for the Installation of Offshore Wind Turbine Foundations	
Credits (ECTS): 30	
Key words: - Wave Theory - Vessel Motions - DAF-Factor - Time Domain Analysis - Frequency Domain Analysis - MOSES Software	Pages: 142 + enclosure: 66 Stavanger, 14.06.2012 Date/year

Abstract

This report looks into the possibility for using modified phased out shuttle tankers to install jacket foundations for offshore wind turbines. New massive wind mill farms are now being planned out in water depths of 40 meters and beyond, making the transition from monopoles to jacket type foundations inevitable. The similarity between these new foundations and the much larger jackets used on oil platforms, makes it natural to look into if the already well-established technology can be applied to these foundations as well. A thorough dynamic analysis is carried out by the use of the computer program MOSES. Included in the analysis is a time domain analysis which will be compared to third party analyses. Further investigations of the non-linear behaviour are made to test the possibility for normalizing into a frequency domain solution. Also, based on these results, ways to reduce the dynamic amplification factors are examined. The main aspects are the lifting methods, the dynamic hook loads and the sea state limitations during installation.

Acknowledgements

This thesis was written as a part of my Master's degree at the University of Stavanger during the spring semester of 2012. It is written in collaboration with Global Maritime.

Firstly, I would like to thank Jan Vatsvåg for giving me the opportunity to work with Global Maritime. His guidance, knowledge and experience have been greatly appreciated when discussing how to attack issues arising during the work with this thesis.

I would also like to thank Thorgeir Anundsen for helping me the computer program MOSES. His experience has proven to be extremely valuable for solving problems occurring during the modelling and simulation phases.

I would also like to express my genuine gratitude towards Ove Tobias Gudmestad at the University of Stavanger, for his guidance, support and proofreading of this report. He has during my years at UiS made me very interested in the fields of marine technology, which I had virtually no knowledge of before attending his two subjects in "Marine Technology and Design" and "Marine Operations".

Table of Contents

Table of Figures

Table of Tables

Definitions

Beam sea	Waves hitting a vessel at an angle of 90 degrees measured from the bow
Head sea	Waves hitting a vessel at an angle of 0 degrees measured from the bow
Hook load	The load experienced by crane vessel from hook
Weather window	The time period when the environmental conditions are equal to or lower than the acceptance criteria.

Abbreviations

DAF	Dynamic Amplification Factor
ISSC	International Ship and Offshore Structure Congress
JONSWAP	Joint North Sea Wave Project
P-M	Pierson-Moskowitz Sea Spectrum
Var	Variance (from statistics)
C.o.G	Centre of Gravity
DOF	Degree of Freedom
MWL	Mean Water Level
RAO	Response Amplitude Operator
SSCV	Semi-Submersible Crane Vessel
SWL	Still Water Level
STF	Storm Factor (equal to 2 in this report)

Nomenclature

A	Area
a	Acceleration
A_γ	Normalizing factor
A_{ij}	Added mass
A_w	Waterline area
B	Centre of buoyancy
B'	Inclined centre of buoyancy
B_{ij}	Damping coefficient
$\overline{BM}$	Distance between the centre of buoyancy and the metacentre
c	Wave speed or celerity
C_D	Drag coefficient
C_{ij}	Spring coefficient
C_L	Lift coefficient
C_M	Mass coefficient
C_S	Slamming coefficient
d	Water depth
d	Draft
D	Diameter
E	Young's modulus
F	Force
f	Force per unit length
f	Freeboard
F_B	Buoyancy force
f_d	Drag force per unit length
f_i	Discrete frequency
f_L	Lift force per unit length
f_M	Mass force per unit length
f_s	Slamming force per unit length
g	Acceleration of gravity
G	Centre of gravity
$\overline{GM}$	Distance between metacentre and c.o.g
G'	Inclined centre of gravity
$\overline{GZ}$	Uprighting arm
H	Wave height
$H_{s_{WF}}$	Maximum forecasted H_s
H_b	Breaking wave height
H_s	Significant wave height
K	Keel
k	Wave number
k	Stiffness of system

Nomenclature

$\overline{KB}$	Distance between the keel and the centre of buoyancy
$\overline{KG}$	Distance between the keel and the centre of gravity
L	Wave length
L	Ship length
l	Length of crane sling in the in-air position
m	Mass
$\dot{m}$	Mass flow
M_ϕ	Metacentre after inclination
M_0	Metacentre before inclination
M_{ij}	Mass
M_n	Spectral moments
M_r	Uprighting moment
n	The normal to a plane
N_ϕ	"False" metacentre
p	Pressure
p_0	Atmospheric pressure
P_d	Dynamic pressure term
r	Relative frequency
S_B	Mean wetted body surface
t	Time
T	Wave Period
$T_{0_{x=y}}$	Jacket eigenperiod in x- and y-direction
T_{0_z}	Jacket eigenperiod in z-direction
T_m	Spectral mean wave period
T_p	Spectral peak wave period
T_z	Zero-up-crossing period
u	Fluid velocity in x-axis
u	Horizontal water particle velocity
U	Current speed
$\vec{U}$	Fluid velocity
$\dot{u}$	Horizontal water particle acceleration
U_0	1 h mean wind speed at 10 m above sea level
U_i	1-hour mean wind speed
V	Volume
v	Fluid velocity in y-axis
w	Fluid velocity in z-axis
w	Vertical water particle velocity
$\dot{w}$	Vertical water particle acceleration

Nomenclature

α	Alpha weather factor from DNV-OS-H101
β	Wave heading
ξ	Wave amplitude
ξ	Relative damping
λ	Wave length
ε	Phase angle
ρ	Density of sea water
η_i	Translation and rotation of a ship
$\dot{\eta}_3$	Velocity in vertical (heave) direction
$\ddot{\eta}_3$	Acceleration in vertical (heave) direction
Φ	Velocity potential
ω	Angular velocity
ω_p	Spectral peak frequency
ω_e	Encounter frequency
∇	Nabla, mathematical operator
∇	Displacement of vessel
τ_{ij}	Stress tensor
ϕ	Velocity potential
ϕ	Inclined (heel) angle
ϕ_i	Phase for the associated wind component
θ	Wave phase
σ	Variance
Γ	Gamma function
γ	Peak shape parameter

1 Introduction

1.1 Background

Due to the international community's ever-increasing demand for more energy, the industry is now investigating new methods in order to increase the production of energy. Renewable energy, which is commonly referred to as "green energy", is now becoming an increasingly important source of energy because of its low impact on the environment. The EU community has proposed that the energy from renewables shall be at least 20% in 2020 and 50% in 2050.

One of the renewable energy sources that have made the most progress is wind energy. Large wind turbines have been installed in groups on suitable locations around the world. These groups of wind turbines are called wind farms and consist of anywhere from a few tens to a few hundred wind turbines. The large land use and noise issues of these wind farms have further led to the development of offshore wind farms.

By locating the wind farms out on the vast ocean, the wind turbines are able to take advantage of the oceans excellent physical environmental conditions for producing wind energy. The uniform surface conditions interfere very little with the wind, leaving the wind speed and direction almost uninterrupted. This provides high wind speeds with low turbulence, which is advantageous when producing wind energy. The wind power offshore is up to 90% higher than onshore, so the energy production is far greater than onshore.

At present, there are two different categories of offshore wind turbines being developed. One of them is the floating wind turbine, which has its main advantage of not being very dependent on water depth. However, the costs of floating wind turbines are very largely dependent on water depth. On the other hand, the bottom fixed wind turbines are attached to the seabed, and the environmental forces (i.e. forces from wind, waves and current) acting on the structure are effectively taken up by the soil beneath the seabed. A plot of foundation cost versus water depth for different types of foundations are shown in Figure 1.1.

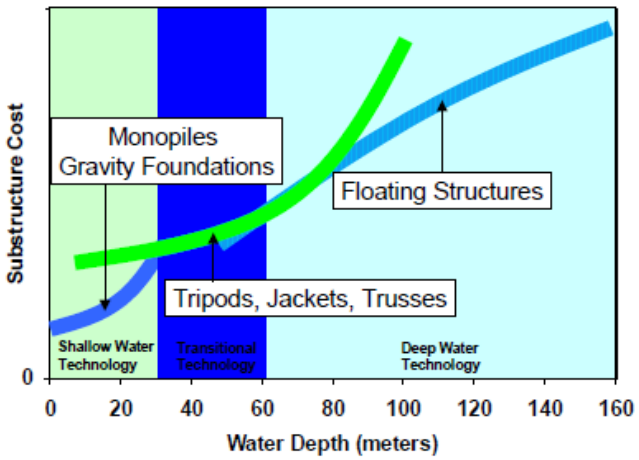

Figure 1.1 – The cost of different types of wind turbine foundations as function of water depth [24]

Starting at water depths of less than 15 meters, the bottom fixed wind turbines normally have a support structure called "monopod". A monopod is a large cylindrical tube with the purpose of acting as the foundation for the wind turbine. When installing bottom fixed wind turbines in larger water depths, the forces acting on the structure are so large that the monopod becomes insufficient as a support structure. An alternative to the monopod is to use a jacket structure as the foundation. A jacket is a structure consisting of tubular members interconnected to form a three-dimensional space frame [1, p.20]. It's a well proven technology from the oil and gas industry, where it's used as support for platform decks. An overview of the existing alternatives for bottom-fixed wind turbine foundations is given in Figure 1.2 below.

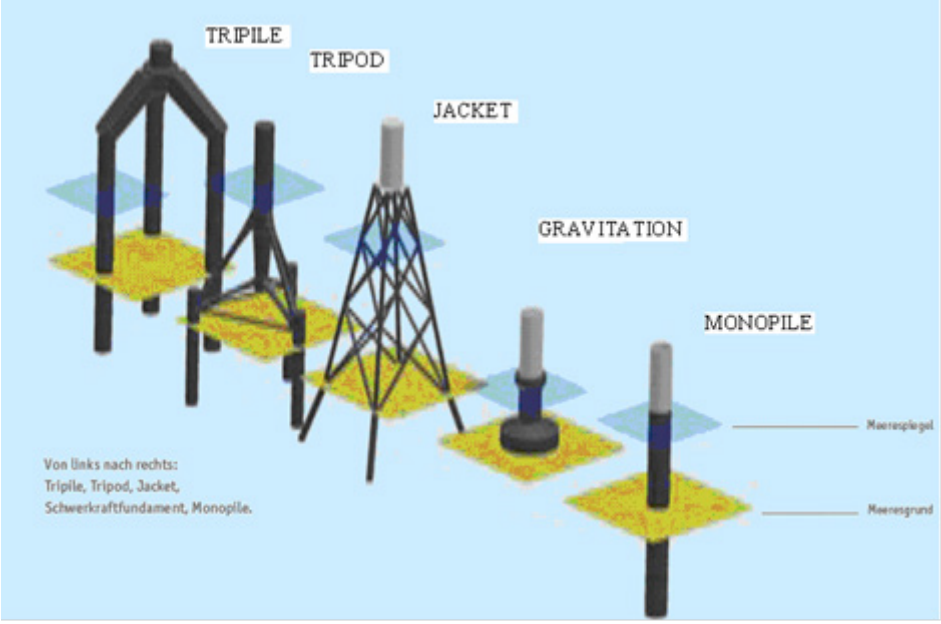

Figure 1.2 – Different types of wind turbine foundations [23]

To install a jacket out at sea, two alternative methods have been developed. The first option is to lift the jacket off the transport barge or vessel with a crane vessel and then lower it through the water and into position. Secondly, a special made launching barge can be used to slide the jacket off the barge and into the water. This is particular used for jackets with weights greater than the lifting capacity of the crane vessels.

Another important factor for offshore wind farms is the overall costs. For the investment to be feasible, the wind turbines must be installed very quickly. It has been suggested using decommissioned shuttle tankers and convert them into transport and installation vessels for jacket wind turbine foundations. The motion characteristics of a shuttle tanker are also far superior compared to a crane barge, but still less superior to a semisubmersible lifting vessel such as the SSCV Thialf and the SSCV S7000. Better motion characteristics give the lifting operations longer "weather windows". Shuttle tankers are only allowed to transport crude oil for 20 years in the North Sea while the life of the vessel is more likely to be 40 years. By using these tankers in the installation industry, the investment cost is therefore limited to the conversion into an installation vessel.

1.2 Study Objectives

The objective of this report is to analyse the lifting operations when installing a wind turbine foundation by the use of a converted shuttle tanker. In this context, the term "converted shuttle tanker" means modifying a standard shuttle tanker to be able to transport and install a four-legged jacket foundation with a height of approximately 68 meters. This is done by equipping the shuttle tanker with a crane and reinforcing the deck to be able to withstand the load from four jackets carried on the deck of each trip.

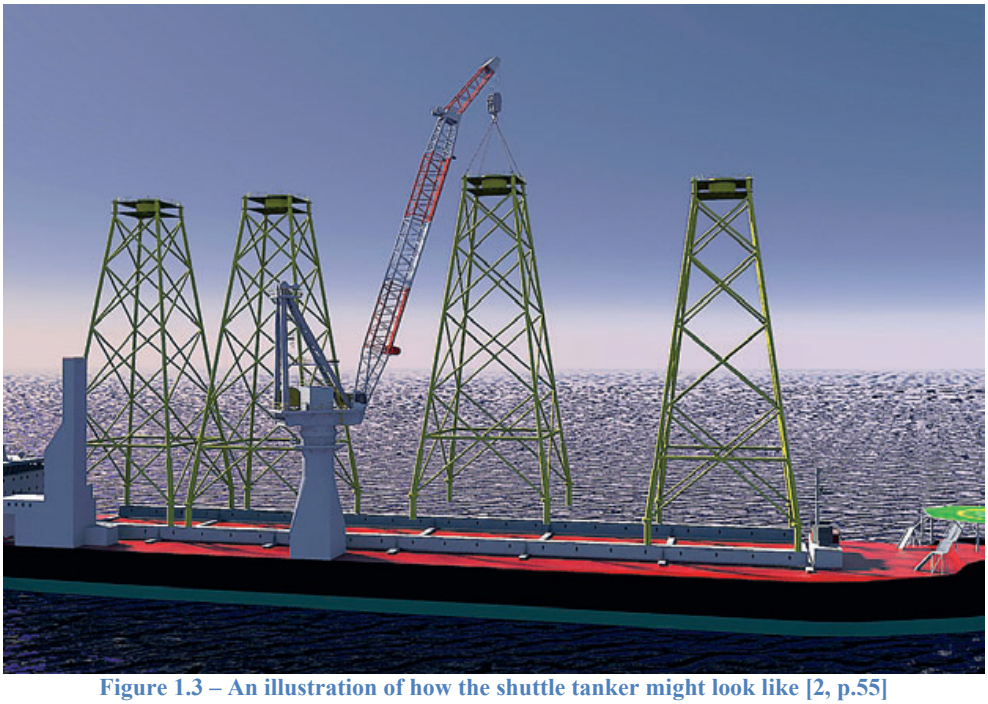

Figure 1.3 – An illustration of how the shuttle tanker might look like [2, p.55]

The key factor for this study is to investigate the possibility for improving the limiting sea state for the installation. A suitable lifting method is presented, and the subjects of interest are mainly the dynamic amplification factors governing from the different sea states used in the analysis. Based on the results from the analysis, limiting sea states for this operation are proposed.

Actual water depth for the analysed installation is 40 meters which suggests intermediate water depths, indicating that bottom effects are likely to occur.

This study requires the use of theories from hydrodynamics, wave theory and mechanical vibrations. The theories needed to solve this problem are presented in a suitable manner in this report. It starts with a description of the ocean environment, and further moves on to describe the motions on the vessel and lifted body by the use of mechanical vibrations theory.

Alongside with the work on this report, the applicable design guidelines are investigated to reveal if they cover this "new" type of lifting vessel. Design guidelines for the offshore industry are provided by Det Norske Veritas (DNV) and Noble Denton.

The computer software used to perform the analysis of the lifting operation is called MOSES. MOSES is a powerful marine simulation software developed by *Ultramarine Inc*. Through this software the lifting operations are analysed by using both time domain analysis and frequency domain analysis.

At the end, the possibility of carrying out a sensitivity analysis is discussed in order to investigate methods of reducing the dynamic amplification factors. A lower dynamic amplification factor is favourable for reducing the overall loads (i.e. maximum load and fatigue loads) during the installation phase or decreasing the sea state limitations.

1.3 Thesis organization

Chapter 1 contains information about the background and study objectives of this report.

Chapter 2 is giving a brief introduction in marine lifting operations and equipment. Especially the different vessel's motion characteristics is highlighted and compared to each other.

Chapter 3 is a thorough review of the theories needed to describe an ocean environment with the purpose of deriving forces and motions of offshore structures.

Chapter 4 is a short introduction in how to determine the stability of a stationary vessel, and how to ensure stability during offshore lifts.

Chapter 5 describes the transaction from wave loads to vessel motions in both the frequency domain and the time domain.

Chapter 6 shows the lifting arrangement chosen for this specific marine operation.

Chapter 7 deals with all the forces acting on the lifted jacket in each phase, and how to calculate them.

Chapter 8 contains information on both how MOSES works, and how this operation is modelled. At the end, there is a section about modelling concerns.

Chapter 9 gives the inputs to, and describes how the analysis is carried out.

Chapter 10 includes all results.

Chapter 11 is a discussion of the obtained results, and suggests ways of increasing the sea state.

Chapter 12 is the conclusions.

2 Marine Lifting Operations

This chapter contains a discussion of the different types of crane vessels the present technology can provide for when carrying out the installation of the wind turbine jacket foundation.

Different types of marine lifting operations have led to the development of a large variety of crane vessels. They vary in lifting capacity, from small crane barges that perform light lifting operations in benign waters, to the large semi-submersible crane vessels used for heavy lifts in almost any environment, although the limiting sea state for these vessels offshore are normally limited to be below 2.5 m significant sea state. Another important factor when selecting a crane vessel is the lift capacity as a function of the crane boom's outreach, i.e. how far out from the crane certain weights can be lifted.

Although the large differences in lifting capacities, most crane vessels can be divided into four groups depending on their hull shape and installation method. The first three groups can be distinguished by their hull shape. Their hull is either shaped as a barge, a ship or a semi-submersible. Some hybrid hulls combining both barge and ship shape has also been made, e.g. the vessel "Oleg Strashnov". The fourth group is called jack-up crane vessel due to its ability to rest on its "legs" during the installation phase. Each vessel type has its clear benefits and disadvantages. They all have their own characteristic motion response to environmental conditions.

2.1 Crane Barge

A crane barge is identified by its rectangular shaped monohull. On deck there is a crane which is used for lifting purposes. The crane can be either mounted onto the deck, or it can be a mobile onshore crane that has been driven onto the barge. Crane barges are widely used in marine operations due to their high availability and relatively low costs. Cargo can be carried on deck or lifted off from another transport barge.

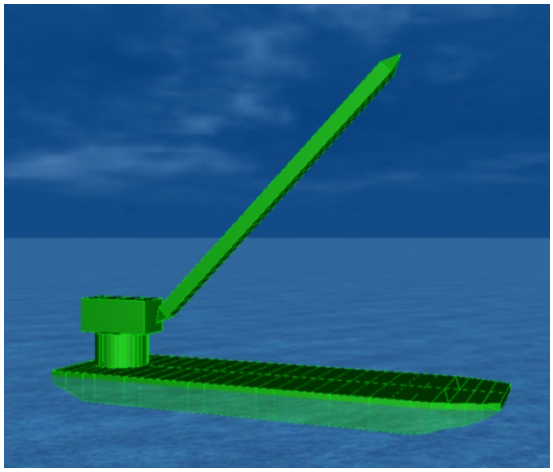

Figure 2.1 – MOSES model of the crane barge "Tonkawa"

However, crane barges have one major drawback: the motion characteristics. A rectangular shaped hull gives the barge a large waterline area compared to the weight of the barge. Further, this causes the vessel to have a relatively low eigenperiod in heave. For a crane barge, heave is the most important degree of freedom when analysing motions and forces in the crane and lifted object. As an example, the RAO in heave for three different wave headings are calculated using MOSES and results are shown in Figure 2.2. The vessel used is the crane barge "Tonkawa" (Figure 2.1) and the model of the vessel is taken from the built-in vessel library in MOSES. On the graph for beam sea there is a large peak at ~7 seconds, this shows where the barge gets into resonance with the waves. By checking the scatter diagram for North Sea conditions in Figure 2.3, it becomes clear that the waves with significant wave height equal to 2-3 meters have a period close to 7 seconds. Resonances between the wave periods and the eigenperiod of the vessel during a lifting operation will be practicable impossible. Most crane barges are outfitted as sheer leg cranes and used for inshore operations in benign waters due to their motion characteristics. This issue was recently experienced by a large Norwegian oil company. In an effort of installing offshore wind turbines at Sheringham Shoal on the east coast of the United Kingdom, they hired the crane vessel "Svanen". "Svanen" is a heavy lift crane barge with a lifting capacity of 8700 tonne. However, due to resonances during a lift which was sensitive to motions, it was not capable of installing the ~500 tonne wind turbines without expecting too much weather downtime. "Svanen" was therefore replaced by a better suited crane ship, forcing the oil company to take a loss in the order of 600 million NOK, see reference [33]

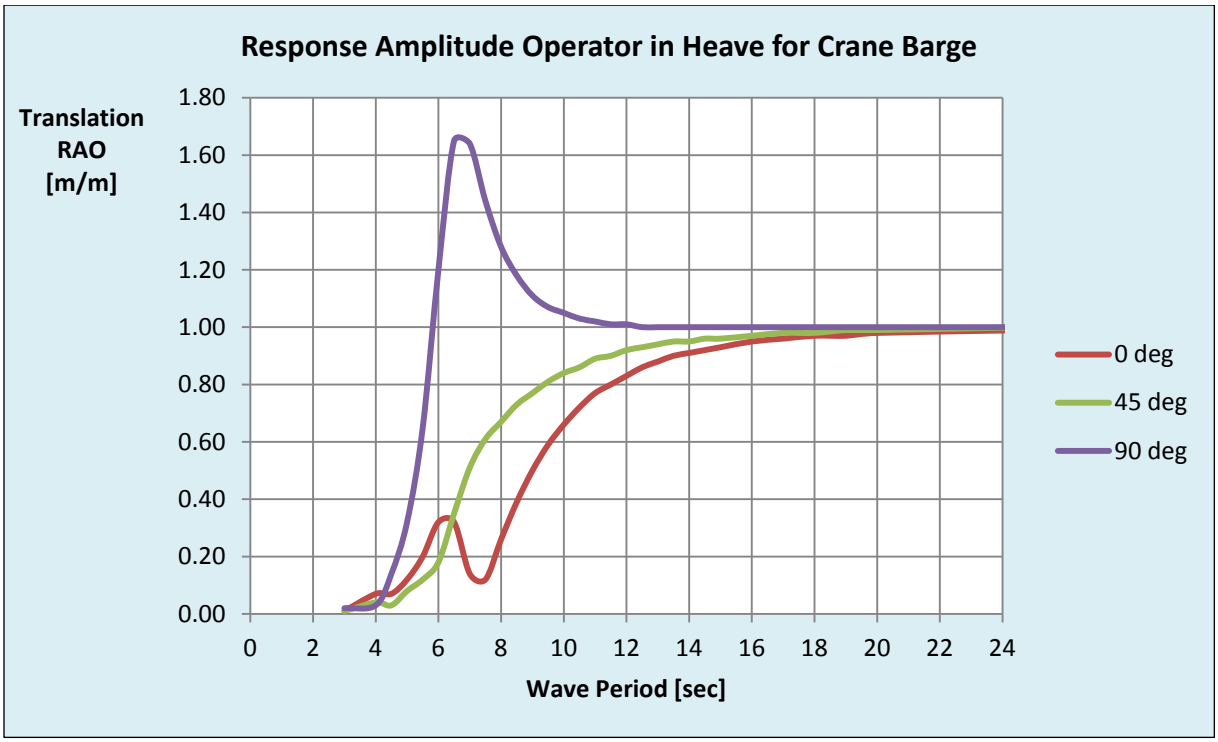

Figure 2.2 – RAO's in heave for the crane barge "Tonkawa" for 0 deg, 45 deg and 90 deg wave heading, respectively.

Table 2.2. *Joint frequency of significant wave height and spectral peak period. Representative data for the northern North Sea*

Significant wave height (m) (upper limit of interval)	Spectral peak period (s)																					Sum
	3	4	5	6	7	8	9	10	11	12	13	14	15	16	17	18	19	21	22			
1	59	403	1061	1569	1634	1362	982	643	395	232	132	74	41	22	12	7	4	2	2			8636
2	9	212	1233	3223	5106	5814	5284	4102	2846	1821	1098	634	355	194	105	56	30	16	17			32 155
3	0	8	146	831	2295	3896	4707	4456	3531	2452	1543	901	497	263	135	67	33	16	15			25 792
4	0	0	6	85	481	1371	2406	2960	2796	2163	1437	849	458	231	110	50	22	10	7			15 442
5	0	0	0	4	57	315	898	1564	1879	1696	1228	748	398	191	84	35	13	5	3			9118
6	0	0	0	0	3	39	207	571	950	1059	885	575	309	142	58	21	7	2	1			4839
7	0	0	0	0	0	2	27	136	347	528	533	387	217	98	37	12	4	1	0			2329
8	0	0	0	0	0	0	2	20	88	197	261	226	138	64	23	7	2	0	0			1028
9	0	0	0	0	0	0	0	2	15	54	101	111	78	39	14	4	1	0	0			419
10	0	0	0	0	0	0	0	0	2	11	30	45	39	22	8	2	1	0	0			160
11	0	0	0	0	0	0	0	0	0	2	7	15	16	11	5	1	0	0	0			57
12	0	0	0	0	0	0	0	0	0	0	1	4	6	5	2	1	0	0	0			19
13	0	0	0	0	0	0	0	0	0	0	0	1	2	2	1	0	0	0	0			6
14	0	0	0	0	0	0	0	0	0	0	0	0	0	1	0	0	0	0	0			1
15	0	0	0	0	0	0	0	0	0	0	0	0	0	0	0	0	0	0	0			0
Sum	68	623	2446	5712	9576	12 799	14 513	14 454	12 849	10 225	7256	4570	2554	1285	594	263	117	52	45			100 001

Figure 2.3 – Scatter diagram representative for the North Sea [3, p.30]

2.2 Jack-Up Crane Vessel

Jack-up crane vessels have a barge shaped hull. The name "jack-up" comes from the vessels ability to "jack up" onto its "legs" during the installation phase, see Figure 2.4. By resting on the legs while installing for instance windmills, the vessel has a completely different motion characteristic compared to floating structures. Less motions result in the opportunity to work in more hostile areas like for instance the North Sea.

Figure 2.4 – Jack-up crane vessel during the installation phase [4]

The main drawback of the jack-up crane vessel is the water depth limitation due to the length of the legs. Another drawback is the limitations related to the operation where the legs are jacked down and hits the sea bottom. Prior to touchdown of the legs, the vessel has motions just like a barge. When the legs hit the sea bottom, there could be initiated a large impact force in the legs and sea ground. For the touchdown to be possible, both the vessel and the sea bed have to be able to withstand this impact force. The foundation might also slide during touchdown, causing damage to the foundation and the legs. All these issues make the vessel sensitive to cargo capacity due to the fatigue capacity of the legs, and the sea state limitations for the touchdown might be as low as between 1-2 meters significant wave height.

2.3 Crane Ship

Crane ships are made in a large variety of sizes and each of them is tailor made for a specific purpose. Common for all of them are the advantages and disadvantages related to the geometry of the ship hull. As a result of this geometry, they all have somewhat similar motion characteristics.

Both crane- ships and barges depend on being able to carry out the lifting operation with the vessel facing the same direction as the waves. This is in many situations a major limitation of these vessels. Beam waves will cause too large motions.

Ships have a high cruising speed and are therefore able to get on loacation faster than any other crane vessel, making them the preferable option for operating in short weather windows, or in remote areas. They are also versatile in terms of cranes, cargo space and equipment.

Within the ship category, for crane ships we distinguish between stern mounted cranes and broadside mounted cranes. Figure 2.5 shows the heavy lift crane vessel "Borealis" with a stern mounted 5 000 tonne crane. The object which is going to be lifted has to be transported in place by a barge, since the crane can't rotate during heavy lifts. Figure 2.6 shows the vessel "Olympic Triton" with a smaller broadside mounted crane. When lifting an object over the side of a ship, the motion characteristics in the roll degree of freedom becomes more important. For crane barges, semi-submersibles and stern mounted cranes on ships, the heave motion is the most important degree of freedom.

Although the ship has a more slender hull geometry compared to a barge, the eigenperiod in heave is only slightly larger than the barge's. Thus the crane ships will encounter the same issues when operating in harsh environments as the North Sea, namely the eigenperiods are too close to the periods of the waves.

Figure 2.5 - Heavy lift crane vessel "Borealis" (HLCV) [5]

Figure 2.6 – Supply vessel "Olympic Triton" [6]

2.4 Semi-Submersible Crane Vessel (SSCV)

Semi-submersible crane vessels consist of a top deck attached to four or more columns which further are attached to two pontoons at the bottom, see Figure 2.7. On deck there are normally two large cranes that are able to work together when lifting one object, also known as tandem lift. A tandem lift provides great stability and the opportunity to rotate large objects such as a jacket from horizontal position to vertical in air. The largest crane vessel in the world designed to operate in offshore areas is at the moment the SSCV "Thialf" [8] with a lifting capacity of 14 000 tonne. During lifting, the vessel is kept stationary by either dynamic positioning or mooring lines.

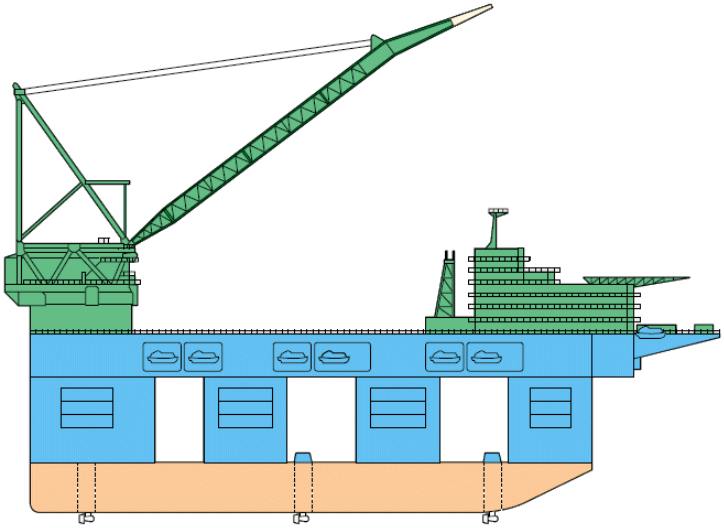

Figure 2.7 – Drawing of a semi-submersible crane vessel (SSCV)

By using columns to penetrate the waterline, the semi-submersible crane vessel obtains a very low waterline area compared to its enormous displacement. Since the formula for calculating the eigenperiod in heave includes the weight divided by waterline area, the SSCV gets a very high eigenperiod. Normally the eigenperiod in heave for a large SSCV is at least 20 seconds, exceeding the wave periods in almost every offshore environment. As a result, this crane type is far superior all other crane types mentioned above when it comes to motion characteristics. The only sea state that leads to large motions for semi-submersibles are swell.

The main reason for why semi-submersibles aren't used in all marine lifting operations is because they are more expensive. High day rates encourage the industry to develop cheaper lifting vessels, or take a higher risk by using a cheaper vessel with lower acceptance criteria. Another negative factor is due to the scarcity and therefore the availability of these vessels. Few vessels built results in long transit routes to reach the destination.

2.5 Motion Comparison for the Different Hull Shapes

The key factor in all marine lifting operations is the motions of the crane vessel during lifting. Wind, wave and current create forces on the vessel and lifted object. Forces initiate accelerations and the equipment starts moving. These movements can be described and calculated using the theory of dynamics.

A good way to compare the above mentioned crane vessels is to plot their Response Amplitude Operator (RAO) in a graph. RAO's tells us how much the vessel will move when excited by a wave with a given wave period. In short words, the vessel with the lowest value on the graph is the preferable one.

Figure 2.8 shows the RAO in the heave degree of freedom for three different vessels in their centre of gravity when exposed to waves with an angle of 90 degrees measured from the vessels bow (beam sea). The RAO's are calculated by using the software MOSES. Two of the vessel models are downloaded from the software's built in vessel library, these are the crane barge "Tonkawa" and the semi-submersible crane "Thialf". The last model is of the shuttle tanker which is going to be studied in the lifting analysis in this report. The model is provided by "Global Maritime".

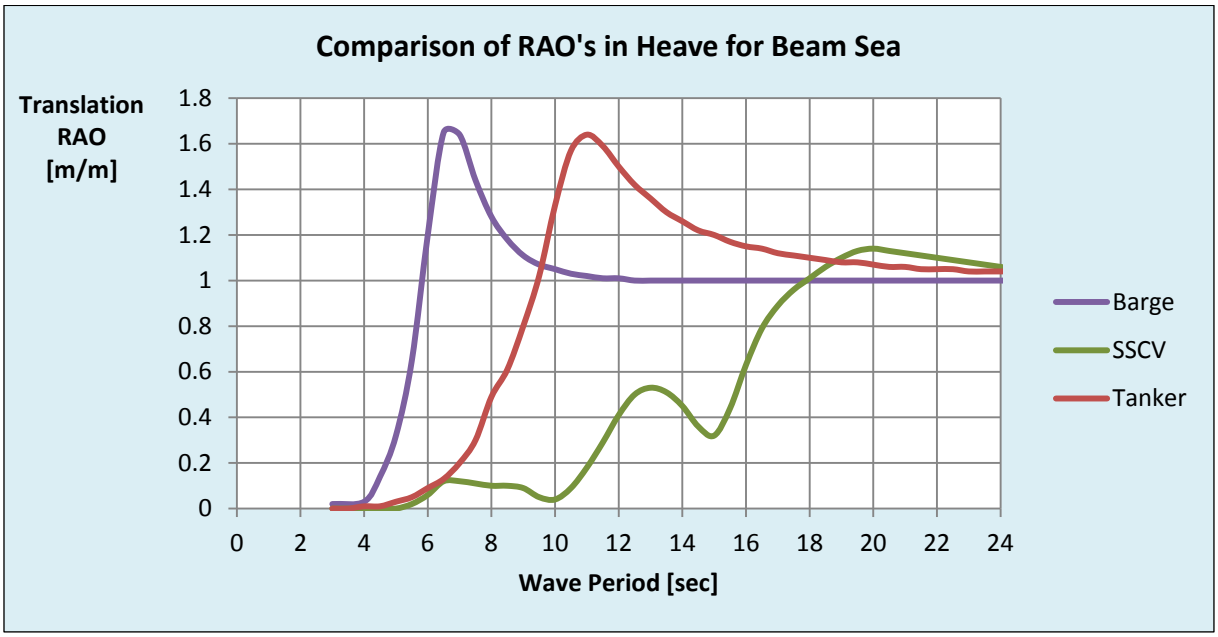

Figure 2.8 – Comparison of RAO's in the vessels centre of gravity in beam sea (90 deg) for typical barge, tanker and sscv in heave

On a calm summer day in areas like the Gulf of Mexico, Brazil or on the west side of Africa, any of these vessels could easily been used for lifting purposes. However, as mentioned above, in harsh environments like the North Sea crane barges cannot be used due to resonance. As a result the barge on Figure 2.8 is inoperable, forcing the industry to use either the slightly better ships or the more expensive semi-submersibles.

2.6 Lifting Equipment

Cranes are made in thousands of different configurations and designs. Their purpose is to lift equipment from one place to another. In the following, there is a description of the most important parts of a crane used in offshore lifting when considering the dynamics.

2.6.1 Crane Boom

The crane boom is the "arm" that is connected to the vessel and reaches out and holds up the crane wire. It is made in steel and can be formed like a truss or a beam.

Closely related to the crane boom size and strength are the lifting capacity as a function of lifting radius. Each crane has its own lifting chart showing the relationship between maximum outreach and weight for the lifted object. A typical lifting chart is shown in Figure 2.9 below.

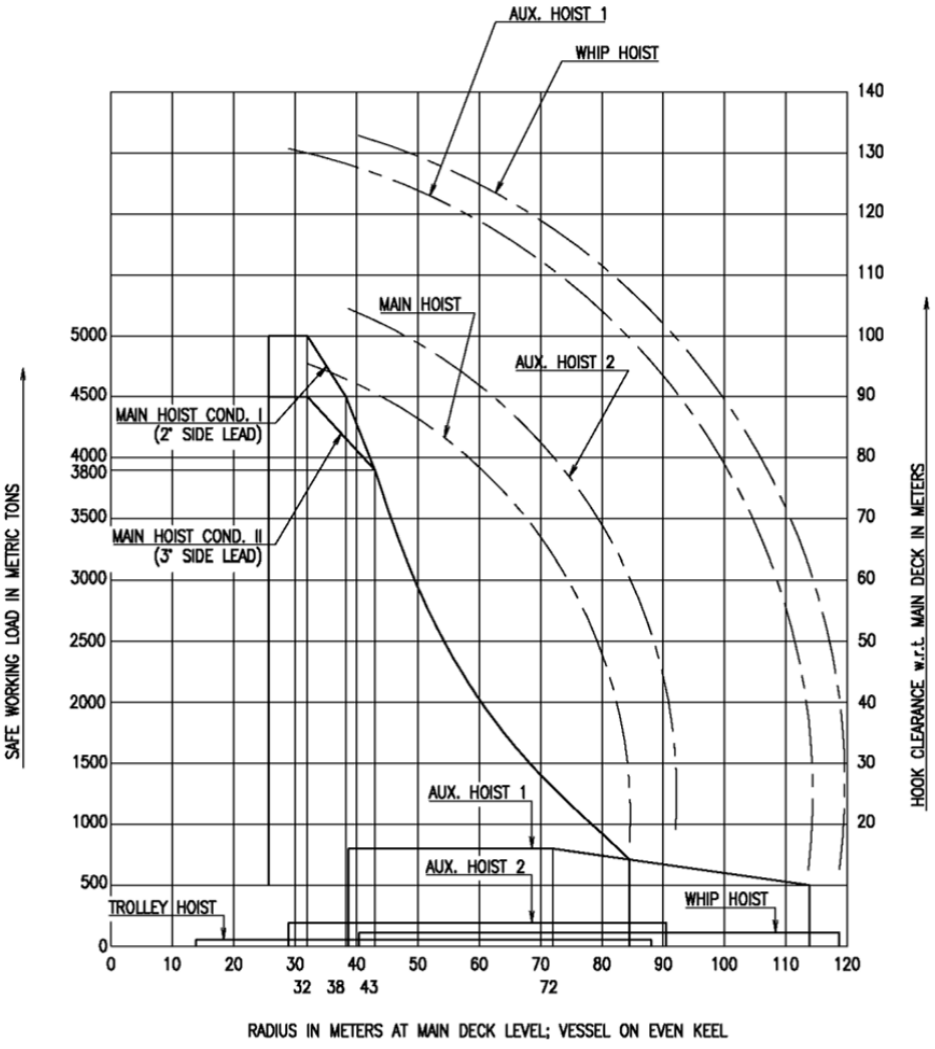

Figure 2.9 – Lifting chart showing the relationship between lifting capacity and lifting radius for the crane vessel "Oleg Strashnov" [9]

2.6.2 Crane Wire and Hook

For the crane to be able to lower and raise an object, it has to have a crane wire which is connected to a winch on the vessel and to the crane hook in the other end. Normally the wire is made by steel, but recent years deep water lowering operations have led to the development of fibre ropes because steel wires went into resonance with the crane tip motion. Fibre ropes are constructed from materials that display visco-elastic properties [10, p.91]. A wire is only able to carry tension loads. The hook is largely self-explanatory. It is a steel part with the purpose of connecting and disconnecting the loads as easily as possible.

2.6.3 Slings

Slings are the parts that connect the lifted object to the crane hook. They are made of steel wire or fibre ropes.

2.6.4 Spreader Beam

Spreader beams are made of steel and is located between the crane hook and lifted object. The purpose of this beam or frame is to reduce the horizontal forces in the lifted object created by the slings when the padeyes aren't located directly beneath the crane hook. Using a spreader beam is not mandatory, but they are very practical in certain lifting operations.

2.6.5 Heave Compensator

Heave compensators are advanced equipment developed for offshore crane vessels. By moving the crane tip in the opposite direction relative to the vessel motion, the heave compensator is able to cancel out some of the motions and hereby the dynamic loads in the lifting slings connected to the lifted object. The result is that the vessel can operate in larger waves and be well suited for deep water lowering operations. Not all cranes have this equipment, though.

Cranes with a high lifting capacity are unable to take advantage of this equipment due to practical issues.

3 Ocean Environment

In order to be able to perform any kind of analysis using floating structures, the theoretical basis must be established. This chapter gives an insight into how the theories for describing the ocean environment are developed, i.e. theories for analysing the effect of the meteorological and oceanographic conditions experienced at sea. The meteorological and oceanographic conditions are [1, p.79]:

- Local surface wind
- Wind-generated local waves
- Swell (long-period waves) generated by distant storms
- Energetic deep water currents associated with low frequency, large basin circulations
- Non-storm-related currents, which are site-specific, such as the loop current in the Gulf of Mexico or the coastal current in the Norwegian northern North Sea

A proper description of the ocean environment is critical so that the designer later on is able to calculate the motions and forces on all the equipment involved. To understand the ocean environment, an appropriate place to start is with the subject of how water flows.

3.1 Hydrodynamics

3.1.1 Basic Assumptions for Ocean Engineering

Hydrodynamics is a subparagraph in the theory of fluid dynamics. It differs from fluid dynamics by the fact that it only describes the dynamics, or flow of fluids (mainly incompressible). Experiments and calculations carried out on water with the purpose of measuring its change in volume when exposed to different pressures, shows that the density of water increases not more than ~5 percent when pressurised equivalent to the deepest part of the ocean (pressure = 1 100 atm) [13, p.95]. Therefore, water is assumed incompressible.

The ocean water is also assumed to be inviscid, meaning that the fluid has no resistance to shear stresses between the fluid elements. The absence of shear forces between the fluid elements results in an irrotational flow.

A fluid which has a flow that can be described by the above assumptions is called an *ideal fluid*. By introducing the assumption that water is an ideal fluid, the water elements can be analysed with the viscous stress tensor deleted [12, p.102]. This causes considerable mathematical simplifications and gives the opportunity to solve a larger number of problems. Each one of these assumptions is a source of some error to the final result. However, the results have proven to be accurate enough approximations to be used for engineering purposes.

3.1.2 Stationary Water Element

Before a fluid in motion can be described, it is appropriate to look into the forces acting on a fluid in the hydrostatic condition, i.e. a fluid with zero velocity. A fluid with no motion is only subjected to pressure variation due to gravitational forces. Considering Figure 3.1, equilibrium states that the net force in the x- and y-direction have to be zero, and the force in z-direction have to be equal to the opposite of the gravitational force. The net force on a stationary water element is calculated by using integration:

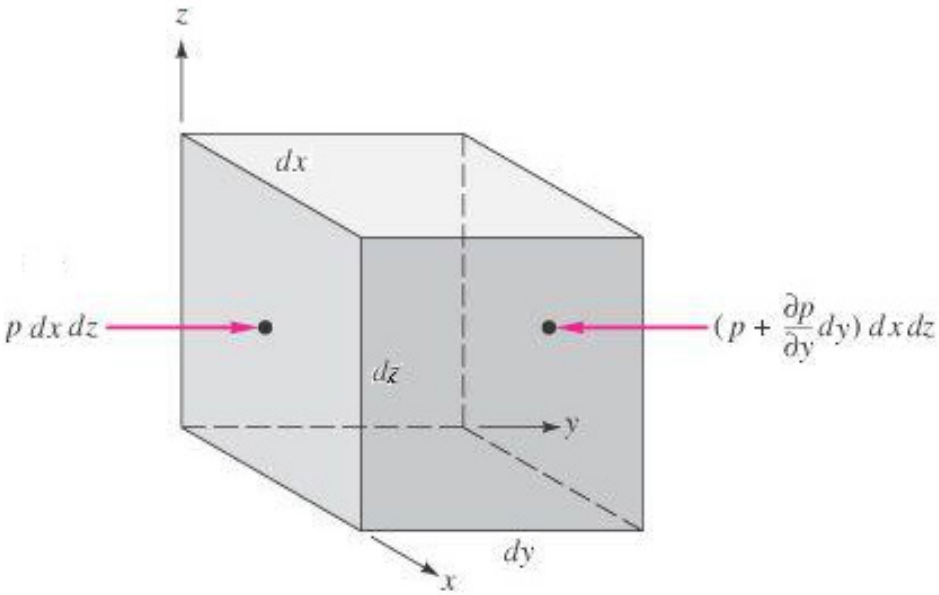

Figure 3.1 – Water element at rest [13, p.92 (modified coordinate system)]

The net force in the three directions on the element in Figure 3.1 before gravity is applied [13, p.91]:

$$d\vec{F_x} = p\,dy\,dz - \left(p + \frac{\partial p}{\partial x}dx\right)\,dy\,dz = -\frac{\partial p}{\partial x}\,dx\,dy\,dz \qquad (3.1\text{-}1)$$

$$d\vec{F_y} = p\,dx\,dz - \left(p + \frac{\partial p}{\partial y}dy\right)\,dx\,dz = -\frac{\partial p}{\partial y}\,dx\,dy\,dz \qquad (3.1\text{-}2)$$

$$d\vec{F_z} = p\,dx\,dy - \left(p + \frac{\partial p}{\partial z}dz\right)\,dx\,dy = -\frac{\partial p}{\partial z}\,dx\,dy\,dz \qquad (3.1\text{-}3)$$

Combining the three above equations into the total force vector for the element due to pressure:

$$d\vec{F} = -\left(\frac{\partial p}{\partial x}\hat{\imath} + \frac{\partial p}{\partial y}\hat{\jmath} + \frac{\partial p}{\partial z}\hat{k}\right)\,dx\,dy\,dz \qquad (3.1\text{-}4)$$

Using the mathematical vector operator *nabla*,∇, to simplify eq. (3.1-4):

$$d\vec{F} = -\nabla\,\mathrm{p}\,dx\,dy\,dz \qquad (3.1\text{-}5)$$

Rewriting eq. (3.1-5) to be a force per unit element volume, $\vec{f}$ $(where\ dx = dy = dz = 1)$:

$$\vec{f} = -\nabla \mathrm{p} \tag{3.1-6}$$

Equation (3.1-6) is the pressure gradient acting on a unit element. The pressure gradient is the sum of all pressure forces acting on the sides of the element. Pressure is therefore called a surface force. The force from the pressure gradient has to be balanced by gravity or acceleration of the element.

Now, the unit element is subjected to a gravity force acting in the negative z-direction while the element is still in a static condition:

$$\vec{f} = -\left(\frac{\partial p}{\partial x}\hat{\imath} + \frac{\partial p}{\partial y}\hat{\jmath} + \frac{\partial p}{\partial z}\hat{k}\right) = -\left(0\hat{\imath} + 0\hat{\jmath} - \rho g\hat{k}\right)$$

$$\vec{f} = -\nabla \mathrm{p} = \rho g\hat{k} \qquad \text{or} \qquad \nabla \mathrm{p} = -\rho g\hat{k} \tag{3.1-7}$$

Eq. (3.1-7) is the fundamental **hydrostatic equation**, also called the hydrostatic distribution of a fluid at rest.

3.1.3 Hydrostatic Pressure in an Ideal Fluid

From a mathematical point of view, the assumption of water being incompressible results in the fact that the density, ρ, now can be treated as a constant rather than a function of the fluid's depth. Equation (3.1-7) states that the pressure in a fluid at rest varies only with vertical distance and the pressure increases with depth.

An expression for the change in pressure can be derived from eq. (3.1-7):

$$\frac{\partial p}{\partial z} = -\rho g \tag{3.1-8}$$

$$p_1 - p_0 = -\int_0^1 \rho g\, dz \tag{3.1-9}$$

$$p_1 = -\rho g[z_1 - z_0] + p_0 \tag{3.1-10}$$

For calculations done in ocean engineering, the still water surface is normally set to be the reference level with the z-axis straight upwards. The variable z_0 then becomes zero, and the variable p_0 is the atmospheric pressure at still water level. Further, the variable p_1 is the pressure at the depth z_1. Since the z-axis is zero at the still water surface, z_1 becomes negative. It can therefore be seen from eq. (3.1-10) that the pressure increases with increasing fluid depth. This pressure distribution is illustrated in Figure 3.2.

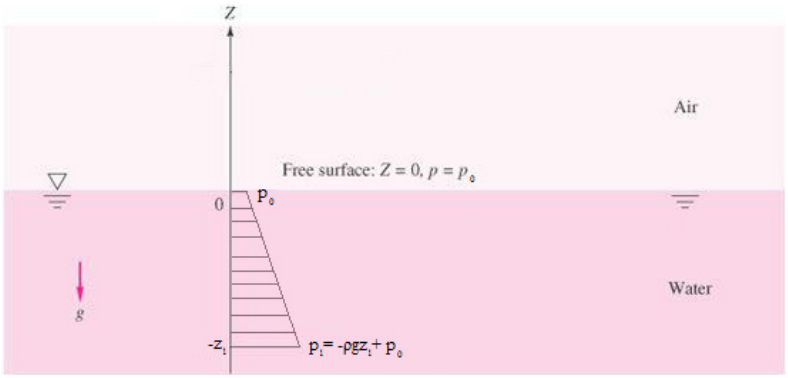

Figure 3.2 – Pressure distribution in an incompressible fluid [13, p.95 (modified to fit eq. (3.1-10))]

3.1.4 Differential Relations for Fluid Flow

There are two different ways of analysing a fluid in motion. The first one is to estimate the effects of energy change, induced force and mass flow in a defined control volume. However, when looking at the vast ocean with its ever changing environments and constraints, it quickly becomes clear that defining this control volume, or finite region, will be difficult and most likely impossible. Therefore the second option of analysing a fluid in motion is used for ocean environment problems like establishing a wave theory and calculating forces on structures due to the water flow. This second option involves seeking the point-by-point details of a flow pattern by analysing an infinitesimal region of the flow [13, p.225]. An infinitesimal region of the flow can be described mathematically by using differential equations. Such basic differential equations are difficult to solve and are therefore simplified by assuming incompressible- and frictionless flow. The last assumption is rather drastic and requires a check of the results afterwards to determine if is realistic and if it is realistic everywhere in the fluid domain.

3.1.4.1 Conservation of Mass

The conservation law for fluid mechanics states that the fluid's mass cannot change when it flows into- or out of an element. This principle is called conservation of mass or the continuity relation and can be presented in differential form by considering Figure 3.3:

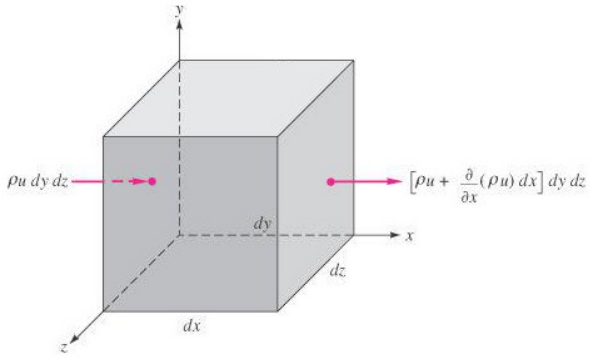

Figure 3.3 – Flow through a fluid element [13, p.227]

Fluid flow velocities are described with the formula:

$$\vec{U} = u\hat{\imath} + v\hat{\jmath} + w\hat{k} \tag{3.1-11}$$

Starting out with the mass conservation relation [13, p.228]:

$$\int \frac{\partial \rho}{\partial t} dV + \sum_i (\rho_i \, A_i \, \vec{U}_i)_{out} - \sum_i (\rho_i \, A_i \, \vec{U}_i)_{in} = 0 \tag{3.1-12}$$

An infinitesimal element yields the first part of eq. (3.1-12) to be:

$$\int \frac{\partial \rho}{\partial t} dV = \frac{\partial \rho}{\partial t} \, dx \, dy \, dz \tag{3.1-13}$$

The flow over an infinitesimal time, dt, in x-, y- and z-direction, respectively:

$$\rho \, u \, dy \, dz \, dt - \left(\rho \, u + \frac{\partial}{\partial x}(\rho \, u) dx\right) dy \, dz \, dt = 0 \tag{3.1-14}$$

$$\rho \, v \, dx \, dz \, dt - \left(\rho \, v + \frac{\partial}{\partial y}(\rho \, v) dy\right) dx \, dz \, dt = 0 \tag{3.1-15}$$

$$\rho \, w \, dx \, dy \, dt - \left(\rho \, w + \frac{\partial}{\partial z}(\rho \, w) dz\right) dx \, dy \, dt = 0 \tag{3.1-16}$$

Combining eqs. 13, 14, 15 and 16 into 12 and simplifying to an infinitesimal element: (dx, dy, dz = 1)

$$\frac{\partial \rho}{\partial t} \, dx \, dy \, dz \, dt + \frac{\partial}{\partial x}(\rho \, u) dx \, dy \, dz \, dt + \frac{\partial}{\partial y}(\rho \, v) dx \, dy \, dz \, dt + \frac{\partial}{\partial z}(\rho \, w) dx \, dy \, dz \, dt = 0$$

$$\frac{\partial \rho}{\partial t} + \frac{\partial}{\partial x}(\rho \, u) + \frac{\partial}{\partial y}(\rho \, v) + \frac{\partial}{\partial z}(\rho \, w) = 0 \tag{3.1-17}$$

Defining the total differential operator, D/Dt [14, p.5]:

$$\frac{D}{Dt} = \frac{\partial}{\partial t} + u\frac{\partial}{\partial x} + v\frac{\partial}{\partial y} + w\frac{\partial}{\partial z} \tag{3.1-18}$$

Using eq. 18 to compress eq. 17 into the compact form of the continuity equation:

$$\frac{D\rho}{Dt} + \nabla \cdot (\rho \, \vec{U}) = 0 \tag{3.1-19}$$

Further simplification is possible because of the assumption of incompressible flow. For incompressible flow, the $\frac{D\rho}{Dt}$ part becomes zero and the **continuity equation for incompressible flow** becomes:

$$\nabla \cdot \vec{U} = 0 \tag{3.1-20}$$

3.1.4.2 Linear Momentum

Another basic law which the flow has to satisfy is the law of linear momentum, i.e. Newton's second law. Starting with the element shown in Figure 3.3, the appropriate form of the linear momentum relation is [13, p.231]:

$$\sum \vec{F} = \frac{\partial}{\partial t}\left(\int \vec{U}\,\rho\; dV\right) + \sum\left(\dot{m}_\iota\, \overrightarrow{U_\iota}\right)_{out} - \sum\left(\dot{m}_\iota\, \overrightarrow{U_\iota}\right)_{in} \tag{3.1-21}$$

From the equation above, it can be shown that the linear momentum differential equation is:

$$\rho\vec{g} - \nabla p + \nabla \cdot \tau_{ij} = \rho\frac{D\vec{U}}{Dt} \tag{3.1-22}$$

where τ_{ij} is the stress tensor:

$$\tau_{ij} = \begin{bmatrix} \tau_{xx} & \tau_{yx} & \tau_{zx} \\ \tau_{xy} & \tau_{yy} & \tau_{zy} \\ \tau_{xz} & \tau_{yz} & \tau_{zz} \end{bmatrix} \tag{3.1-22}$$

The full derivation on how to get from equation 21 to 22 can be found in reference [14].

As previously mentioned, the flow of ocean water is assumed to be inviscid, i.e. there are no shear forces between the water particles. This assumption offers great mathematical simplifications in the linear momentum equation since all parts in the stress tensor becomes zero. Deleting the stress tensor from equation (3.1-22) yields the *Euler's equation* for inviscid flow:

$$\rho\vec{g} - \nabla p = \rho\frac{D\vec{U}}{Dt} \tag{3.1-23}$$

3.1.4.3 Non-Rotational Flow

The differential relation for deformation of a fluid is derived using the assumption that the water particles in waves are irrotational. In other words, the particles can deform, but it does not have an angular velocity with respect to its mass centre. Consider Figure 3.4, the angular velocity, ω_z about the z-axis is [13, p.246]:

$$\omega_z = \frac{1}{2}\left(\frac{d\alpha}{dt} - \frac{d\beta}{dt}\right) \tag{3.1-24}$$

where

$$d\alpha = \lim_{dt\to 0}\left[\tan^{-1}\frac{\frac{\partial v}{\partial x}dx\,dt}{dx+\frac{\partial u}{\partial x}dx\,dt}\right] = \frac{\partial v}{\partial x}dt \tag{3.1-25}$$

$$d\beta = \lim_{dt\to 0}\left[\tan^{-1}\frac{\frac{\partial u}{\partial y}dy\,dt}{dy+\frac{\partial v}{\partial y}dy\,dt}\right] = \frac{\partial u}{\partial y}dt \tag{3.1-26}$$

Combining eqs. 25 and 26 with 24:

$$\omega_z = \frac{1}{2}\left(\frac{\partial v}{\partial x} - \frac{\partial u}{\partial y}\right) \tag{3.1-27}$$

Using the same procedure about the x- and y-axis:

$$\omega_x = \frac{1}{2}\left(\frac{\partial w}{\partial y} - \frac{\partial v}{\partial z}\right) \tag{3.1-28}$$

$$\omega_y = \frac{1}{2}\left(\frac{\partial u}{\partial z} - \frac{\partial w}{\partial x}\right) \tag{3.1-29}$$

By comparing the $\vec{\omega}$ vector with the curl of the velocity vector, $\vec{U}$, it becomes clear that the $\vec{\omega}$ vector is half the curl of the velocity vector:

$$\vec{\omega} = \frac{1}{2}\left(\nabla \times \vec{U}\right) \tag{3.1-30}$$

Assuming zero angular velocity for an irrotational fluid is therefore the same as defining the curl of the velocity vector to be equal to zero:

$$\nabla \times \vec{U} \equiv \vec{0} \tag{3.1-31}$$

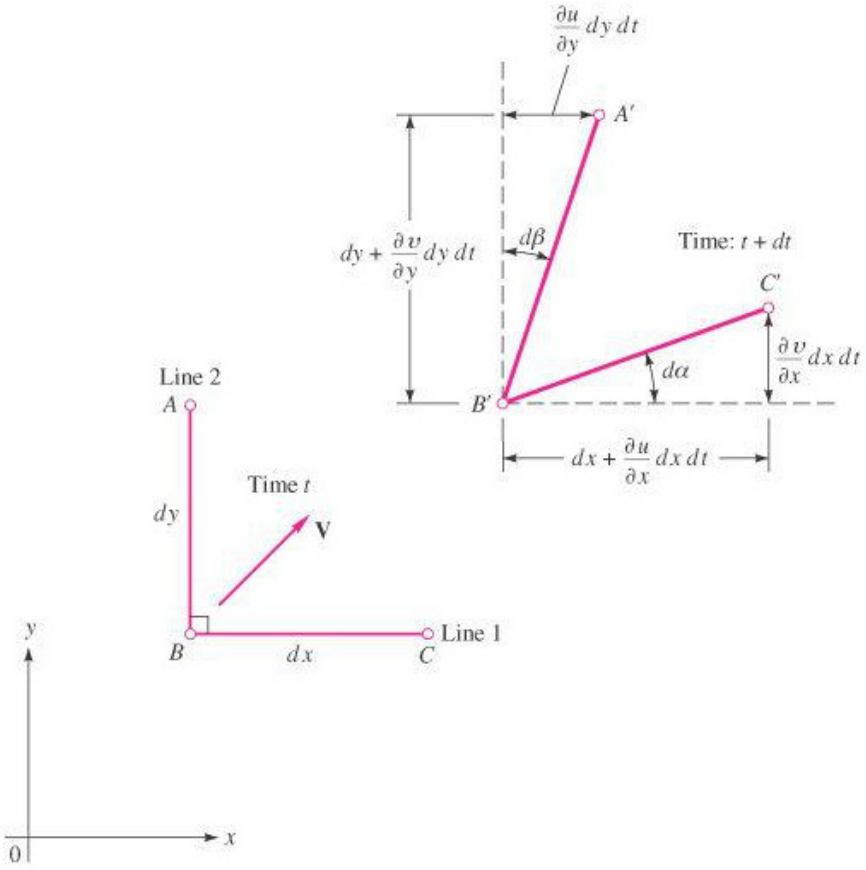

Figure 3.4 – Deformation of two fluid lines in a water particle [13, p.246]

3.1.4.4 Potential Flow

Two important subjects using potential flow theory are aerodynamics and hydrodynamics. Potential theory seeks to find a scalar function $\phi = \phi(x, y, z, t)$ on a specific form so that its partial derivatives yields functions for the velocities in the x-, y- and z-directions, respectively. The function is called the velocity potential and its partial derivatives have to be continuous. And when a function is continuous, it is possible to change the order of derivation [14, p.8]:

$$\frac{\partial}{\partial z}\left(\frac{\partial \phi}{\partial x}\right) = \frac{\partial}{\partial x}\left(\frac{\partial \phi}{\partial z}\right) \Rightarrow \frac{\partial u}{\partial z} = \frac{\partial w}{\partial x} \tag{3.1-32}$$

$$\frac{\partial}{\partial z}\left(\frac{\partial \phi}{\partial y}\right) = \frac{\partial}{\partial y}\left(\frac{\partial \phi}{\partial z}\right) \Rightarrow \frac{\partial v}{\partial z} = \frac{\partial w}{\partial y} \tag{3.1-33}$$

$$\frac{\partial}{\partial y}\left(\frac{\partial \phi}{\partial x}\right) = \frac{\partial}{\partial x}\left(\frac{\partial \phi}{\partial y}\right) \Rightarrow \frac{\partial u}{\partial y} = \frac{\partial v}{\partial x} \tag{3.1-34}$$

The equations above are equivalent to equation (3.1-31) meaning that the fluid flow must be irrotational for a velocity potential to exist. Now, the continuity equation for incompressible flow (eq. (3.1-20)) is used to find the equation for the velocity potential, ϕ:

$$\nabla \cdot \vec{U} = 0$$
$$\frac{\partial u}{\partial x} + \frac{\partial v}{\partial y} + \frac{\partial w}{\partial z} = 0$$
$$\frac{\partial}{\partial x}\left(\frac{\partial \phi}{\partial x}\right) + \frac{\partial}{\partial y}\left(\frac{\partial \phi}{\partial y}\right) + \frac{\partial}{\partial z}\left(\frac{\partial \phi}{\partial z}\right) = 0$$

$$\nabla^2 \phi = 0 \tag{3.1-35}$$

Equation (3.1-35) is recognised as the Laplace equation and is known to be much easier to solve compared to fully viscous Navier-Stokes equations. It should also be noted that the Laplace equation is fully three-dimensional.

Also, when assuming potential flow, the linear momentum differential equation (3.1-22) reduces to Bernoulli's equation [13, p.485]:

$$\frac{\partial \phi}{\partial t} + \frac{p}{\rho} + \frac{1}{2}|\nabla \phi|^2 + gz = constant \tag{3.1-36}$$

3.1.5 Boundary Conditions

Solving the 2nd order Laplace equation requires a set of boundary conditions. These boundary conditions must be related to the physical environment of the ocean to yield any kind of realistic answer. Assuming linear (Airy) wave theory, the solution should contain sinusoidal waves at the surface. This section contains only a discussion about the boundary conditions, while the solution for the Laplace equation is given in section 3.2.1.

3.1.5.1 Bottom Condition

Water cannot flow through the sea floor because the bottom is assumed impermeable. This constrain is equivalent to the vertical velocity, w, at the water depth, -d, always being equal zero. Assuming a completely horizontal and frictionless sea floor, the first boundary condition is mathematically described as:

Vertical velocity:

$$w = 0 \qquad \text{for} \qquad z = -d$$

Is the same as:

$$w|_{z=-d} = 0 \tag{3.1-37}$$

Gives the bottom boundary condition:

$$\frac{\partial \phi}{\partial z} = 0 \qquad \text{for} \qquad z = -d \tag{3.1-38}$$

3.1.5.2 Wall Condition

This condition is similar to the bottom condition above. No water is allowed through a vertical wall, giving the boundary condition for a wall at the position $x = a$:

Horizontal velocity:

$$u|_{z=a} = 0 \tag{3.1-39}$$

Wall boundary condition:

$$\frac{\partial \phi}{\partial x} = 0 \qquad \text{for} \qquad z = a \tag{3.1-40}$$

It should here be noted that the linear wave theory is only two dimensional with the x-axis horizontal and the z-axis vertical and positive upwards. Therefore, there is no boundary condition involving the y-axis.

The wall condition can be used to constrain the water from flowing through the hull of a ship, using the boundary condition:

$$\left.\frac{\partial \phi}{\partial n}\right|_{(x_i,y_i,z_i)} = 0 \tag{3.1-41}$$

Equation (3.1-41) is a mathematical expression showing that the velocity component perpendicular to the ship is equal to zero in a coordinate system moving with the ship [14, p.10].

3.1.5.3 Surface Conditions

At the sea surface, the water cannot flow through the surface because the surface adjusts its elevation automatically. To describe this mathematically it is necessary to develop both the kinematical- and the dynamical surface condition.

3.1.5.3.1 The Kinematic Surface Condition

The kinematic surface condition is based on the assumption "A water particle at the free surface will always remain at the free surface" [14, p.10]. Sea surface elevation is in two dimensions described by the formula $\xi = \xi(x,t)$, where ξ is the surface elevation at position x at time t. Consider the vertical velocity, w, at the wave surface:

$$w = \frac{\partial \phi}{\partial z} \tag{3.1-42}$$

Using the total differential operator and expanding the formula at $z = \xi$, the eq (3.1-42) becomes [14, p.10]:

$$w = \frac{\partial \phi}{\partial z} = \left.\frac{Dz}{Dt}\right|_{z=\xi(x,t)} = \left.\left(\frac{\partial z}{\partial t} + u\,\frac{\partial z}{\partial x}\right)\right|_{z=\xi(x,t)}$$

$$w = \left(\frac{\partial \xi}{\partial t} + u\,\frac{\partial \xi}{\partial x}\right) \tag{3.1-43}$$

Equation (3.1-43) is linearized by deleting the non-linear factor $u\,\frac{\partial \xi}{\partial x}$:

$$w = \left.\frac{\partial \phi}{\partial z}\right|_{z=\xi(x,t)} \tag{3.1-44}$$

Now, it is assumed that the velocity at the wave surface is equal to the velocity at still water level, making the boundary condition only applicable to small waves:

$$w = \frac{\partial \phi}{\partial z} = \frac{\partial \xi}{\partial t} \qquad \text{for} \qquad z = 0 \tag{3.1-45}$$

3.1.5.3.2 The Dynamic Surface Condition

The dynamic surface condition is developed by setting the pressure at the free surface level to be equal to the atmospheric pressure, p_0. Using the Bernoulli equation (3.1-36) with the constant equal to $\frac{p_0}{\rho}$ at $z = \xi(x,t)$, the equation becomes:

$$\frac{\partial \phi}{\partial t}\Big|_{z=\xi} + \frac{p_0}{\rho} + \frac{1}{2}|\nabla\phi|^2\Big|_{z=\xi} + g\xi = \frac{p_0}{\rho}$$

$$g\xi + \frac{\partial \phi}{\partial t}\Big|_{z=\xi} + \frac{1}{2}|\nabla\phi|^2\Big|_{z=\xi} = 0 \qquad (3.1\text{-}46)$$

Again, linearizing by deleting the non-linear term and assuming that the velocity at the wave surface is equal to the velocity at still water level:

$$g\xi + \frac{\partial \phi}{\partial t}\Big|_{z=0} = 0$$

$$\xi = -\frac{1}{g}\frac{\partial \phi}{\partial t} \qquad \text{for} \qquad z = 0 \qquad (3.1\text{-}47)$$

Combining the kinematic- (3.1-45) and the dynamic (3.1-47) surface condition into the same equation:

$$\frac{\partial \phi}{\partial z} = \frac{\partial \xi}{\partial t} = \frac{\partial}{\partial t}\left(-\frac{1}{g}\frac{\partial \phi}{\partial t}\right)$$

$$\frac{\partial^2 \phi}{\partial t^2} + g\frac{\partial \phi}{\partial z} = 0 \qquad \text{for} \qquad z = 0 \qquad (3.1\text{-}48)$$

3.1.6 Summary of Hydrodynamic Equations and Boundary Conditions

Hydrodynamic equations for water flow:

The fundamental hydrostatic equation: $\nabla \mathrm{p} = -\rho g \hat{k}$

Continuity equation for incompressible flow: $\nabla \cdot \vec{U} = 0$

Definition of irrotational flow: $\nabla \times \vec{U} \equiv \vec{0}$

Laplace equation for potential flow: $\nabla^2 \phi = 0$

Bernoulli's equation: $\frac{\partial \phi}{\partial t} + \frac{p}{\rho} + \frac{1}{2}|\nabla \phi|^2 + gz = const.$

Boundary conditions:

Bottom condition:	$\frac{\partial \phi}{\partial z} = 0$	for	$z = -d$
Wall condition:	$\frac{\partial \phi}{\partial \mathrm{x}} = 0$	for	$z = \mathrm{a}$
Ship condition:	$\frac{\partial \phi}{\partial n}\Big\|_{(x_i, y_i, z_i)} = 0$		
Kinematic surface condition:	$\frac{\partial \phi}{\partial z} = \frac{\partial \xi}{\partial t}$	for	$z = 0$
Dynamic surface condition:	$\xi = -\frac{1}{g}\frac{\partial \phi}{\partial t}$	for	$z = 0$

3.2 Wave Theory

Local winds and distant storms are the most important sources generating ocean waves. Ocean waves are difficult to describe exactly due to their natural randomness. However, in many cases the waves can be given a regular form and described by only a few parameters. Then the waves can be described by a deterministic theory such as linear wave theory or higher order Stokes theory. These theories are used for many design purposes and provide good results when applied properly. However, it is important to be aware of the applicability limits arising because of the assumptions made.

3.2.1 Linear Wave Theory

The most basic wave theory is the linear wave theory (also called Airy wave theory). This theory uses the potential flow theory derived in section 3.1.4.4 together with the linear boundary conditions for solving the Laplace equation (3.1-35). Further, it assumes regular waves with sinusoidal periods, giving the opportunity to consider only a few cyclic periods instead of long time periods.

Figure 3.5 shows a regular wave travelling along the positive x-axis with the wave speed, c, shown at time t = 0. H is the wave height, d is the water depth, L is the wave length and ξ is the surface elevation at time t and position x.

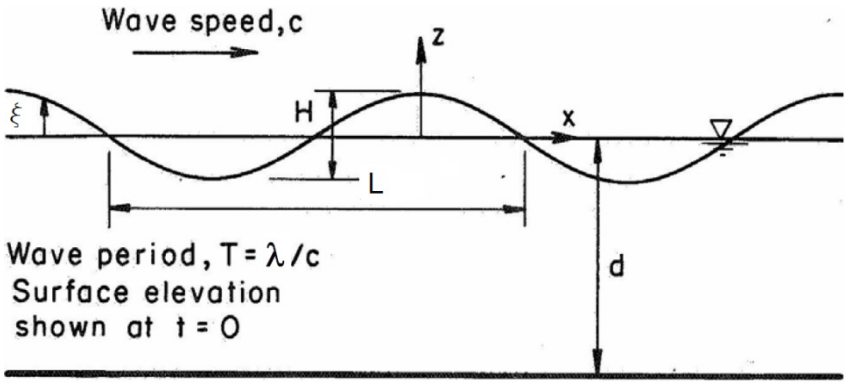

Figure 3.5 – Properties of a regular wave [15, p.25]

Linear wave theory requires three parameters for describing the waves. The first one is the wave period, T, which is the time it takes a wave to travel from the still water level and past the wave crest and trough and to the same still water level again. The second parameter is the wave height, H, defined to be the vertical distance between the crest and trough, also known as two times the wave amplitude for a linear wave. At last, the third parameter is the water depth, d, which is the vertical distance between the sea bottom and the still water level.

A linear wave's free surface profile in two dimensions is described by the following formula:

$$\xi(x,t) = \xi_0 \sin(\omega\, t - k\, x) \tag{3.2-1}$$

where ξ_0 is the wave amplitude
ω is the angular wave frequency
k is the wave number
x is the position on the x-axis

This is a simple harmonic function varying between the wave crest which have the value $+\xi_0$ and the wave trough with the value $-\xi_0$. In front of the wave number there is a minus sign with the intention of making the wave propagate in the positive x-direction. The argument $\omega t - kx$ is called the phase of the wave.

From the free surface formula (3.2-1), a set of relations can be derived:

The phase velocity associated with the wave, also called the celerity, c, of propagation along the x-axis is:

$$c = \lim_{\Delta t \to 0} \frac{\omega}{k} = \frac{\omega}{k} \tag{3.2-2}$$

Angular frequency, ω, can be written as:

$$\omega = \frac{2\pi}{T} \tag{3.2-3}$$

The wave number, k, has the relation:

$$k = \frac{2\pi}{L} \tag{3.2-4}$$

Inserting equation (3.2-3) and (3.2-4) into (3.2-2), the celerity becomes:

$$c = \frac{\frac{2\pi}{T}}{\frac{2\pi}{L}} = \frac{L}{T} \tag{3.2-5}$$

3.2.1.1 Velocity Potential

Newton's second law states that the force is equal to mass multiplied with acceleration. In wave theory, the only fluid involved is water and its mass is well known. Finding the forces on structures subjected to waves then becomes an issue of whether or not the acceleration of the waves can be found. In physics the acceleration is known as the derivative of the velocity. This means that if the formula for velocity is known, the acceleration can be easily calculated. By using the potential theory derived in an earlier chapter, the function for the velocity

potential, ϕ, for the waves can be calculated. The function for the velocity potential, considering an incompressible- and irrotational flow, is found by solving the Laplace equation (3.1-35), using the boundary conditions in eq. (3.1-38) and (3.1-47). To solve this second order differential equation, the method of separation of variables is used [16]:

Boundary conditions:

$$\frac{\partial \phi}{\partial z} = 0 \qquad \text{for} \quad z = -d \tag{3.1-38}$$

$$\xi = -\frac{1}{g}\frac{\partial \phi}{\partial t} \qquad \text{for} \quad z = 0 \tag{3.1-47}$$

Laplace equation for two dimensions:

$$\nabla^2 \phi = 0 \tag{3.1-35}$$

$$\frac{\partial^2 \phi}{\partial x^2} + \frac{\partial^2 \phi}{\partial z^2} = 0 \qquad \text{for} \quad -\infty < x < \infty\,, \qquad -d < z < 0$$

The solution after separation of variables and assuming T is a harmonic function:

$$\phi(x,z,t) = \qquad X(x) \qquad Z(z) \qquad T(t)$$

$$\phi(x,z,t) = [A\sin(kx) + B\cos(kx)] \cdot (Ce^{kz} + De^{-kz}) \cdot [E\sin(\omega t) + F\cos(\omega t)] \tag{3.2-6}$$

Using the boundary conditions and the formula for the free surface (eq. (3.2-1)) to determine the A to F constants, yields the velocity potential:

$$\phi(x,z,t) = \frac{\xi_0\, g}{\omega} \cdot \frac{\cosh k(z+d)}{\cosh(k\,d)} \cdot \cos(\omega\, t - k\, x) \tag{3.2-7}$$

3.2.1.2 Horizontal Particle Velocity and Acceleration

As previously mentioned, the derivative of the velocity potential gives the velocity, and hence the horizontal velocity is:

$$u = \frac{\partial \phi}{\partial x} = \frac{\xi_0\, g\, k}{\omega} \cdot \frac{\cosh k(z+d)}{\cosh(k\,d)} \cdot \sin(\omega\, t - k\, x) \tag{3.2-8}$$

The sinus part in the equation above shows that the function is in-phase with the free surface, meaning that the velocity has its maximum at the wave crest and minimum at the trough. Figure 3.6 shows how the horizontal particle velocity decays with an exponential form as it moves down into the water. The formula for velocity is only valid up to the still water level. However, it is normal to just extend the function up to the wave crest.

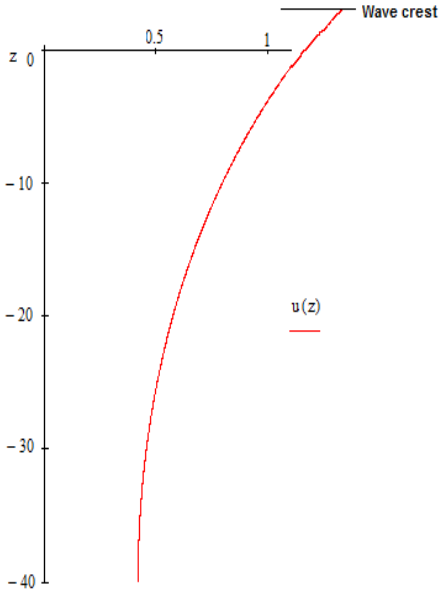

Figure 3.6 – Horizontal velocity when the water depth is 40 meters

Figure 3.7 shows the horizontal velocity for different water depths and positions at time $t = 0\ s$.

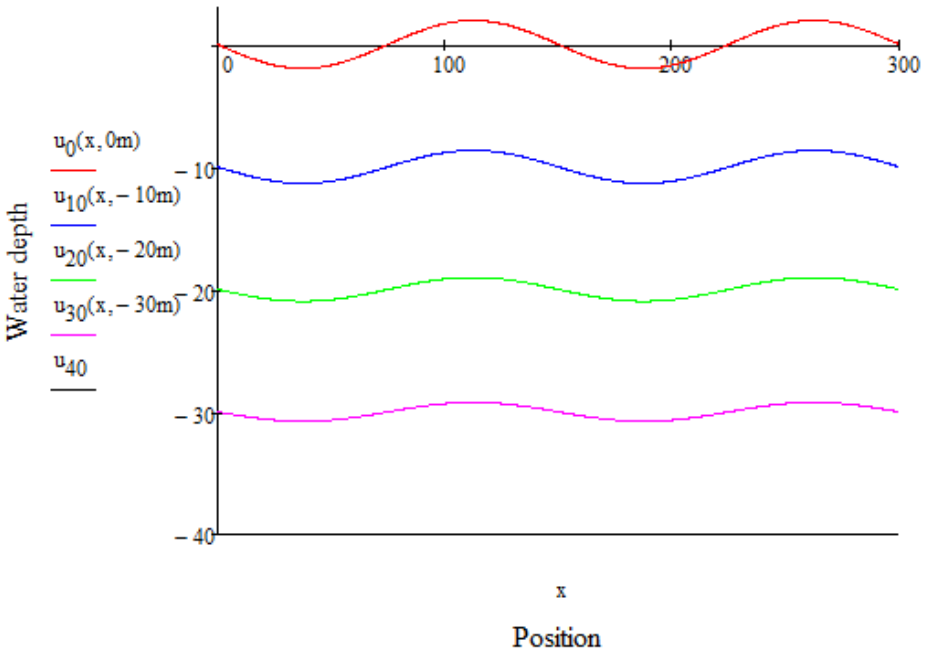

Figure 3.7 – Horizontal velocity for different water depths

The acceleration is obtained from the formula for horizontal velocity:

$$\dot{u} = \frac{\partial u}{\partial t} = \xi_0 \, g \, k \cdot \frac{\cosh k(z+d)}{\cosh(k \, d)} \cdot \cos(\omega \, t - k \, x) \qquad (3.1\text{-}9)$$

Figure 3.7 shows an example of the velocity plotted together with the acceleration, note the 90 degrees phase shift.

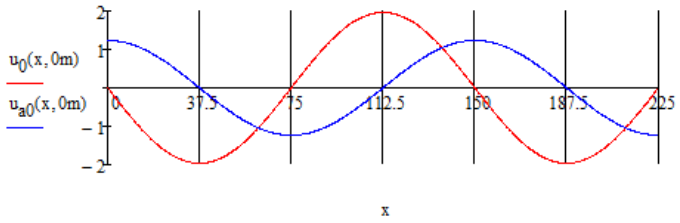

Figure 3.8 - Horizontal velocity with its corresponding acceleration

3.2.1.3 Vertical Particle Velocity and Acceleration

Again, the vertical particle velocity is found by taking the derivative of the velocity potential (3.1-7) with respect to the z-axis:

$$w = \frac{\partial \phi}{\partial z} = \frac{\xi_0 \, g \, k}{\omega} \cdot \frac{\sinh k(z+d)}{\cosh(k \, d)} \cdot \cos(\omega \, t - k \, x) \qquad (3.2\text{-}10)$$

Taking the time-derivative of the velocity to find the formula for acceleration:

$$\dot{w} = \frac{\partial w}{\partial t} = -\xi_0 \, g \, k \cdot \frac{\sinh k(z+d)}{\cosh(k \, d)} \cdot \sin(\omega \, t - k \, x) \qquad (3.2\text{-}11)$$

Figure 3.9 shows a plot of the horizontal- and vertical particle velocity at the surface for a water depth is 40 meters. The phase shift is 90 degrees.

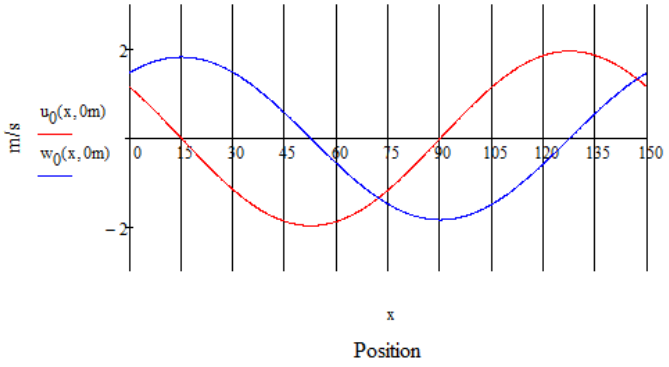

Figure 3.9 – Plot of the horizontal and vertical particle velocity

3.2.1.4 Shallow and Deep Water

While the offshore industry classifies shallow- and deep waters only by the water depth, it is in normal to relate the water depth to the wave length when using the wave theories. Normally the water depth is classified according to Table 3.1:

Table 3.1 – Classification of water depths

Shallow waters:	$\frac{d}{L} \lesssim \frac{1}{2}$
Finite/intermediate waters:	$\frac{1}{20} \lesssim \frac{d}{L} \lesssim \frac{1}{2}$
Deep waters:	$\frac{d}{L} \lesssim \frac{1}{20}$

Some mathematical simplifications can be made to the velocity potentials for shallow and deep water. Assuming shallow water the hyperbolic functions are simplified to:

$$\sinh d \approx \tanh d \approx d \tag{3.2-12}$$

and

$$\cosh d = \frac{e^{d}+e^{-d}}{2} \approx \frac{1+1}{2} = 1 \tag{3.2-13}$$

Similar for deep water where d becomes a large number:

$$\sinh d = \frac{e^{d}-e^{-d}}{2} \approx \frac{e^{d}}{2} \tag{3.2-14}$$

and

$$\cosh d = \frac{e^{d}+e^{-d}}{2} \approx \frac{e^{d}}{2} \tag{3.2-15}$$

These simplifications are applied to the velocity potential in Table 3.2.

3.2.1.5 Dynamic Pressure under a Wave

An ocean wave has both kinematic and dynamic properties. The kinematic properties are known as the velocities and accelerations of the wave, while the dynamic property is the pressure in the wave. For potential flow, the pressure under a wave is calculated from the linearized Bernoulli equation with the constant set to $\frac{p_0}{\rho}$:

$$\frac{\partial \phi}{\partial t} + \frac{p}{\rho} + gz = \frac{p_0}{\rho}$$

$$p = p_0 - \rho\, g\, z - \rho\, \frac{\partial \phi}{\partial t} \tag{3.2-16}$$

Consider the equation above; this is almost the same equation as the equation for hydrostatic pressure in an ideal fluid, eq. (3.1-10). The only difference is the last term $-\rho\, \frac{\partial \phi}{\partial t}$, which is commonly called the dynamic pressure term P_d. Inserting the velocity potential into the dynamic pressure term:

$$P_d = -\rho\, \frac{\partial \phi}{\partial t} = \rho\, \xi_0\, g\, \cdot \frac{\cosh k(z+d)}{\cosh(k\, d)} \cdot \sin(\omega\, t - k\, x) \tag{3.2-17}$$

Figure 3.10 shows the pressure variation in a linear wave, the dynamic pressure term is labelled “Linear dynamic pressure”.

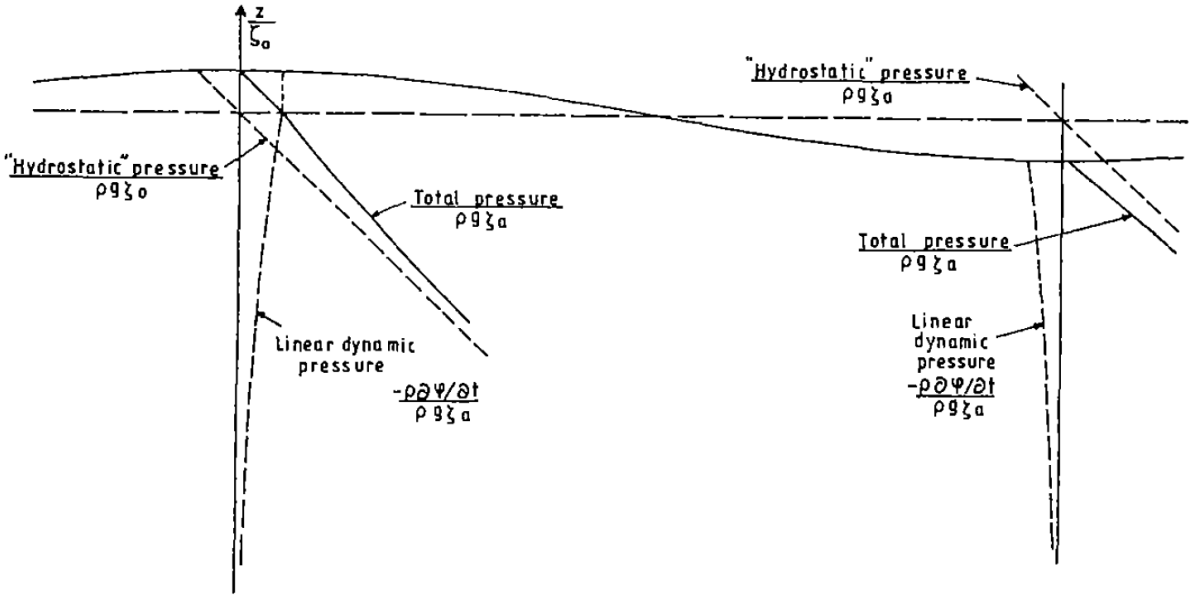

Figure 3.10 – Pressure variation in a linear wave [3, p.20]

3.2.1.6 Dispersion Relation

The combination of the kinematic- (3.1-45) and the dynamic (3.1-47) surface condition was not used to find the solution for the Laplace equation. However, this combination can be used to develop a relationship between wave length and wave period, called the dispersion relationship. Inserting the velocity potential (3.2-7) into the equation (3.1-48) gives an equation for finding the wave length, L:

$$\frac{\partial^2 \phi}{\partial t^2} + g\,\frac{\partial \phi}{\partial z} = 0 \qquad \text{for} \qquad z = 0 \tag{3.1-48}$$

$$L = \frac{g}{2\pi}\,T^2\,\tanh(k\,d) \tag{3.2-18}$$

3.2.1.7 Water Particle Motions

Although it might look like the water particles moves along with the wave's surface form, this is not the case. An object floating on the ocean surface moves vertically according to the surface profile, but it does not move much in the horizontal direction as long as there is no strong surface current. The explanation is that the water particles move in another pattern, they have their own orbits. From the formulas for horizontal- and vertical velocities it can be shown that the water particles move in elliptical orbits. These orbits are illustrated in Figure 3.11 for the case with a water depth of 40 meters. When the water particle approaches the sea floor, the vertical motions decrease faster than the horizontal motions.

A decrease in the vertical particle motion should therefore result in a decrease in heave motion for a floating structure located in such conditions where the sea bottom interferes with the fluid motion. This subject is investigated later on by calculating the RAO's for the shuttle tanker at different water depths.

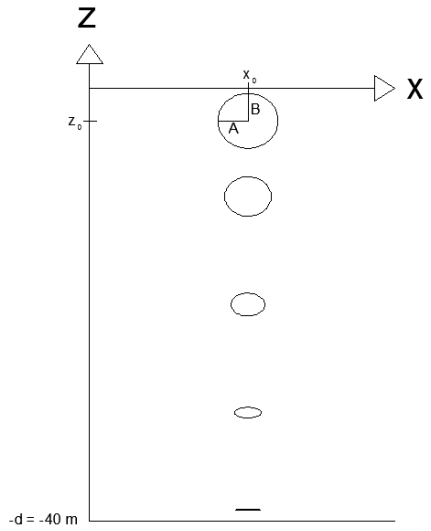

Figure 3.11 – Water particle motions at different depths

3.2.1.8 Summary of Linear Wave Theory

Table 3.2 – Linear Theory Equations [16]

Linear Wave Theory Review			
Wave Property	**Shallow Water** $d/L<1/20$	**Intermediate Water** $1/20<d/L<1/2$	**Deep Water** $d/L>1/2$
Velocity potential	$\varphi=\frac{\xi_0\cdot g}{\omega}\cdot\cos(\omega t-kx)$	$\varphi=\frac{\xi_0\cdot g}{\omega}\cdot\frac{\cosh k(z+d)}{\cosh(kd)}\cdot\cos(\omega t-kx)$	$\varphi=\frac{\xi_0\cdot g}{\omega}\cdot e^{kz}\cdot\cos(\omega t-kx)$
Dispersion relation	$\omega^2=g\cdot d\cdot k^2$ $L=\sqrt{g\cdot d\cdot T^2}$	$\omega^2=g\cdot k\cdot\tanh(kd)$ $L=\frac{g}{2\pi}\cdot T^2\cdot\tanh(kd)$	$\omega^2=g\cdot k$ $L=\frac{g}{2\pi}\cdot T^2$
Wave profile	$\xi=\xi_0\sin(\omega t-kx)$	$\xi=\xi_0\sin(\omega t-kx)$	$\xi=\xi_0\sin(\omega t-kx)$
Dynamic pressure	$P_d=\rho\cdot\xi_0\cdot g\cdot\sin(\omega t-kx)$	$P_d=\rho\cdot\xi_0\cdot g\cdot\frac{\cosh k(z+d)}{\cosh(kd)}\cdot\sin(\omega t-kx)$	$P_d=\rho\cdot\xi_0\cdot g\cdot e^{kz}\cdot\sin(\omega t-kx)$
Horizontal particle velocity	$u=\frac{\xi_0\cdot k\cdot g}{\omega}\cdot\sin(\omega t-kx)$	$u=\frac{\xi_0\cdot k\cdot g}{\omega}\cdot\frac{\cosh k(z+d)}{\cosh(kd)}\cdot\sin(\omega t-kx)$	$u=\frac{\xi_0\cdot k\cdot g}{\omega}\cdot e^{kz}\cdot\sin(\omega t-kx)$
Vertical particle velocity	$w=\frac{\xi_0\cdot k^2\cdot g}{\omega}\cdot(z+d)\cdot\cos(\omega t-kx)$	$w=\frac{\xi_0\cdot k\cdot g}{\omega}\cdot\frac{\sinh k(z+d)}{\cosh(kd)}\cdot\cos(\omega t-kx)$	$w=\frac{\xi_0\cdot k\cdot g}{\omega}\cdot e^{kz}\cdot\cos(\omega t-kx)$
Horizontal particle acceleration	$\dot{u}=\xi_0\cdot k\cdot g\cdot\cos(\omega t-kx)$	$\dot{u}=\xi_0\cdot k\cdot g\cdot\frac{\cosh k(z+d)}{\cosh(kd)}\cdot\cos(\omega t-kx)$	$\dot{u}=\xi_0\cdot k\cdot g\cdot e^{kz}\cdot\cos(\omega t-kx)$
Vertical particle acceleration	$\dot{w}=-\xi_0\cdot k^2\cdot g\cdot(z+d)\cdot\sin(\omega t-kx)$	$\dot{w}=-\xi_0\cdot k\cdot g\cdot\frac{\sinh k(z+d)}{\cosh(kd)}\cdot\sin(\omega t-kx)$	$\dot{w}=-\xi_0\cdot k\cdot g\cdot e^{kz}\cdot\sin(\omega t-kx)$
Phase velocity c	$c^2=g\cdot d$	$c^2=\frac{g}{k}\cdot\tanh(kd)$	$c^2=\frac{g}{k}$
$\omega=2\pi/T$, $k=2\pi/L$ T = wave period L = wave length ξ_0 = wave amplitude g = acceleration of gravity $c=\omega/k=L/T$ = phase velocity		t = time x = direction of propagation z = vertical co-ordinate, positive upward, origin at still water level d = water depth P_d = dynamic pressure P_0 = atmospheric pressure	

3.2.2 Stokes' Fifth Order Wave Theory

Far from every sea states can be analysed using linear wave theory and obtain a satisfactory result. Linear wave theory depends on the assumption that the wave height is small compared to the wave length to yield good results. Stokes found a method of extending the validity range of the theory by taking into consideration the non-linear terms for wave kinematics and boundary conditions, which were neglected when developing the linear wave theory. This theory is named "Stokes' Fifth Order Wave Theory" and provides five components (a trigonometric series) for the wave kinematics, compared to the single component used in linear wave theory. The first component for Stokes' theory is exactly the same as the component in linear wave theory. Components 2-5 are non-linear and decreases in magnitude as the order increases. In other words, the first order term is the largest and the fifth order term is the smallest. The horizontal velocity is expressed by a series on the form [1, p.94]:

$$u = \sum_{n=1}^{5} u_n \cosh[n\,k\,(z+d)] \sin[n(\omega t - kx)] \qquad (3.2\text{-}19)$$

It should be noted from the equation above that the higher order components have a frequency which is a multiplication of n times the fundamental wave frequency. This becomes important when analysing structures that might get into resonance with the higher frequencies. Also, the component u_n is a series that converges towards 1 when n increases.

An example of the five components is given in Figure 3.12. Stokes' fifth order waves are more realistic compared to linear waves as they have higher and steeper crests and lower troughs, similar to real ocean waves.

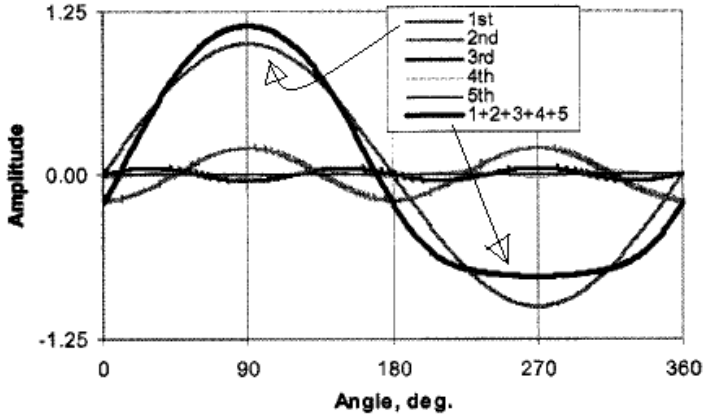

Figure 3.12 – Stokes' fifth order velocity components [1, p94]

Figure 3.13 shows a plot of the horizontal velocity for a Stokes fifth order wave compared to the velocity of the equivalent wave described by linear wave theory. Note that the only place where the non-linear Stokes fifth order theory will give any significant effect is close to the free surface. Stokes theory is therefore a very useful tool for analysing floating structures.

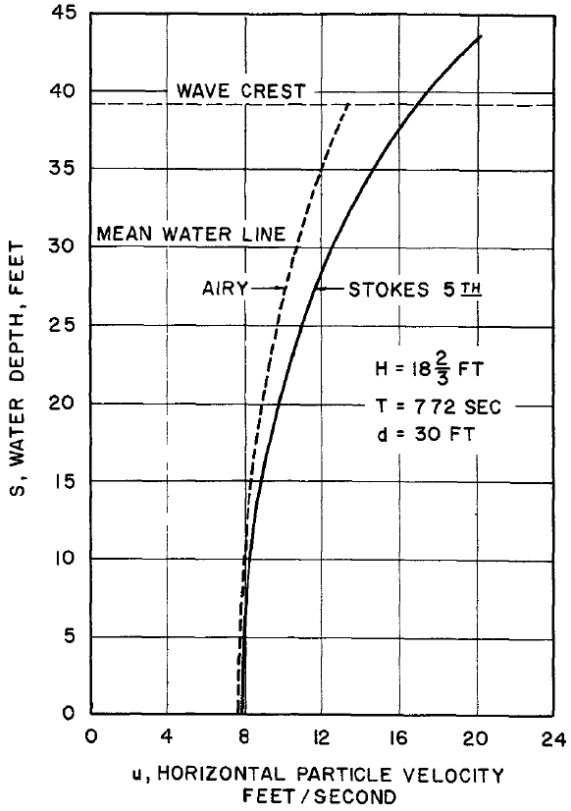

Figure 3.13 – Plot of the horizontal velocity for a Stokes fifth order wave compared to a linear (Airy) wave. [17]

3.2.3 Applicability of Regular Deterministic Wave Theory

As mentioned before, both linear- and Stokes wave theory are based upon a couple of assumptions that limits their validity range when it comes to wave height and length and the water depth. *Det Norske Veritas* have developed clear rules for when the different theories for regular deterministic waves are to be used for practical purposes. The offshore standard DNV-OS-H101 states in Table 3.3:

Table 3.3 – DNV-OS-H101 wave theory requirements

$\frac{d}{L} \leq 0.1$	Solitary wave theory for particularly shallow water
$0.1 < \frac{d}{L} \leq 0.3$	Stokes 5th order wave theory or Stream Function wave theory
$\frac{d}{L} > 0.3$	Linear wave theory (or Stokes 5th order)

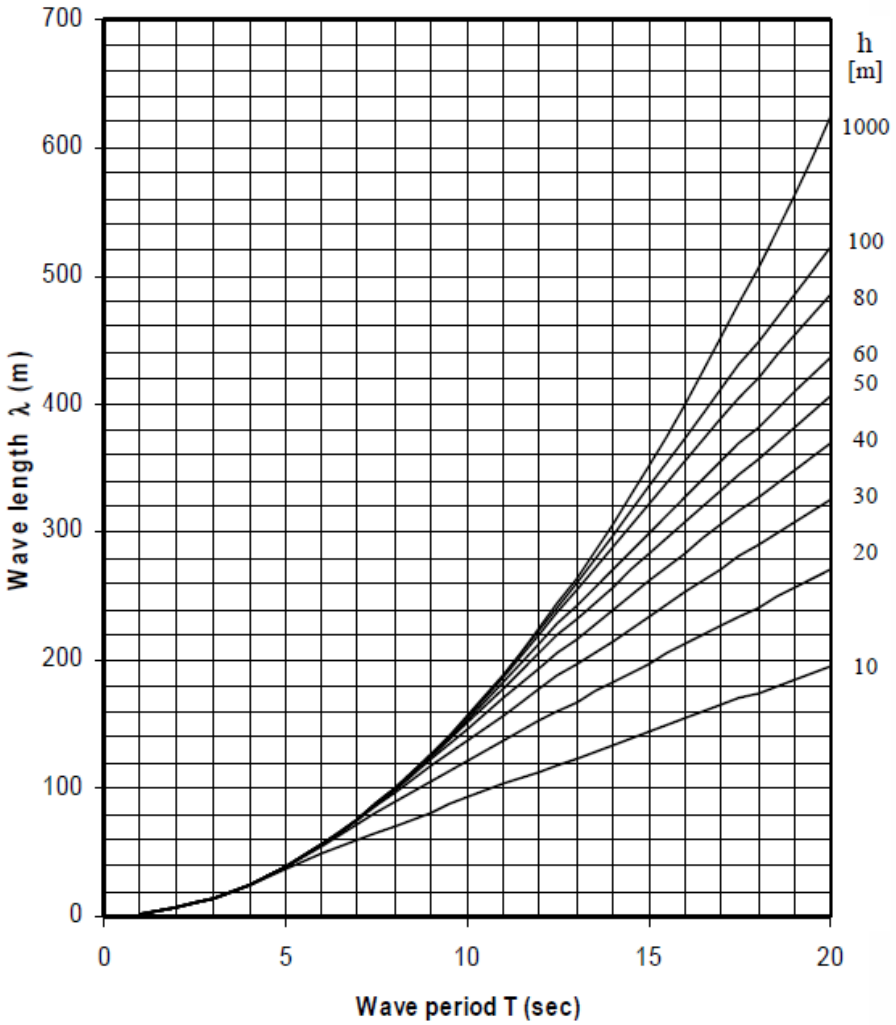

Figure 3.14 – Relationship between wave length, wave period and water depth (h) [18, p24]

Determining the deterministic wave theory for use in the analysis of the shuttle tanker:

Table 3.4 – Location characteristics for determining applicable wave theory

Location:	North Sea
Water depth:	40 meters
Wave period:	5-13 seconds
Assumed wave height limit:	$H = STF \times H_s = 2 \times 3.5\ m = 7\ m$

The location and water depth is given in the project. Relevant wave periods are determined by the North Sea representative scatter diagram in Figure 2.3. The wave height is assumed upon an initial guess of the limiting significant wave height being 3.5 m, and then multiplied with the STF factor in accordance with DNV-OS-H101 Sec. 3, C303.

Applying the information in Table 3.4 to the DNV-OS-H101 wave theory requirements in Table 3.3:

Figure 3.14 gives the wave lengths for the wave periods 5-13 second to be:

$$L = 40\ m\ to\ 220\ m$$

$$\left.\frac{d}{L}\right|_{min} = \frac{40\ m}{220\ m} = 0.18 \Longrightarrow Stokes\ 5^{th}\ order\ wave\ theory \quad (3.2\text{-}20)$$

$$\left.\frac{d}{L}\right|_{max} = \frac{40\ m}{40\ m} = 1.0 \Longrightarrow Linear\ wave\ theory \quad (3.2\text{-}21)$$

Eq. (3.2-20) states that if the analysis of the shuttle tanker is going to be analysed by regular deterministic waves, the Stokes 5th order theory (or Stream theory) must be used to be in accordance with the offshore standard DNV-OS-H101.

3.3 Breaking Waves

Everyone who has been to the beach and watched the waves rolling onto it has probably seen the waves grow to a certain height, before turning into foam and spilling from the crest and down on the forward face on the wave. This phenomena is called breaking waves and will eventually happen to all growing waves at some point, independent if the waves are close to the shore or not. It happens because the wave slope becomes too steep, making the wave unstable. The breaking height for a wave is limited only by wavelength and water depth and is calculated by the formula [1, p.105]:

$$H_b = 0.142\ L\ \tanh(k\ d) \qquad (3.3\text{-}1)$$

For the case of deep waters, the $\tanh(k\ d)$ term is simplified and to equal one, making the breaking height only a function of wave length:

$$H_b = 0.142\ L \qquad (3.3\text{-}2)$$

Breaking waves causes very large slamming loads on structures and none of the before mentioned wave theories can describe the kinematics and dynamic properties of these waves very well. Researchers are currently working on this subject with the objective of developing a theory. Some theories have been suggested, but none of them are commonly used for design purposes.

In this report, the subject of breaking waves is taken care of by only considering waves with a lower height than the breaking height. Figure 3.15 shows the relationship between breaking wave height and wave period.

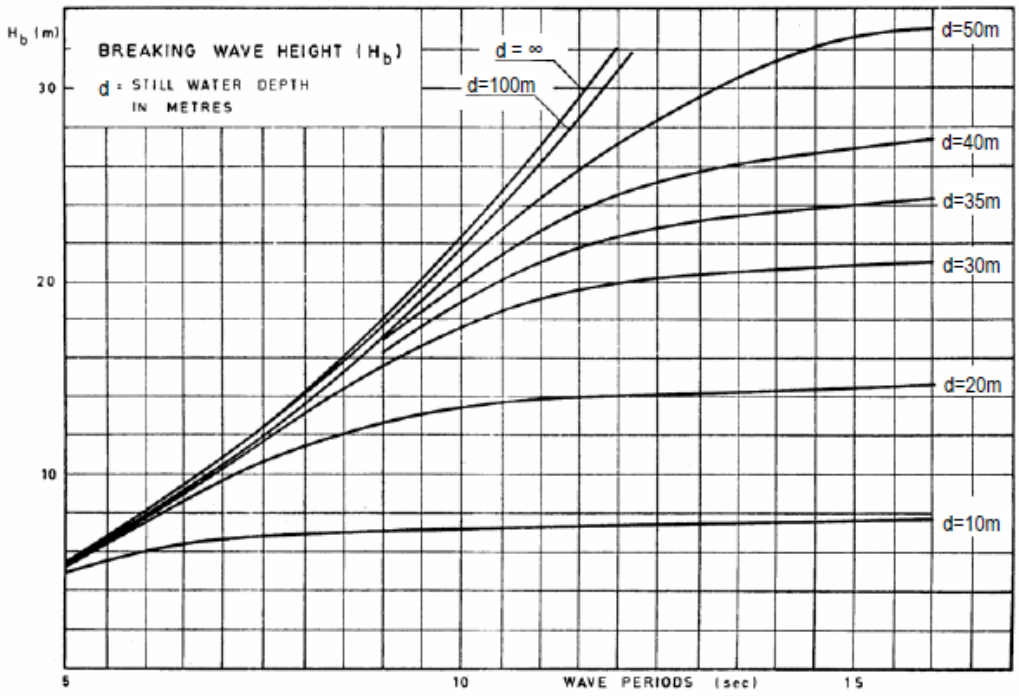

Figure 3.15 – Breaking wave height [15, p.31]

3.4 Swell Waves

Ocean waves are divided into two categories, waves that are generated by local winds and swell waves. Swells are generated from distant storms and have no connection to the local weather conditions. Since they travel over long distances they have a narrower range of frequencies and directions compared to local wind waves. The wave periods for swell waves are higher than those for normal waves, and the wave lengths are normally around 100 meters. However, for severe storms, the wave lengths can easily exceed 500 meters.

An example of a breaking swell wave is given in Figure 3.16. The surface profile of a swell wave is actually the closest the nature gets to the surface profile assumed in linear wave theory.

Figure 3.16 – A swell wave breaking at Hermosa Beach, California [19]

For marine operations it is critical to be aware of the local wave conditions. Swell seas carries a lot more energy than shorter wind seas, this causes floating structures to have considerable motions even when there is no resonance between the vessels eigenperiod and the wave period. During the past decades, many on-going marine operations have had to be aborted due to unexpected swell waves.

3.5 Sea Spectrum

Regular wave theories are mainly used to determine the extreme response of a structure initiated by a single wave. Marine operations will never be carried out during extreme weather conditions and are hence dependent upon a more suitable theory for describing the sea state on a relatively calm day. If one were to measure the sea surface on any given day, it would quickly become clear that the sea surface does not look very similar to the sinusoidal surface assumed in the linear wave theory. The ocean waves are more random and are generally better described by statistical parameters.

Another way of solving the Laplace equation is by adding many different sinusoidal waves together into one solution. By considering only a limited time period, the height of the sea surface can be described by a Fourier series. The many different regular waves create an irregular sea state similar to the one illustrated in Figure 3.17.

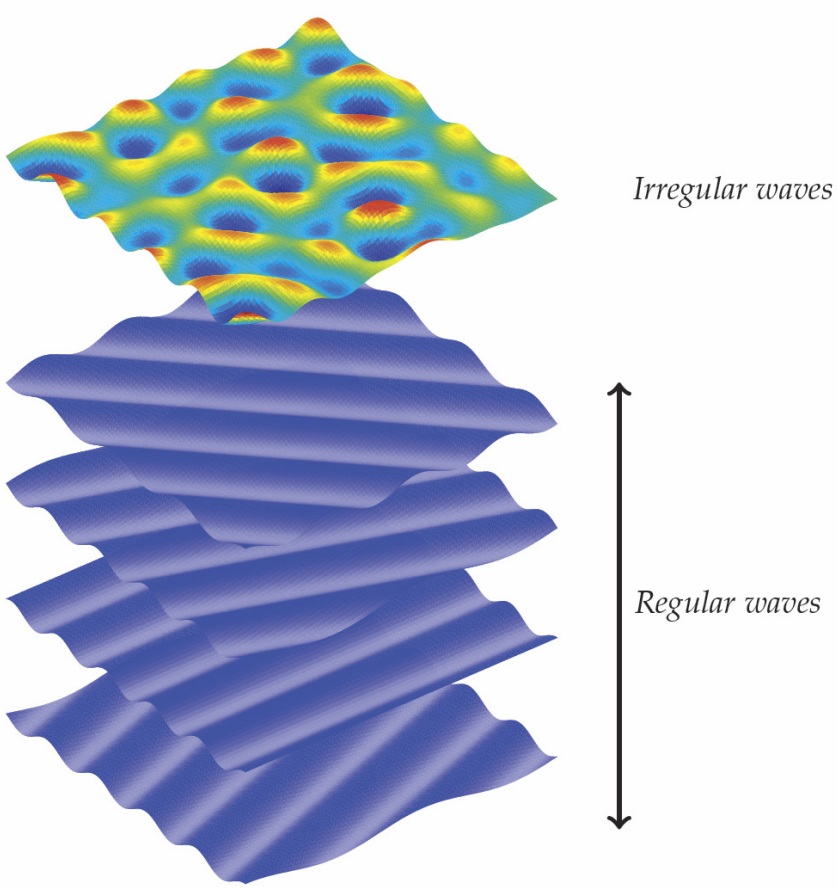

Figure 3.17 – A set of regular waves added together by superposition to obtain a sea state of irregular waves [20, p.34]

Starting with the Fourier series [21]:

$$\xi(t) = a_0 + \sum_{n=1}^{\infty}\left[a_n \cos\left(\frac{2\,n\,\pi}{T}\,t\right) + b_n \sin\left(\frac{2\,n\,\pi}{T}\,t\right)\right] \qquad (3.5\text{-}1)$$

where

T is the time period of the Fourier series

$$a_0 = \frac{1}{T}\int_{-T/2}^{T/2} \xi(t)\ dt$$

$$a_n = \frac{2}{T}\int_{-T/2}^{T/2} \xi(t)\cos\left(\frac{2\,n\,\pi}{T}\,t\right)\ dt$$

$$b_n = \frac{2}{T}\int_{-T/2}^{T/2} \xi(t)\sin\left(\frac{2\,n\,\pi}{T}\,t\right)\ dt$$

Rewriting equation (3.5-1) for a wave process with Origo at mean sea level and using trigonometric manipulations:

$$\xi(t) = \sum_{n=1}^{\infty} \xi_n\ \cos(\omega_n t - \theta_n) \qquad (3.5\text{-}2)$$

where

ω_n is the angular velocity for the n-component

$$\xi_n = \sqrt{{a_n}^2 + {b_n}^2} \qquad \text{(Wave amplitude)}$$

$$\theta_n = \tan^{-1}\left(\frac{b_n}{a_n}\right) \qquad \text{(Wave phase)}$$

From equation (3.5-2) it is seen that the wave process is described by the sum of cosine waves. The components are calculated for each period $\frac{2\,\pi}{T}$, giving the opportunity to obtain a smoother curve by increasing the time period T.

The same approach can be done to obtain to simulate the horizontal fluid velocity and acceleration [3, p.27]:

$$u = \sum_{n=1}^{\infty} \omega_n\ \xi_n\ e^{k_n z}\ \sin(\omega_n t - k_n x + \theta_n) \qquad (3.5\text{-}3)$$

$$\dot{u} = \sum_{n=1}^{\infty} {\omega_n}^2\ \xi_n\ e^{k_n z}\ \cos(\omega_n t - k_n x + \theta_n) \qquad (3.5\text{-}4)$$

If one were to measure two or more time series of the surface height of the same sea state, they would not be very similar to each other. This is typical for a stochastic process and the origin for the development of sea spectra.

A sea spectrum is a function $S(\omega)$, showing how the energy in the sea is distributed over the range of frequencies. Harmonic waves contain an energy amount which is proportional to the amplitude squared. Hence the function for sea spectrum is introduced as:

$$S(\omega_n) = \frac{{\xi_n}^2}{2\Delta\omega} \tag{3.5-5}$$

where

$$\Delta\omega = \frac{2\pi}{T} \qquad \text{(Difference between two successive frequencies)}$$

Now, the equation for surface elevation (3.5-2) is assumed to be a stochastic process with deterministic amplitude and an arbitrary phase angle [21]. The expected value and the variance of $\xi(t)$ can then be calculated, and the result is the expected value equal to zero and the variance is $\frac{1}{2}\,\xi^2$. Further, the phase angles are assumed to be statistically independent, and the variance becomes:

$$Var[\xi(t)] = \sum_{n=1}^{\infty} S(\omega_n)\Delta\omega$$

$$\lim_{T\to\infty} Var[\xi(t)] = \int_0^{\infty} S(\omega_n)\, d\omega = {\sigma_\xi}^2 \tag{3.5-6}$$

The largest amplitude in each simulation of the stochastic process will now be different. Faltinsen (1993) suggests approximating the most probable value of the amplitude with the formula:

$$\xi_{max} = \left(2M_0 \log\left(\frac{t}{T_z}\right)\right)^{\frac{1}{2}} \tag{3.5-7}$$

Here, M_0 is the zeroth spectral moment, t is the time duration and T_z is the zero-up-crossing period.

3.5.1 Sea Spectrum Parameters

The recommended practice standard DNV-RP-C205 uses the following parameters:

The **spectral moments** are defined as:

$$M_n = \int_0^{\infty} \omega^n\, S(\omega)\, d\omega \tag{3.5-8}$$

$$M_0 = {\sigma_\xi}^2 \tag{3.5-9}$$

The **significant wave height**:

$$H_s = H_{m0} = 4\sqrt{M_0} = 4\,{\sigma_\xi}^2 \tag{3.5-10}$$

The **zero-up-crossing period**:

$$T_z = T_{m02} = 2\pi\sqrt{\frac{M_0}{M_2}} \tag{3.5-11}$$

The **spectral peak period**:

$$T_p = \frac{2\pi}{\omega_p} \tag{3.5-12}$$

3.5.2 Sea Spectrum Models

Sea spectrum models are developed from measurements of real ocean waves over long time periods and are therefore empirical. The most common spectrums are the ISSC model, the Pierson-Moskowitz model and the JONSWAP model. These models will distribute a given amount of energy differently over the frequency range and hence estimate different responses of the structures involved. It is therefore important to choose the most accurate spectrum for the given location. Table 3.5 suggests which model should be used for some locations around the world.

Table 3.5 – Spectral models applied to different regions [1, p.112]

Location	Operational	Survival
Gulf of Mexico	P-M	P-M or JONSWAP
North Sea	JONSWAP	JONSWAP
Northern North Sea	JONSWAP	JONSWAP
Offshore Brazil	P-M	P-M or JONSWAP
Western Australia	P-M	P-M
Offshore Newfoundland	P-M	P-M or JONSWAP
West Africa	P-M	P-M

3.5.2.1 Pierson-Moscowitz

The Pierson-Moscowitz spectrum was developed by measurements done by ships in the North Atlantic. It is used to describe a fully developed sea, meaning that the waves are developing from all directions. The PM-spectrum is described by the following formula [15, p.33]:

$$S_{PM}(\omega) = \frac{5}{16}\,{H_s}^2\,{\omega_p}^4\,\omega^{-5}\,exp\left(-\frac{5}{4}\left(\frac{\omega}{\omega_p}\right)^{-4}\right) \tag{3.5-13}$$

3.5.2.2 JONSWAP

The JONSWAP spectrum was developed by measurements of waves in the Southern North Sea and has therefore a narrower distribution of wave directions. This causes the spectrum to have a narrower and higher energy distribution at the peak period. The spectrum is suitable for describing a sea state in a fetch limited situation [15, p.33]:

$$S_J(\omega) = A_\gamma \, S_{PM}(\omega) \, \gamma^{exp\left(-0.5\left(\frac{\omega-\omega_p}{\sigma\,\omega_p}\right)^2\right)} \qquad (3.5\text{-}14)$$

where

γ is a non-dimensional peak shape parameter

σ is a spectral width parameter

$\sigma = \sigma_a$ for $\leq \omega_p$
$\sigma = \sigma_b$ for $> \omega_p$

$A_\gamma = 1 - 0.287\ln(\gamma)$ (Normalizing factor)

Figure 3.18 shows a comparison between the JONSWAP- and the Pierson-Moscowitz spectra when the significant wave height is 3.5, the wave peak period is 8 sec and the peak parameter is calculated to be 5 (DNV-RP-C205 3.5.5.5).

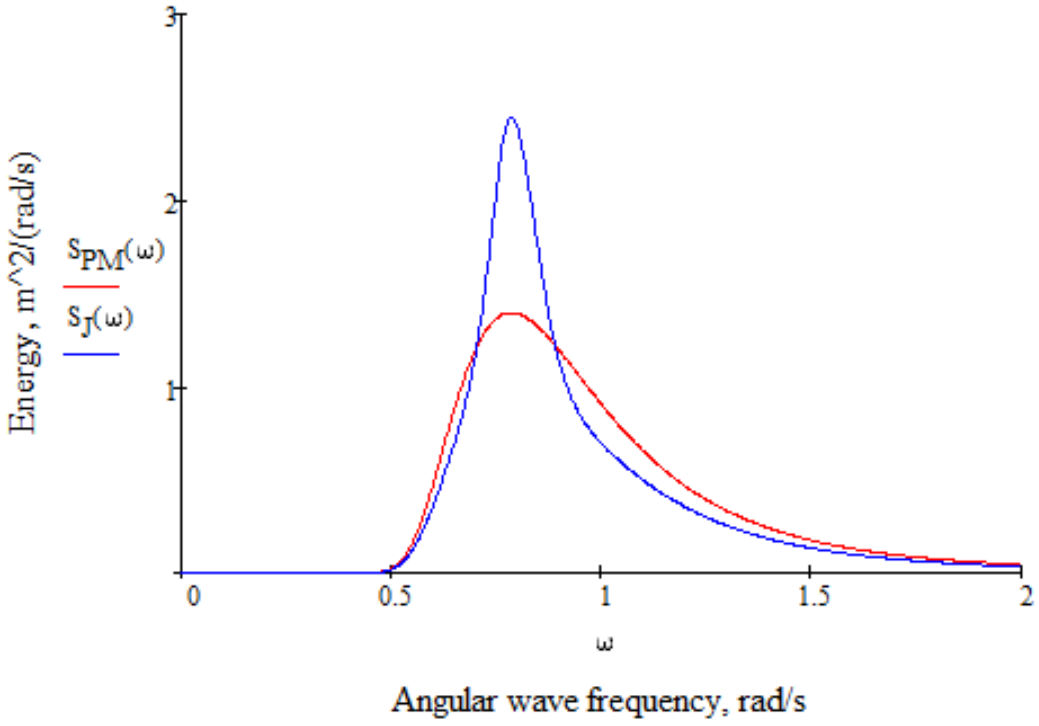

Figure 3.18 – Comparison between JONSWAP and Pierson-Moscowitz spectra

3.5.3 Directional Distribution of the Sea Spectrum

The sea spectrum is made directional by introducing a spreading function. This function is multiplied with the unidirectional spectrum, giving the formula for directional spectrum:

$$S(\omega,\theta) = S(\omega)\, D(\omega,\theta) \tag{3.5-15}$$

Here, the directionality function $D(\omega,\theta)$ has to fulfil the requirement from DNV-RP-C205:

$$\int_{\theta} D(\omega,\theta)\, d\theta = 1 \tag{3.5-16}$$

And a common directional function is [15, p35]:

$$D(\omega,\theta) = \frac{\Gamma\left(1+\frac{n}{2}\right)}{\sqrt{\pi}\,\Gamma\left(\frac{1}{2}+\frac{n}{2}\right)}\, cos^{n}\left(\theta-\theta_p\right) \tag{3.5-17}$$

where

Γ is the Gamma function tabulated in many mathematics textbooks

n is typically in the range of 2 to 4 for wind seas

$$\left|\theta-\theta_p\right| \leq \frac{\pi}{2}$$

A plot of the directional function is given in Figure 3.19 for different values of s. Note that a higher value of s makes the spreading narrower, almost unidirectional.

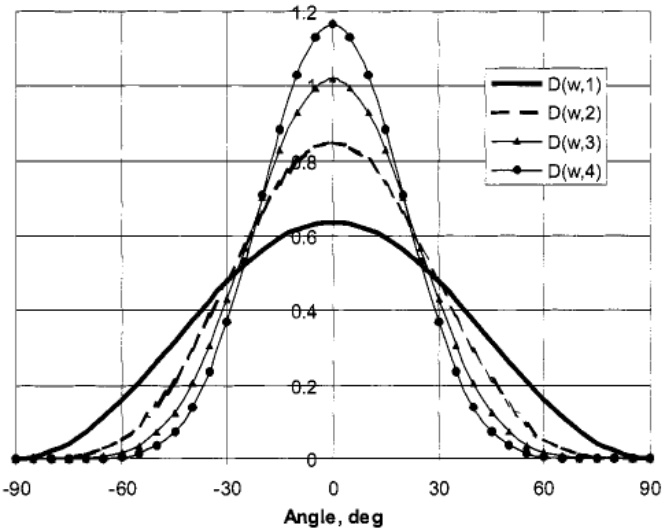

Figure 3.19 – Directional function for different values of s [1, p.116]

After introducing the directionality function, the two-dimensional sea spectrum shown in Figure 3.18 transforms into a three-dimensional directional sea spectrum shown in Figure 3.19.

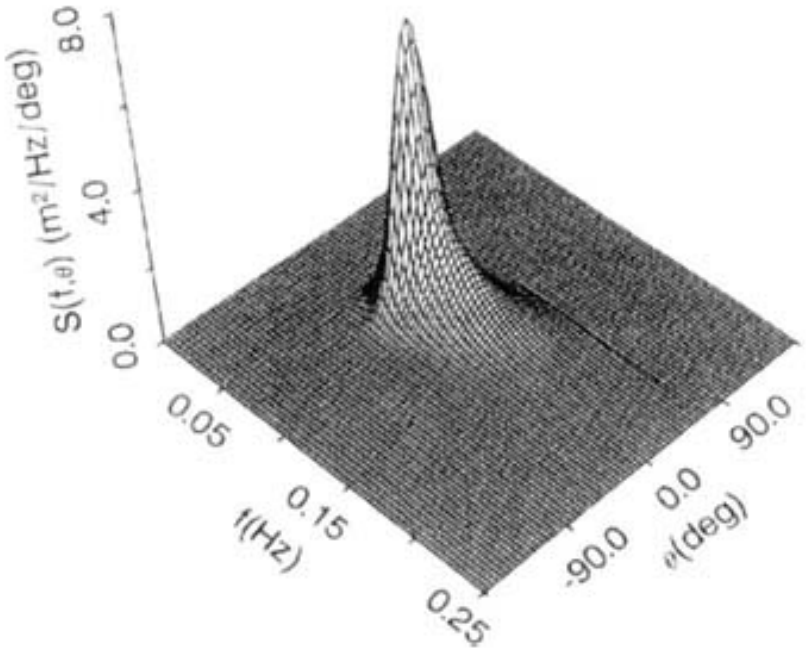

Figure 3.20 – Directional sea spectrum [1, p.117]

3.6 Simulating the Sea Surface

Both frequency-domain design and time-domain design uses a wave spectrum to simulate the sea. A frequency-domain analysis can only be applied to linear systems. If the system is non-linear, a time-domain analysis has to be conducted. Time-domain analysis calculates the surface elevation at every small time-step over the whole time period. This requires an enormous amount of calculations, making time-domain analysis very time consuming.

Figure 3.21 shows an illustration of the connection between frequency- and time-domain analyses. The frequency-domain is only considering a single wave component each time, whereas the time-domain frequency creates an irregular sea state by adding together all the regular wave components with different frequencies.

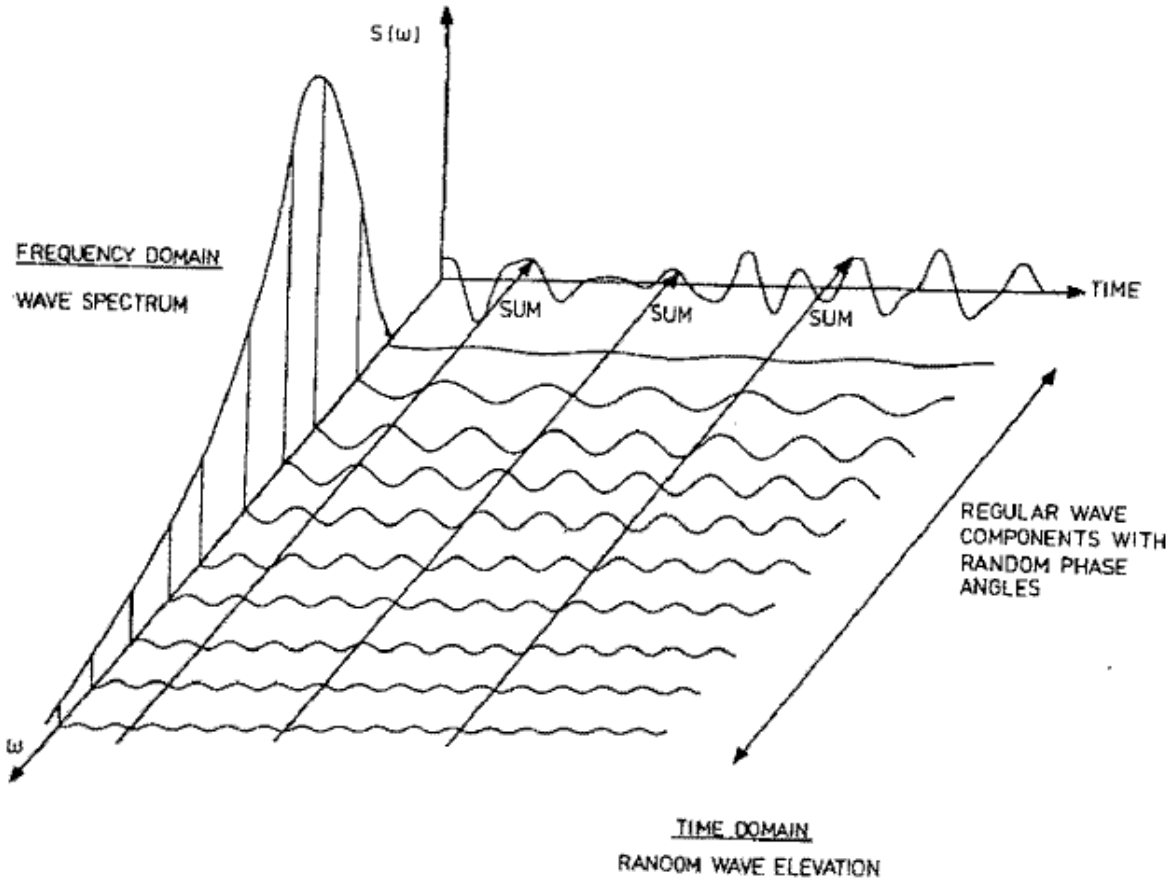

Figure 3.21 – Connection between frequency- and time-domain representation of waves [3, p.24]

MOSES is able to simulate both frequency- and time-domain analysis using ISSC, Pierson-Moscowitz or JONSWAP spectrum. An example of a time-domain representation of the sea surface elevation is shown in Figure 3.22 and Table 3.6. The JONSWAP sea spectrum has been chosen together with a significant wave height of 3.5 meters and a spectral peak period of 8 seconds, given by the scatter diagram for the North Sea in Figure 2.3. The peak shape parameter is calculated automatically by MOSES in accordance with DNV-RP-C205.

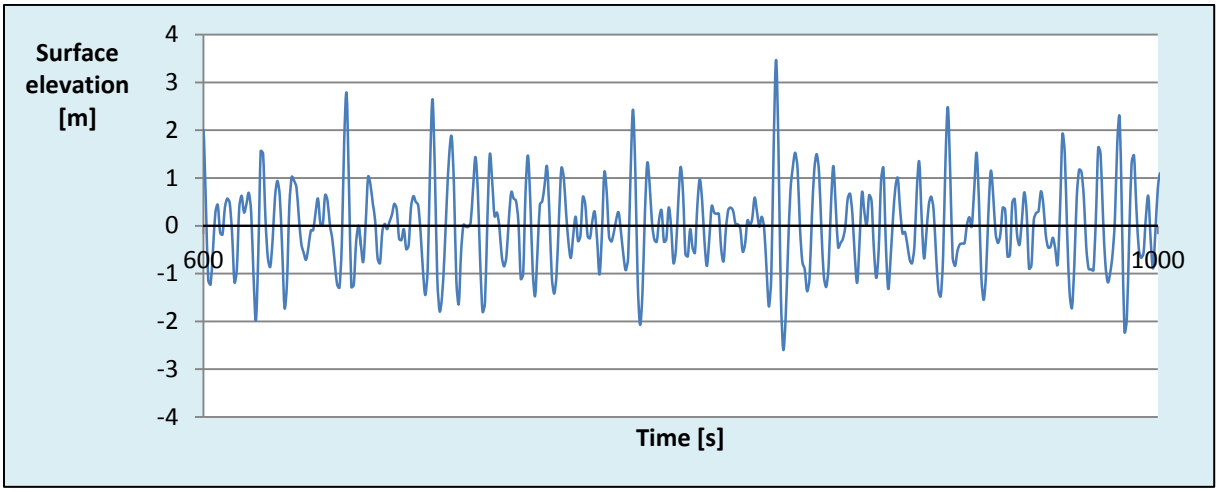

Figure 3.22 - Time series from MOSES showing the surface elevation of the sea at point (0,0,0) using the JONSWAP sea spectrum. The significant wave height is 3.5 meters, the spectral peak period is 8 seconds and the gamma factor has been calculated by MOSES using DNV-RP-C205

Table 3.6 – Properties of surface elevation time series

Standard Deviation	0.875	
H_s = 4 x Std.Dev.	3.50	m
Max Elevation:	3.47	m
Min Elevation:	-2.59	m

3.7 Wind

Wind creates forces on structures above the sea surface, and is characterised by two effects, namely the mean wind speed and the fluctuation about this mean speed (turbulence). The mean wind speed is treated as a steady load, while the turbulence is treated as a dynamic load.

The randomness of the blowing wind has resulted in the development of wind spectrums similar to the sea spectrums. Wind speeds are measured for a period of 1-hour at a height of 10 meters above still water level and these measurements are the basis for the empirical formulas used in the wind spectrums. The fluctuating wind speed is represented by a Fourier series containing harmonic components [22]:

$$u(t) = \sum_{i=1}^{\infty} U_i \cos(2\pi f_i t - \phi_i) \tag{3.7-1}$$

where

U_i is the 1 h mean wind speed

f_i is a discrete frequency

ϕ_i is the phase for the associated component

And the wind spectrum is expressed by the formula:

$$S(f_i) = \frac{{U_i}^2}{2\,\Delta f} \tag{3.7-2}$$

where

Δf is a small interval along the frequency axis

This report is examining a marine operation located in the North Sea where the NORSOK standards are governing. The correct choice of wind spectrum is therefore the *Frøya spectrum* from the NORSOK N-003 "Actions and action effects" standard developed by Andersen and Løvseth (1992):

$$S(f) = 320\,\frac{\left(\frac{U_0}{10}\right)^2 \left(\frac{z}{10}\right)^{0.45}}{\left(1+\tilde{f}^n\right)^{\frac{5}{3\,n}}} \tag{3.7-3}$$

where

$$\tilde{f} = 172\,f\left(\frac{z}{10}\right)^{\frac{2}{3}}\left(\frac{U_0}{10}\right)^{-0.75}$$

where

$S(f)$ is the spectral density at frequency f

z is the height above sea level

U_0 is the 1 h mean wind speed at 10 m above sea level

Figure 3.23 below shows an example of the Frøya wind spectrum:

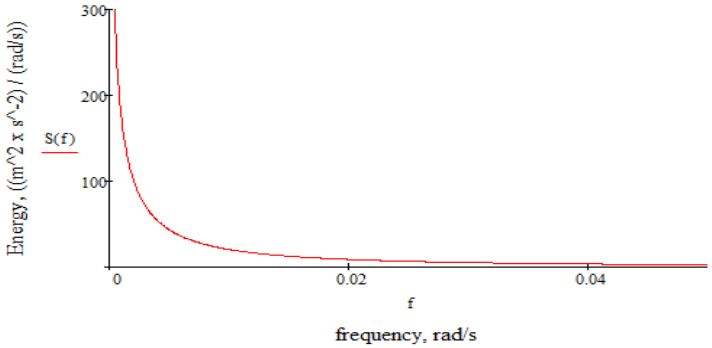

Figure 3.23 – Frøya wind spectrum for 25 knots 1 h mean wind speed at 75 meters above sea level

Marine operations are carried out only when the weather conditions are within the acceptance criteria. It is therefore important to know which magnitude of wind speeds to apply in the analysis for different significant wave heights. Table 3.7 shows how the wind speed is related to the significant wave height for measurements done in the North Atlantic and North Pacific.

Table 3.7 – The relationship between significant wave height and wind speed [3, p.32]

					North Atlantic			North Pacific		
Sea state no.	Significant wave height (m) Range	Mean	Sustained wind speed (knots)[a] Range	Mean	Percentage probability of sea state	Modal wave period (s) Range[b]	Most probable[c]	Percentage probability of sea state	Modal wave period (s) Range[b]	Most probable[c]
0–1	0–0.1	0.05	0–6	3	0.70	—	—	1.30	—	—
2	0.1–0.5	0.3	7–10	8.5	6.80	3.3–12.8	7.5	6.40	5.1–14.9	6.3
3	0.5–1.25	0.88	11–16	13.5	23.70	5.0–14.8	7.5	15.50	5.3–16.1	7.5
4	1.25–2.5	1.88	17–21	19	27.80	6.1–15.2	8.8	31.60	6.1–17.2	8.8
5	2.5–4	3.25	22–27	24.5	20.64	8.3–15.5	9.7	20.94	7.7–17.8	9.7
6	4–6	5	28–47	37.5	13.15	9.8–16.2	12.4	15.03	10.0–18.7	12.4
7	6–9	7.5	48–55	51.5	6.05	11.8–18.5	15.0	7.00	11.7–19.8	15.0
8	9–14	11.5	56–63	59.5	1.11	14.2–18.6	16.4	1.56	14.5–21.5	16.4
>8	>14	>14	>63	>63	0.05	18.0–23.7	20.0	0.07	16.4–22.5	20.0

[a] Ambient wind sustained at 19.5 m above surface to generate fully-developed seas. To convert to another altitude, H_2, apply $V_2 = V_1(H_2/19.5)^{\frac{1}{7}}$.
[b] Minimum is 5 percentile and maximum is 95 percentile for periods given wave height range.
[c] Based on periods associated with central frequencies included in Hindcast Climatology.

3.8 Current

Surface currents are mainly generated by wind, variation in the atmospheric pressure and the tide. These currents are very site-specific and the design values should therefore be determined from measurements at the site. However, if there is no exact measured data available, the NORSOK N-003 standard suggests that the wind induced current velocity at the still water level may be taken as:

$$U_i(0\ m) = 0.02\ U_0 \tag{3.8-1}$$

In the equation above, the current is assumed to have a steady mean flow. This is an approximation of the real current which has a more turbulent flow.

The velocity profile of a surface current is assumed to be linear and decreasing with water depth. Faltinsen [3] proposes the following formula to calculate the local wind generated current at increasing water depths:

$$U_i(z) = \begin{cases} U_i(0\ m)\frac{h_0+z}{h_0}, & for -h_0 \le z \le 0 \\ 0, & for\ z < -h_0 \end{cases} \tag{3.8-2}$$

where

h_0 is chosen to be 50 meters

Ships and floating structures will start to drift when subjected to surface currents. To counteract this effect, ships are normally equipped with a dynamic positioning system (DP) and floating structures stay at rest by the help of mooring lines connected to anchors on the sea floor.

Another type of current is the ones travelling below the sea surface or close to the sea floor. When a loop current like the Gulf Stream travels near the sea floor, it introduces irregularities and eddies by interacting with the sea floor. For deep waters, the velocity of the current disappears, and for shallow water it is assumed to decrease in a logarithmic form. These currents are especially important to be aware of when lowering objects like the wind turbine foundation close to the sea floor.

4 Ship Stability

4.1 Stability

Stability is the ability of a body, in this setting a shuttle tanker, to resist the overturning forces and return to its original position after the disturbing forces are removed [30]. During the lifting operation, the shuttle tanker will encounter environmental forces from winds, waves and current, combined with forces due to the lifting itself in the form of varying crane sling forces, tugger wire forces and shifting of jacket loads. All these forces are altering the stability in a greater or lesser extent during the whole operation.

A ship is said to have **initial stability** if it returns to its original position after a force which gives it a small deviation (heel angle) is removed.

The stability of a ship is divided into two categories; longitudinal- and transverse stability. Since the ship is almost six times longer in the longitudinal direction than the transverse, and the jacket is lifted over the ship's side, only the ships transverse stability is considered here.

To ensure stability at all times, ships are equipped with ballast tanks to alter the centre of gravity and keep as much weight as possible low in the hull. By pumping water into the correct ballast tanks, the ship can remain at an even keel also when the jackets are lifted over the ship's side, see Figure 4.2.

4.1.1 Determining the Stability

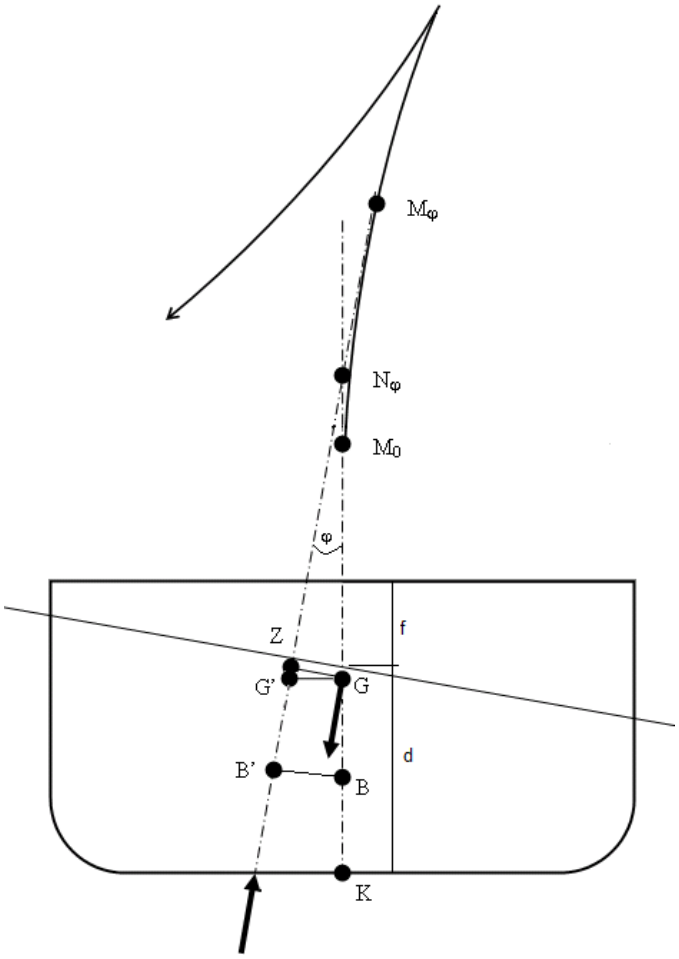

Figure 4.1 - Inclined ship hull [32]

Figure 4.1 shows an illustration of an inclined ship hull with the following nomenclature:

- K is the keel
- G is the centre of gravity (c.o.g)
- B is the centre of buoyancy
- G' is the inclined centre of gravity
- B' is the inclined centre of buoyancy
- ϕ is the inclined (heel) angle
- N_ϕ is the "false" metacentre
- M_0 is the metacentre before inclination
- M_ϕ is the metacentre after inclination
- f is the freeboard
- d is the draft

For a floating ship to have initial stability, the metacentre *must* be located above the centre of gravity (c.o.g) on Figure 4.1. The distance between metacentre and c.o.g is denoted $\overline{GM}$ and calculated by the formula:

$$\overline{GM} = \overline{KB} + \overline{BM} - \overline{KG} \tag{4.1-1}$$

where

$\overline{KB}$ is the distance between the keel and the centre of buoyancy

$\overline{BM}$ is the distance between the centre of buoyancy and the metacentre

$\overline{KG}$ is the distance between the keel and the centre of gravity

It should be noted that this equation is only valid for small inclination angles, ϕ.

When the distance to the metacenter is known, it is possible to calculate the moment acting against the inclination, i.e. the uprighting moment, M_r [30]:

$$M_r = \overline{GZ}\ \rho g \nabla = \overline{GM} \sin(\phi)\ \rho g \nabla \approx \overline{GM}\ \phi\ \rho g \nabla \tag{4.1-2}$$

where

$\overline{GZ}$ is the uprighting arm (see figure 4.1)

∇ is the displacement of the vessel

A metacenter located above the centre of gravity results in a positive $\overline{GM}$ value, which further gives a uprighting moment acting against the inclination and the ship has a certain magnitude of stability. Requirements to $\overline{GM}$ and freeboard is given by companies like *Det Norske Veritas* and *Noble Denton*.

4.2 Stability During Lifting

The stability of the ship must be monitored at all times during the operating. Lifting these jackets in an offshore environment comprises risks that have to be addressed with caution. Before a lift begins, the slings are tightened such that the crane hook is placed vertically above the jacket's centre of gravity to prevent motions at lift off.

Figure 4.2 shows how the ship uses ballast water during the lift to minimize the heel angle. It is utmost important that the heel angle is at a minimum when the jacket is lifted off from rest. At this moment the jacket's centre of gravity moves from the initial position and upwards to the crane tip. If the lift-off is done when the ship has a large heel angle, the jacket moves sideways and the situation might get out of control. This alteration in centre of gravity reduces the ships $\overline{GM}$, i.e. the ship is less stable with the jacket is hanging in the crane tip, compared to when it is standing on the rests (skid system).

During the slewing of the crane, the ships centre of gravity changes continuously. This change in centre of gravity is counteracted and controlled by continuously pumping ballast water to ensure sufficient stability at all times.

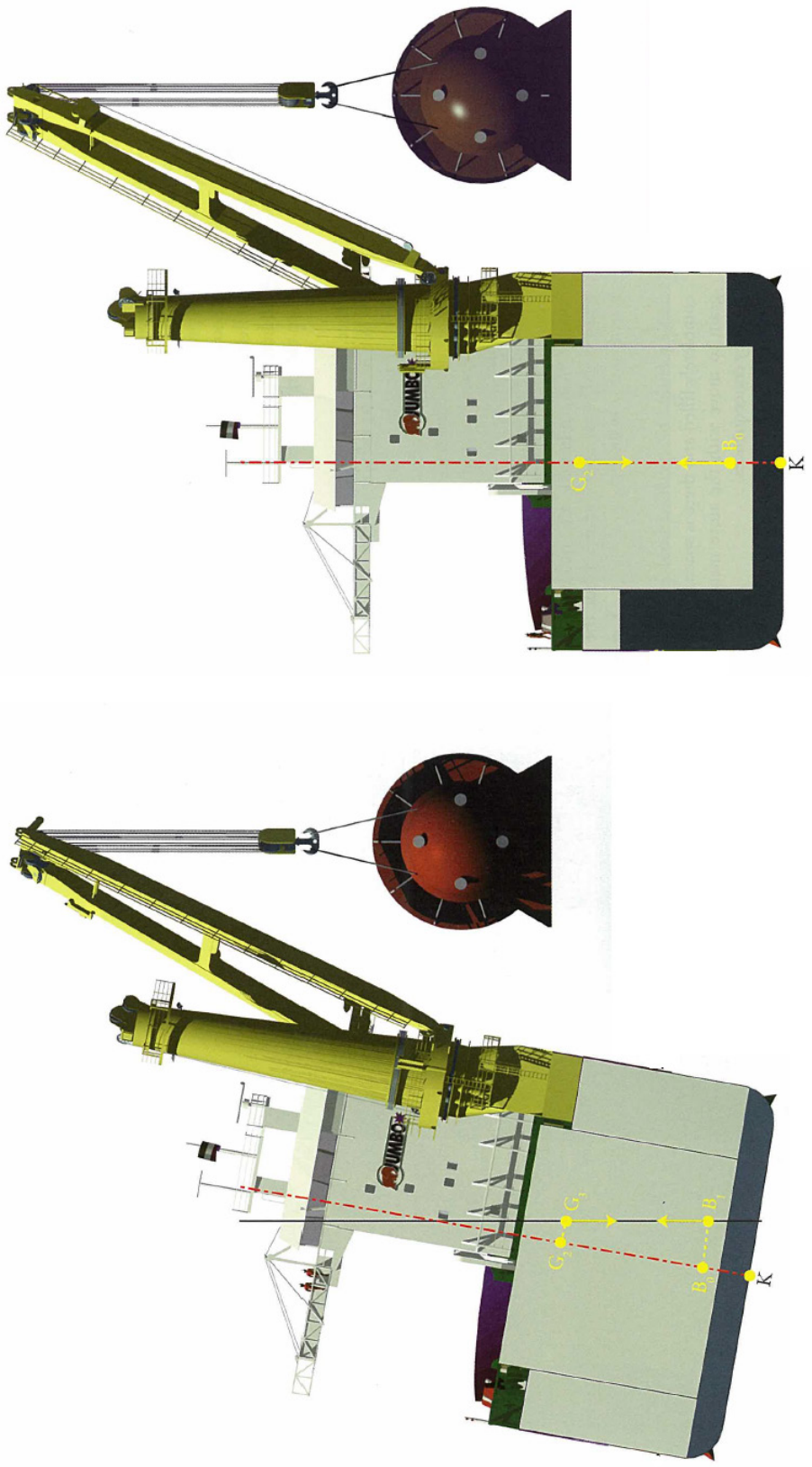

Figure 4.2 - The effect of ballast water while lifting [31, p.63]

5 Ship Motions

The motion characteristics of the lifting vessel are of great importance for determining if the operation can be carried out in the given weather conditions. Waves and wind forces on the vessel causes motions in the crane tip. These results are accelerations and velocities in the lifted object. Since the crane tip motion changes direction all the time, the acceleration varies and hence the force on the lifted object varies. A varying load is referred to as a dynamic load.

A ship floating on water can move in three uncoupled translatory directions and is therefore said to have three rigid-body translatory degrees of freedom (DOF). If a coordinate system is placed according to Figure 5.2, the motions in the x-, y- and z-axis are called surge, sway and heave respectively. Also, the ship can rotate around the same three axes, giving it three rotational degrees of freedom called roll, pitch and yaw.

The translations along the x-, y- and z-axis are commonly denoted as η_1, η_2 and η_3, respectively. And the rotations around the x-, y- and z-axis are commonly denoted as η_4, η_5 and η_6.

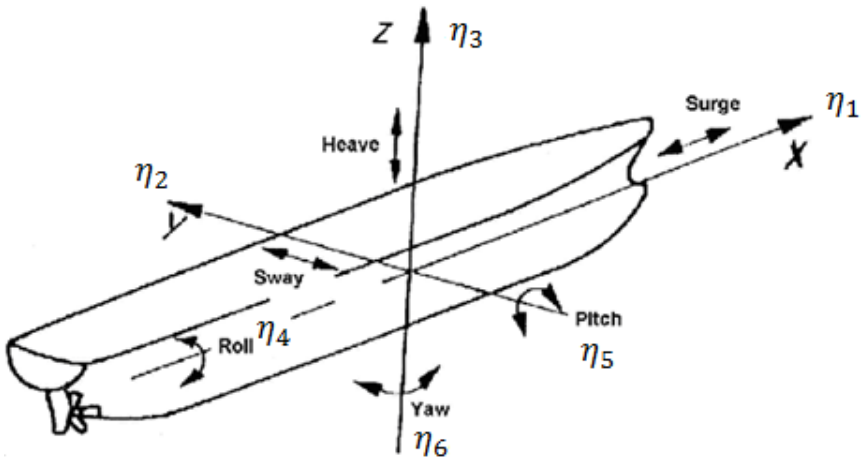

Figure 5.1 - Degrees of freedom for a ship [25]

For the surge, sway and yaw degrees of freedom, the system can be viewed as a simple mass-damper system; all the positions for each degree of freedom are equilibrium positions, as there is no hydrostatic stiffness [20].

For the heave, roll and pitch degrees of freedom, the system can be viewed as a mass-spring-damper system, where the stiffness is determined by the hydrostatic characteristics of the floating ship [20].

5.1 Mass-Spring-Damper System

The heave motion of a floating ship is modelled as a single degree of freedom system subjected to a harmonic excitation force from the sea, see Figure 5.2.

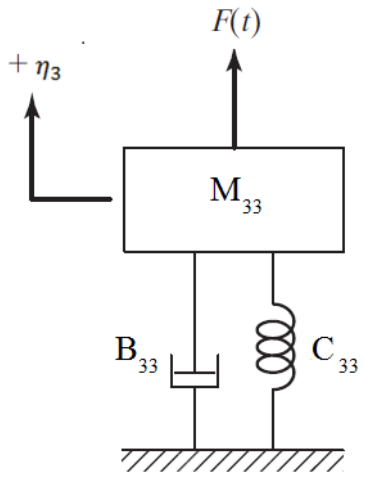

Figure 5.2 - Spring-mass-damper system [26, p.262]

The **equation of motion** is derived from Figure 5.2 and Newton's second law:

$$M_{33}\ddot{\eta}_3 + B_{33}\dot{\eta}_3 + C_{33}\eta_3 = F_3(t) \qquad (5.1\text{-}1)$$

where

M_{33} is the mass of the system (hydrodynamic mass added later on)

B_{33} is the damping coefficient associated with the fluid

C_{33} is the "spring" constant equal to the increased buoyancy force when increasing the draft by one meter

η_3 is the position along the z-axis

$\dot{\eta}_3$ is the velocity in the z-direction (time derivative of the position)

$\ddot{\eta}_3$ is the acceleration in the z-direction (time derivative of the velocity)

$F_3(t)$ is a function describing the force acting on the ship in the z-direction at time t

For surge, sway and yaw, the simple mass-damper system is equivalent to the system in Figure 5.2 only with the spring removed, i.e. the term $C_{33}\eta_3$ is removed from the equation of motion.

5.2 Response Amplitude Operators

All ships have different motion characteristics making them respond and move differently in the same sea state. To determine the motions of a ship on the basis of a given sea state, a function can be developed that transfers a sea state into a function that shows how the ship responds to it. This transfer function is called the Response Amplitude Operator (RAO) and every ship has its own unique RAO. An illustration of how wave excitation becomes ship motions is given in Figure 5.4. RAO's can only be developed for linear motion responses.

The RAO's for the shuttle tanker model used in this report is given in **Appendix B** for two points, the crane tip and the ships centre of gravity. These RAO's are only valid when the ship has a draft of 13 meters and is located in a water depth of 40 meters. Figure 5.3 shows the RAO's in the crane tip for head- and beam seas.

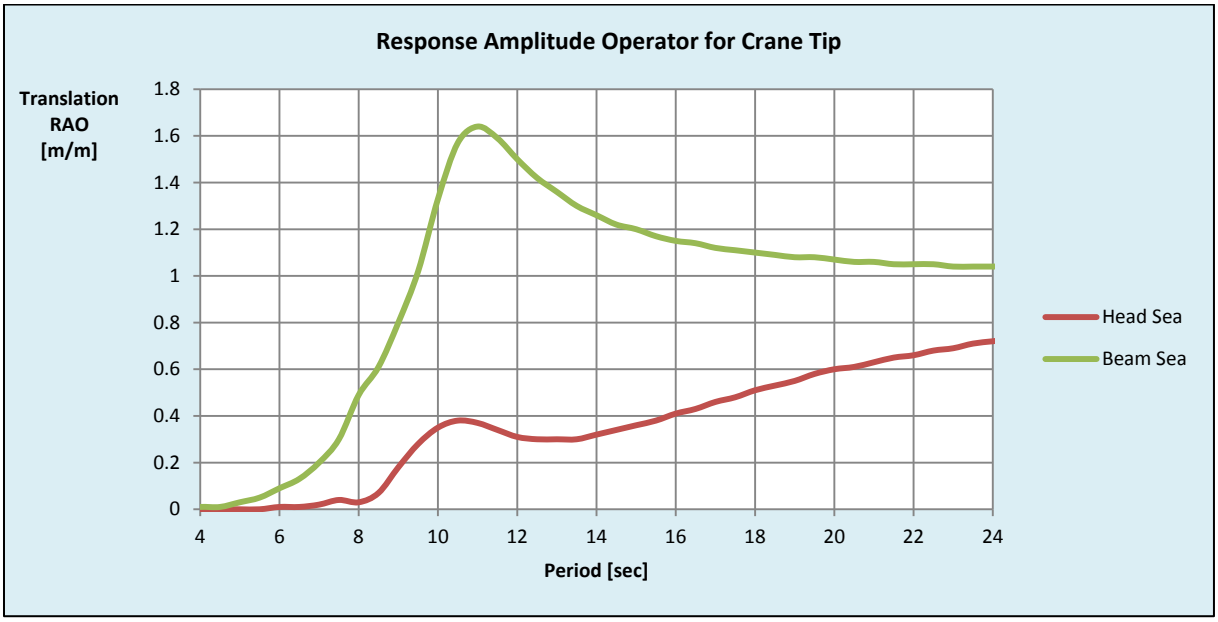

Figure 5.3 – RAO for Crane Tip

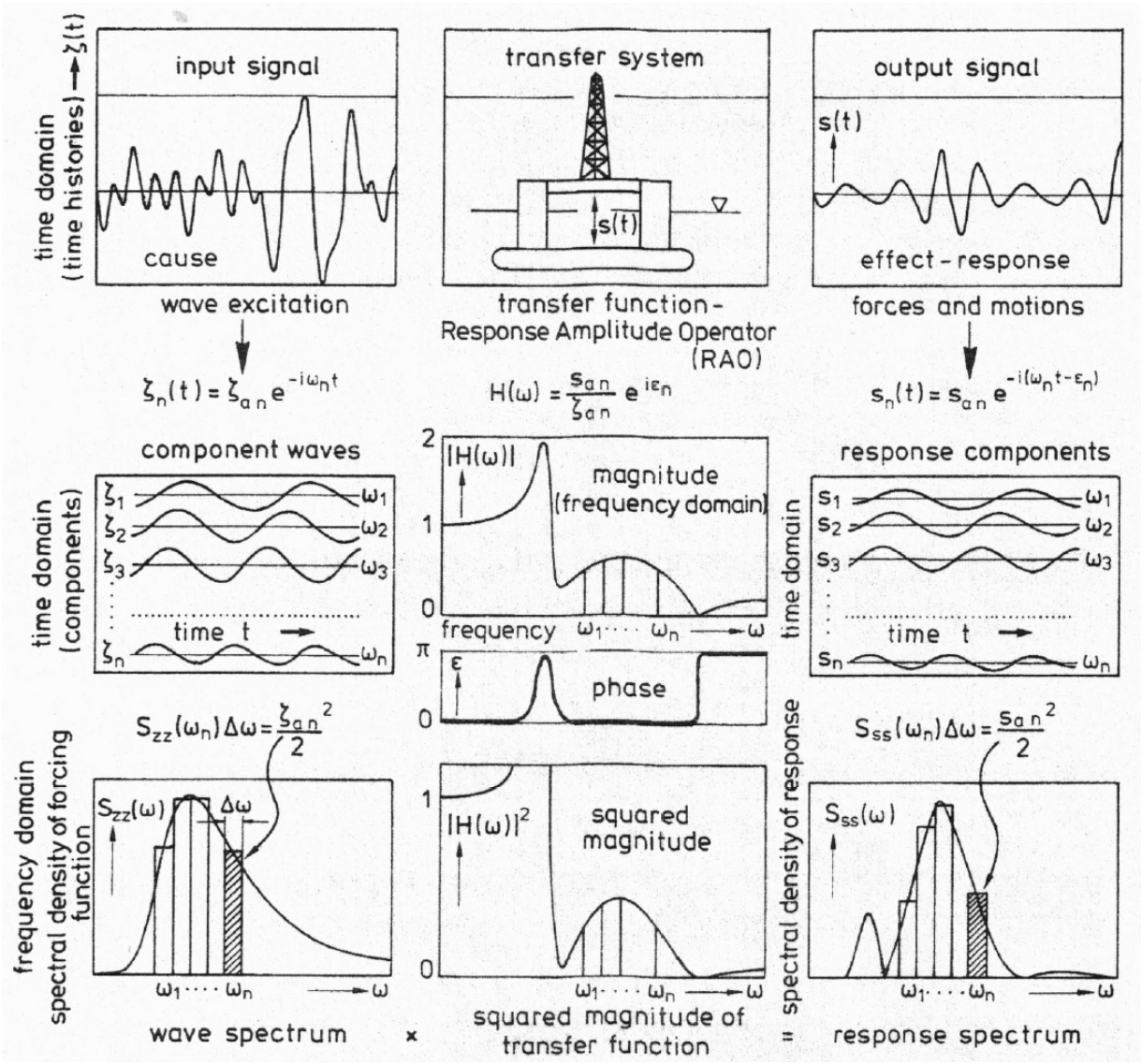

Figure 5.4 – Illustration of how to use RAO's to calculate vessel motions from wave excitation [27, p.36]

5.3 Frequency Domain Analysis

As illustrated in Figure 5.4, the frequency domain analysis uses the wave spectrum and the squared magnitude of the transfer function to generate a response spectrum for the ship. This method requires much less computational power than time domain analysis. However, frequency domain analysis can only be carried out with acceptable results for linear systems. This might make the forces in the tugger wires unpredictable.

The transfer function, $H(\omega)$ is found by setting the forcing function $F_3(t)$ in equation (5.1-1) equal to the harmonic forcing function $F_0 e^{-i\omega t}$ such that the **equation of motion** becomes:

$$M_{33}\ddot{\eta}_3 + B_{33}\dot{\eta}_3 + C_{33}\eta_3 = F_0 e^{-i\omega t} \tag{5.3-1}$$

It should here be noted that the actual wave excitation is given only by the real part of $F_0 e^{-i\omega t}$ and the response is hence only the real part of the complex solution $x(t)$ of the differential equation above [26, p.278].

From equation (5.3-1), the mechanical **transfer function** is found to be [28]:

$$|H(\omega)| = \frac{1}{k[(1-\xi^2)^2+(2r\xi)^2]^{0.5}} \tag{5.3-2}$$

where

k is the stiffness of the system

r is the relative frequency ratio $\left(\frac{\omega}{\omega_0} = \frac{loading\ frequency}{system's\ eigen-frequency}\right)$

ξ is the relative damping $\left(\frac{B_{33}}{2M_{33}\omega_0} = \frac{actual\ damping}{critical\ damping}\right)$

Figure 5.5 shows the **Dynamic Amplification Factor** (DAF) and phase angles as function of frequency ratio. The DAF factor is defined as the dynamic displacement divided by the static displacement [28]:

$$DAF = \frac{(\eta_3|_{max})_{dynamic}}{(\eta_3)_{static}} = \frac{1}{[(1-\xi^2)^2+(2r\xi)^2]^{0.5}} \tag{5.3-3}$$

After establishing the transfer function, the motion of the ship in heave is found by first carrying out a Fourier transform of the loading from the sea. Then the equation of motion is solved using the transfer function and the result is transformed back to the time domain.

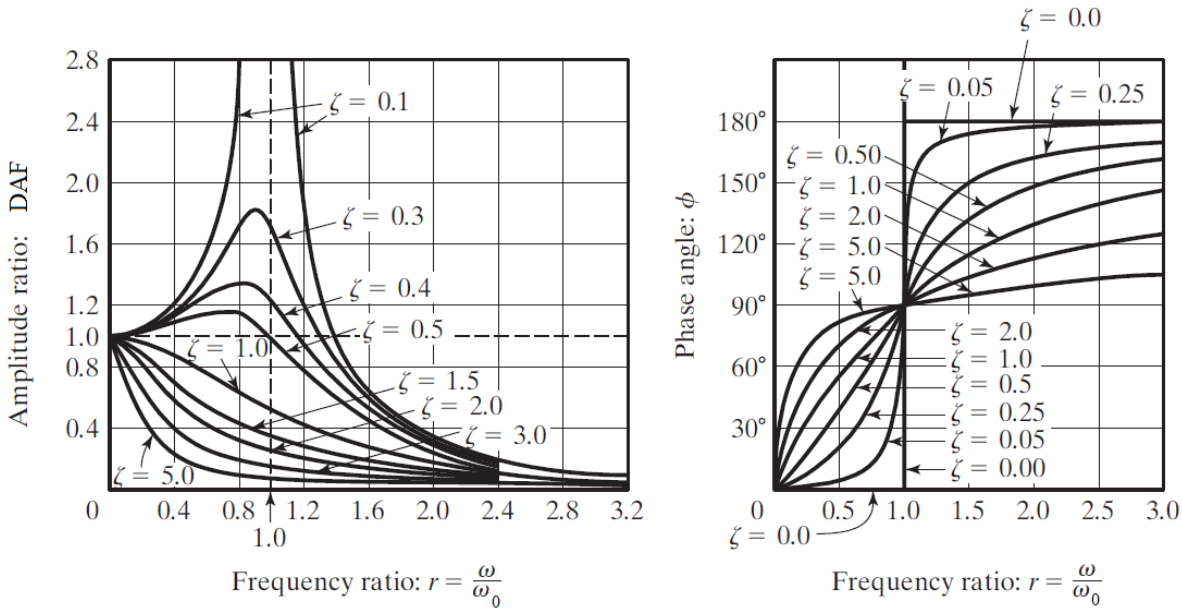

Figure 5.5 – DAF and phase angle as function of frequency ratio

A response spectrum for a vessel is shown in the bottom right corner in Figure 5.4. Here, the wave spectrum is multiplied with the squared magnitude of the transfer function:

$$S_R(\omega) = |H(\omega)|^2 \, S(\omega) \tag{5.3-4}$$

A disadvantage of the response operator approach is that one can only look at the response due to wave frequency excitation. This excludes the effects from wind or slow drift wave excitation [11]. To include all environmental forces in a frequency domain analysis, the spectral response must be developed, and this spectral response is only applicable to the specified environment. This obviously limits the versatility of the frequency response analysis.

5.4 Time Domain Analysis

The connection between frequency- and time domain sea simulation was illustrated in Figure 3.21 in Section 3.6. While frequency domain simulates the sea by a unit amplitude wave with only one wave frequency, the time domain analysis uses a large number of different wave components. Each wave component has its own amplitude and frequency and the superposition of all these waves creates the sea state. The many different wave frequencies enhance the risk for resonances between one wave frequency and one of the systems eigen-frequencies, bearing in mind that resonances not only appear for wave frequencies exactly equal to the eigen-frequency, but also for frequencies close to and even frequencies equal to the eigen-frequency multiplied with an integer ($\omega = n \times \omega_0$ where $n = 1,2,3$ ...). In other words, non-linear systems are best analysed in the time domain.

In time domain analysis, the equation of motion is solved with respect to time for each discrete time interval Δt throughout the whole assigned time period. The discrete time interval is user defined and should at least be lower than the lowest eigenperiod of the system. Solving the equation of motion with respect to time is done by integration methods (default in MOSES is the Newmark method). These integration methods have two fundamental characteristics: They are only valid solutions to the governing differential equations at discrete time intervals Δt apart. And a suitable type of variation of displacement, velocity and acceleration is assumed within each time interval [29].

5.5 Regular Wave Induced Motions

Ship motions during the lift can be described fairly well by linear waves. However, one exception where non-linear effects have to be taken into account is the horizontal slow drift motions. Here, a steady state condition is assumed, meaning there are no transient effects present due to initial conditions [3, p.39].

Now, the hydrodynamic loads on the ship can be calculated by dividing the problem into two sub-problems according to Figure 5.6. And because linearity is assumed, both contributions can be superpositioned together:

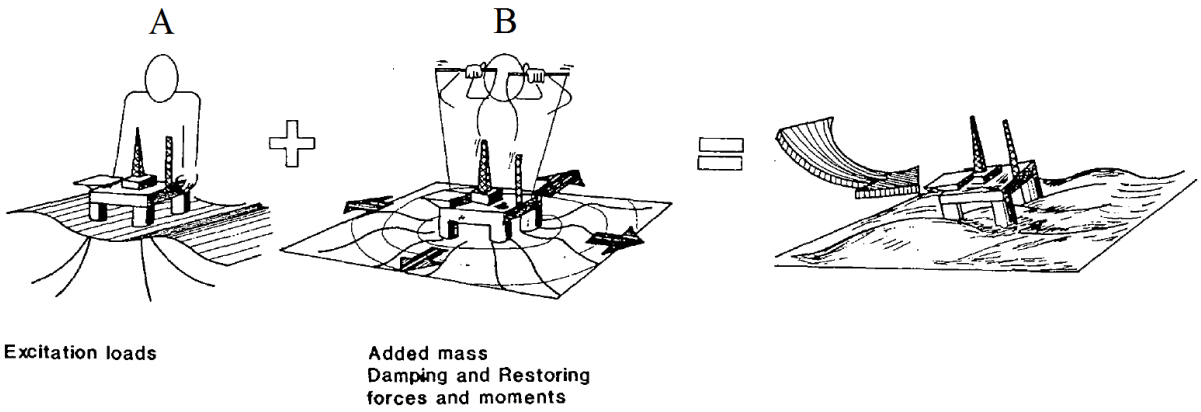

Figure 5.6 – Superposition of wave excitation forces (I) and added mass, damping and restoring forces (II) [3, p.38]

The first sub-problem (A) deals with the forces and moments on the body when the ship is restrained from oscillating and there are incident regular waves. The hydrodynamic loads are called wave excitation loads and composed of so-called Froude-Kriloff and diffraction forces and moments [3, p.39].

The second sub-problem (B) deals with the forces and moments on the body when the ship is forced to oscillate with the wave excitation frequency in any rigid-body motion mode. There are no incident waves. The hydrodynamic loads are identified as added mass, damping and restoring forces [3, p.39].

To describe the motion of a point on the ship, the following formula is used [3, p.41]:

$$\vec{s} = \eta_1\vec{\imath} + \eta_2\vec{\jmath} + \eta_3\vec{k} + \vec{\omega} \times \vec{r} \qquad (5.5\text{-}1)$$

where

$$\vec{\omega} = \eta_4\vec{\imath} + \eta_5\vec{\jmath} + \eta_6\vec{k}$$

$$\vec{r} = x\,\vec{\imath} + y\,\vec{\jmath} + z\,\vec{k}$$

The equation for heave motion becomes:

$$\sum F_3 = M_{33}\,\ddot{\eta}_3 \tag{5.5-2}$$

Similarly to the linear wave surface profile (eq. (3.2-1)), the amplitude of the ship in heave at time, t is:

$$\eta_3 = \eta_{3_0}\,\cos(\omega t + \varepsilon_3) \tag{5.5-3}$$

where

η_{3_0} is the maximum amplitude in heave

ε_3 is the phase angle

5.5.1 Added Mass and Damping

A ship with heave motion in water creates a pressure field in the fluid. The effect of this pressure field can be calculated using the velocity potential, ϕ and the boundary conditions developed in section on boundary conditions. Then the pressure in the fluid is found by using Bernoulli's equation (3.2-16).

Finally, the force in the heave direction is found by excluding the hydrostatic pressure and integrating the remaining pressure over the ship's length, giving the force [3, p.42]:

$$F_3 = -A_{33}\frac{d^2\eta_3}{dt^2} - B_{33}\frac{d\eta_3}{dt} \tag{5.5-4}$$

A_{33} is the **added mass** or the mass of the fluid that is influenced by the motion of the ship in heave. And B_{33} is the before mentioned heave damping. The ship has 6 degrees of freedom which results in the added mass being a 6 by 6 matrix, i.e. there is 36 added mass coefficients and 36 damping coefficients. Another important fact for this report is that these coefficients also are influenced by finite water effects, due to the solution of Laplace's equation in the velocity potential.

5.5.1.1 Strip Theory

Strip theory is a method used to make the two dimensional added mass- and damping coefficients three dimensional. The idea is to divide the ship in around 20 parts, or strips along the longitudinal direction, see Figure 5.7. This theory implies that the variation of the flow in the cross-sectional plane is much larger than the variation of the flow in the longitudinal direction [3, p.50].

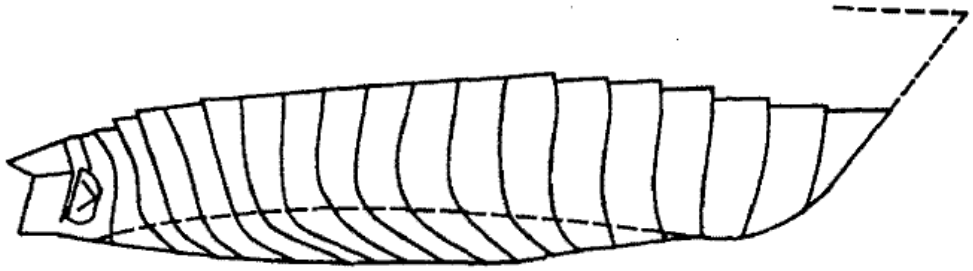

Figure 5.7 – Strip Theory [3, p.50]

Added mass and damping coefficients are calculated for each strip and then combined. These coefficients tend to vary significantly for different ship shapes, and are therefore calculated by numerical methods like source techniques or conformal mapping to get good approximations.

5.5.2 Restoring Forces and Moments

The restoring forces and moments are also calculated by finding coefficients and multiplying with position. These coefficients are found using hydrostatic and mass considerations, and the coefficient for heave is [3, p.58]:

$$F_3 = -C_{33}\eta_3 = -\rho g A_w \eta_3 \qquad (5.5\text{-}5)$$

where

C_{33} is the restoring coefficient

A_w it the ship's waterline area

5.5.3 Excitation Loads

Now, the ship is restrained and subjected to incident waves. The waves create an unsteady fluid pressure which is divided into two effects. First there is a force initiated by the unsteady fluid pressure from the undisturbed waves, called the **Froude-Kriloff force**. When this pressure field hits the ship, a force is initiated so that the previously undisturbed waves pass around the ship hull. This is the second effect called **diffraction forces**.

The diffraction force is found by using the velocity potential together with the boundary condition on the body, and using the fact that the normal derivative of the diffraction velocity potential has to be opposite and of identical magnitude as the normal velocity of the undisturbed wave system [3, p.59].

Faltinsen shows in his book (1993) how to derive an equation including both the Froude-Kriloff force and the diffraction forces for the vertical excitation force of a ship, based upon the wave potential and Bernoulli's equation:

$$\begin{aligned} F_3(t) = & -\iint_{S_B} p_I n_3 \, ds \\ & -\int_L dx \; \omega \, \xi_0 e^{k\, z_{mean}} \{ {A_{33}}^{(2D)} \omega \; \sin(\omega t - kx \; \cos(\beta)) \\ & -{B_{33}}^{(2D)} \cos(\omega t - kx \; \cos(\beta)) \} \end{aligned} \qquad (5.5\text{-}6)$$

where

$p_I = \rho g \xi_0 e^{kz} \sin(\omega_e t - kx \; \cos(\beta) - ky \; \sin(\beta))$

n_3 is a unit vector perpendicular to the vertical axis

S_B is the mean wetted body surface, i.e. the limits for the integral

L is the ship length

z_{mean} is the mean z value for the strip

${A_{33}}^{(2D)}$ is the added mass in heave derived from Strip theory

${B_{33}}^{(2D)}$ is the damping coefficient in heave derived from Strip theory

β is the wave heading

ω_e is the wave encounter frequency

5.5.4 The Ship's Equations of Motion

The coefficients and forcing functions derived in the previous sections can now be inserted into the equation of motion for the ships 6 degrees of freedom:

$$\sum_{k=1}^{6}\left[\left(M_{jk}+A_{jk}\right)\ddot{\eta}_k + B_{jk}\dot{\eta}_k + C_{jk}\eta_k\right] = F_j e^{-i\omega_e t} \qquad (5.5\text{-}7)$$

5.6 Ir-Regular Wave Induced Motions

Ship motions in ir-regular waves are described stochastically by using the transfer function and superposition. The response from adding all the wave components together then becomes [3, p38]:

$$\sum_{i=1}^{\infty} \xi_i |H(\omega_i)| \ \sin(\omega_i t + \delta(\omega_i) + \theta_i) \qquad (5.5\text{-}8)$$

5.7 Dynamic Positioning

The shuttle tanker used in this report has a dynamic positioning system (DP). This system uses thrusters located at the bow and stern to hold the ship in the right position at all times during the operation by the help of a navigation system.

6 Lifting Arrangement

6.1 Transport Phase

The jacket foundations are transported out to the location on a skidding system specifically made to carry them, see Figure 1.3 in Section 1.2. This system has a built in sea fastening system to ensure the safety during transit. Another important feature of this system is that it is able to slide the foundations close to the crane, reducing the crane's reach-out requirements drastically.

6.2 Lift Phase

The lifting arrangement is shown in Figure 6.1. A crane is mounted on the starboard side. And a lifting sling is assembled by four slings connected to a pad eye in each of the top corners on the spreader frame. Further, the four slings are joined into one at a height of 13 meters above the spreader in the jackets centre of gravity with respect to the x-y plane. This is done to obtain an angle of at least 60 degrees measured between a horizontal plane at the top of the spreader and the slings. The slings are made by steel wire with a diameter of 120 mm and an E-module of 65 GPa. Between the spreader frame and the jacket, there are 3 meter steel wires of the same type as the lifting slings.

Two "tugger wires" are connected between the jacket and lifting vessel. The purpose of these wires is to reduce and keep control over the horizontal motions. Both tugger wires are made by steel wires with a diameter of 30 mm and have an E-module of 65 GPa. To restrain the motions even more, they are pre-tensioned to a force of 6 tonne (~60 kN). These tugger lines are disconnected when the jacket is lowered so far that the water dampens the motions.

During the lifting operation the shuttle tanker is ballasted down to a draft of 13 meters, and a dynamic positioning system is used to keep the vessel in the right position. However, for simplicity reasons, the analysis in MOSES is carried out using mooring lines to keep the vessel positioned.

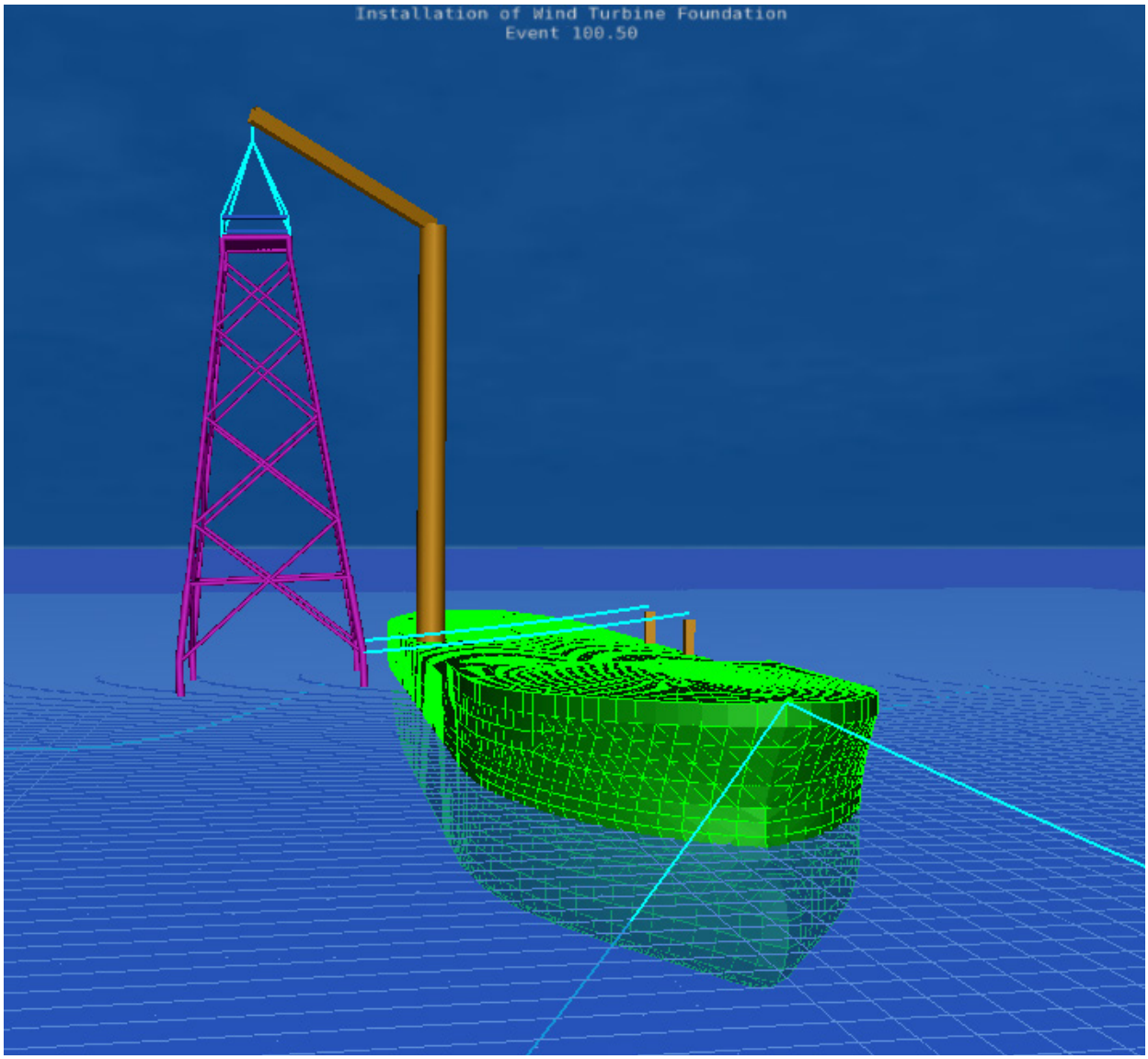

Figure 6.1 - Screen shot from MOSES showing the lifting arrangement

7 Forces on the Jacket during Installation

During the lifting phase the jacket is going through a set of different phases between lift off and touchdown. The phases of concern in this analysis are:

- Lift-Off
- In-air
- Through the Splash Zone
- Close to Sea Bed

Figure 7.1 shows a drawing of the jacket and a more detailed drawing showing the jacket dimensions and profiles are given in **Appendix A**.

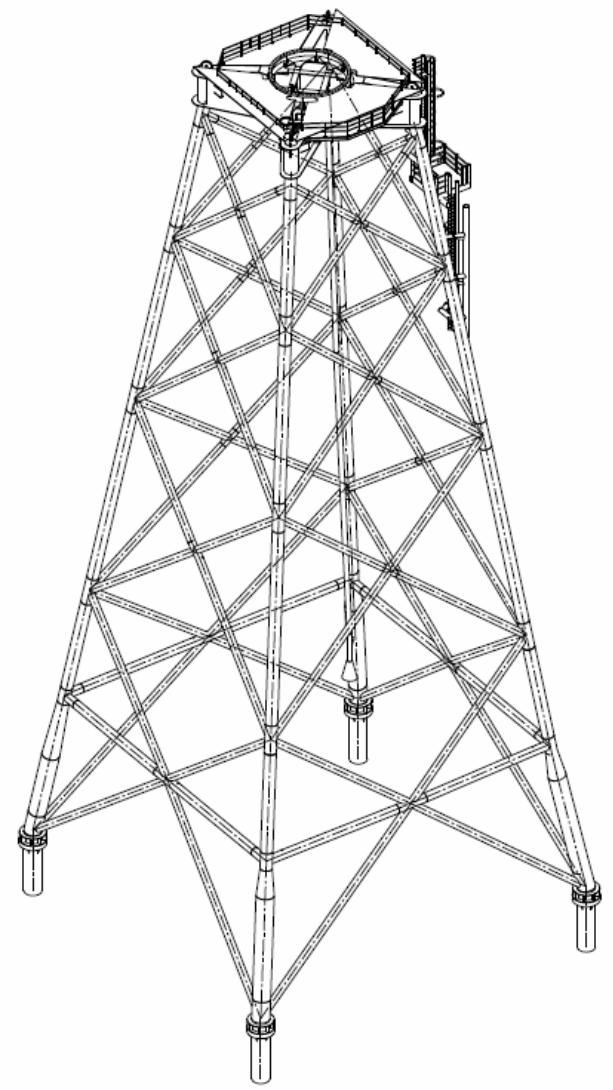

Figure 7.1 – Jacket Drawing provided by Global Maritime

7.1 Lift-Off

Since the transportation and lifting of the jacket is done with one vessel, both jacket and crane tip will have approximately the same motions. This is important information because it drastically reduces the risk of accidental impacts between the jacket and deck due to relative motion, which is a concern when using a dedicated lifting vessel and cargo barge. The lift-off now reduces to making sure that there is sufficient clearance between the jacket and other equipment and personnel. Prior to the lift, all lifting equipment has to be double checked for faults and the sea fastening must be removed.

At lift-off and during the hoisting, the force in the crane tip is written as:

$$F = m\,(g + a) \tag{7.1-1}$$

where

m is the mass of the lifted object

a is the acceleration in the crane wire during hoisting

The a term in the equation is positive when the crane lifts the jacket upwards (against the gravitational force), giving a dynamic load in the crane tip. However, since the upwards hoisting of the jacket only is carried out when it's located vertically above the deck (before the slewing starts), the velocity and accelerations in the crane tip, due to ship motions, are smaller compared to after the slewing is complete and the jacket is hanging over the ship's side. By also adding the fact that the hoisting and slewing speed of the cane is very low, and hence making the a term in the equation above small, the force contribution from equation (7.1-1) is assumed to be smaller compared to the dynamic load initiated by ship motions during the "In-air" phase in Section 7.2.

The ships stability concerns while lifting are covered in the section on Ship Stability.

7.2 In-air

In this report, the "in-air" phase is defined as to when the jacket is hanging in its highest point after it has been lifted off of the deck and the crane slewing is complete, see Figure 7.2.

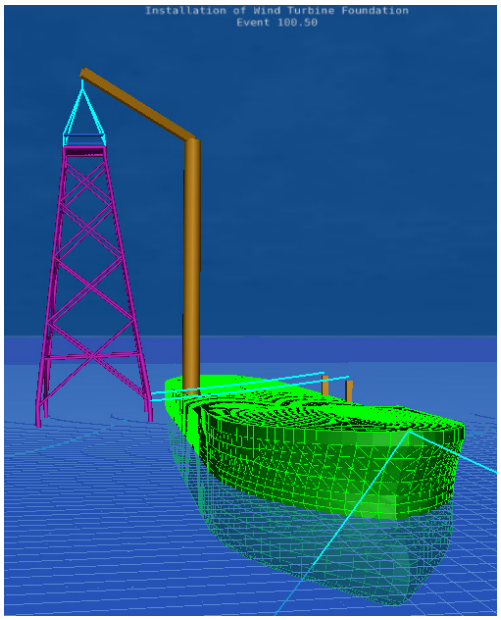

Figure 7.2 – Jacket "in air" position

Environmental forces on the ship initiates motions in the crane tip which are further transferred as dynamic loads in the crane slings and into the jacket. Together with wind loads acting on the jacket, these forces make the jacket oscillate like a pendulum both in the x- and y-direction and a spring-mass system in the z-direction (the coordinate system in Figure 5.1 is used consistently throughout the whole report).

To reduce the horizontal motions of the jacket, two "tugger lines" are connected between the jacket and ship. These are made as long as possible to take advantage of the reduction in stiffness as the length increases ($k = EA/L$). Extensive testing in the computer simulation program MOSES of different angles and heights of the tugger line attachment points on the ship, suggests that the force in the lines is smallest when all angles are zero and the lines are horizontal. In order to reduce the motions even more and at the same time prevent slack in the lines, they have to be pre-tensioned. If the tugger lines were to go slack during the lifting, large snap-loads will appear and cause hazardous events, and even a possibility of fatalities, if a wire or chain breaks.

Characteristic for this phase is the very low damping the jacket is exposed to in the x- and y-directions. Air does not dampen the motions very much compared to water; hence the damping coefficient in the equation of motion is low. Another characteristic of this system is the short crane wire. As the jacket is hanging in this position, the short distance from the jacket to the crane tip results in a very high stiffness in the z-direction.

The forces on the jacket in this position are shown in Figure 7.3. These forces vary both with time and angle of attack as the system starts to move. Wind forces are calculated using the Frøya wind spectrum described in the section on Wind.

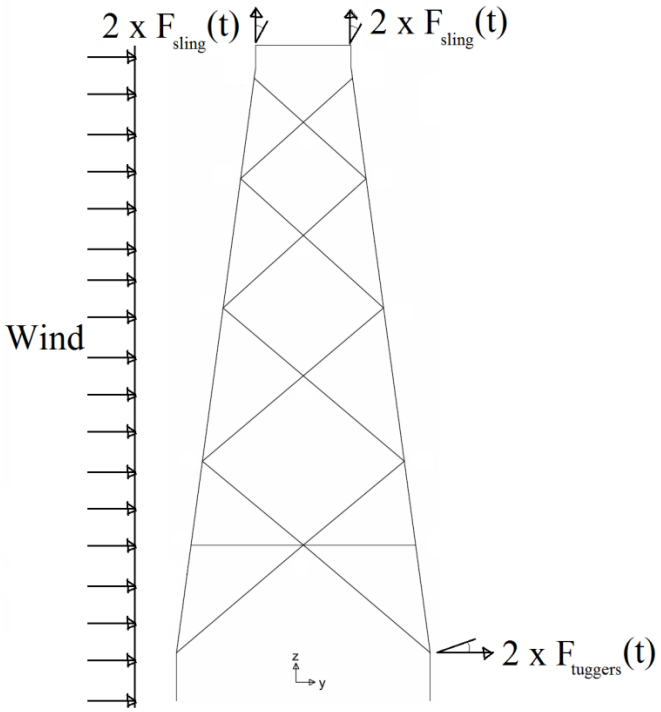

Figure 7.3 – Forces on jacket "in-air"

The system consists of three parts (called bodies in MOSES); the shuttle tanker the jacket and the crane spreader. Every one of them has 6 degrees of freedom, giving the system a total of 18 degrees of freedom. However, simplified analysis is normally carried out saying that the tugger lines eliminate rotations in the lifted object. Applying this to both the jacket and crane spreader, reduces the system to 12 degrees of freedom, see Figure 7.4.

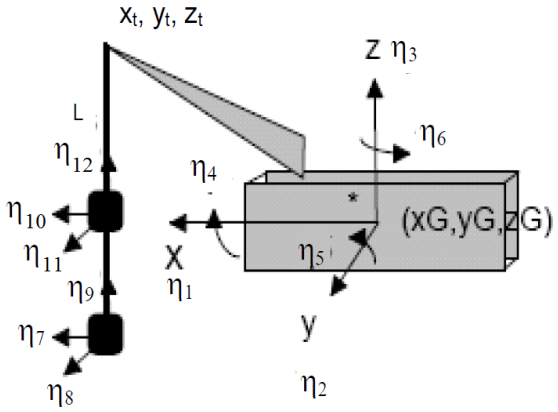

Figure 7.4 – Simplified lifting system [10, p.133 (modified)]

Even after the reduction in degrees of freedom, this is a highly complex system and should therefore be analysed by a numerical computer program such as MOSES. A computer program is also able to analyse all 18 degrees of freedom and the effect of the tugger lines.

7.3 Through the Splash Zone

The "through the splash zone" phase starts when the jacket is lowered down and the bottom end of the jacket begins submerging into the water, see Figure 7.5. At this moment, waves and current start to hit the submerged part of the jacket, and since no water can flow through the walls of the jacket's tube elements, a force is created from the jacket's surface such that the water flows around the jacket's elements. This force has one contribution from steady flow past the elements (current) and one contribution from accelerating flow past the elements (waves). The "new" force compared to the "in-air" phase is the buoyancy force on the jacket.

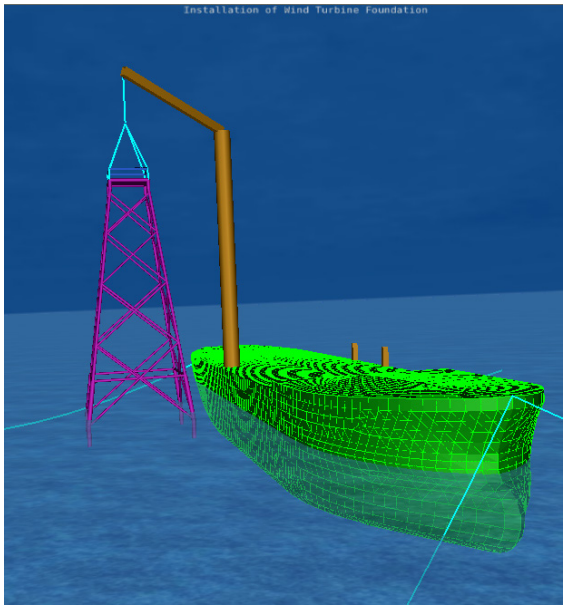

Figure 7.5 – Jacket position when starting on the splash zone phase

Characteristic for this phase is the concern that the above mentioned forces shall become large enough in the vertical direction to create slack in the crane slings. This would cause large snap-loads in the slings and crane structure, which would further develop into a hazardous event if the slings break. However, this might be seen as an unlikely event, since the elements are open and water then floods the whole jacket, giving the structure considerably less buoyancy compared to a subsea template which often is water tight inside. Also, the jacket is tall and narrow causing the buoyancy force to start at a low magnitude and increase slowly compared to the weight of the jacket.

When the jacket has been lowered far enough into the water such that the motions in the horizontal direction are considerably damped due to the water, the tugger lines are disconnected.

The hydrostatic (buoyancy) and hydrodynamic forces are illustrated in Figure 7.6. Each vertical element of the jacket has a buoyancy force, a horizontal and a lift force. For the inclined elements, the lift force is calculated using the projected area, and the horizontal force now gets a normal- and a tangential force component, see Figure 7.7.

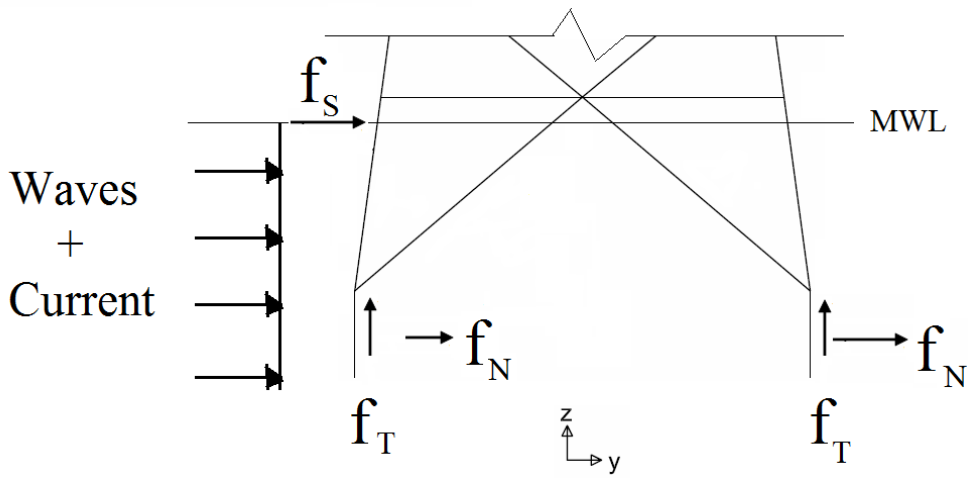

Figure 7.6 – Forces from waves, current and buoyancy, all elements have forces according to Figure 7.7

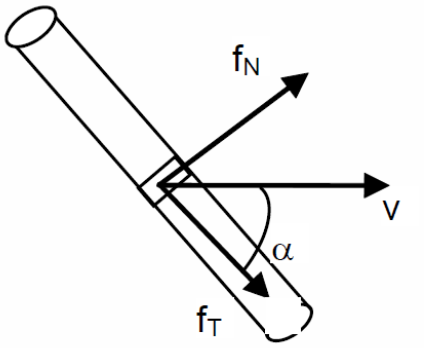

Figure 7.7 – Morison's force on an inclined cylinder [10, p.37]

7.3.1 Hydrostatic Force

The buoyancy force is the weight of the displaced water:

$$F_B = \rho g \sum V_i \qquad (7.3\text{-}1)$$

where

$\sum V_i$ is the volume of all the submerged elements

It should here be noted that the jacket is flooded and V_i is only the volume of the steel for each element.

7.3.2 Slamming Force

The surface crossing element will experience a slamming impact force equal to:

$$f_s = \frac{1}{2}\rho\, C_S\, D\, u\, |u| \qquad (7.3\text{-}2)$$

where

f_s is the unit slamming force

C_S is a theoretical or experimental determined slamming coefficient

D is the diameter of the jacket element

u is the current or water particle velocity

7.3.3 Current Force

A current creates a perpendicular and a parallel force on the submerged jacket elements. These forces are difficult to describe by linear theory due to eddy currents, and is therefore approximated by the empirical formula:

$$f_d = \frac{1}{2}\rho\, C_D\, D\, u|u| \qquad (7.3\text{-}3)$$

where

f_d is the unit force parallel to the current direction, called drag force

C_D is an experimental dimension less coefficient determined from *Reynolds* number and the roughness of the cylinder

To find the total force acting on the jacket, equation (7.3-2) must be calculated for each of the submerged elements and integrated over the length of it.

The force perpendicular to the current direction is called the lift force and is also approximated in the same manner as the drag force:

$$f_L = \frac{1}{2}\rho\, C_L\, D\, u\, |u| \qquad (7.3\text{-}4)$$

where

f_L is the unit force perpendicular to the current direction, called lift force

C_L is an experimental determined dimension less coefficient

7.3.4 Morison's Equation

Wave forces on slender cylinders can be approximated with good results by using Morison's equation. A cylinder is considered as slender if the wave length is at least 5 times the element's diameter. The smallest relevant wave length is found to be ~30 m in Figure 3.14, and **Appendix A** states that the largest diameter of a jacket element is 1.22 m, hence the jacket elements are well within the limit for using Morison's equation.

Morison's equation is based on experiments and assumes that the acceleration is constant over the cylinder [20]:

$$f(z,t) = f_M + f_D = \frac{\pi D^2}{4}\,\rho\, C_M \ddot{u} + \frac{1}{2}\rho\, C_D\, D\, \dot{u}\,|\dot{u}| \qquad (7.3\text{-}5)$$

where

$f(z,t)$ is the force on a unit length of the cylinder

f_M is the mass force

f_D is the drag force

C_M is the mass coefficient (including the hydrodynamic added mass)

C_D is the drag coefficient

It should also be noted that Morison's equation is not valid for breaking waves or cylinders with a larger amplitude than 0.2 times the diameter.

One can determine if it is the drag or the mass force that is dominating by calculating the *Keulegan-Carpenter* number.

The wave force will also give a force in the vertical direction on the inclined elements. Then the Morison's force is decomposed into a normal and a tangential equation according to Figure 7.7.

If waves and currents are acting on the jacket simultaneously, it is normal to add vectorially the wave-induced velocity and the current velocity in the velocity term of the Morison's equation [3, p.226]. The presence of a current will also affect the drag- and mass coefficients.

7.3.5 Total Force on the Submerged Part

The total force on the jacket due to buoyancy and hydrodynamic forces is found by integrating the unit forces for current and waves over the length of the whole element for every element, and then adding the buoyancy force. This force is varying with time and the draft/submergence of the jacket.

7.4 Close to Sea Bed

The “close to sea bed” phase is in this report defined as to be when the jacket is lowered 39 meters from the “in air” phase. Then the jacket then has a bottom clearance of ~3.9 meters in static position.

In this phase, the jacket is exposed to the same hydrostatic and hydrodynamic forces as in the splash zone phase (except for the slamming load). Further characteristic for this phase is the concern that the motions of the whole system will cause impacts between the jacket and sea bottom, or the jacket and ship. The increase in hydrodynamic forces will result in a larger offset from the jacket’s static position vertically below the crane tip. This concern is taken care of by monitoring the jacket’s location during the analysis.

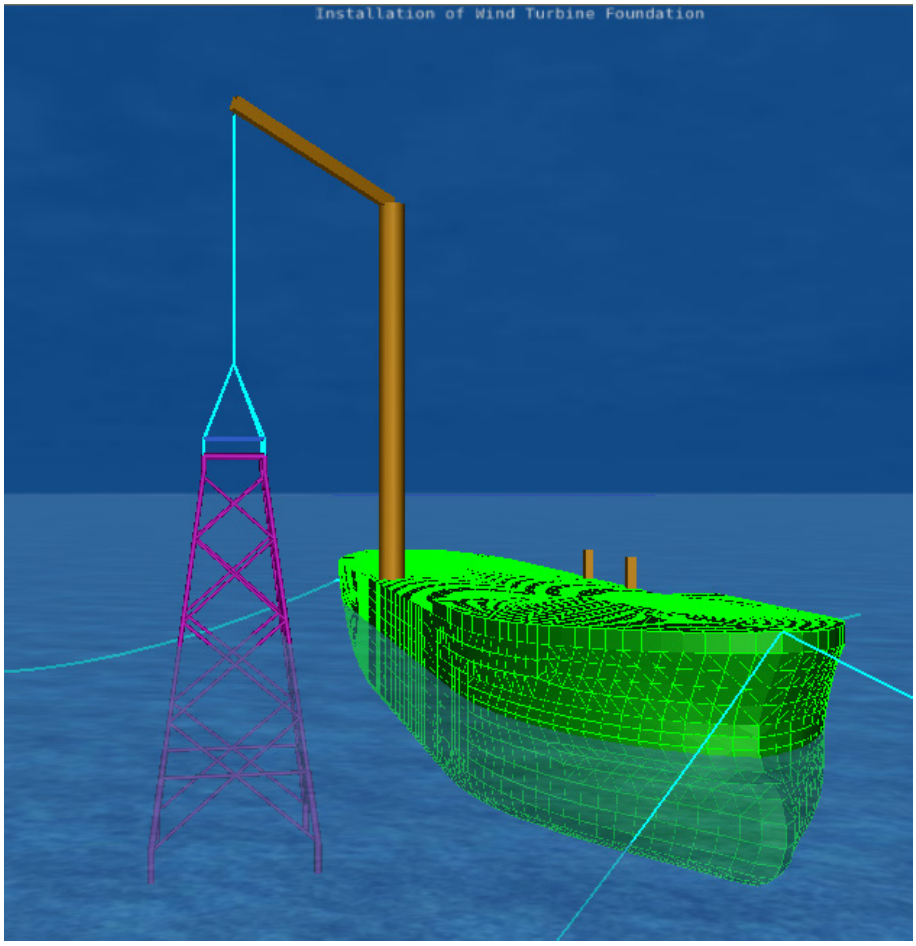

Figure 7.8 – Jacket in “close to sea bed” position

8 MOSES Modelling

8.1 Introduction

MOSES is a computer software developed by Ultramarine, Inc. with the purpose of being able to do a complete analyse of a marine operation within only one software. In other words, MOSES is a computer program capable of modelling, simulating and analysing the stresses which arise in marine situations [11, p.1].

Examples where MOSES is used are:

- Lifting operations
- Load out
- Towing
- Jacket launch
- Pipe laying
- Stress analysis during the operations above

8.2 Analysis Flow

All structures, i.e. the shuttle tanker, jacket and crane spreader is in MOSES called a body. These bodies are made by multiple elements called structural classes. A body can in MOSES be exposed to four different forces; wind, waves, inertia and applied forces. Each of the bodies is in this report analysed as rigid bodies, meaning that they have 6 degrees of freedom and deformation of the bodies is neglected.

The software allows the user to choose between three different hydrodynamic theories to calculate the bodies' interaction with water; Morison's equation, Two Dimensional Diffraction and Three Dimensional Diffraction.

To connect bodies together and transfer forces between them, MOSES employs a set of elements called connectors. There are five different types of connectors; slings, flexible connectors, rigid constraints, pipes and launch ways.

Now that the bodies have been connected, an environment is defined and the simulations can begin. MOSES can perform static, frequency- and time domain analysis. When the simulations are complete, the post-processing menu offers the results as reports, graphs and pictures. If the structural solver is used, the results are given in deflections, reactions and stresses which can be checked against structural standards.

A flowchart of the procedure above is given in Figure 8.1.

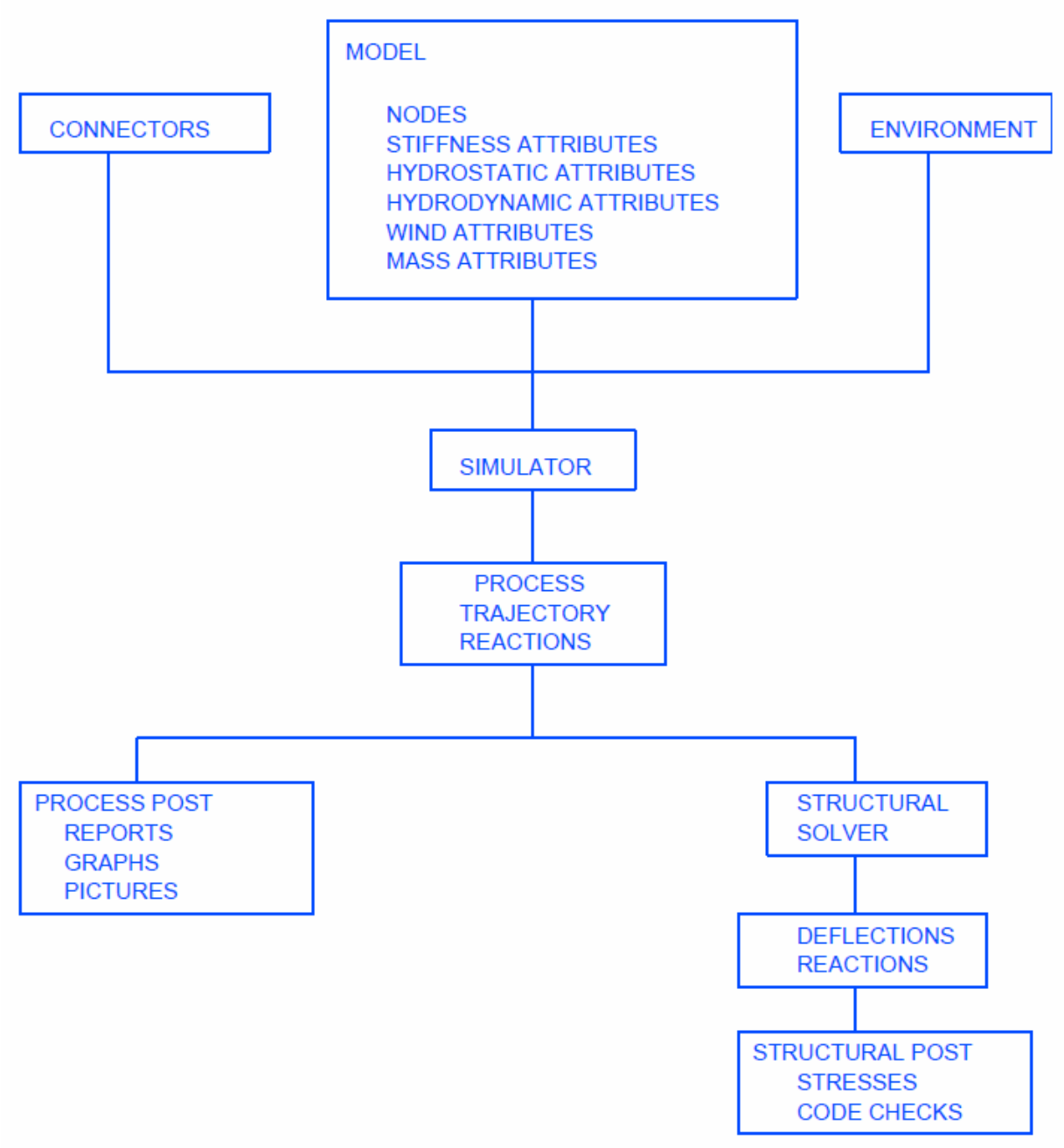

Figure 8.1 – Analysis flow in MOSES [11, p.6]

8.3 Coordinate System and Environmental Headings

MOSES distinguishes between local and global coordinates. It assigns each body its own local coordinate system which is user defined. These bodies are inserted into MOSES' global coordinate system at the desirable position. In the global coordinate system, the vertical axis is always the z-axis with the positive direction pointing upwards, and with Origo placed at the mean water level (MWL), see Figure 8.2.

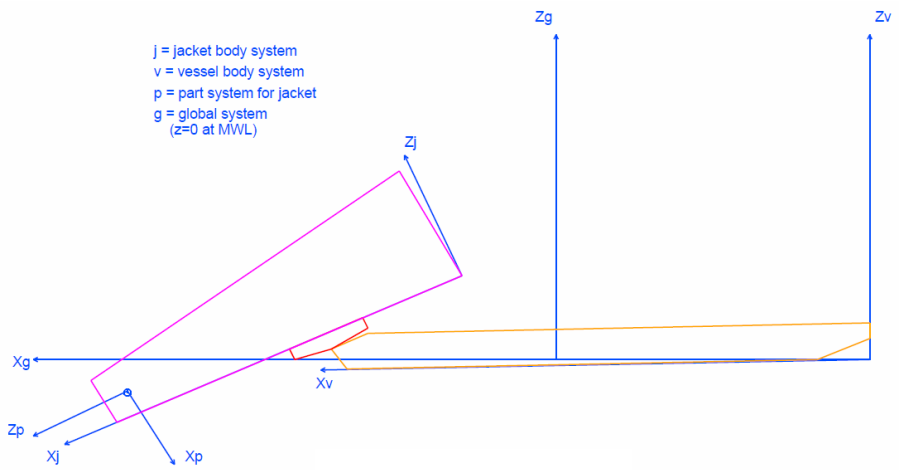

Figure 8.2 – Global- and local coordinate system in MOSES [11, p.174]

Environmental headings are in MOSES defined as shown in Figure 8.3. Here, the vessels local coordinate system is located with the x-axis starting in the bow with positive direction towards the stern. This is exactly opposite of the x-axis previously defined in Figure 5.1 as standard for this report. Head sea has therefore an environmental heading of 0 degrees in this report instead of 180 degrees, which would be normal when using MOSES' notation.

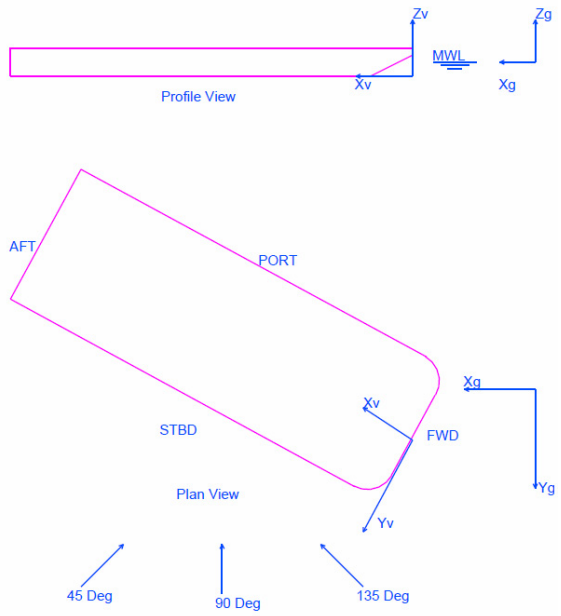

Figure 8.3 - Environmental headings in MOSES [11, p.162]

8.4 Model of the Shuttle Tanker

The model of the shuttle tanker has been created by Global Maritime. First the model was drawn in *Autodesk 3ds Max*, and then it was converted into a file format readable in the *DNV Software; Sesam GeniE*. From this software it is possible to write the model to a text file consisting of only points and plates. This text file is then easily read by MOSES.

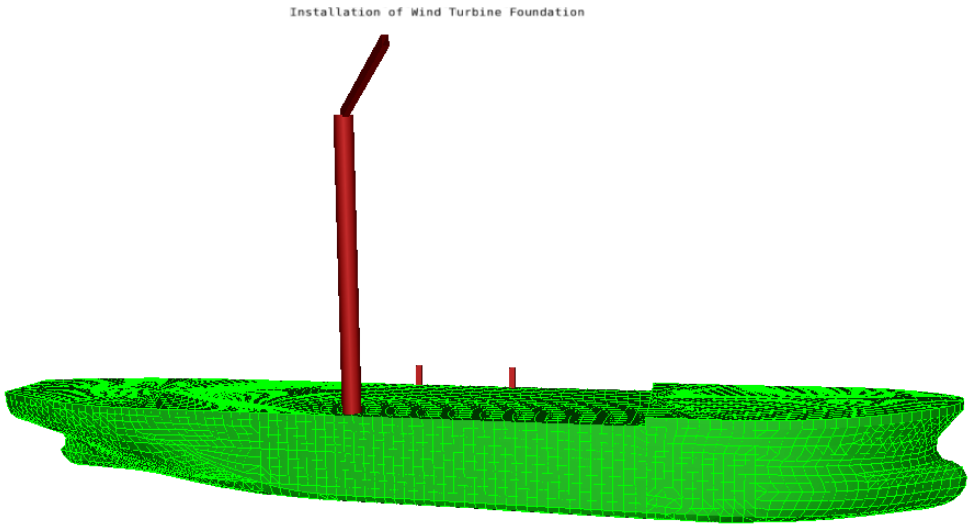

Figure 8.4 - Model of the shuttle tanker in MOSES

This shuttle tanker model is 244 meters long and 42 meters wide, see Figure 8.4. It contains 7215 points used to create hull consisting of 7010 plates and a "virtual crane" consisting of tubes and boxes. The crane is said to be only "virtual" due to the fact that crane tips are in MOSES only defined as a point belonging to a body. Hence the crane is considered to have an infinite stiffness.

The crane is located on the tanker's starboard side 120 meters from the stern, or approximately in the ships longitudinal direction. To allow enough clearance during the whole lifting operation, the crane tip is placed 47 meters from the centre of the ship's beam (negative y-direction) and 103 meters above the ship keel (z-direction), see Table 8.1.

Due to user preferences, the x-axis is zero at the stern and is positive in the forward direction (as shown in Figure 5.1). This is opposite to the MOSES' notation shown in Figure 8.3, resulting in the previously mentioned 180 degrees shift in environmental heading, and making MOSES define starboard as port and port as starboard.

An issue with this model is that there is no information about the tanker's centre of gravity and radii's of gyration. MOSES is therefore set to compute the weight of the tanker based on the assumption that the distance from centre of gravity to the metacentre, $\overline{GM}$ is 3 meters. Also, the pitch and yaw radii of gyration are approximated as 0.25 times the ship length, and the roll radii of gyration is approximated as 0.35 times the beam [3, p.71].

The draft is set to be 13 meters during the operation.

Table 8.1 – Shuttle Tanker Properties

Draft:	13 m
Length:	244 m
Beam:	42 m
Number of Plates:	7010
Crane Tip Position:	x = 120 m y = -47 m z = 103 m
$\overline{GM}$:	3 m
Roll Radii of Gyration:	14.7 m
Pitch Radii of Gyration:	60.7 m
Yaw Radii of Gyration:	60.7 m

8.5 Model of the Crane Spreader Frame

The most efficient method of modelling the crane spreader was chosen to simply write directly into the text file using *Notepad*. For the complete MOSES file, see **Appendix C**.

Only five points are need; one at each of the four corners, and one in Origo of the local coordinate system. All elements in the spreader are built up by the element class called box in the MOSES Manual, i.e. by 500x250x15 mm hollow rectangular elements. Points and elements are connected through a connectivity table. The fifth point in Origo is only used to calculate crane sling distance later on.

A picture of the crane spreader is given in Figure 8.5.

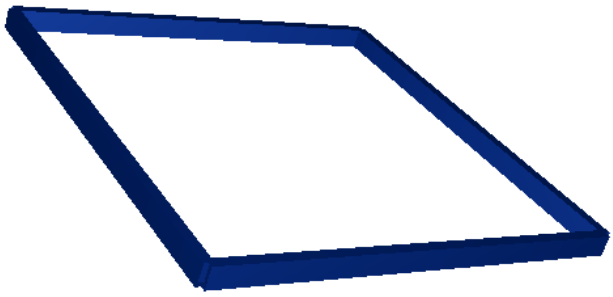

Figure 8.5 – Model of spreader frame in MOSES

8.6 Model of the Jacket Model

The MOSES jacket model was developed with *Microsoft Excel* from the drawings in **Appendix A**. First, all nodes were numbered as shown on the first four pages in **Appendix F**. Then the coordinates of the nodes were calculated by *Excel* using only the coordinates of the top plate, the heights h1 to h8 and the slope. At last *Excel* was set up in such a manner that the points and connectivity was written in MOSES notation and could easily be copied into a text file. The complete "jacket.dat" file is provided in **Appendix D**.

A picture of the jacket model is shown in Figure 8.6. Note that there is a plate on the top of it. This is a 135 mm thick steel plate made to account for the weight of 105.6 tonne of equipment used to connect the jacket to the wind turbine, and being able to carry out inspections and maintenance on the wind turbine. See **Appendix G** for thickness calculation and **Appendix A** for drawing of the top. The total weight of the jacket is calculated by MOSES.

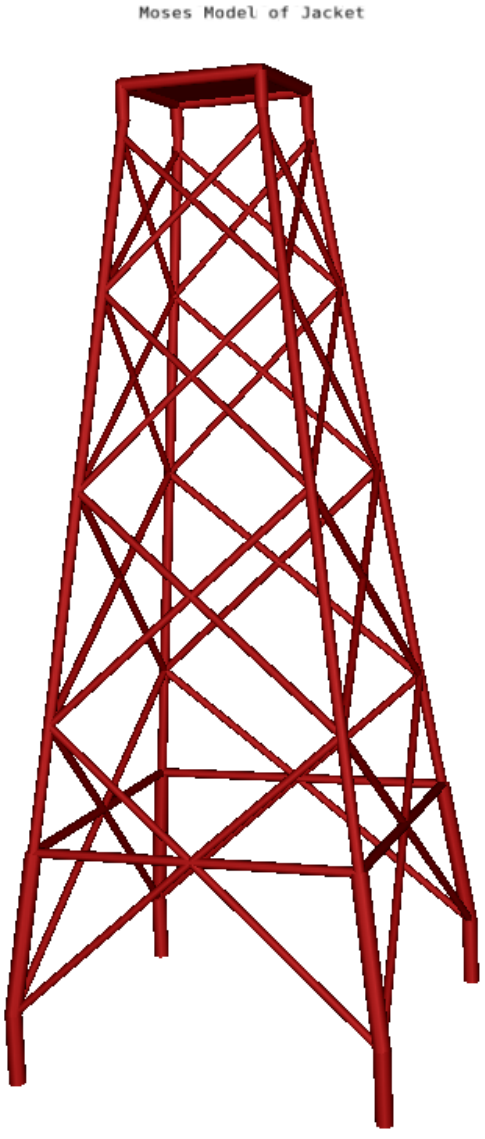

Figure 8.6 - Model of the jacket in MOSES

8.7 The Complete System in MOSES

All the bodies are now inserted into a global coordinate system. For basic parameters in MOSES, see Table 8.2:

Table 8.2 – Basic MOSES parameters

Dimensions: - Length: - Force:	 Meters Metric tons (tonne)
Water depth:	40 meters
Diftyp:	3D diffraction
Flood jacket:	Yes
Roll damping:	Tanaka

The modelling begins by inserting the shuttle tanker at the coordinates x=0, y=0 and z= -13, giving the body a draft of 13 meters. Then a "dummy" weight equivalent to the jacket weight is applied in the crane tip. This weight is only used to make sure that the tanker has no initial heel angle after MOSES has computed its weight.

Now that the tanker has been placed in the right position, the jacket is inserted directly below the crane tip point with the crane spreader 3 meters above the jacket. The crane spreader is then connected to the jacket with four flexible connectors from the "h_cat" class in MOSES. Further, the crane slings connecting the crane tip to the crane spreader is created by the "t-h_definition" command. This command is specifically made for the purpose of dividing a sling from the crane tip into 2-4 slings connected to a pad eye, and the only allowed flexible connector class for using this command is "sling". Afterwards, the command "&instate –sl_set" should be used to make sure there is no initial slack in the slings.

The tugger lines are modelled in the same way as the connectors between the crane spreader and jacket. Only here, the option "exact" is activated. This option instructs MOSES to also take into account the weight of the connector. The reason for this is discussed in Section 8.8. To avoid snap loads, the tugger lines are pre-tensioned by simply reducing the lines by 4 meters.

Mooring lines are used to keep the tanker in place, since MOSES does not have the option to simulate a dynamic positioning system. These lines are modelled with the "b_cat" class including the "-depanchor" and "-anchor" options. To obtain the catenary geometry of a mooring line, the lines are pre-tensioned to 80 tonne.

At last, the whole system is ready to start simulating after being moved into equilibrium with the "&equi" command.

This whole procedure is programmed into MOSES as shown in **Appendix E**. And the complete system is previously shown for the three phases in Figure 7.2, Figure 7.5 and Figure 7.8.

Three-dimensional diffraction is chosen to calculate the hydrodynamic forces on the basis of recommendations in the MOSES Reference Manual.

8.8 Modelling Concerns

8.8.1 Interpretation Errors

MOSES seldom reports modelling errors, and it is therefore utmost important that the user utilize commands like "&status" to manually check if the software has interpret all inputs correctly. Some variables that must be checked and evaluated are the buoyancy, weight, draft and radii of gyration of all the bodies, the tip-hook properties and the connector forces and their geometry.

8.8.2 Mooring Lines

Mooring lines must be used with caution in this analysis because of the relatively small water depth. Small water depths force the mooring lines to touchdown on the sea bed close to the moored structure. The result is a high stiffness and a low ability to move around without initiating snap loads in the mooring lines. These snap loads during the MOSES simulations are highly unwanted because they don't represent a realistic situation for a tanker kept in place with dynamic positioning.

8.8.3 Numerical Issues

The numerical methods in MOSES are believed to cause issues for simulating certain lifting operations involving crane spreaders. This is experienced when trying to move the jacket into equilibrium before the simulation starts. MOSES is not able to move it into equilibrium after 51 iterations with the crane spreader activated, although equilibrium is easily obtained without the crane spreader. However, this issue is seen acceptable after a review of all the connector forces and the position of both crane spreader and jacket.

8.8.4 Connector Instability

The tugger lines were found guilty of causing "instability crashes" during the simulations. This issue was solved by instructing MOSES to also consider the weight of the tugger lines with the "exact" command for this connector.

9 Analysis

9.1 Introduction

As mentioned in the study objectives, the main interest in this analysis is the dynamic amplification factor in the crane sling during installation. This means that the shuttle tanker is located at the installation site, and the analysing begins after the sea fastening is removed. The lifting is modelled and simulated using MOSES.

Three phases are considered as sufficient to cover the range of different forces on the jacket; the in-air-, through splash zone- and close to sea bed phase.

The parameters initially given for this operation are given in Table 9.1:

Table 9.1 – Initial parameters

Lifting vessel:	Converted shuttle tanker
Location:	North Sea
Water depth:	40 meters
Lifted Structure:	Jacket given in **Appendix A**
Weather window:	Preferably 1-2 days

9.2 Method

The analysis begins with investigating how the water depths of only 40 meters influences the motion characteristics of the shuttle tanker, compared to infinite water depths. According to the water particle motion theory in Section 3.2.1.7, the shuttle tanker should be affected by the water particles interaction with the sea bottom.

JONSWAP sea spectrum is used, and the ten spectral peak periods shown in Table 9.2 are derived from the guidelines in DNV-OS-H101, Sec.3 C 803 and DNV-RP-C205 3.5.3. The complete calculations are shown in **Appendix G**. DNV-RP-C205 3.5.8.6 states that a typical value for the spreading constant, n in equation (3.5-17) is in the range of 2 to 4. Numerous short simulations in MOSES have determined that worst case for this operation is when n=4. Furthermore, the wave height is too low for the wave to break (see Figure 3.15) and no swells are assumed present in the area. Also current is assumed to be of a negligible magnitude on the jacket and the tankers DP system will balance out the effect it.

The relationship between wind speeds and significant wave height for wind seas is shown in Table 3.7. And the wind speed is for this operation set to have a mean value of 24.5 knots (or 12.6 m/s). Wind loads are calculated by the Frøya wind spectrum given in Section 3.7. Worst case wind direction is assumed to be in the same direction as the wave heading. Squalls are considered as not present in this area.

Table 9.2 – JONSWAP spectral peak periods

H_s [m]	T_z [s]	γ [-]	T_p [s]	T_m [s]
3.0	4.92	3.84	6.4	4.9
3.0	5.82	1.72	8.1	6.3
3.0	6.72	1.00	9.5	7.3
3.0	7.61	1.00	10.8	8.3
3.0	8.51	1.00	12.1	9.3
3.0	9.41	1.00	13.4	10.3
3.0	10.31	1.00	14.6	11.3
3.0	11.20	1.00	15.9	12.3
3.0	12.10	1.00	17.2	13.3
3.0	13.00	1.00	18.4	14.2

H_s [m]	T_z [s]	γ [-]	T_p [s]	T_m [s]
3.5	5.32	3.84	6.9	5.3
3.5	6.17	1.89	8.5	6.6
3.5	7.02	1.00	10.0	7.7
3.5	7.88	1.00	11.2	8.6
3.5	8.73	1.00	12.4	9.6
3.5	9.58	1.00	13.6	10.5
3.5	10.44	1.00	14.8	11.4
3.5	11.29	1.00	16.0	12.3
3.5	12.15	1.00	17.2	13.3
3.5	13.00	1.00	18.4	14.2

Then the marine operation is analysed for the three phases using time domain analysis. A significant wave height of 3 meters is assumed as a good starting point. The simulations are carried out for a length of 20 minutes, and then the results are statistically extended to be the predicted maximum value for a 3-hour period. A time increment of 0.25 seconds is considered to be satisfyingly low due to the fact that it is smaller than the following simplified calculation of the jacket's eigenperiods:

Eigenperiod in x- and y-direction (pendulum):

$$T_{0_{x=y}} = 2\pi\sqrt{\frac{l}{g}} = 2\pi\sqrt{\frac{15m}{9.81ms^{-2}}} = 7.8\ sec \qquad (10.2\text{-}1)$$

Eigenperiod of jacket in z-direction (spring-mass system):

$$T_{0_z} = 2\pi\sqrt{\frac{m}{k}} = \sqrt{\frac{515\,000\ kg}{\frac{65\ GPa*\pi\ 60mm^2}{15m}}} = 0.64\ sec \qquad (10.2\text{-}2)$$

The Newmark method is used in MOSES to integrate the equations of motion.

All analyses are carried out for the environmental headings; 0, 22.5, 45, 67.5, 90, 112.5, 135, 157.5 and 180 degrees. Headings from 180 to 360 degrees are not needed due to the symmetry of the tanker.

Due to the enormous amount of calculations needed to run time domain analysis, only the 3 m significant wave height is analysed in the time domain. Also, the "splash zone" phase is analysed only when the jacket is submerged 6 meters. Ideally the jacket should be analysed in multiple positions through the splash zone. This is not done purely because of time limitations. As an example, if one were to analyse a 10 meter lowering in steps of 0.5 m, the time needed would be $\sim 6500\ sec.per\ period\ \times 10\ periods\ \times 9\ headings \times 20\ steps = 135\ days$, when using a computer with a single core Pentium 3 GHz processor.

To compensate for the somewhat short simulation time in the splash zone, this phase is also analysed using the simplified method in DNV-RP-H103 Section 4.

After the analysis has been completed for $H_s = 3m$ in the time domain, a frequency domain analysis is carried out with the exact same parameters. This makes it possible to compare the results from the two different analysing methods. Also, frequency domain analysis is carried out for $H_s = 3.5m$.

10 Results

All units in this section are degrees, meters and metric tons (tonne).

10.1 Weight, Buoyancy and Hydrostatic Parameters of the Involved Bodies

Prior to the start of the simulations in both time- and frequency domain, the program MOSES is asked to provide information on how it has interpreted the inputs from Chapter 8.

10.1.1 Shuttle Tanker

The shuttle tanker was given an initial condition with a draft of 13 meters, $\overline{GM}$ was assumed to be 3 meters and the radii's of gyration was approximated using suggestions from Faltinsen's book, see reference [3]. Results from MOSES showing the shuttle tankers weight, buoyancy and hydrostatic parameters are shown in Table 10.1, Table 10.2, Table 10.3 and Table 10.4. The main purpose of these tables is to check that MOSES has computed the tanker's weight correctly and given it the correct initial condition in the global coordinate system.

Table 10.1 – Shuttle tanker MOSES outputs for all phases

Draft:	13.01
Roll Angle: - In air - Splash zone - Close to sea bed	 0.23 0.00 0.02
Pitch Angle:	0.00
Radii of Gyration about C.o.G: - K-X - K-Y - K-Z	 15.07 60.69 60.62
$\overline{GM}$	2.99

Table 10.2 – Shuttle tanker weight and buoyancy for the in air phase

		Centre of Gravity		
		x	y	z
Displacement	105 192.46	125.30	0.23	15.11
Buoyancy	105 842.76	125.27	0.05	6.77

Table 10.3 - Shuttle tanker weight and buoyancy for the splash zone phase

		Centre of Gravity		
		x	y	z
Displacement	105 196.45	125.30	0.23	15.11
Buoyancy	105 842.27	125.27	0.00	6.77

Table 10.4 - Shuttle tanker weight and buoyancy for the close to sea bed phase

		Centre of Gravity		
		x	y	z
Displacement	105 224.45	125.30	0.22	15.11
Buoyancy	105 844.16	125.27	0.00	6.77

Note: The shuttle tankers local coordinate system is equal to the global

10.1.2 Jacket

MOSES has located the jacket according to Table 10.5, Table 10.6, Table 10.7 and Table 10.8 for the three analysed phases. The jacket is seen to have an initial roll angle in the in-air phase as a direct result of the pre-tensioning in the tugger lines. Further, it is confirmed that there is no buoyancy on the jacket in the in-air phase, small buoyancy in the splash zone phase and large buoyancy during the close to sea bed phase.

Table 10.5 – Jacket MOSES outputs for all phases

Roll Angle: - In air - Splash zone - Close to sea bed	 2.60 0.00 0.00
Pitch Angle:	0.00

Table 10.6 – Jacket weight and buoyancy for the in air phase

		Centre of Gravity		
		x	y	z
Weight	514.86	0.00	0.00	-27.91
Buoyancy	0.00	0.00	0.00	0.00

Table 10.7 - Jacket weight and buoyancy for the splash zone phase

		Centre of Gravity		
		x	y	z
Weight	514.86	0.00	0.00	-27.91
Buoyancy	3.59	0.00	0.00	-65.38

Table 10.8 - Jacket weight and buoyancy for the close to sea bed phase

		Centre of Gravity		
		x	y	z
Weight	514.86	0.00	0.00	-27.91
Buoyancy	29.48	0.00	0.00	-51.77

Note: The coordinates above is in the jacket's local coordinate system. To convert them into global coordinates, the x- and y-coordinate must be added together with 120 and -47, respectively. Also, the z-coordinate must be added together with 72.07, 61.71, and 32.31 for the in air-, splash zone- and close to sea bed phase, respectively.

10.1.3 Crane Spreader

The crane spreader is also confirmed to be located at the correct starting position 3 meters above the jacket, see Table 10.9, Table 10.10, Table 10.11 and Table 10.12. Just like the jacket, it has a small roll angle in the first phase. Also, there is no buoyancy force on the crane spreader in any of the phases.

Table 10.9 – Crane Spreader MOSES outputs for all phases

Roll Angle: - In air - Splash zone - Close to sea bed	 2.59 0.00 0.00
Pitch Angle:	0.00

Table 10.10 – Crane Spreader weight and buoyancy for the in air phase

		Centre of Gravity		
		x	y	z
Weight	6.78	0.00	0.00	0.00
Buoyancy	0.00	0.00	0.00	0.00

Table 10.11 - Crane Spreader weight and buoyancy for the splash zone phase

		Centre of Gravity		
		x	y	z
Weight	6.78	0.00	0.00	0.00
Buoyancy	0.00	0.00	0.00	0.00

Table 10.12 - Crane Spreader weight and buoyancy for the close to sea bed phase

		Centre of Gravity		
		x	y	z
Weight	6.78	0.00	0.00	0.00
Buoyancy	0.00	0.00	0.00	0.00

Note: The coordinates above is in the crane spreader's local coordinate system. To convert them into global coordinates, the x- and y- coordinate must be added together with 120 and -47, respectively. Also, the z-coordinate must be added together with 75.07, 64.71, and 35.31 for the in air-, splash zone- and close to sea bed phase, respectively.

10.2 Static Connector Forces

After MOSES has confirmed that all bodies are in the correct initial condition, all the connector forces between the bodies must be assessed. Static connector forces are here defined as the forces in the connectors prior to the simulations, hence no motions and static equilibrium. Results from MOSES for the three phases are shown in Table 10.13, Table 10.14 and Table 10.15. The total force or magnitude in a connector is calculated by the equation:

$$Mag. = \sqrt{FX^2 + FY^2 + FZ^2} \qquad (10.2\text{-}1)$$

Table 10.13 – Static connector forces for the in-air phase

Connector	Connecting Bodies	FX	FY	FZ	Mag.
Crane Sling (Wire)	Tanker - (Hook)*	0.0	14.6	-520.6	521
Crane Sling 1	(Hook)* - Spreader	52.8	52.8	137.4	156
Crane Sling 2	(Hook)* - Spreader	-52.8	52.8	137.4	156
Crane Sling 3	(Hook)* - Spreader	-47.3	-47.3	122.9	140
Crane Sling 4	(Hook)* - Spreader	47.3	-47.3	123.0	140
Spreader Sling 1	Spreader - Jacket	0.0	-2.9	-135.8	136
Spreader Sling 2	Spreader - Jacket	0.0	-2.9	-135.7	136
Spreader Sling 3	Spreader - Jacket	0.0	-2.6	-121.2	121
Spreader Sling 4	Spreader - Jacket	0.0	-2.6	-121.3	121
Tugger Line 1	Tanker - Jacket	0.0	-6.2	-0.9	6
Tugger Line 2	Tanker - Jacket	0.0	-6.2	-0.9	6
Mooring Line 1	Tanker	51.9	52.1	-32.3	80
Mooring Line 2	Tanker	-52.0	52.1	-31.1	80
Mooring Line 3	Tanker	-52.0	-51.8	-31.6	80
Mooring Line 4	Tanker	51.1	-51.8	-32.7	80

*) The (Hook) is not really a body, the term is only used to differentiate the sling that goes to the tanker (crane tip) with the ones that goes to the crane spreader

The first connector in Table 10.13 is the crane wire connected to the crane tip. This connector has the expected magnitude equal to the weight of the jacket and crane spreader (514.86 + 6.78 = 521.64). The crane wire is divided into the next four crane slings in the table above. Summing the forces for these four connectors in the x-direction yields the expected value of zero. The forces in the y-direction are a bit more complex as both jacket and crane spreader are rotated, the weight of the tugger lines apply and the slings must also counteract the force from the tugger lines. However, they all seem to have a realistic magnitude. Four spreader slings are connecting the crane spreader to the jacket. All these has zero force in the x-direction (the reason they are there), and a small force in the y-direction due to the rotation. Furthermore, the tugger lines are seen to have the desired magnitude.

All mooring lines in these three tables have equal magnitude, and balance each other when calculating the resulting force from them.

Table 10.14 – Static connector forces for the splash zone phase

Connector	Connecting Bodies	FX	FY	FZ	Mag.
Crane Sling (Wire)	Tanker - (Hook)*	0.0	0.0	-518.0	518
Crane Sling 1	(Hook)* - Spreader	49.8	49.8	129.5	147
Crane Sling 2	(Hook)* - Spreader	-49.8	49.8	129.5	147
Crane Sling 3	(Hook)* - Spreader	-49.8	-49.8	129.5	147
Crane Sling 4	(Hook)* - Spreader	49.8	-49.8	129.5	147
Spreader Sling 1	Spreader - Jacket	0.0	0.0	-127.9	128
Spreader Sling 2	Spreader - Jacket	0.0	0.0	-127.9	128
Spreader Sling 3	Spreader - Jacket	0.0	0.0	-127.9	128
Spreader Sling 4	Spreader - Jacket	0.0	0.0	-127.9	128
Mooring Line 1	Tanker	51.9	51.9	-32.5	80
Mooring Line 2	Tanker	-52.0	52.0	-31.3	80
Mooring Line 3	Tanker	-52.0	-52.0	-31.3	80
Mooring Line 4	Tanker	51.9	-51.9	-32.5	80

*) The (Hook) is not really a body, it's only used to differentiate the sling that goes to the tanker (crane tip) with the ones that goes to the crane spreader

All connectors in the splash zone- and the sea bed phase (Table 10.14 and Table 10.15, respectively) are considered to have the correct values. It should be noted that the crane wire forces of 518 and 492 tonne is equal to the weight of the jacket and crane spreader minus the buoyancy of 3.59 and 29.48 tonne, respectively.

Table 10.15 – Static connector forces for the close to sea bed phase

Connector	Connecting Bodies	FX	FY	FZ	Mag.
Crane Sling (Wire)	Tanker - (Hook)*	0.0	-0.2	-492.2	492
Crane Sling 1	(Hook)* - Spreader	47.3	47.3	123.0	140
Crane Sling 2	(Hook)* - Spreader	-47.3	47.3	123.0	140
Crane Sling 3	(Hook)* - Spreader	-47.3	-47.3	123.0	140
Crane Sling 4	(Hook)* - Spreader	47.3	-47.3	123.0	140
Spreader Sling 1	Spreader - Jacket	0.0	0.0	-135.8	121
Spreader Sling 2	Spreader - Jacket	0.0	0.0	-135.7	121
Spreader Sling 3	Spreader - Jacket	0.0	0.0	-121.2	121
Spreader Sling 4	Spreader - Jacket	0.0	0.0	-121.3	121
Mooring Line 1	Tanker	51.9	51.9	-32.5	80
Mooring Line 2	Tanker	-52.0	51.9	-31.4	80
Mooring Line 3	Tanker	-52.0	-52.0	-31.3	80
Mooring Line 4	Tanker	51.9	-52.0	-32.5	80

*) The (Hook) is not really a body, it's only used to differentiate the sling that goes to the tanker (crane tip) with the ones that goes to the crane spreader

10.3 Finite Water Depth Effects

This section contains comparisons of the shuttle tankers RAO's for infinite water depth and 40 meters water depth. Figure 10.1, Figure 10.2 and Figure 10.3 show the motion comparisons for heave, pitch and surge in head sea. And Figure 10.4, Figure 10.5 and Figure 10.6 show the motion comparisons for heave, roll and sway.

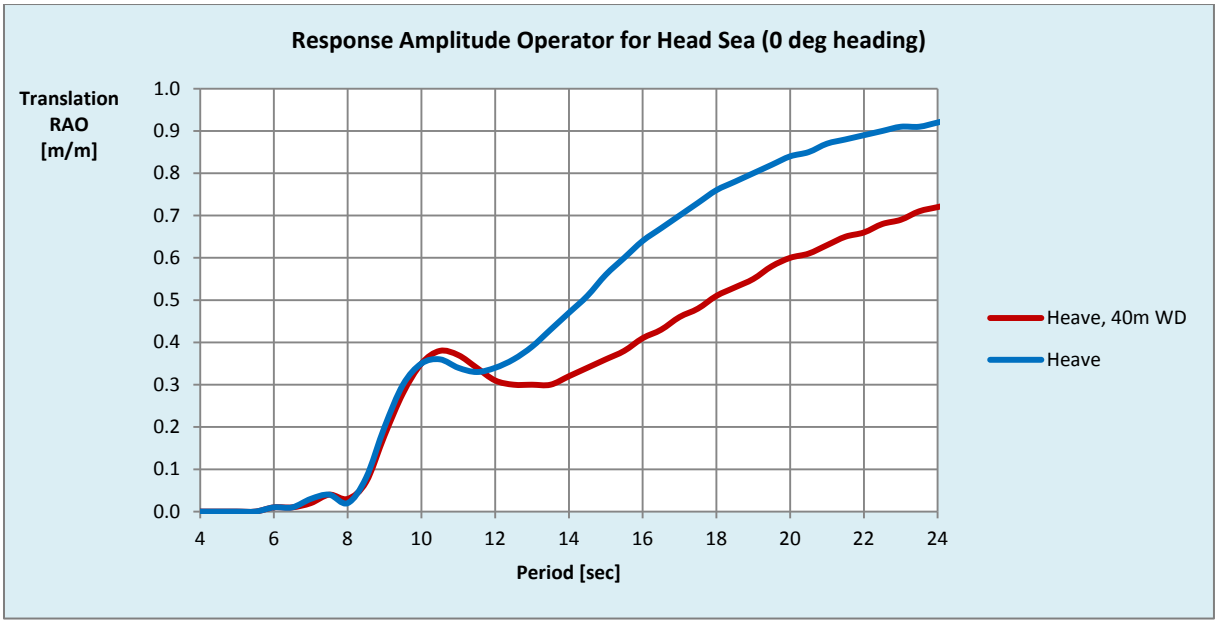

Figure 10.1 - RAO comparison in heave for two water depths in head sea

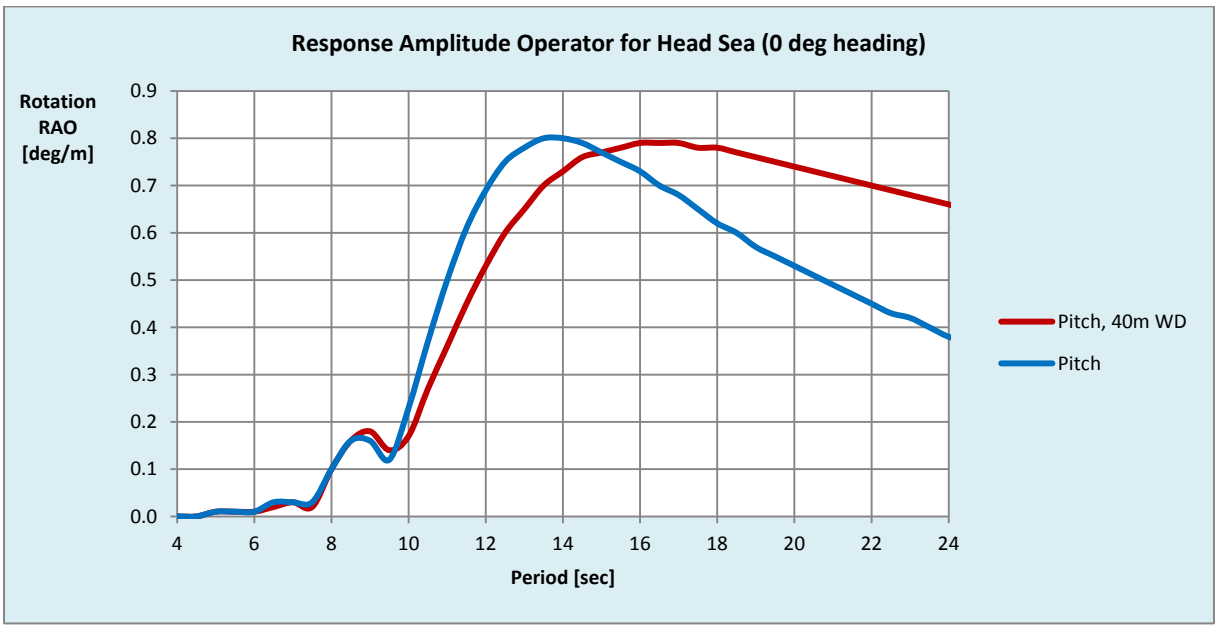

Figure 10.2 - RAO comparison in pitch for two water depths in head sea

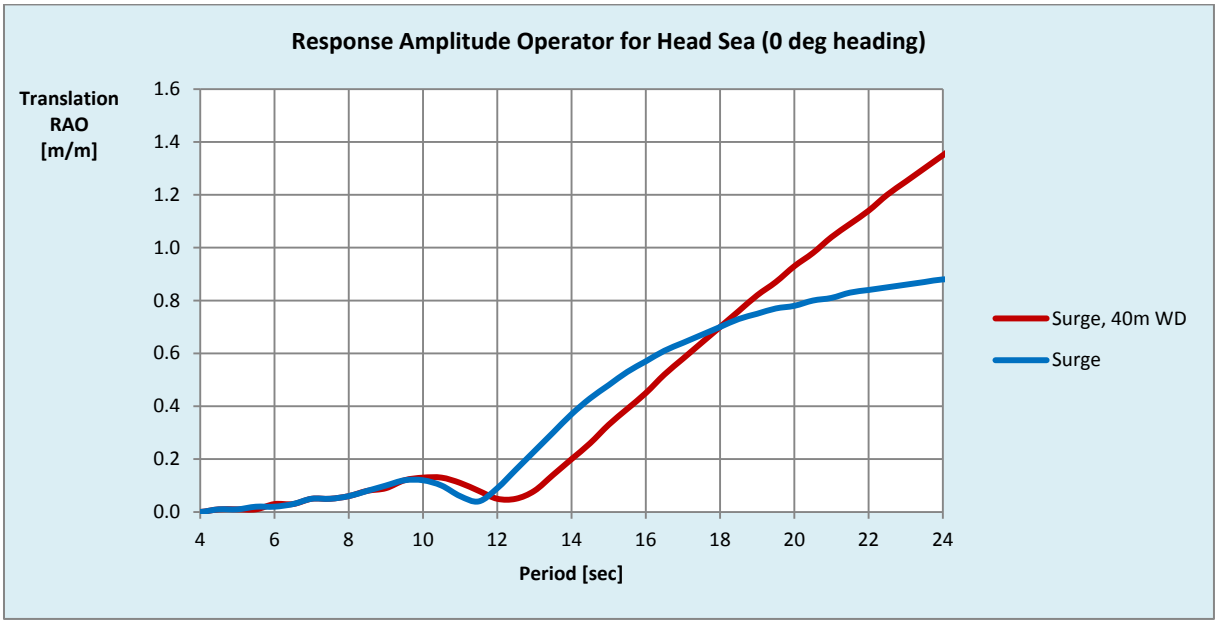

Figure 10.3 - RAO comparison in surge for two water depths in head sea

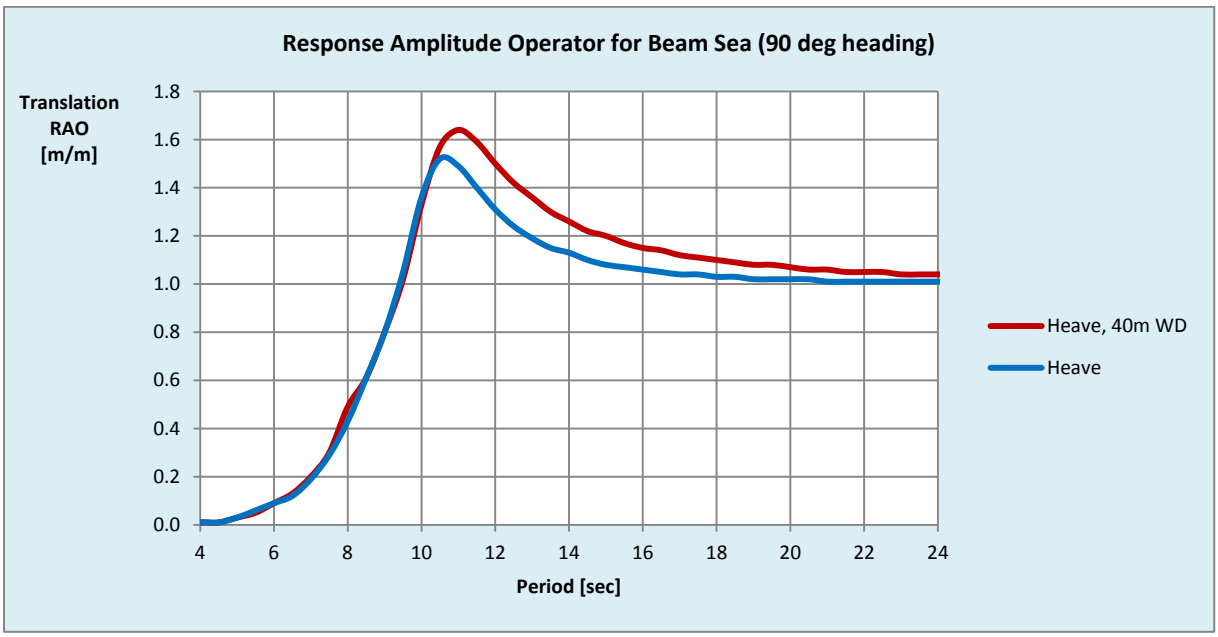

Figure 10.4 - RAO comparison in heave for two water depths in beam sea

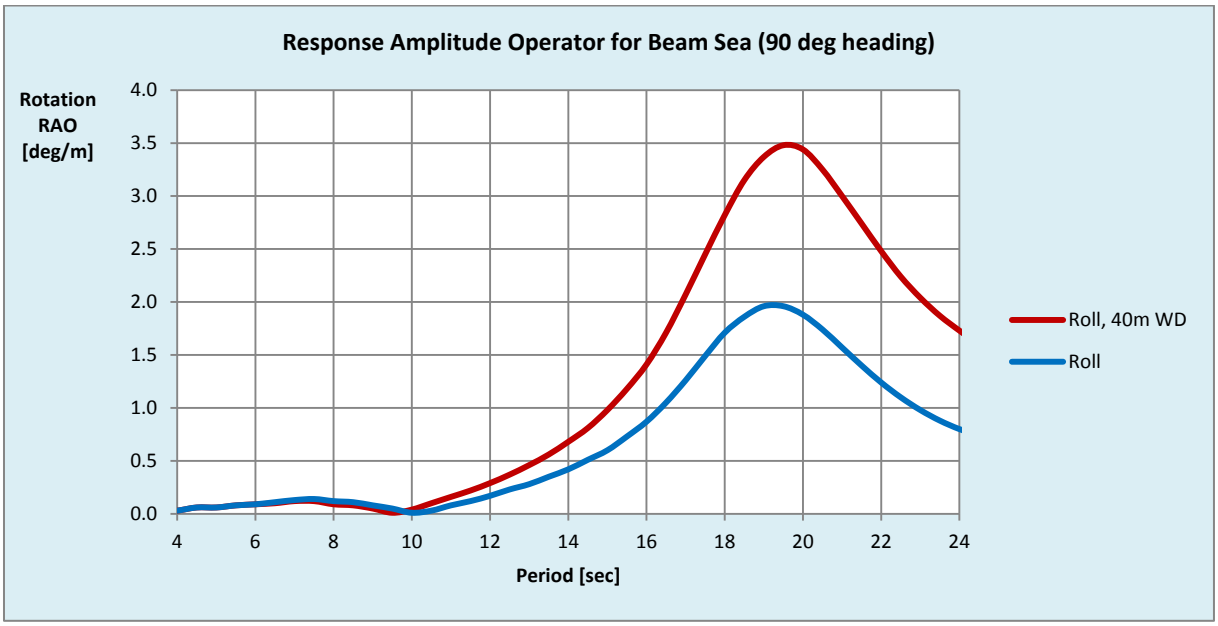

Figure 10.5- RAO comparison in roll for two water depths in beam sea

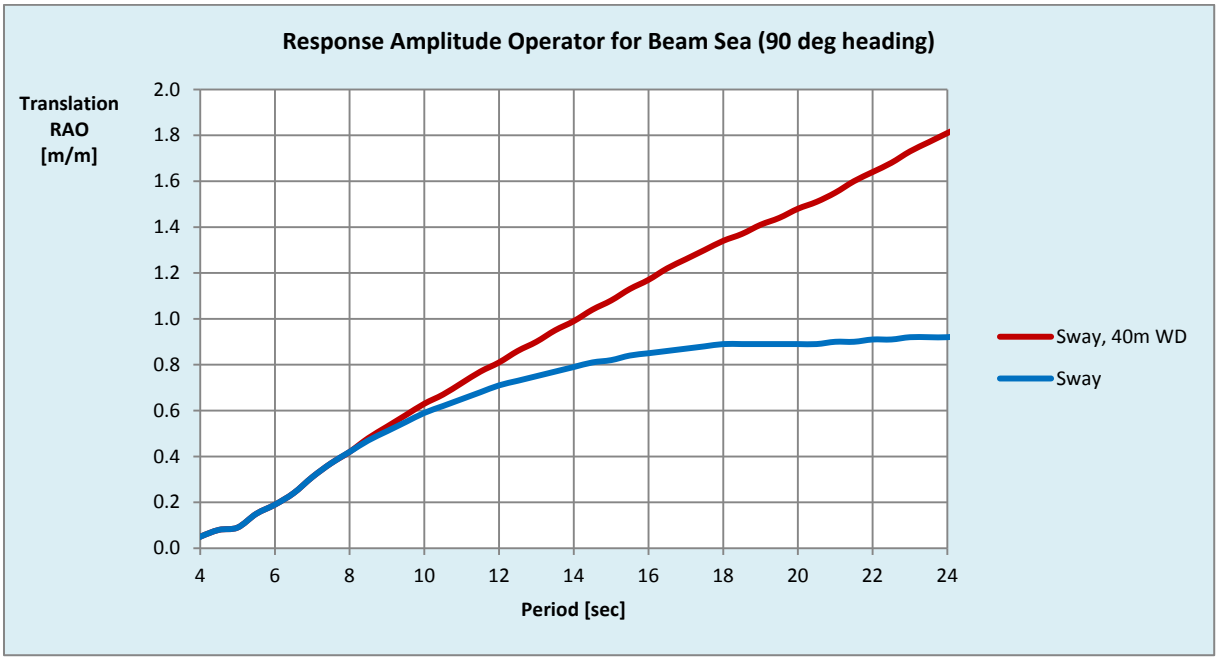

Figure 10.6- RAO comparison in sway for two water depths in beam sea

10.4 DAF-Factor

The dynamic amplification factor in the crane sling is defined as in DNV-RP-H103:

$$DAF = \frac{F_{total}}{F_{in\ air}} \tag{10.5-1}$$

where

F_{total} is the largest crane sling force

$F_{in\ air}$ is the weight of the jacket times the acceleration of gravity

Another way to define the dynamic amplification factor is by using the submerged weight in the denominator of equation (10.5-1):

$$DAF_{sub} = \frac{F_{total}}{F_{submerged}} \tag{10.5-2}$$

where

$F_{submerged}$ is $F_{in\ air}$ minus the buoyancy in the current phase

10.5 Time Domain Analysis Results for H_s = 3.0 m

The time domain analysis was carried out for 20 minutes for each period for each heading. These results are then statistically extended to find the highest predicted value for a 3-hour run. In order to get more accurate results, the first 200 seconds of each run were deleted because the system will always need some time to start moving after the environmental forces have started hitting it.

Figure 10.7 is a rosette showing the relationship between environmental heading and DAF-factor for the analysed zero-up-crossing periods, T_z. Simulations are carried out for headings 0-180 degrees and then extended to be valid for 180-360 degrees due to symmetry. Values for the two largest periods are omitted from this figure since they include extreme values. They are however included in Table 10.16.

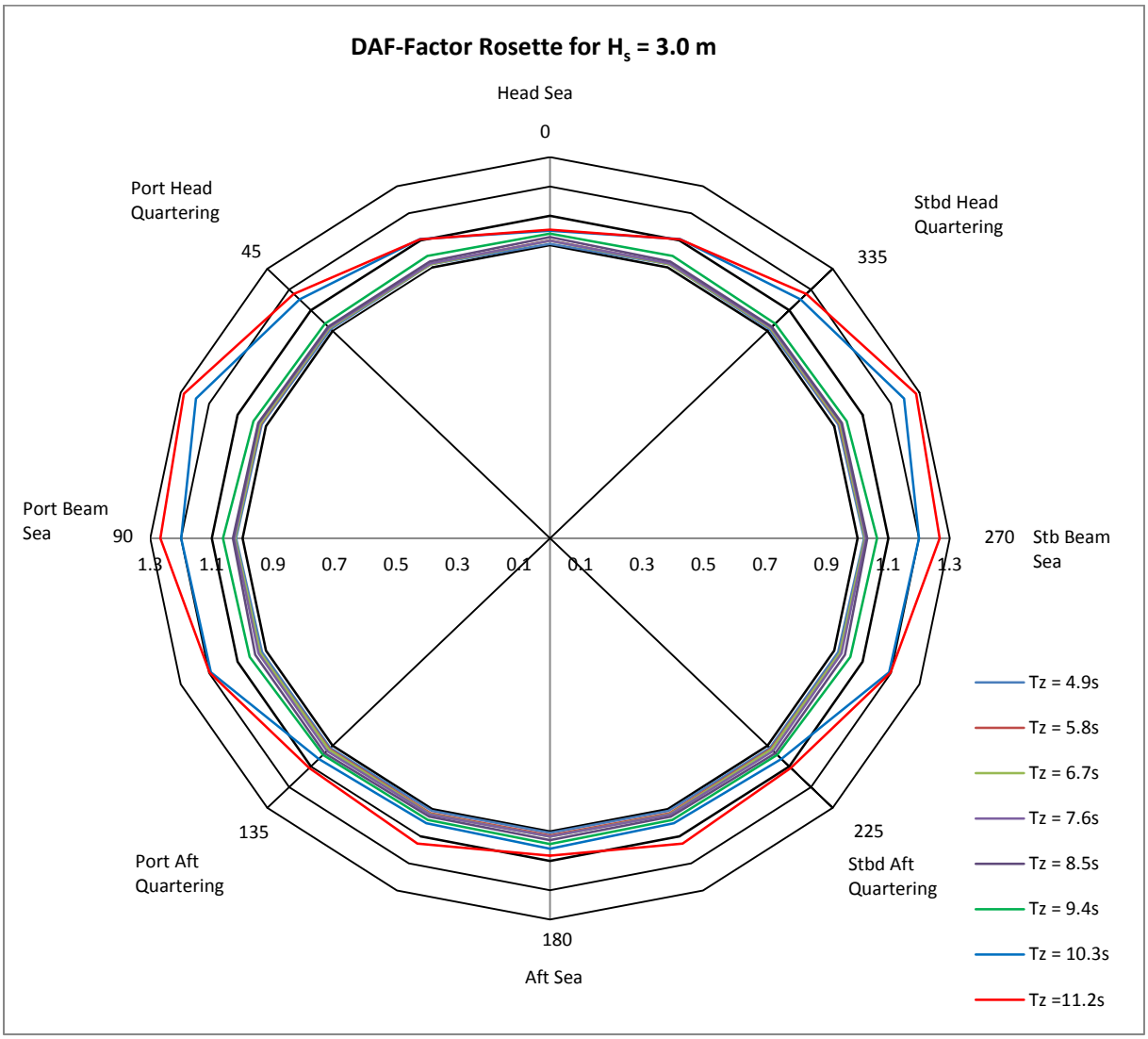

Figure 10.7 –Rosette showing the relationship between environmental heading and DAF-factor

The DAF-factors for the three phases are shown in Table 10.17, Table 10.18 and Table 10.19. These three tables are assembled into Table 10.16 and Figure 10.7, which show the maximum DAF-factor for each period. Factors written in red colour means that for this period, snap loads in the tugger lines will most likely appear and compromise the operation.

Table 10.16 – DAF-Factor for H_s = 3.0 m (Max value of the three phases)

DAF-Factor for Significant Wave Height, H_s = 3.0 m										
Heading		0	22.5	45	67.5	90	112.5	135	157.5	180
T_z(s)	T_p(s)									
4.9	6.4	1.008	1.013	1.011	1.014	1.021	1.015	1.009	1.012	1.010
5.8	8.1	1.014	1.015	1.015	1.021	1.025	1.019	1.014	1.013	1.016
6.7	9.5	1.017	1.018	1.018	1.020	1.024	1.021	1.014	1.012	1.015
7.6	10.8	1.017	1.020	1.026	1.026	1.027	1.025	1.017	1.015	1.015
8.5	12.1	1.029	1.027	1.037	1.038	1.031	1.027	1.020	1.022	1.027
9.4	13.4	1.042	1.039	1.045	1.057	1.063	1.044	1.036	1.042	1.039
10.3	14.6	1.058	1.052	1.064	1.194	1.200	1.246	1.152	1.105	1.049
11.2	15.9	1.082	1.127	1.107	1.198	1.267	1.289	1.179	1.104	1.053
12.1	17.2	1.054	1.052	1.229	1.283	2.812	4.006	1.260	1.144	1.053
13.0	18.4	1.048	1.047	1.188	158.784	Error	4.079	1.478	1.133	1.046

Note: Red colour is used to show at which period and headings snap forces appeared in the tugger lines

Table 10.17 – DAF-Factor for H_s = 3.0 m during in-air phase

DAF-Factor for the In-Air Phase for Significant Wave Height, H_s = 3.0 m										
Heading		0	22.5	45	67.5	90	112.5	135	157.5	180
T_z(s)	T_p(s)									
4.9	6.4	1.004	1.006	1.011	1.014	1.021	1.015	1.009	1.012	1.010
5.8	8.1	1.013	1.015	1.015	1.021	1.025	1.019	1.014	1.013	1.016
6.7	9.5	1.017	1.018	1.018	1.020	1.024	1.021	1.014	1.012	1.015
7.6	10.8	1.017	1.020	1.026	1.026	1.027	1.025	1.017	1.015	1.015
8.5	12.1	1.029	1.027	1.037	1.038	1.031	1.027	1.020	1.022	1.027
9.4	13.4	1.042	1.039	1.045	1.057	1.063	1.044	1.036	1.042	1.039
10.3	14.6	1.058	1.052	1.064	1.194	1.200	1.246	1.152	1.105	1.049
11.2	15.9	1.082	1.127	1.107	1.198	1.267	1.289	1.179	1.104	1.053
12.1	17.2	1.054	1.052	1.229	1.283	2.812	4.006	1.260	1.144	1.053
13.0	18.4	1.048	1.047	1.188	158.784	Error	4.079	1.478	1.133	1.046

Note: Red colour is used to show at which period and headings snap forces appeared in the tugger lines

Table 10.18 – DAF- Factor for H_s = 3.0 m during the splash zone phase

DAF-Factor for the Splash Zone Phase for Significant Wave Height, H_s = 3.0 m										
Heading		0	22.5	45	67.5	90	112.5	135	157.5	180
T_z(s)	T_p(s)									
4.9	6.4	1.008	1.013	1.012	1.014	1.019	1.013	1.007	1.010	1.015
5.8	8.1	1.014	1.010	1.013	1.016	1.020	1.015	1.009	1.007	1.013
6.7	9.5	1.010	1.012	1.014	1.016	1.018	1.018	1.008	1.009	1.011
7.6	10.8	1.011	1.014	1.020	1.020	1.020	1.017	1.009	1.006	1.010
8.5	12.1	1.010	1.015	1.025	1.027	1.026	1.017	1.011	1.006	1.007
9.4	13.4	1.010	1.015	1.028	1.031	1.029	1.021	1.012	1.006	1.007
10.3	14.6	1.011	1.017	1.030	1.033	1.030	1.025	1.015	1.007	1.007
11.2	15.9	1.013	1.017	1.029	1.033	1.031	1.027	1.016	1.008	1.008
12.1	17.2	1.014	1.017	1.027	1.033	1.032	1.027	1.017	1.008	1.008
13.0	18.4	1.014	1.016	1.023	1.034	1.034	1.028	1.016	1.009	1.008

Table 10.19 - DAF-Factor for H_s = 3.0 m during the close to sea bed

DAF-Factor for the Close to Sea Bed Phase for Significant Wave Height, H_s = 3.0 m										
Heading		0	22.5	45	67.5	90	112.5	135	157.5	180
T_z(s)	T_p(s)									
4.9	6.4	0.964	0.955	0.961	0.966	0.975	0.975	0.968	0.975	0.969
5.8	8.1	0.971	0.967	0.968	0.971	0.979	0.975	0.965	0.968	0.970
6.7	9.5	0.974	0.970	0.975	0.974	0.982	0.978	0.970	0.970	0.972
7.6	10.8	0.974	0.971	0.979	0.982	0.987	0.979	0.972	0.972	0.972
8.5	12.1	0.974	0.972	0.988	0.994	0.998	0.990	0.979	0.969	0.970
9.4	13.4	0.972	0.974	0.997	1.008	1.009	1.000	0.984	0.972	0.969
10.3	14.6	0.971	0.979	1.008	1.022	1.023	1.011	0.989	0.975	0.968
11.2	15.9	0.968	0.981	1.017	1.032	1.034	1.021	1.000	0.978	0.967
12.1	17.2	0.966	0.983	1.018	1.036	1.040	1.026	1.008	0.980	0.965
13.0	18.4	0.964	0.983	1.017	1.035	1.045	1.032	1.012	0.982	0.963

Note: All headings are individually height adjusted such that the jacket does not hit the sea bed during simulation

On the next page there is a table (Table 10.20) showing the forces in the tugger lines during the in-air phase. Large forces are experienced for unfavourable environmental headings and high periods.

Table 10.20 – Force in tugger lines for H_s = 3.0 m

Force in Tugger Lines for Significant Wave Height, H_s = 3.0 m																				
Heading			0		22.5		45		67.5		90		112.5		135		157.5		180	
T_z(s)	T_p(s)		Line 1	Line 2	Line 1	Line 2	Line 1	Line 2	Line 1	Line 2	Line 1	Line 2	Line 1	Line 2	Line 1	Line 2	Line 1	Line 2	Line 1	Line 2
4.9	6.4	Max	6.91	6.70	7.22	7.09	7.83	7.54	8.34	7.89	9.25	9.37	9.00	8.51	7.57	7.89	11.06	10.85	10.88	10.55
		Min	5.85	5.74	5.54	5.45	4.74	4.40	4.04	4.10	1.81	1.93	3.68	3.65	5.41	4.86	3.46	3.02	3.27	2.59
5.8	8.1	Max	6.89	6.72	7.25	7.34	7.90	8.25	8.87	8.97	10.96	13.36	9.85	10.03	8.42	8.32	7.58	7.72	6.98	6.81
		Min	5.74	5.76	5.36	5.16	4.26	3.81	2.93	2.23	1.93	1.61	2.93	2.79	4.63	4.37	5.41	5.25	5.93	5.45
6.7	9.5	Max	7.03	6.82	7.60	7.62	8.39	8.99	9.84	10.67	15.84	15.03	12.90	13.11	8.97	9.08	8.09	8.05	7.20	7.21
		Min	5.43	5.45	5.14	4.69	3.92	3.32	2.12	1.43	0.89	0.59	1.26	1.00	3.61	3.13	4.67	4.99	5.43	5.13
7.6	10.8	Max	8.33	8.21	8.68	8.70	10.64	10.70	12.77	13.62	20.45	16.34	23.10	17.72	9.65	10.43	9.01	9.05	7.99	7.94
		Min	4.42	4.67	4.33	3.54	3.27	2.78	1.23	1.10	0.67	0.37	0.62	0.31	3.08	2.13	3.77	3.99	4.65	4.66
8.5	12.1	Max	12.28	11.43	11.89	11.59	14.16	14.40	28.54	21.37	24.09	20.85	30.64	30.74	15.46	16.37	11.12	11.28	11.18	11.22
		Min	2.85	2.80	2.71	2.19	2.15	2.09	0.37	0.27	0.30	0.09	0.25	0.02	1.77	0.77	2.14	1.93	2.84	2.95
9.4	13.4	Max	17.26	16.18	17.43	18.43	18.03	18.45	52.11	25.92	66.60	57.56	56.27	53.79	31.38	33.21	19.47	20.58	16.45	15.50
		Min	1.68	1.49	1.19	0.86	1.37	0.93	-0.32	-0.30	-0.36	-0.44	-0.32	-0.40	0.08	-0.14	0.51	0.49	1.57	1.74
10.3	14.6	Max	24.25	22.95	31.70	27.83	34.52	27.07	87.30	55.09	111.9	76.37	104.3	73.84	73.78	57.24	63.09	37.32	19.88	18.86
		Min	0.44	0.35	0.12	0.10	-0.03	-0.13	-0.55	-0.54	-0.55	-0.55	-0.57	-0.55	-0.49	-0.53	-0.29	-0.09	1.02	1.00
11.2	15.9	Max	29.20	31.39	38.34	35.66	64.67	62.61	102.5	80.6	147.4	134.4	136.1	111.7	110.1	78.60	57.13	43.15	20.95	20.20
		Min	0.07	0.00	-0.24	-0.20	-0.50	-0.58	-0.64	-0.62	-0.74	-0.67	-0.64	-0.64	-0.65	-0.65	-0.31	-0.31	0.71	0.86
12.1	17.2	Max	25.12	23.23	25.87	26.39	93.47	95.29	115.7	112.4	170.9	126.8	171.2	158.8	137.4	94.75	70.71	51.17	19.07	19.20
		Min	0.31	0.41	0.73	0.17	-0.72	-0.70	-0.75	-0.78	-0.82	-0.83	-0.85	-0.85	-0.74	-0.70	-0.54	-0.49	1.13	1.03
13.0	18.4	Max	18.38	18.80	20.75	20.99	131.4	96.41	1674	2583	Error	Error	212.6	198.1	146.3	143.5	70.26	55.73	17.56	17.27
		Min	1.16	0.88	0.79	0.45	-0.76	-0.79	-1.00	-1.06	Error	Error	-2.19	-2.21	-0.73	-0.72	-0.46	-0.50	1.65	1.32

Note: "Error" is used for the periods and environmental headings for which the simulation was terminated due to instability

10.6 Frequency Domain Analysis Results for H_s = 3.0 m

A frequency domain analysis was carried out for the exact same system as in Section 10.5 in order to investigate the differences in results for both analysis types. Table 10.21 shows the maximum DAF-factor for the three phases for each period and heading. This table is in Table 10.22 compared to Table 10.16.

Table 10.21 – Frequency domain analysis DAF-Factor for H_s = 3.0 m (Max value of the three phases)

DAF-Factor for Significant Wave Height, H_s = 3.0 m										
Heading		0	22.5	45	67.5	90	112.5	135	157.5	180
T_z(s)	T_p(s)									
4.9	6.4	1.009	1.013	1.026	1.041	1.048	1.043	1.029	1.016	1.013
5.8	8.1	1.057	1.081	1.151	1.232	1.279	1.264	1.194	1.119	1.090
6.7	9.5	1.053	1.076	1.135	1.198	1.231	1.215	1.155	1.092	1.069
7.6	10.8	1.044	1.062	1.104	1.145	1.162	1.145	1.103	1.060	1.044
8.5	12.1	1.037	1.052	1.087	1.119	1.132	1.118	1.084	1.049	1.035
9.4	13.4	1.033	1.044	1.072	1.098	1.108	1.097	1.070	1.042	1.030
10.3	14.6	1.030	1.039	1.062	1.083	1.092	1.082	1.060	1.038	1.028
11.2	15.9	1.028	1.036	1.055	1.073	1.080	1.073	1.054	1.036	1.028
12.1	17.2	1.027	1.034	1.051	1.068	1.074	1.068	1.052	1.036	1.029
13.0	18.4	1.029	1.036	1.052	1.067	1.073	1.068	1.053	1.038	1.031

The variation between the results from time- and frequency domain analysis as given in Table 10.22 is computed by the simple formula:

$$\Delta = Frequency\ Domain\ DAF\ Factor - Time\ Domain\ DAF\ Factor \qquad (10.6\text{-}1)$$

Table 10.22 - Comparison of DAF-factors from time- and frequency domain analysis

Comparison of DAF-Factors Calculated with Time- and Frequency Domain Analysis for Significant Wave Height, H_s = 3.0 m										
Heading		0	22.5	45	67.5	90	112.5	135	157.5	180
T_z(s)	T_p(s)									
4.9	6.4	0.001	0.000	0.014	0.027	0.027	0.028	0.020	0.004	0.003
5.8	8.1	0.043	0.066	0.135	0.211	0.253	0.245	0.179	0.106	0.074
6.7	9.5	0.036	0.058	0.117	0.177	0.207	0.194	0.140	0.081	0.054
7.6	10.8	0.027	0.042	0.079	0.119	0.135	0.120	0.085	0.046	0.029
8.5	12.1	0.008	0.025	0.050	0.081	0.100	0.091	0.063	0.028	0.008
9.4	13.4	-0.010	0.005	0.028	0.041	0.045	0.053	0.034	-0.001	-0.009
10.3	14.6	-0.029	-0.013	-0.002	-0.110	-0.108	-0.164	-0.092	-0.067	-0.021
11.2	15.9	-0.055	-0.091	-0.053	-0.125	-0.187	-0.216	-0.124	-0.068	-0.025
12.1	17.2	-0.027	-0.018	-0.177	-0.215	-1.738	-2.938	-0.207	-0.108	-0.024
13	18.4	-0.019	-0.012	-0.136	-157.717	Error	-3.012	-0.425	-0.096	-0.016

Table 10.23 shows the calculated tugger line forces. A comparison of the tugger line forces for H_s = 3.0 m for the two analysis types is given in Table 10.24.

Table 10.23 – Frequency domain calculated force in tugger lines for H_s = 3.0 m

Force in Tugger Lines Calculated with Frequency Domain Analysis for Significant Wave Height, Hs = 3.0 m																			
Heading		**0**		**22.5**		**45**		**67.5**		**90**		**112.5**		**135**		**157.5**		**180**	
T_z(s)	**T_p(s)**	Line 1	Line 2	Line 1	Line 2	Line 1	Line 2	Line 1	Line 2	Line 1	Line 2	Line 1	Line 2	Line 1	Line 2	Line 1	Line 2	Line 1	Line 2
4.9	6.4	9.19	9.40	9.84	10.04	11.49	11.78	13.23	13.74	14.26	14.97	14.09	14.85	12.75	13.40	11.04	11.44	10.20	10.44
5.8	8.1	18.45	18.98	21.28	21.73	27.93	28.46	34.56	35.37	38.39	39.44	37.83	38.88	32.98	33.78	26.63	27.03	23.53	23.67
6.7	9.5	16.11	16.62	18.68	18.92	24.29	24.27	29.67	29.67	32.87	32.96	32.55	32.60	28.52	28.39	22.96	22.66	20.12	19.81
7.6	10.8	13.66	13.86	15.69	15.41	19.86	19.15	23.47	22.98	25.31	25.23	24.76	24.81	21.82	21.65	17.86	17.42	15.81	15.30
8.5	12.1	13.55	13.01	15.64	14.65	19.87	18.59	23.40	22.43	24.92	24.37	23.98	23.56	20.87	20.29	17.00	16.26	15.04	14.28
9.4	13.4	14.39	13.43	16.77	15.58	21.58	20.31	25.55	24.54	27.12	26.30	25.89	24.92	22.26	21.00	17.82	16.48	15.54	14.26
10.3	14.6	16.23	15.41	19.11	18.22	24.98	24.12	29.76	29.05	31.59	30.74	30.03	28.67	25.62	23.75	20.20	18.26	17.36	15.55
11.2	15.9	19.00	18.60	22.62	22.26	30.00	29.78	35.98	35.74	38.22	37.49	36.25	34.63	30.73	28.40	23.92	21.51	20.31	18.08
12.1	17.2	23.05	23.38	27.53	28.04	36.70	37.46	44.10	44.62	46.87	46.41	44.48	42.67	37.70	34.96	29.21	26.42	24.70	22.16
13.0	18.4	27.27	28.65	32.25	33.94	42.63	44.62	51.01	52.46	54.19	54.14	51.59	49.77	43.98	41.10	34.34	31.53	29.24	26.77

Table 10.24 - Comparison of tugger line forces from time- and frequency domain analysis

Difference in Tugger Line Force for Time- and Frequency Domain Analysis for Significant Wave Height, Hs = 3.0 m																			
Heading		**0**		**22.5**		**45**		**67.5**		**90**		**112.5**		**135**		**157.5**		**180**	
T_z(s)	**T_p(s)**	Line 1	Line 2	Line 1	Line 2	Line 1	Line 2	Line 1	Line 2	Line 1	Line 2	Line 1	Line 2	Line 1	Line 2	Line 1	Line 2	Line 1	Line 2
4.9	6.4	2.28	2.70	2.62	2.95	3.66	4.24	4.89	5.85	5.01	5.60	5.09	6.34	5.18	5.51	-0.02	0.59	-0.68	-0.11
5.8	8.1	11.56	12.26	14.03	14.39	20.03	20.21	25.69	26.40	27.43	26.08	27.98	28.85	24.56	25.46	19.05	19.31	16.55	16.86
6.7	9.5	9.08	9.80	11.08	11.30	15.90	15.28	19.83	19.00	17.03	17.93	19.65	19.49	19.55	19.31	14.87	14.61	12.92	12.60
7.6	10.8	5.33	5.65	7.01	6.71	9.22	8.45	10.70	9.36	4.86	8.89	1.66	7.09	12.17	11.22	8.85	8.37	7.82	7.36
8.5	12.1	1.27	1.58	3.75	3.06	5.71	4.19	-5.14	1.06	0.83	3.52	-6.66	-7.18	5.41	3.92	5.88	4.98	3.86	3.06
9.4	13.4	-2.87	-2.75	-0.66	-2.85	3.55	1.86	-26.56	-1.38	-39.48	-31.26	-30.38	-28.87	-9.12	-12.21	-1.65	-4.10	-0.91	-1.24
10.3	14.6	-8.02	-7.54	-12.59	-9.61	-9.54	-2.95	-57.54	-26.04	-80.27	-45.63	-74.22	-45.17	-48.16	-33.49	-42.89	-19.06	-2.52	-3.31
11.2	15.9	-10.20	-12.79	-15.72	-13.40	-34.67	-32.83	-66.52	-44.84	-109.2	-96.89	-99.84	-77.07	-79.37	-50.20	-33.21	-21.64	-0.64	-2.12
12.1	17.2	-2.07	0.15	1.66	1.65	-56.77	-57.83	-71.60	-67.78	-124.1	-80.42	-126.7	-116.1	-99.71	-59.79	-41.50	-24.75	5.63	2.96
13.0	18.4	8.89	9.85	11.50	12.95	-88.72	-51.79	-1623	-2531	-	-	-161.0	-148.3	-102.3	-102.4	-35.92	-24.20	11.68	9.50

10.7 Frequency Domain Analysis Results for H_s = 3.5 m

Table 10.25 shows the frequency domain analysis results for a significant wave height of 3.5 meters and a wind speed of 24.5 knots.

Table 10.25- Frequency domain analysis DAF-Factor for H_s = 3.5 m (Max value of the three phases)

DAF-Factor for Significant Wave Height, H_s = 3.5 m										
Heading		0	22.5	45	67.5	90	112.5	135	157.5	180
T_z(s)	T_p(s)									
4.9	6.4	1.011	1.016	1.032	1.050	1.059	1.053	1.036	1.020	1.016
5.8	8.1	1.074	1.105	1.194	1.297	1.357	1.339	1.251	1.156	1.119
6.7	9.5	1.067	1.096	1.170	1.249	1.292	1.273	1.198	1.119	1.089
7.6	10.8	1.054	1.076	1.128	1.178	1.199	1.180	1.128	1.076	1.056
8.5	12.1	1.046	1.064	1.106	1.145	1.161	1.145	1.104	1.062	1.044
9.4	13.4	1.039	1.054	1.087	1.119	1.132	1.119	1.086	1.052	1.037
10.3	14.6	1.035	1.047	1.075	1.101	1.111	1.101	1.074	1.046	1.035
11.2	15.9	1.033	1.043	1.066	1.088	1.097	1.088	1.066	1.043	1.034
12.1	17.2	1.032	1.041	1.061	1.081	1.089	1.082	1.063	1.043	1.035
13.0	18.4	1.034	1.042	1.062	1.080	1.087	1.081	1.063	1.045	1.036

10.8 Simplified Splash Zone Analysis

A simplified splash zone analysis is carried out in accordance with DNV-RP-H103 Sec. 4. Accelerations, velocities and amplitude in the crane tip are obtained from frequency domain analysis in MOSES. The results are shown in Table 10.26, and the complete calculations are provided in **Appendix G**.

Table 10.26 – DAF-factors for simplified splash zone analysis

	DAF-Factor	
Load Case	H_s = 3m	H_s = 3.5m
1	1.098	1.350
2	1.122	1.346

It should here be noted that these values are calculated using the largest amplitude, velocity and acceleration in the crane tip for all periods and headings. The results are only used to confirm the previous assumption of the splash zone as a non-critical phase for this operation.

Check of the "slack sling criterion":

For H_s = 3m:

Load Case 1: $F_{hyd.up} \leq 0.9\, F_{static}$

$$785\ kN \leq 0.9 \times 4\,825\ kN = 4\,342\ kN \rightarrow OK$$

Load Case 2: $F_{hyd.up} \leq 0.9\, F_{static}$

$$776\ kN \leq 0.9 \times 4\,825\ kN = 4\,342\ kN \rightarrow OK$$

For H_s = 3.5m:

Load Case 1: $F_{hyd.up} \leq 0.9\, F_{static}$

$$905\ kN \leq 0.9 \times 4\,825\ kN = 4\,342\ kN \rightarrow OK$$

Load Case 2: $F_{hyd.up} \leq 0.9\, F_{static}$

$$895\ kN \leq 0.9 \times 4\,825\ kN = 4\,342\ kN \rightarrow OK$$

Conclusion: No slack criterion is fulfilled, i.e. the slings will not go slack during lowering through the splash zone.

10.9 Analysis Conclusion

The water depth of 40 meters is confirmed to have an effect on the shuttle tankers motion characteristics and must further be assumed to have influence on the DAF-factor and forces in the tugger lines.

Time domain analysis is considered more accurate compared to frequency domain analysis when approaching the limit for snap loads in tugger lines and large motions of the lifted object. The tugger line results from the time domain analysis are also considered to give a better understanding of when they are close to becoming slack. However, the frequency domain results yields acceptable results for periods well outside the non-linear forces area.

The installation is feasible in waves with a significant height of 3 meters, given the requirement that it's carried out outside of the red area in Table 10.16. According to DNV-OS-H101, the significant wave height should be multiplied with an alpha-factor to cover the uncertainty in forecasted and monitored values. Assuming the weather is monitored at all times and the operational period is less than 12 hours, the maximum forecasted $H_{s_{WF}}$ become:

$$H_{s_{WF}} = \alpha \times H_s = 0.855 \times 3m = 2.56m$$

For a significant wave height of 3.5 meters, further analysis in the time domain should be carried out to investigate the behaviour of the tugger lines.

The sudden change in DAF-factor between T_z=9.4s and T_z=10.3s in Figure 10.7, indicates that this is the area at which the shuttle tanker goes into resonance with the waves. Although the motions are still low at head sea, this is normally an area avoided for carrying out a lifting operation.

11 Discussion

The weight, buoyancy and hydrostatic parameters are important to check to ensure that if MOSES has interpreted the system as desired. All results in this section are as anticipated, except for maybe the shuttle tankers roll angle in the beginning of the in-air phase. Although the shuttle tanker was ballasted to an even keel with a "dummy" weight in the crane tip, the angle is still 0.23. Not much, but still a deviation compared to the two other angles which were 0.00 and 0.02. The most probable reason for this is that the pre-tensioning of the tugger lines has changed the jacket's centre of gravity slightly in the global coordinate system. However, this initial roll angle is assumed not to have any considerable effect on the result. Further, the radii's of gyration and $\overline{GM}$-distance are obvious sources of errors since there is not really given any more information about the shuttle tanker than the hull geometry (MOSES model).

All connector forces are found to be as desired in the static equilibrium. It's here observed that the crane- and spreader slings do not have any weight, while the tugger lines do (due to the "exact" command). This is in accordance with the MOSES Reference Manual, see reference [11], which states that connectors don't have any weight unless it's specified by the user, and no environmental forces are applied on the connectors.

Section 10.3 clearly shows how the motion characteristics of the shuttle tanker changes as it travel into shallower waters. The eigenperiods are also seen to increase for shallower waters. These RAO's comply very well with the theory given in Section 3.2.1.7. Ultimately, this shows that the DAF-factors depend on the water depth at the installation site.

The DAF-factor rosette in Figure 10.7 shows very well the importance of environmental headings during lifting operations carried out with crane ships. For a heading of 0 degrees, none of the zero-up-crossing periods creates a DAF-factor which exceeds 1.082 or initiates snap loads in the tugger lines. However, as soon as the heading deviates from 0, the DAF-factor increases quickly for high (> 10s) zero-up-crossing periods. This can, to a large extent, be explained by considering the RAO's in **Appendix B**. These high periods are close to the tanker's eigenperiod in heave. Although the eigenperiod is more or less the same for all headings, the RAO's have a much larger peak value (DAF-factor) when the heading increases towards 90 degrees. The RAO in heave for head sea peaks at less than 0.4, while it exceeds 1.6 for beam sea. This is caused by the relative relationship between the wave length of the wave passing the tanker in head sea is L/245m (ship length) while it for head sea is L/42m (ship width). Hence giving all crane ships much better motion characteristics in the crane tip for head sea.

Another interesting effect discovered in the DAF-factor rosette, is that the DAF-factor is seen to be larger in the interval from 0 to 90 degrees environmental headings compared to 90 to 180 degrees, especially for high wave periods. The DAF-factor for T_z = 11.2s and 45 degrees is clearly larger than the one calculated for 135 degrees. Again, the RAO's in **Appendix B** is checked for differences in ship motions for 45 and 135 degrees. Here it's found that the dynamic amplification in heave is actually larger for 45 degrees compared to 135 degrees,

making it worse to operate with the waves 45 degrees from the bow than 45 degrees from the stern. Also, the DAF-factor seems to be at its highest not for 90 degrees, but for angles between 67.5 and 90. The linear line between the 67.5 to 90 degrees interval in Figure 10.7 is likely to hide the maxima point for the DAF-factor. This might not be so surprising considering that linear waves hitting a perfectly symmetric body at an angle of 90 degrees only would create sway, roll and heave motions, whereas waves hitting with an angle of almost 90 degrees would cause approximately the same sway, heave and roll motion combined with some pitch, yaw and surge motions.

It should also be mentioned that the DAF-factors shown in the rosette clearly states that the factors remain low for all environmental headings as long as the wave periods remain out of the tankers eigenperiod.

The calculated results show that the limiting phase (where the DAF-factor is at its highest) is the in-air phase. As soon as the jacket starts submerging into the water, the jacket motions are dampened by the water (mathematically described with a larger damping coefficient in the equations of motion). Further, the buoyancy force on the jacket is contributing to reduce the experienced DAF-factor in the crane tip.

Moving on to the tugger line results in Table 10.20, both tugger lines were initially tensioned to a force of 6 tonnes in an effort to avoid them from going slack. A tugger line going slack due to jacket motion relative to the shuttle tanker will turn into a snap load (impact force) causing a hazardous event. The forces in these two tugger lines are to a large extent acting as expected, meaning that they are low when the shuttle tankers motions are low. Important here is to be aware of how they are modelled in MOSES. The tugger lines are modelled as class "h_cat" flexible connectors. These connectors can only handle tension forces, meaning that there is no such thing as negative forces. Forces below zero in Table 10.20 is therefore interpreted as the point where the tugger lines go slack and snap loads appear. Also the calculated maximum force when snap loads appear is considered questionable due to the concern that the snap loads are believed to apply for a shorter time than the 0.25 seconds time step in the time domain analysis. It's therefore believed that maximum forces should be larger when the minimum force is below zero. However, during a real marine operation, an experienced person will be monitoring the tugger line force at all times with the ability of adjusting the length of the lines or terminate the operation if necessary.

Time domain analysis has been experienced to be an extremely time consuming type of analysis. Almost three weeks of calculations were consumed to obtain the results in Section 10.5, whereas the same system was analysed in the frequency domain in 180 seconds. Frequency domain analysis is therefore preferred for all systems that can be considered as linear. For this specific lifting operation, frequency domain is found to yield acceptable and conservative results for the DAF-factors when the zero-up-crossing period is less than ~9 seconds, see Table 10.22. For larger periods, the time domain analysis returns larger DAF-factors, especially for unfavourable environmental headings. The reason for this is the time domain analysis' ability to capture non-linear effects.

A suggestion of how to reduce the need for computational power could be to reduce the number of plates used to describe the shuttle tanker. ~7000 plates is about 7 times more than the number of plates MOSES recommends to obtain good hydrodynamic results.
The comparison of the calculated tugger line forces for time- and frequency domain analysis does not show any good correlation for the two types of analysis. For periods below $T_z = 8.5s$, the frequency domain results are much higher than the time domain results. And for periods above 8.5s, the results are opposite. It's likely to believe that this is caused by a combination of non-linear forces, and the fact that the forces in the tugger lines are not very well described as a function of the wave frequency, ω. Time domain analysis is therefore superior for calculation of tugger line forces.

All results in this report are based upon the assumption that the JONSWAP sea spectrum does describe the local sea conditions to a satisfactory extent. If e.g. swell waves are present at the time of installation, none of the results in this report will be realistic. A good option would then be to use the two peaked Torsethaugen wave spectrum. Furthermore, the assumptions executed to develop the wave theory; the description of wind and ship motions are sources of errors in the final results. It has also been informed in the MOSES manual that the calculations do not cover interaction in fluid flow between the sea bottom and jacket, giving a small source of error in the calculations during the "close to sea bed" phase.

A number of alternatives to increase the allowable sea state can be suggested on the basis of this report. The results clearly determine the in-air phase to be the limiting and it might therefore be suggested methods to carry out the in-air phase with the ship always facing the waves (head sea) for every lift. And then, after the jacket has been submerged and the motions are damped by the water, rotate the whole ship to the correct position. Then all installations will benefit from the shuttle tanker's great motion characteristics in head sea. Alternatively, the crane spreader could be made rotatable such that the tanker can be dynamically positioned to face the waves at all times. Another and even more drastic suggestion is to design a circular jacket able of being installed at an arbitrary angle, such that the lifting always is carried out in head sea.

Another way to increase the allowable sea state is by use of a roll tank which would reduce the roll motions of the shuttle tanker and include the roll tank in the MOSES modelling.

Increasing the draft will slightly improve the motion characteristics. However, this does not prevent resonances for large wave periods.

Tugger lines could also be even more pre-tensioned, making the in-air phase more resisting to snap loads. This requires consultancy with the designer in order to check the structural integrity for this type of loading on the jacket. Also, this requires the designer to check the jacket for fatigue damage due to load cycling during the installation.

Easier methods to reduce the DAF-factors are to use a crane wire with a smaller diameter, hence reducing the stiffness. The analysis is carried out with a conservative crane wire diameter of 120 mm. Further, other materials than steel wire could be evaluated, for instance using fibre rope on the tugger lines to lower the stiffness.

At last, the alpha factor is simply increased to almost one if the operational period is defined as less than 4 hours.

12 Conclusions and Recommendations

By using typical environmental conditions experienced in the North Sea, this report is positive that a converted shuttle tanker can be used to install the jacket foundation for a wind turbine. Carrying out the operation in a significant wave height of 3 meters is confirmed feasible for specific environmental headings, i.e. the ones where snap loads in the tugger lines does not occur. DAF-factors and tugger line loads depend strongly on non-linear effects for large zero-up-crossing periods, and time domain analysis must therefore be recommended as the safest analysing method. Frequency domain analysis is only found to yield good results well outside of the area where there is a possibility for snap loads in the tugger lines.

The results show how the motion characteristics for the shuttle tanker changes for varying water depth, making these results only valid for 40 meters water depth. Also, the DAF-factor Rosette illustrates very clearly how the shuttle tanker goes into resonance with a sudden large increase in DAF-factor between T_z=9.4s and T_z=10.3s.

In other words, all ship captains rotate their ship such that the bow is facing large waves head on. The same principle must be used for this lifting operation to achieve good results.

References

[1] Chakrabarti, Subrata K.; "Handbook of Offshore Engineering - Volume 1", 1st ed., Plainfield, Illinois, USA – Elsevier, 2005

[2] "Teknisk Ukeblad NR 07/23. Februar 2012", Teknisk Ukeblad Media AS, Majorstuen, Oslo – 2012

[3] Faltinsen, O.M.; "Sea Loads on Ships and Offshore Structures", Cambridge University Press – 1993

[4] Picture downloaded from: http://www.hebezeuge-foerdermittel.de/sites/dev.hebezeugefoerdermittel.de/files/bilder/jacked%20crane%20up%2005_klein.jpg – February 2012

[5] Picture downloaded from: http://www.ship-technology.com/projects/hlcv-borealis/hlcv-borealis3.html – February 2012

[6] Picture downloaded from: http://www.ulstein.com/kunder/ulstein/mm.nsf/lupGraphics/Yard%20278%20_Olympic%20Triton.pdf/$file/Yard%20278%20_Olympic%20Triton.pdf – February 2012

[7] Picture downloaded from: http://www.globalsecurity.org/military/systems/ship/crane-comp.htm – February 2012

[8] Picture downloaded from: http://www.marineinsight.com/marine/marine-news/featured/sscv-thialf-unbelievably-big-crane-ship/ – February 2012

[9] Copied from the 2011 spring exam paper in the "MOM480 Marine Technology and Design" course taught by Ove Tobias Gudmestad at University of Stavanger, 2011

[10] DNV Recommended Practice DNV-RP-H103 "Modelling and Analysis of Marine Operations, April 2011

[11] "Reference Manual for MOSES", Ultramarine, Inc. Houston, Texas, USA – 2010 Downloaded from http://ultramarine.com//hdesk/document/a4.pdf - 02 Jan. 2012

[12] Newman, J.N.; "Marine Hydrodynamics", MIT Press, Cambridge, MA – 1977

[13] White, Frank M.; "Fluid Mechanics", 7th ed., University of Rhode Island, McGraw-Hill Science/Engineering/Math – 2010

[14] Lecture notes on hydrodynamics from the "MOM480 - Marine Technology and Design" course taught by Ove Tobias Gudmestad at University of Stavanger, spring 2011

[15] DNV Recommended Practice DNV-RP-C205 "Environmental Conditions and Environmental Loads", October 2010

[16] Lecture notes on linear wave theory from the "MOM480 - Marine Technology and Design" course taught by Ove Tobias Gudmestad at University of Stavanger, spring 2011

[17] Skjelbreia & Hendrickson; "Fifth Order Gravity Wave Theory" - 1961

[18] DNV Offshore Standard DNV-OS-H101 "Marine Operations, General", October 2011

[19] Picture downloaded from: http://upload.wikimedia.org/wikipedia/commons/d/d2/Early_90%27s_Bangs.jpg – April 2012

[20] Gaggiotti , Federico; "Deep Water Pipe Laying: from Mooring-Based Station Keeping to Dynamic Positioning", Università Politecnica delle Marche, Italy

[21] Lecture notes on the description of ocean waves from the "MOM480 - Marine Technology and Design" course taught by Ove Tobias Gudmestad at University of Stavanger, spring 2011

[22] Lecture notes on wind loads from the "MOM480 - Marine Technology and Design" course taught by Jasna B. Jakobsen at University of Stavanger, spring 2011

[23] Böttcher, Jörg; "Handbuch Offshore-Windenergie", Oldenbourg Wissenschaftsverlag - 2012

[24] Musial, W.D.; Butterfield, S.; Ram, B.; "Energy from Offshore Wind", Offshore Technology Conference – 2006

[25] Picture downloaded from: http://212.201.38.20/siw/paper/heft5/beitrag10 - May 2012

[26] Rao, Singiresu S.; "Mechanical Vibrations" 5th ed., University of Miami, USA – Prentice Hall - 2010

[27] Clauss, Günther; Lehmann, Eike; Östergaard, Carsten; "Offshore Structures Vol. 1, Conceptual Design and Hydromechanics" – Springer Verlag – 1992

[28] Lecture notes on dynamics from the "MOM480 - Marine Technology and Design" course taught by Ove Tobias Gudmestad at University of Stavanger, spring 2011

[29] Anundsen, Thorgeir; "Operability comparison of three ultra-deepwater and harsh environment drilling vessels" – University of Stavanger – 2008

[30] Lecture notes on stability of vessels from the "MOM480 - Marine Technology and Design" course taught by Ove Tobias Gudmestad at University of Stavanger, spring 2011

[31] Dokkum, Klaas van, et al; "Ship Stability", 2nd ed, DOKMAR, Enkhuizen, The Netherlands – 2007

[32] Picture downloaded from: http://upload.wikimedia.org/wikipedia/commons/thumb/4/41/GNfiguur.PNG/220px-GNfiguur.PNG - May 2012

[33] Internet article from www.dn.no; "Bestilte skip som ikke tålte sjø", Published 23.08.11 http://www.dn.no/energi/article2203122.ece - May 2012

Appendix A

Jacket Drawings

Jacket Foundation for Installing Wind Turbines in 40 meters Water Depth

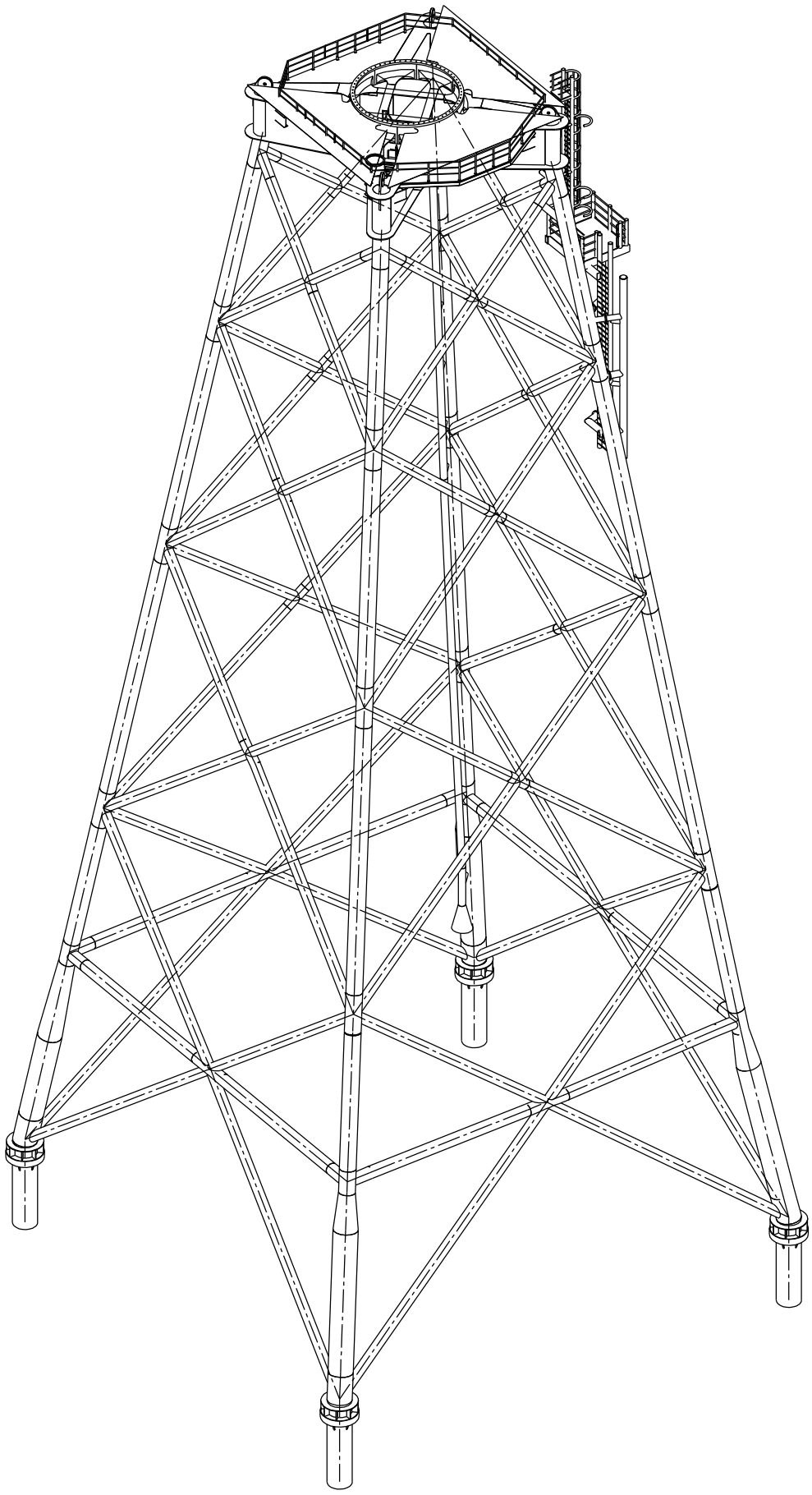

(Drawing provided by Global Maritime)

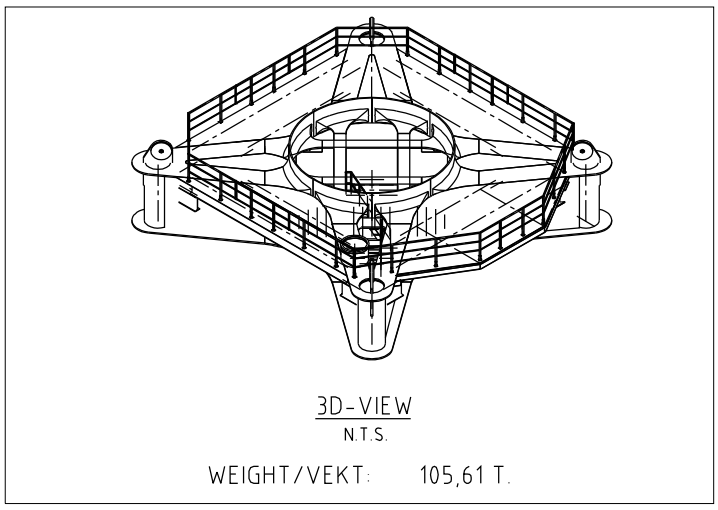

3D-VIEW
N.T.S.

WEIGHT/VEKT: 105,61 T.

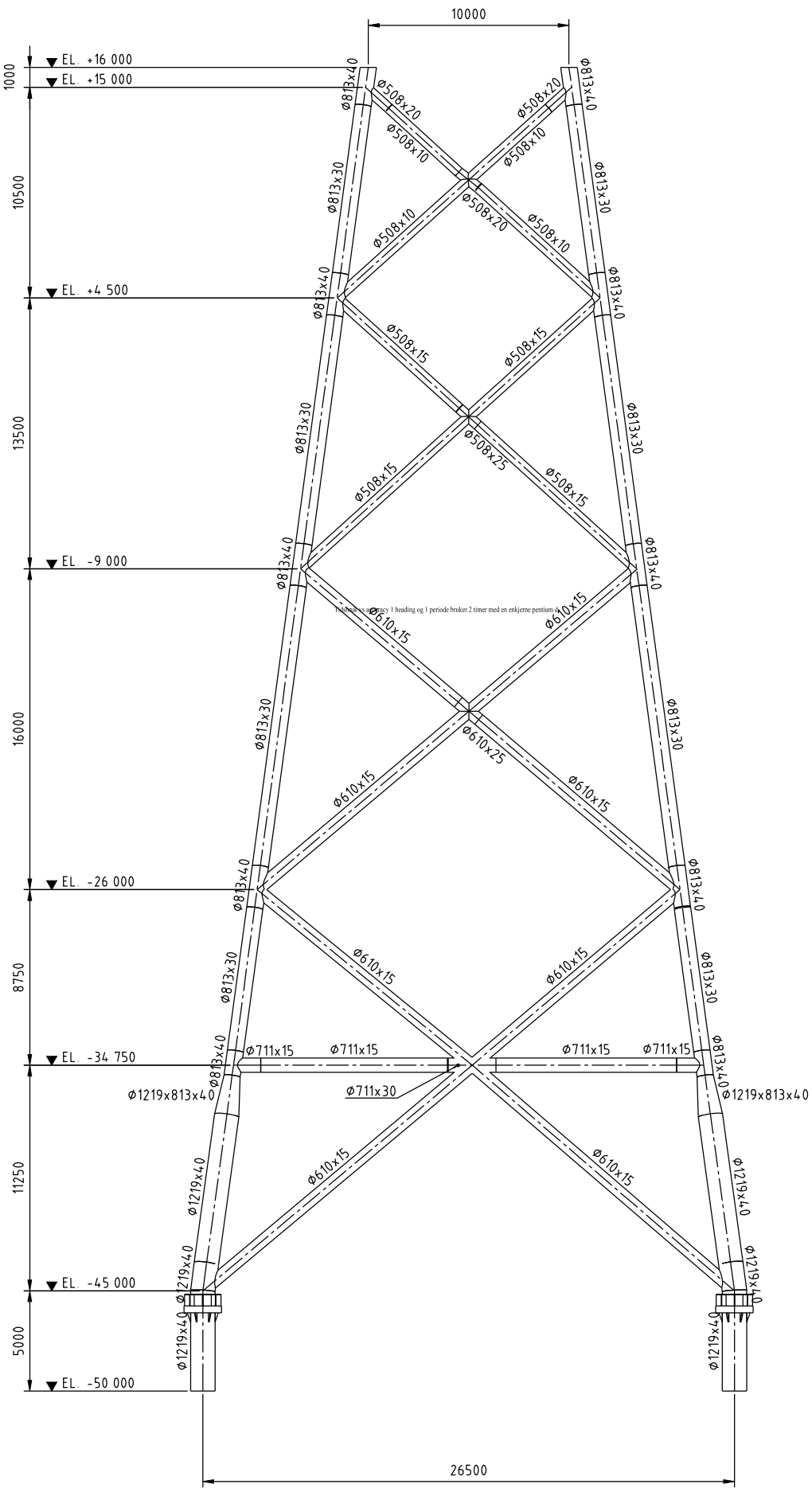

(Drawing provided by Global Maritime)

Appendix B

Response Amplitude Operators for the Shuttle Tanker

Response Amplitude Operators for the shuttle tanker's <u>crane tip</u> with a draft of 13 meters. The ship is located in 40 meters water depth.

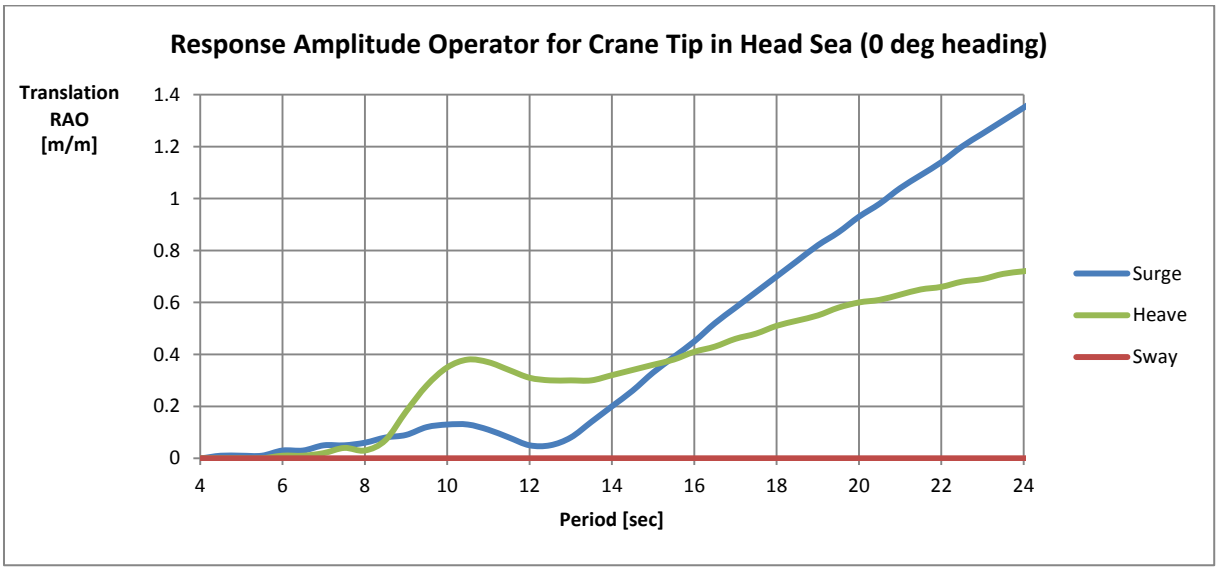

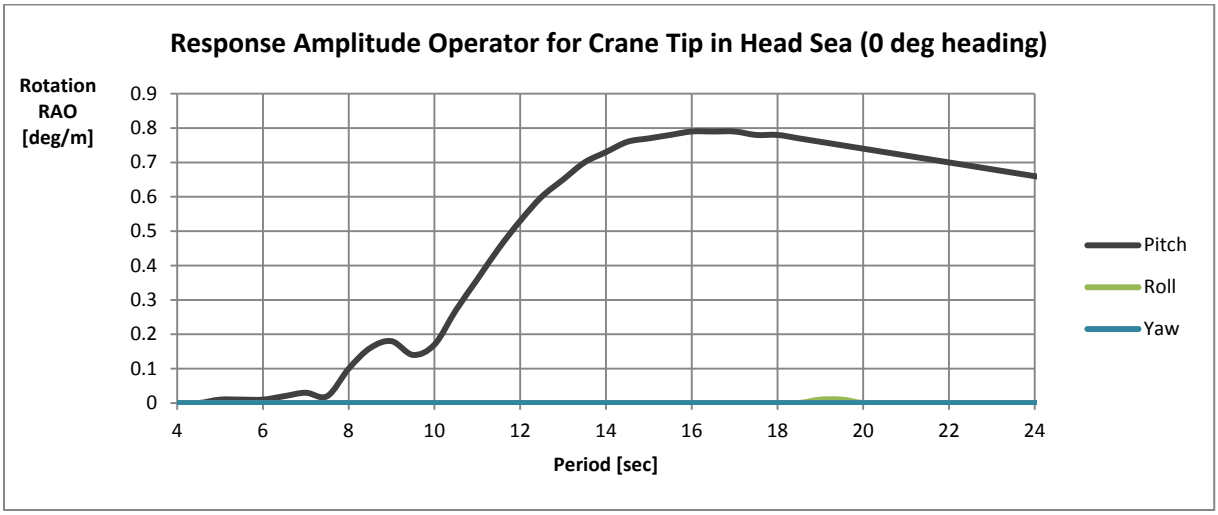

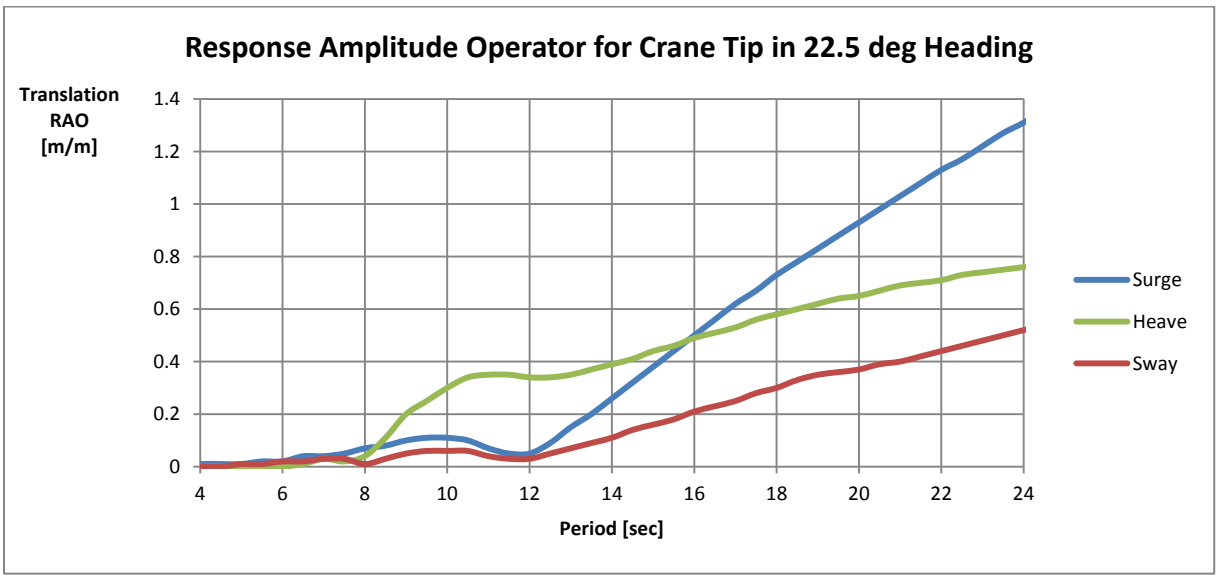

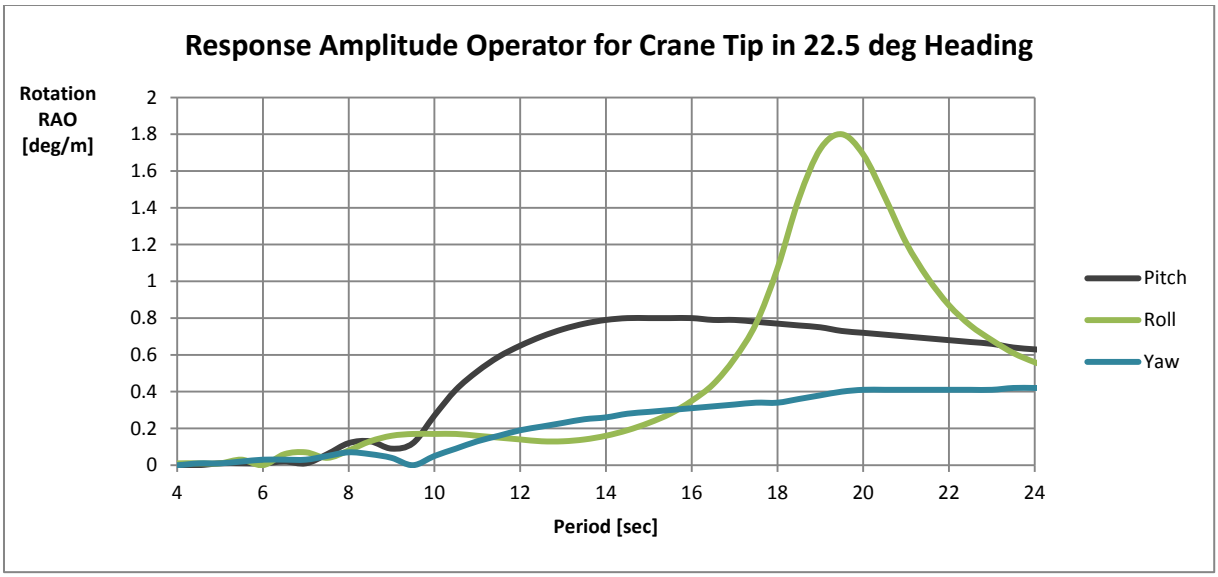
Response Amplitude Operator for Crane Tip in 22.5 deg Heading
Rotation RAO [deg/m]
2
1.8
1.6
1.4
1.2
1
0.8
0.6
0.4
0.2
0
4
6
8
10
12
14
16
18
20
22
24
Period [sec]
Pitch
Roll
Yaw

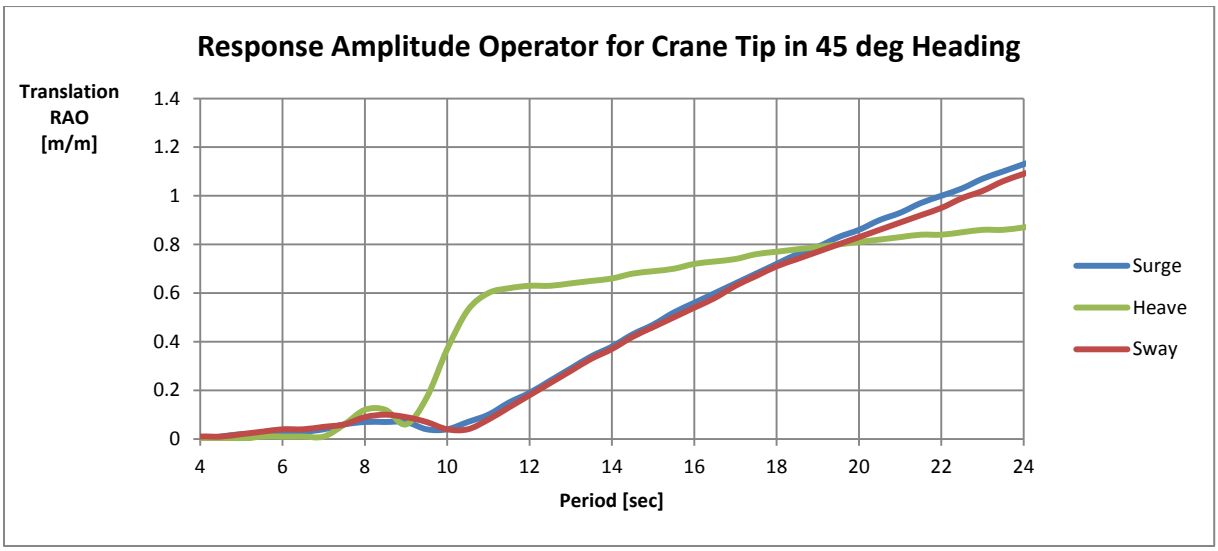
Response Amplitude Operator for Crane Tip in 45 deg Heading
Translation RAO [m/m]
1.4
1.2
1
0.8
0.6
0.4
0.2
0
4
6
8
10
12
14
16
18
20
22
24
Period [sec]
Surge
Heave
Sway

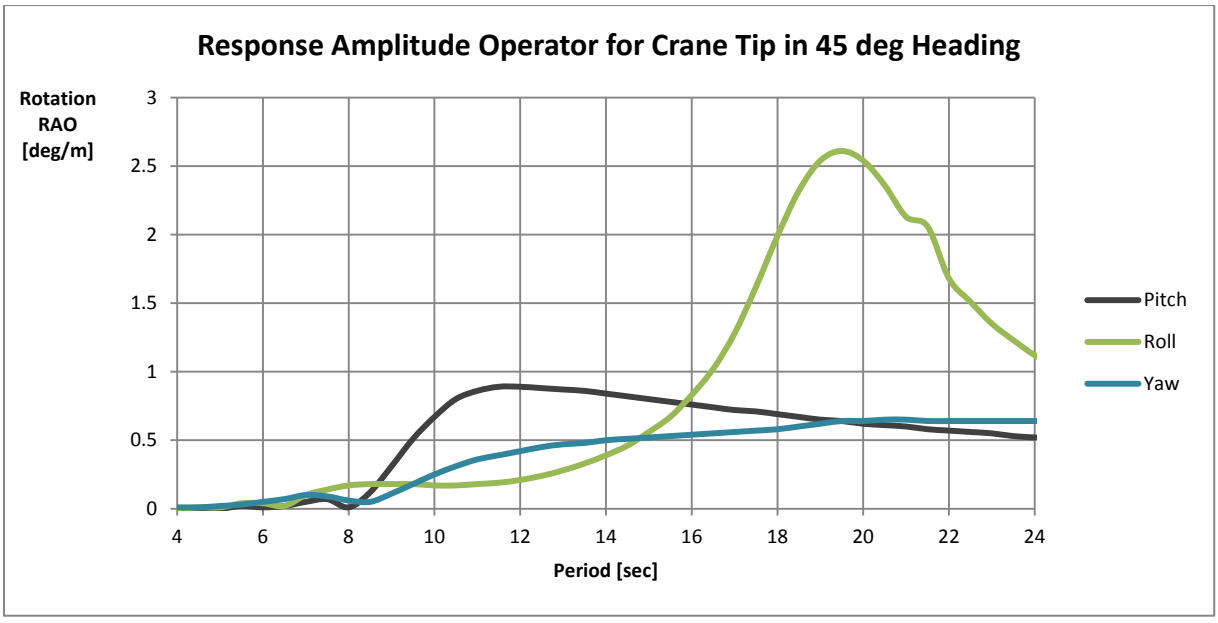
Response Amplitude Operator for Crane Tip in 45 deg Heading
Rotation RAO [deg/m]
3
2.5
2
1.5
1
0.5
0
4
6
8
10
12
14
16
18
20
22
24
Period [sec]
Pitch
Roll
Yaw

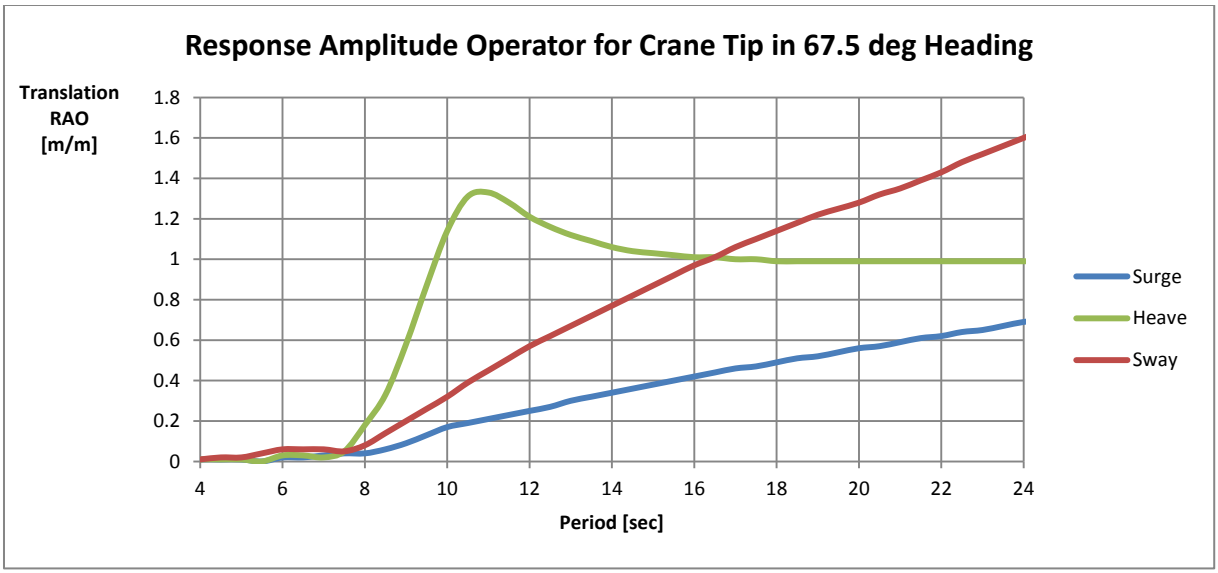
Response Amplitude Operator for Crane Tip in 67.5 deg Heading
Translation RAO [m/m]
1.8
1.6
1.4
1.2
1
0.8
0.6
0.4
0.2
0
4
6
8
10
12
14
16
18
20
22
24
Period [sec]
Surge
Heave
Sway

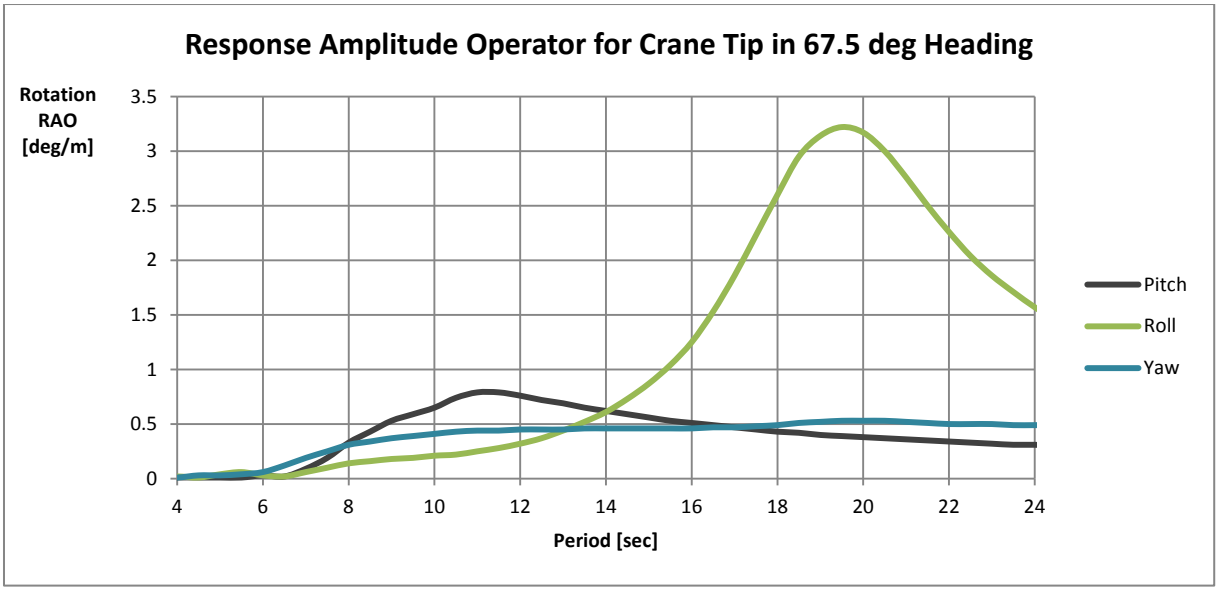
Response Amplitude Operator for Crane Tip in 67.5 deg Heading
Rotation RAO [deg/m]
3.5
3
2.5
2
1.5
1
0.5
0
4
6
8
10
12
14
16
18
20
22
24
Period [sec]
Pitch
Roll
Yaw

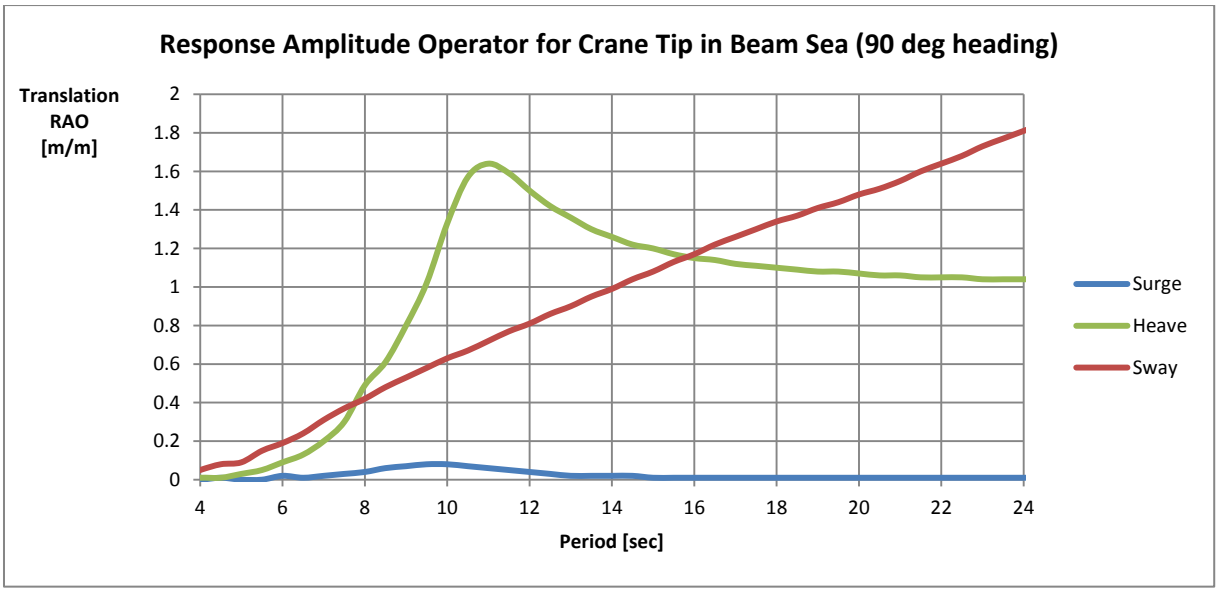
Response Amplitude Operator for Crane Tip in Beam Sea (90 deg heading)
Translation RAO [m/m]
2
1.8
1.6
1.4
1.2
1
0.8
0.6
0.4
0.2
0
4
6
8
10
12
14
16
18
20
22
24
Period [sec]
Surge
Heave
Sway

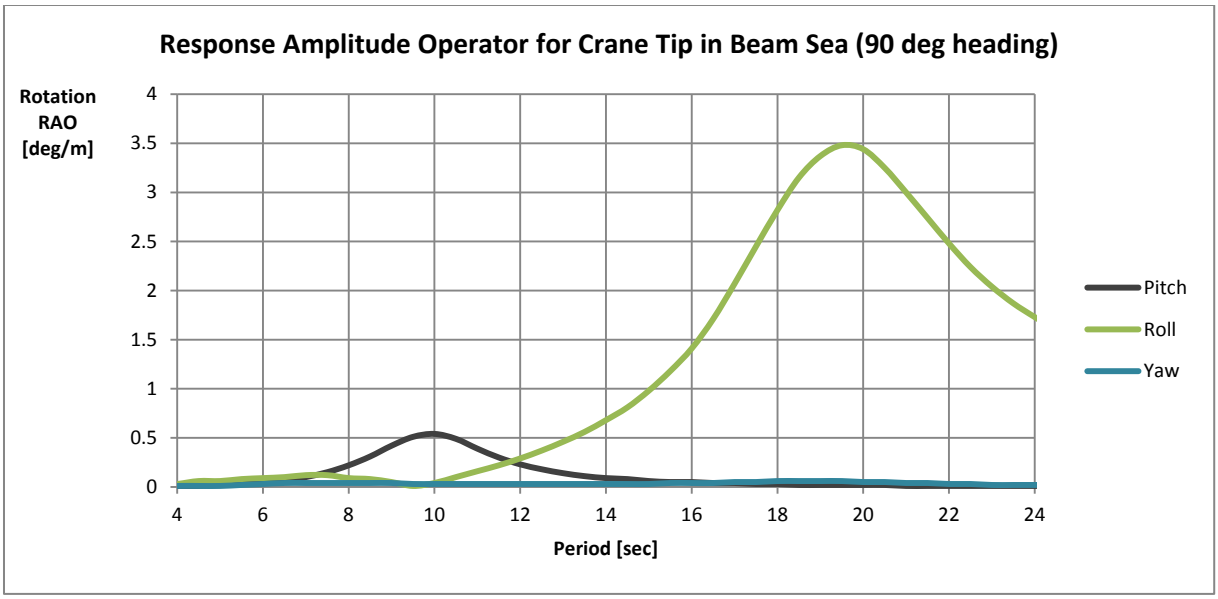
Response Amplitude Operator for Crane Tip in Beam Sea (90 deg heading)
Rotation RAO [deg/m]
4
3.5
3
2.5
2
1.5
1
0.5
0
4
6
8
10
12
14
16
18
20
22
24
Period [sec]
Pitch
Roll
Yaw

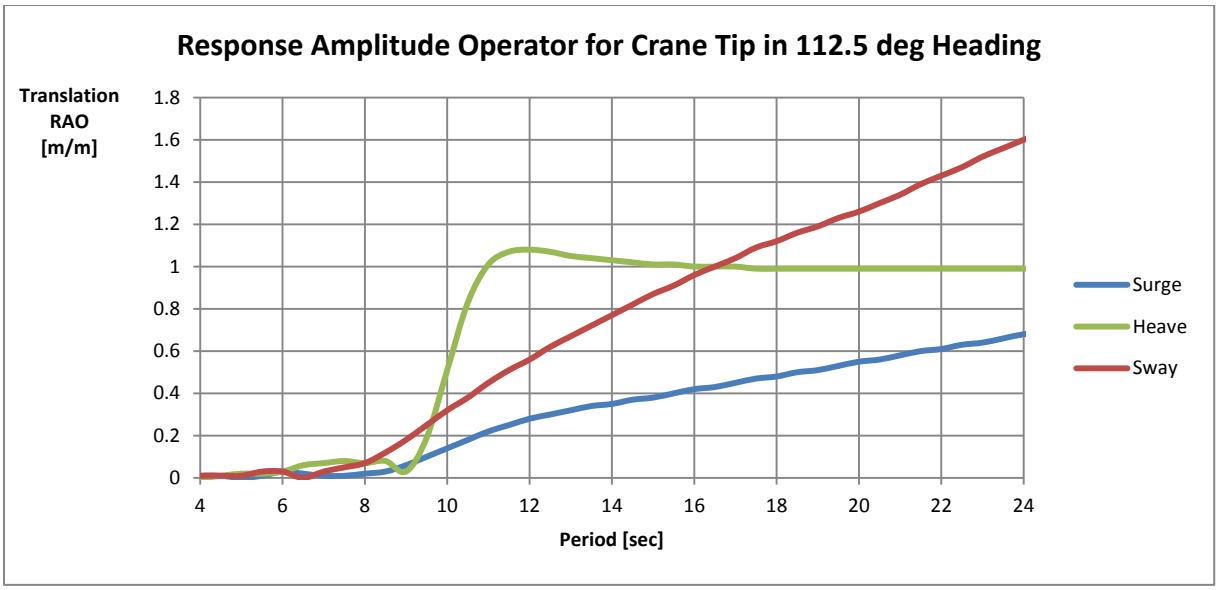
Response Amplitude Operator for Crane Tip in 112.5 deg Heading
Translation RAO [m/m]
1.8
1.6
1.4
1.2
1
0.8
0.6
0.4
0.2
0
4
6
8
10
12
14
16
18
20
22
24
Period [sec]
Surge
Heave
Sway

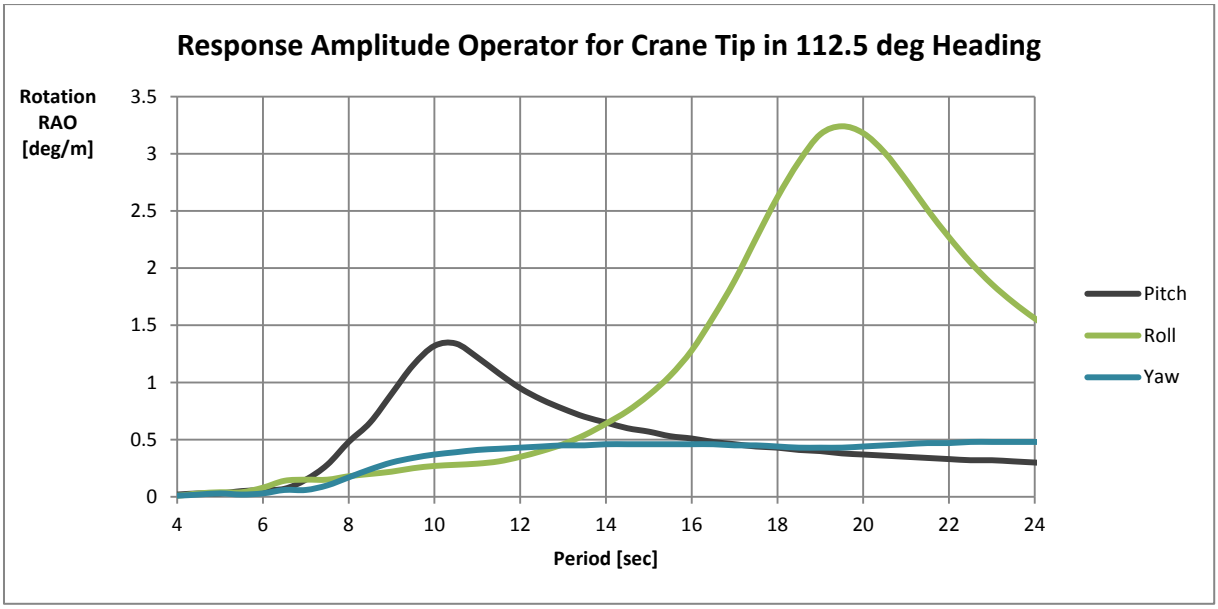
Response Amplitude Operator for Crane Tip in 112.5 deg Heading
Rotation RAO [deg/m]
3.5
3
2.5
2
1.5
1
0.5
0
4
6
8
10
12
14
16
18
20
22
24
Period [sec]
Pitch
Roll
Yaw

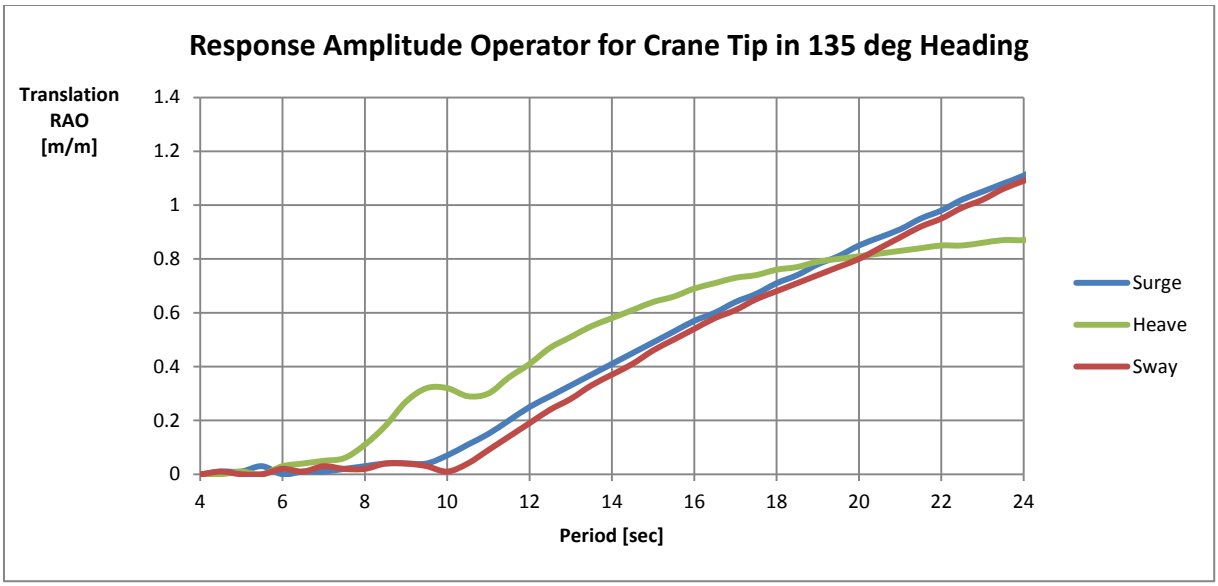
Response Amplitude Operator for Crane Tip in 135 deg Heading
Translation RAO [m/m]
1.4
1.2
1
0.8
0.6
0.4
0.2
0
4
6
8
10
12
14
16
18
20
22
24
Period [sec]
Surge
Heave
Sway

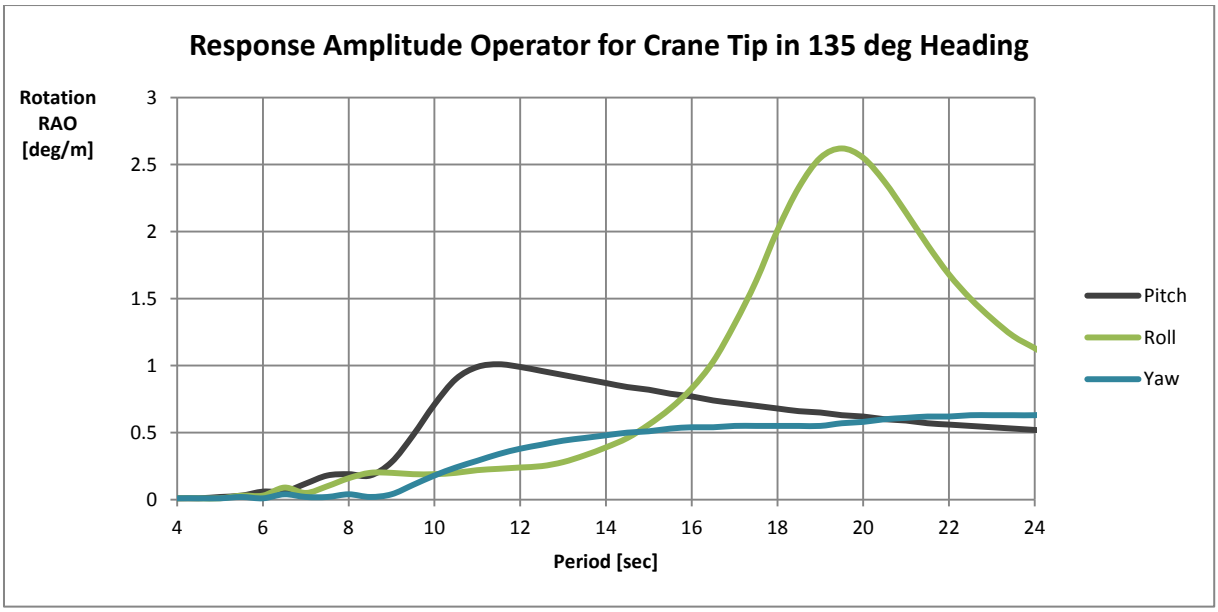
Response Amplitude Operator for Crane Tip in 135 deg Heading
Rotation RAO [deg/m]
3
2.5
2
1.5
1
0.5
0
4
6
8
10
12
14
16
18
20
22
24
Period [sec]
Pitch
Roll
Yaw

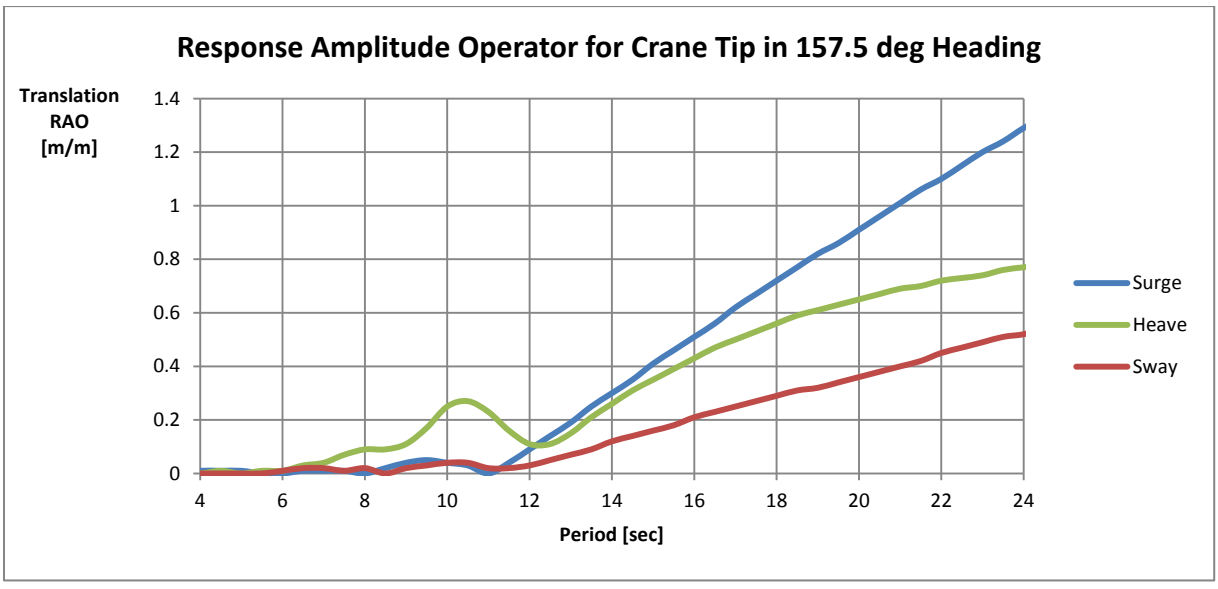
Response Amplitude Operator for Crane Tip in 157.5 deg Heading
Translation RAO [m/m]
1.4
1.2
1
0.8
0.6
0.4
0.2
0
4
6
8
10
12
14
16
18
20
22
24
Period [sec]
Surge
Heave
Sway

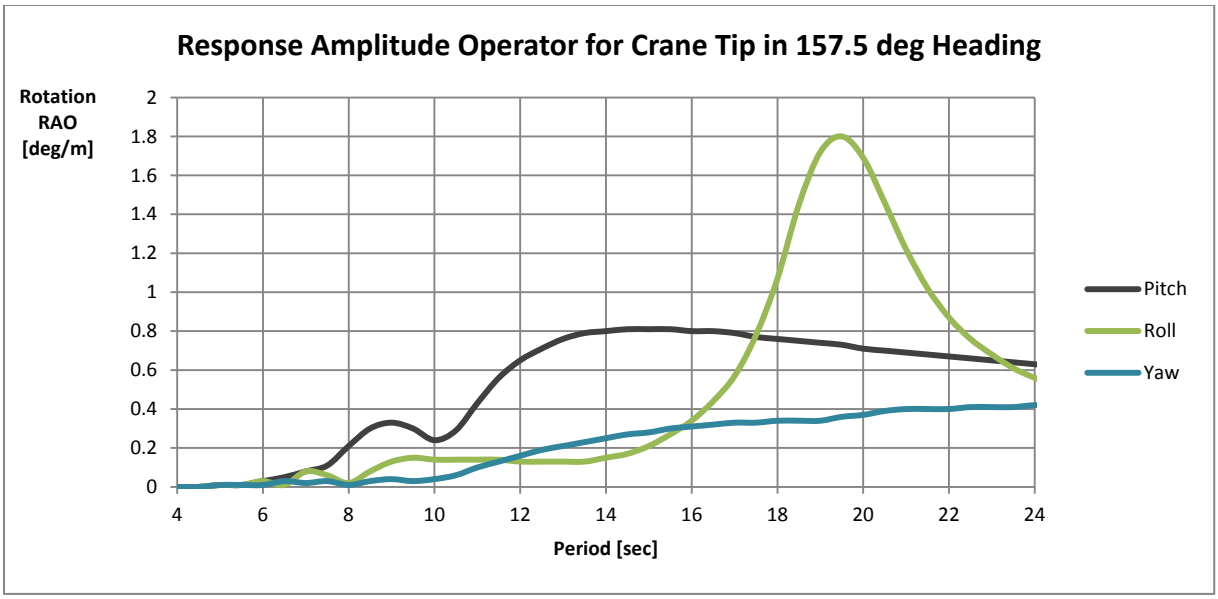
Response Amplitude Operator for Crane Tip in 157.5 deg Heading
Rotation RAO [deg/m]
2
1.8
1.6
1.4
1.2
1
0.8
0.6
0.4
0.2
0
4
6
8
10
12
14
16
18
20
22
24
Period [sec]
Pitch
Roll
Yaw

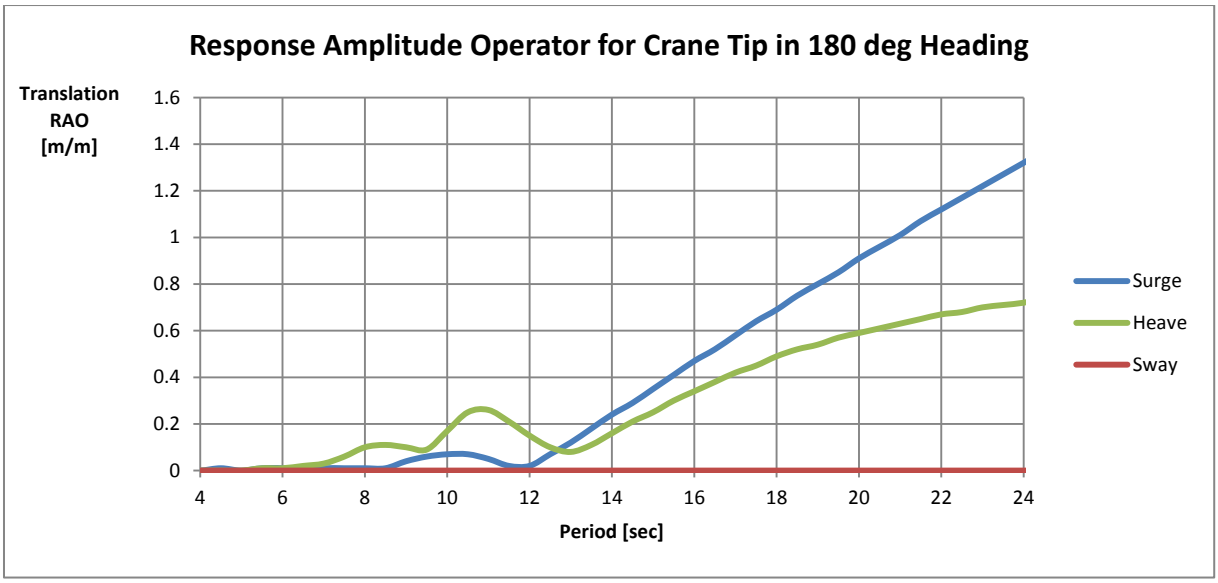
Response Amplitude Operator for Crane Tip in 180 deg Heading
Translation RAO [m/m]
1.6
1.4
1.2
1
0.8
0.6
0.4
0.2
0
4
6
8
10
12
14
16
18
20
22
24
Period [sec]
Surge
Heave
Sway

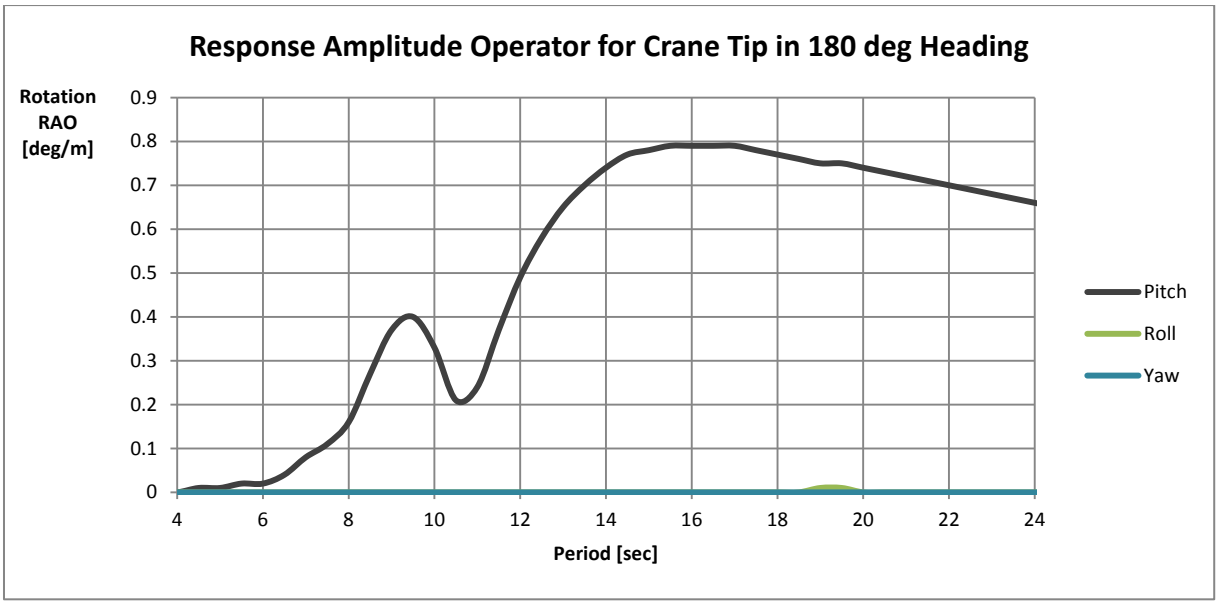
Response Amplitude Operator for Crane Tip in 180 deg Heading
Rotation RAO [deg/m]
0.9
0.8
0.7
0.6
0.5
0.4
0.3
0.2
0.1
0
4
6
8
10
12
14
16
18
20
22
24
Period [sec]
Pitch
Roll
Yaw

Response Amplitude Operators for the shuttle tanker's centre of gravity with a draft of 13 meters. The ship is located in 40 meters water depth.

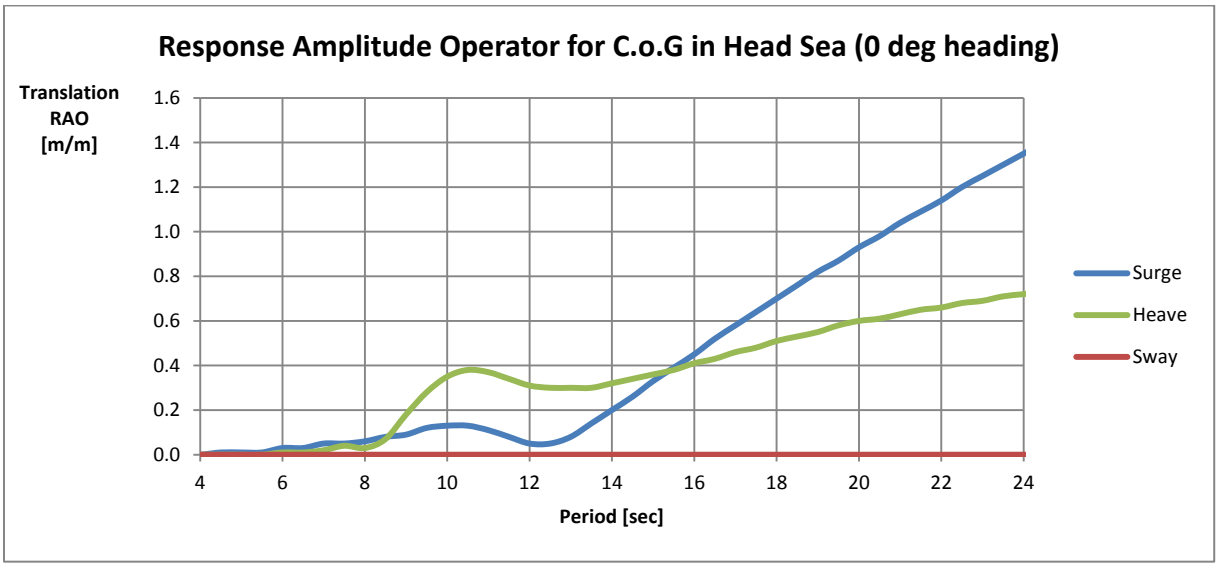

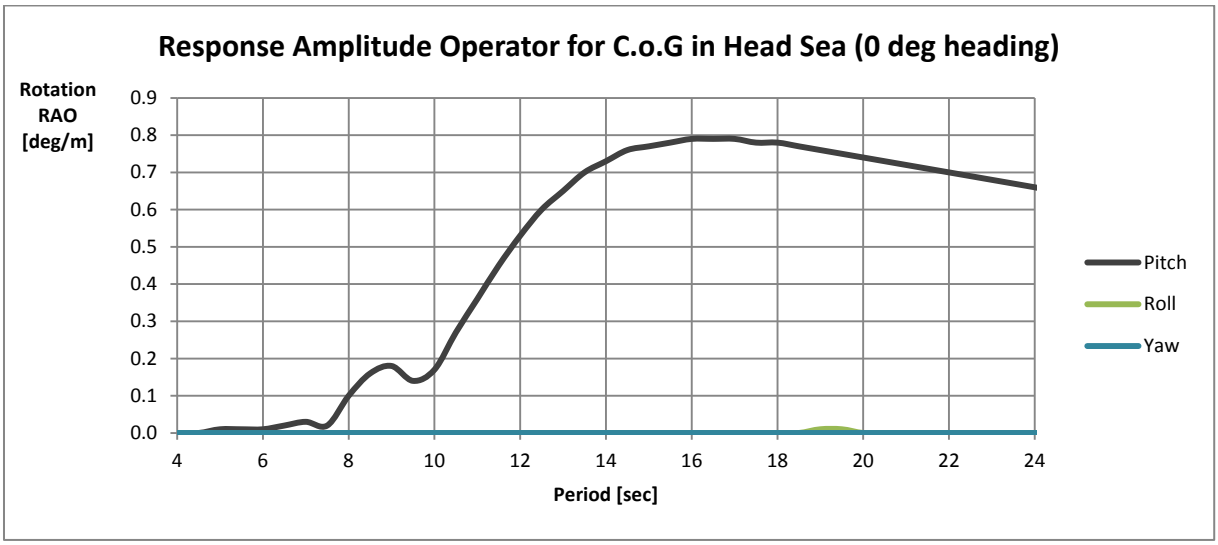

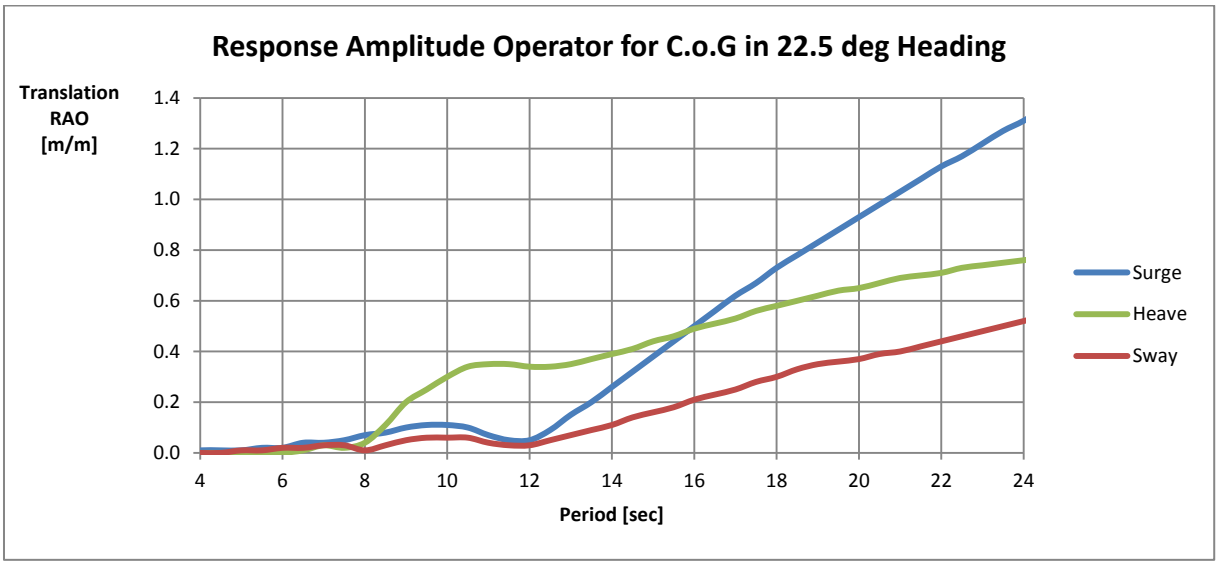

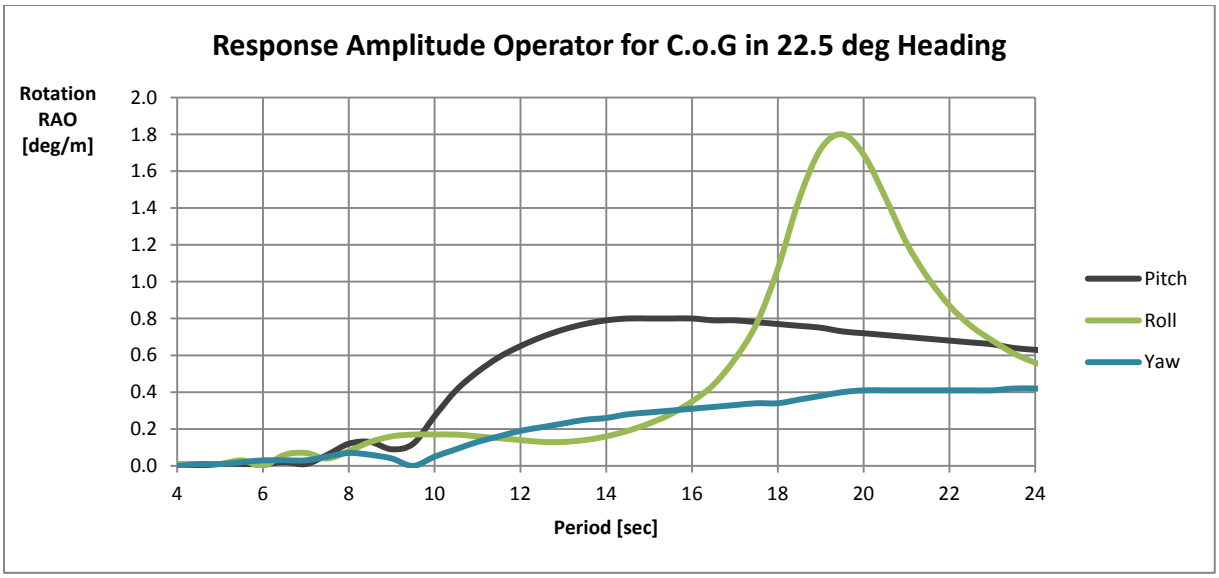
Response Amplitude Operator for C.o.G in 22.5 deg Heading
Rotation RAO [deg/m]
2.0
1.8
1.6
1.4
1.2
1.0
0.8
0.6
0.4
0.2
0.0
4
6
8
10
12
14
16
18
20
22
24
Period [sec]
Pitch
Roll
Yaw

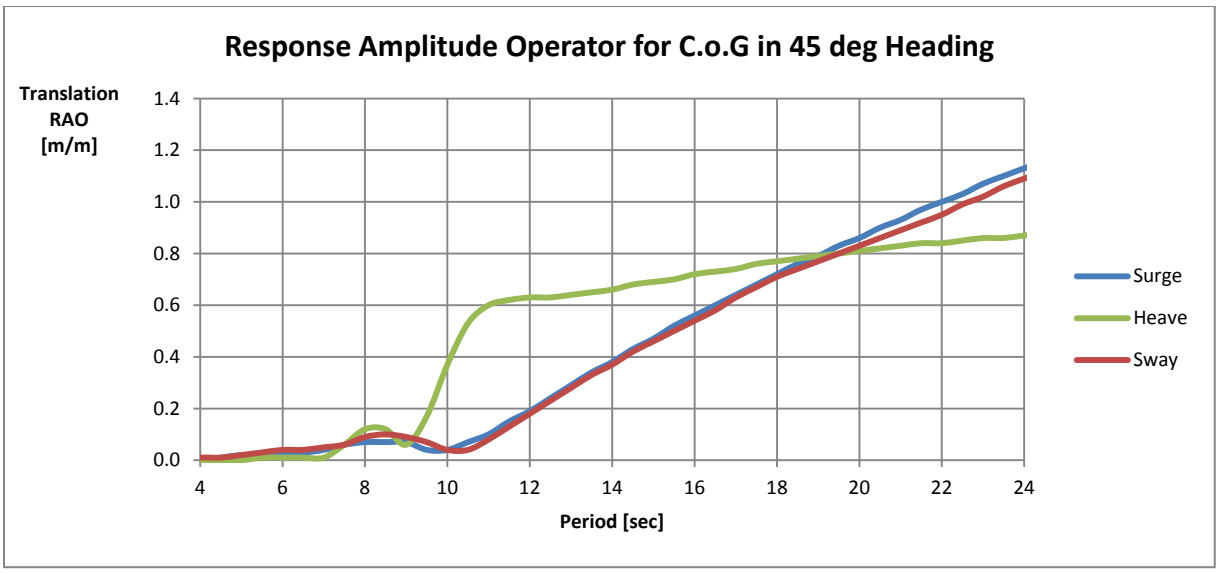
Response Amplitude Operator for C.o.G in 45 deg Heading
Translation RAO [m/m]
1.4
1.2
1.0
0.8
0.6
0.4
0.2
0.0
4
6
8
10
12
14
16
18
20
22
24
Period [sec]
Surge
Heave
Sway

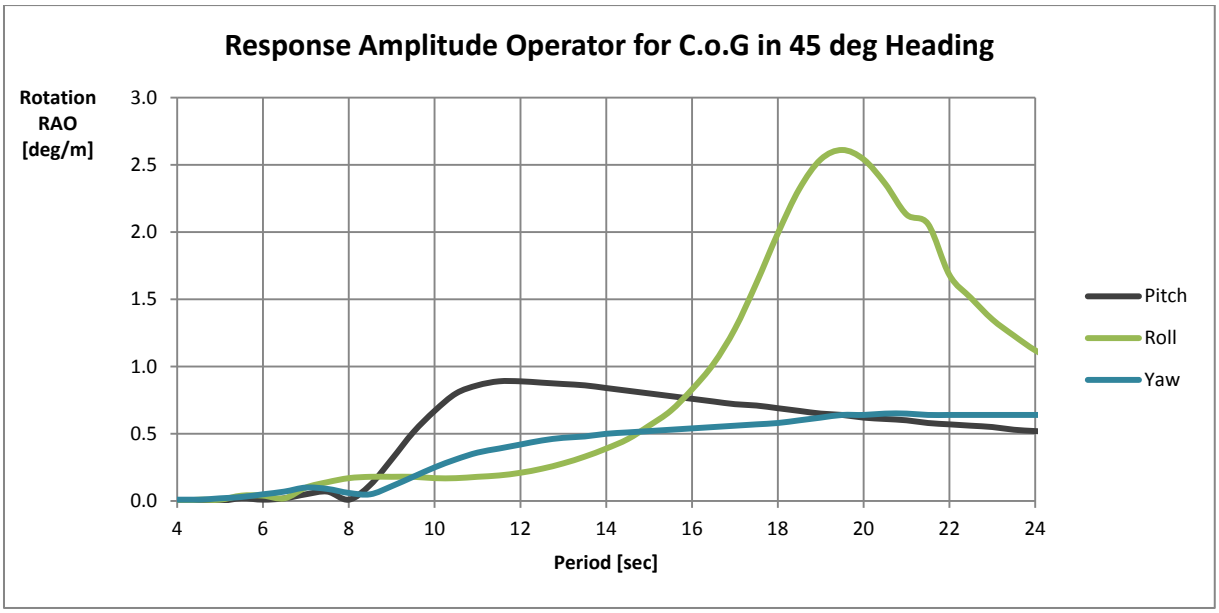
Response Amplitude Operator for C.o.G in 45 deg Heading
Rotation RAO [deg/m]
3.0
2.5
2.0
1.5
1.0
0.5
0.0
4
6
8
10
12
14
16
18
20
22
24
Period [sec]
Pitch
Roll
Yaw

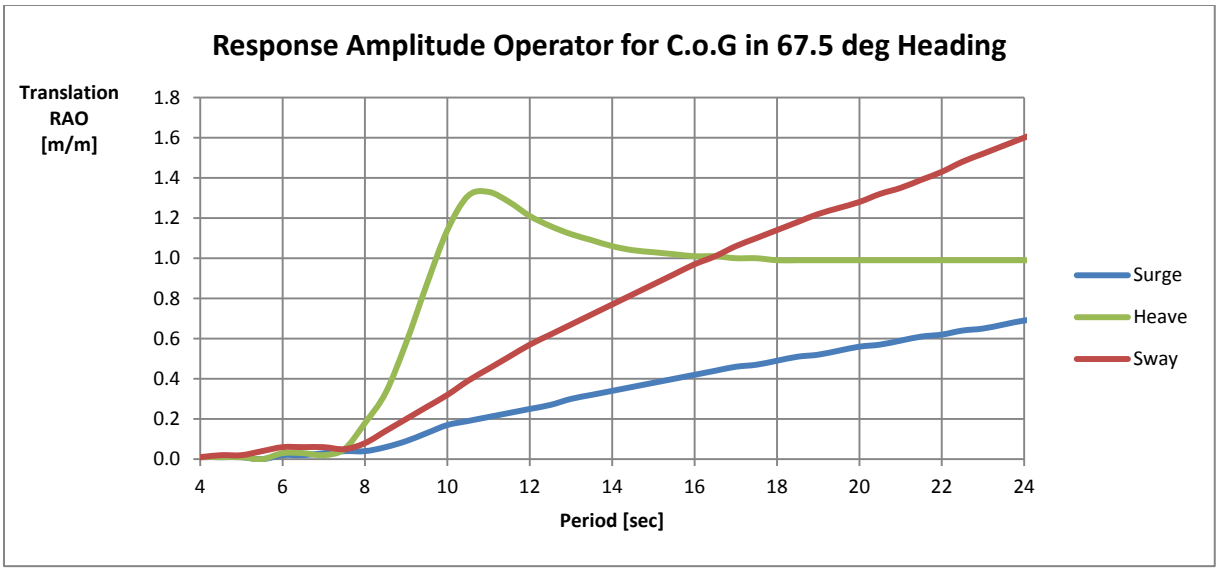
Response Amplitude Operator for C.o.G in 67.5 deg Heading
Translation RAO [m/m]
1.8
1.6
1.4
1.2
1.0
0.8
0.6
0.4
0.2
0.0
4
6
8
10
12
14
16
18
20
22
24
Period [sec]
Surge
Heave
Sway

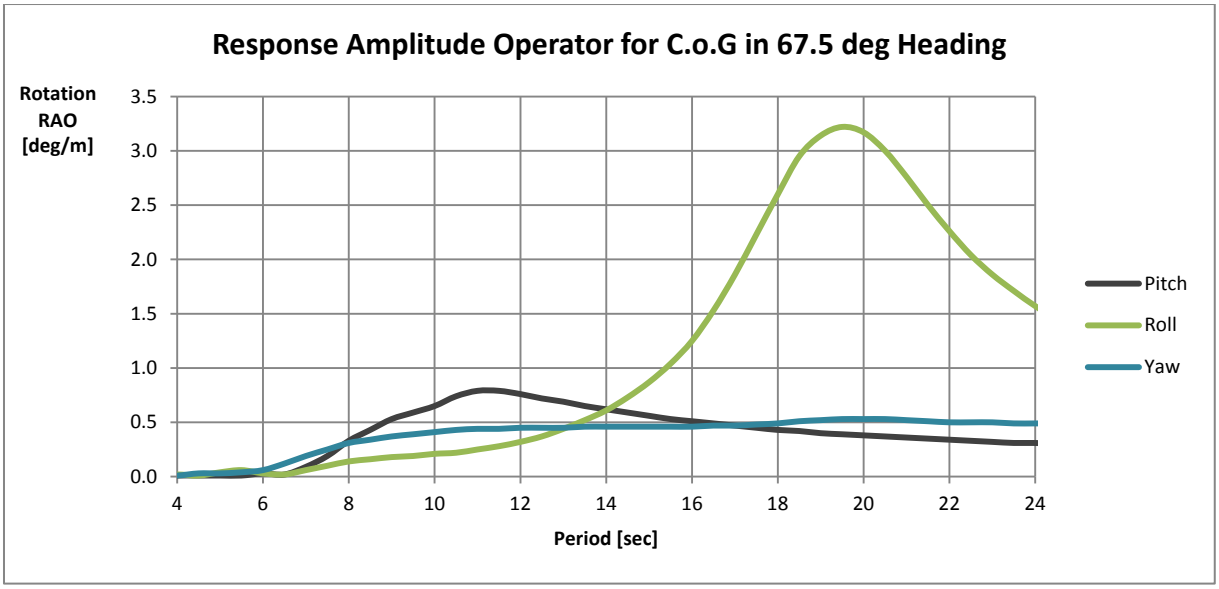
Response Amplitude Operator for C.o.G in 67.5 deg Heading
Rotation RAO [deg/m]
3.5
3.0
2.5
2.0
1.5
1.0
0.5
0.0
4
6
8
10
12
14
16
18
20
22
24
Period [sec]
Pitch
Roll
Yaw

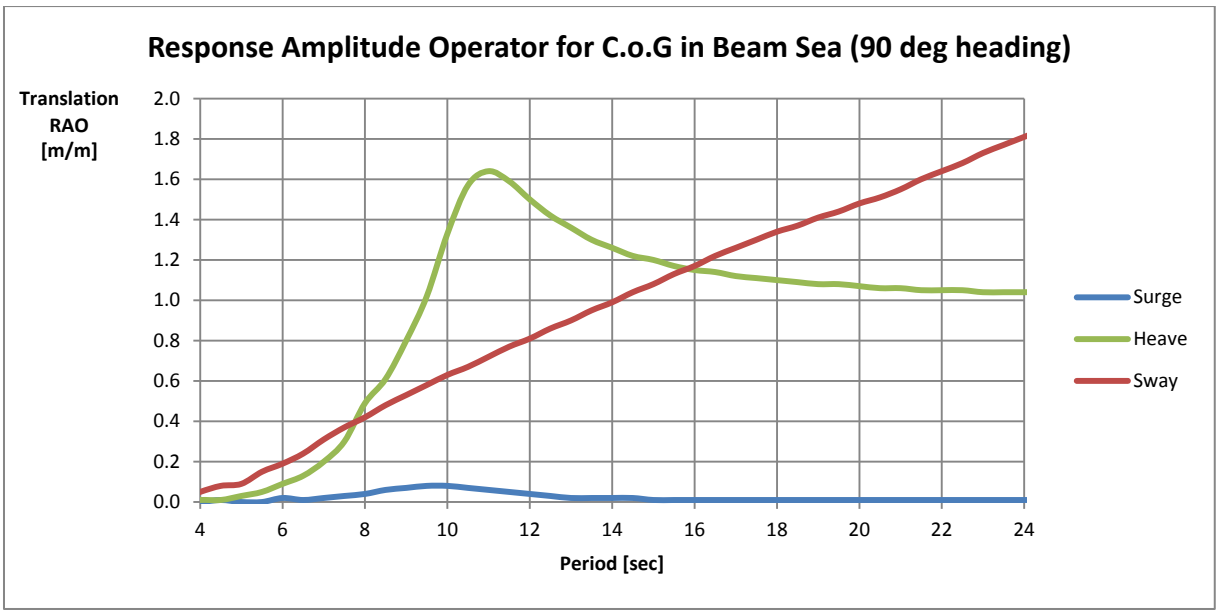
Response Amplitude Operator for C.o.G in Beam Sea (90 deg heading)
Translation RAO [m/m]
2.0
1.8
1.6
1.4
1.2
1.0
0.8
0.6
0.4
0.2
0.0
4
6
8
10
12
14
16
18
20
22
24
Period [sec]
Surge
Heave
Sway

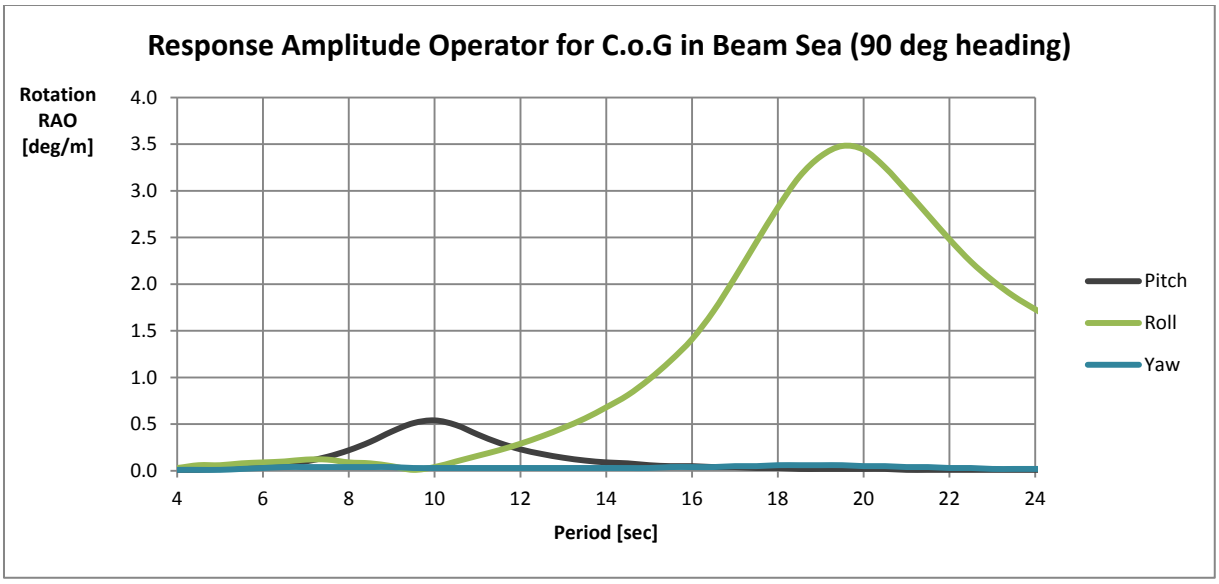
Response Amplitude Operator for C.o.G in Beam Sea (90 deg heading)
Rotation RAO [deg/m]
4.0
3.5
3.0
2.5
2.0
1.5
1.0
0.5
0.0
4
6
8
10
12
14
16
18
20
22
24
Period [sec]
Pitch
Roll
Yaw

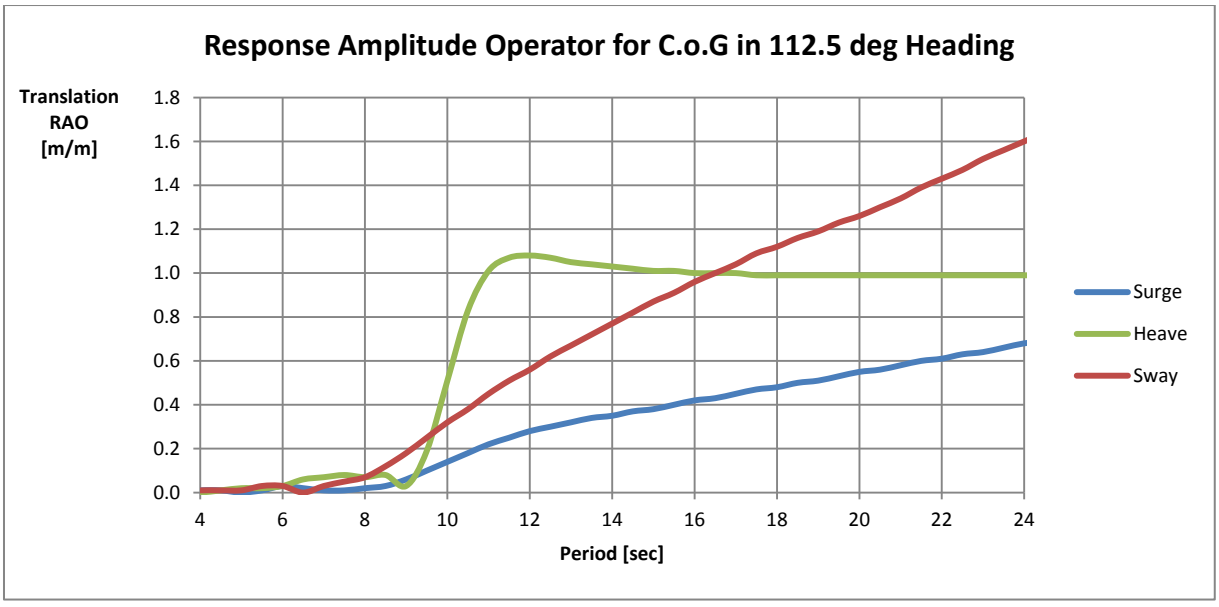
Response Amplitude Operator for C.o.G in 112.5 deg Heading
Translation RAO [m/m]
1.8
1.6
1.4
1.2
1.0
0.8
0.6
0.4
0.2
0.0
4
6
8
10
12
14
16
18
20
22
24
Period [sec]
Surge
Heave
Sway

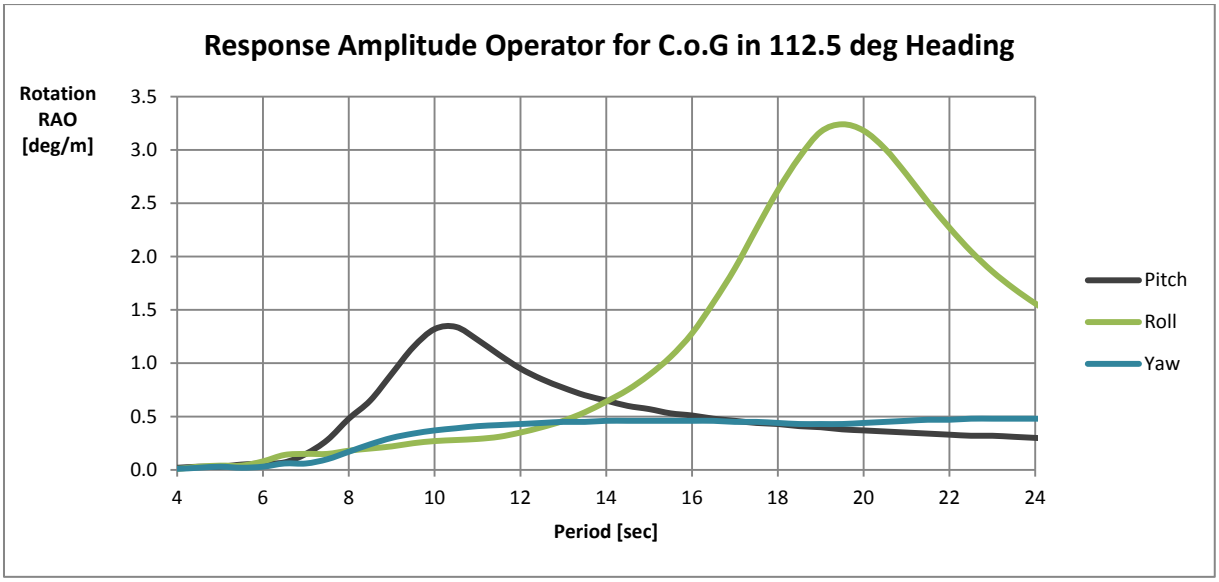
Response Amplitude Operator for C.o.G in 112.5 deg Heading
Rotation RAO [deg/m]
3.5
3.0
2.5
2.0
1.5
1.0
0.5
0.0
4
6
8
10
12
14
16
18
20
22
24
Period [sec]
Pitch
Roll
Yaw

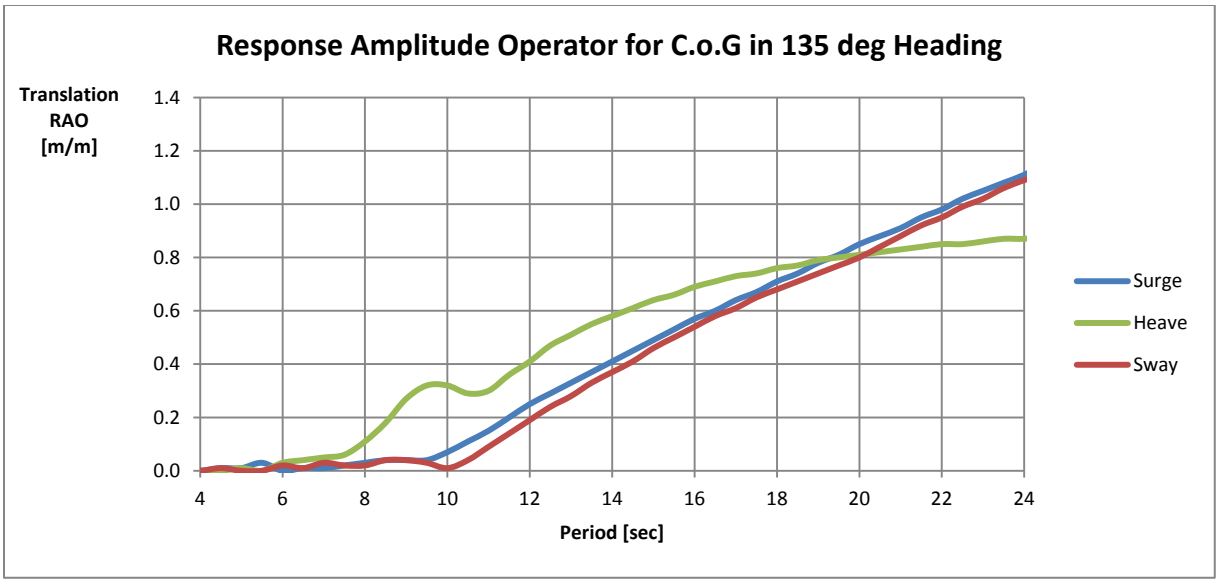
Response Amplitude Operator for C.o.G in 135 deg Heading
Translation RAO [m/m]
1.4
1.2
1.0
0.8
0.6
0.4
0.2
0.0
4
6
8
10
12
14
16
18
20
22
24
Period [sec]
Surge
Heave
Sway

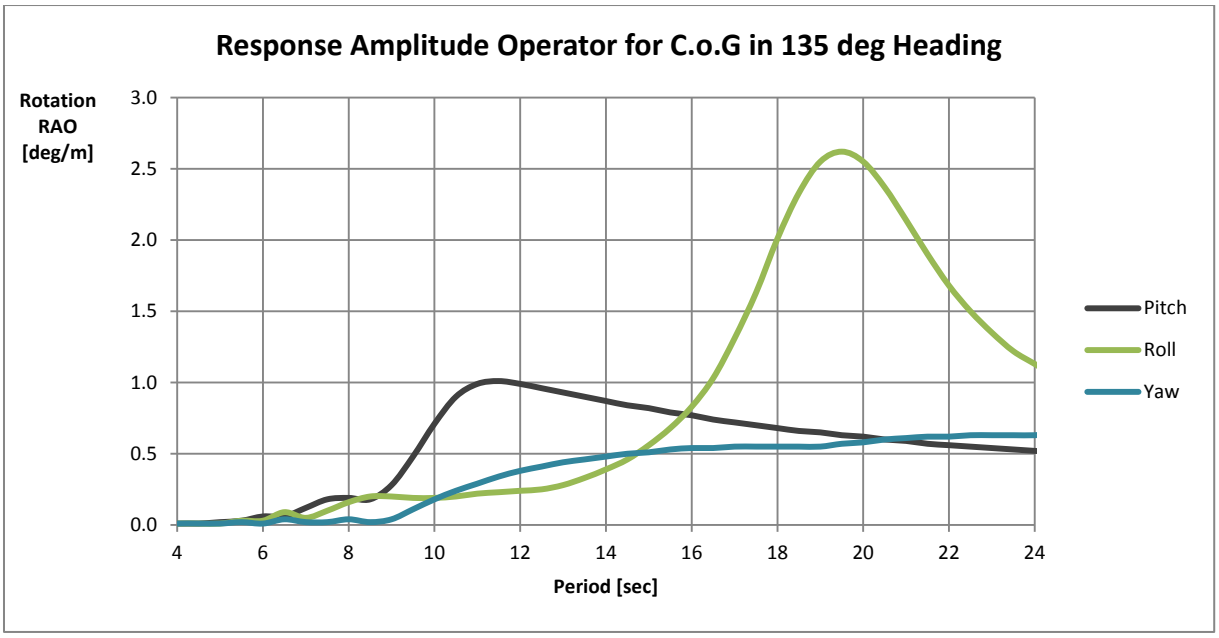
Response Amplitude Operator for C.o.G in 135 deg Heading
Rotation RAO [deg/m]
3.0
2.5
2.0
1.5
1.0
0.5
0.0
4
6
8
10
12
14
16
18
20
22
24
Period [sec]
Pitch
Roll
Yaw

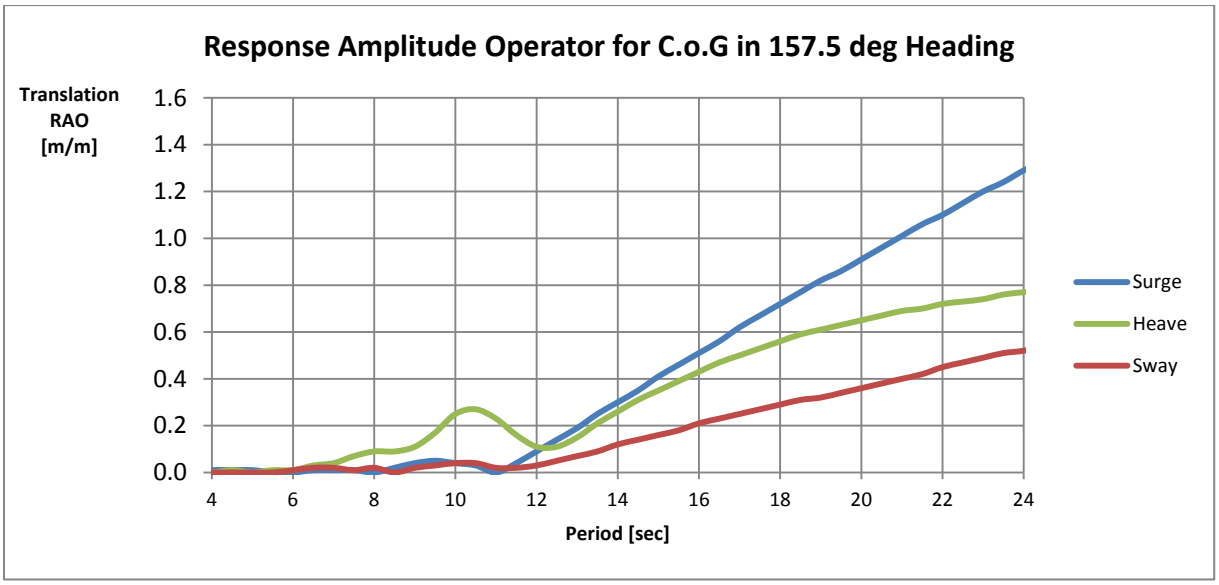
Response Amplitude Operator for C.o.G in 157.5 deg Heading
Translation RAO [m/m]
1.6
1.4
1.2
1.0
0.8
0.6
0.4
0.2
0.0
4
6
8
10
12
14
16
18
20
22
24
Period [sec]
Surge
Heave
Sway

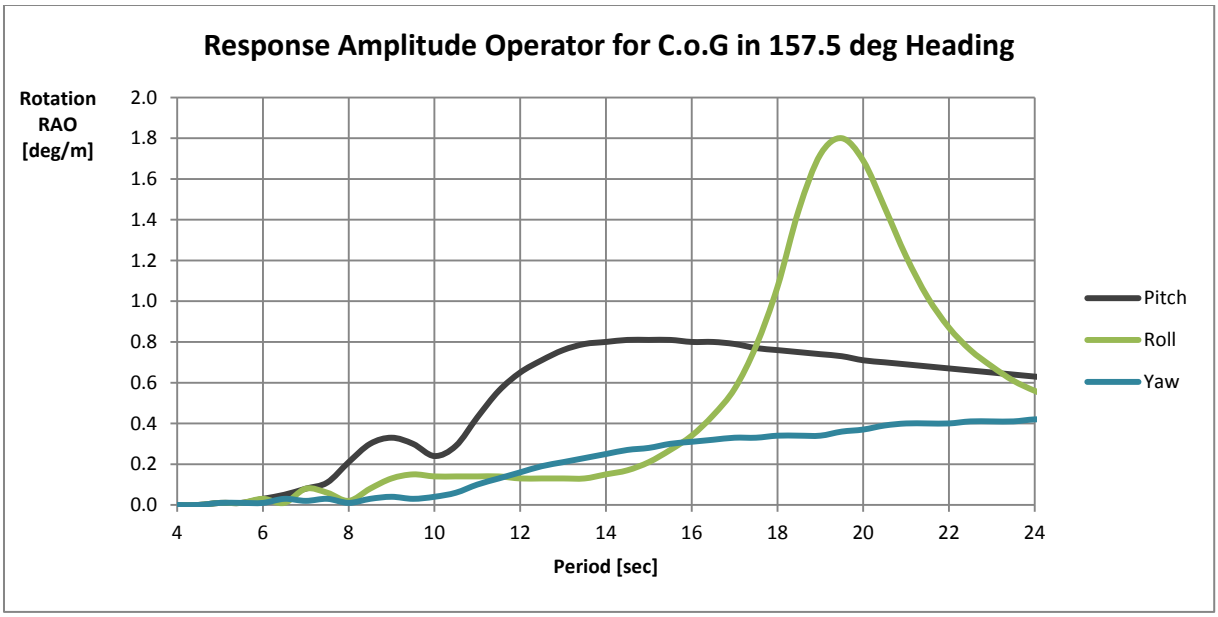
Response Amplitude Operator for C.o.G in 157.5 deg Heading
Rotation RAO [deg/m]
2.0
1.8
1.6
1.4
1.2
1.0
0.8
0.6
0.4
0.2
0.0
4
6
8
10
12
14
16
18
20
22
24
Period [sec]
Pitch
Roll
Yaw

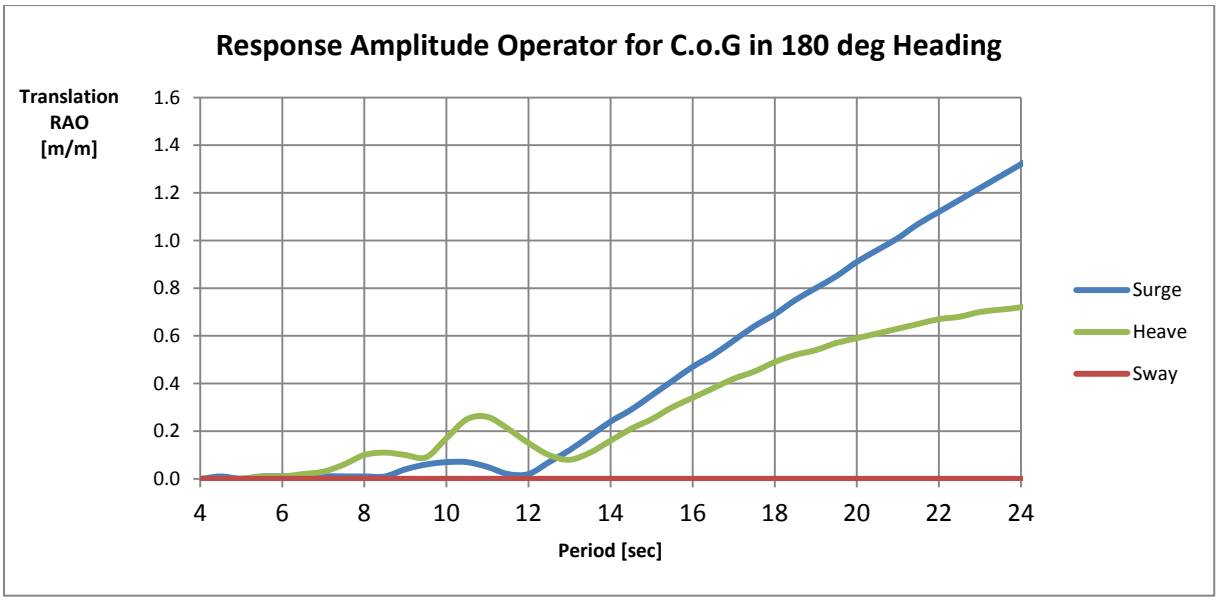
Response Amplitude Operator for C.o.G in 180 deg Heading
Translation RAO [m/m]
1.6
1.4
1.2
1.0
0.8
0.6
0.4
0.2
0.0
4
6
8
10
12
14
16
18
20
22
24
Period [sec]
Surge
Heave
Sway

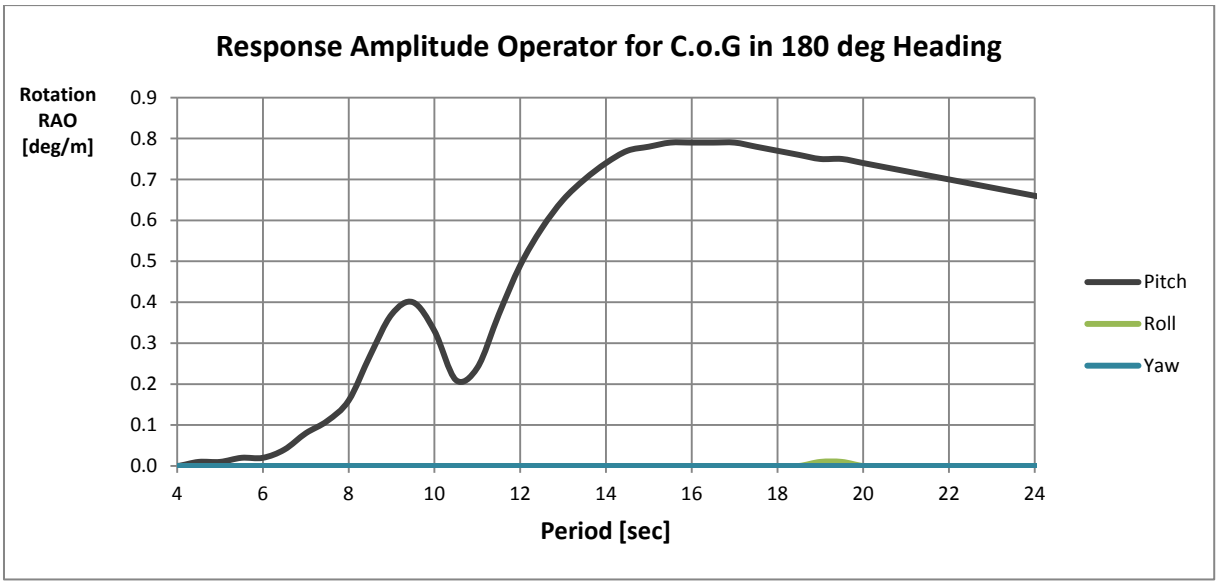
Response Amplitude Operator for C.o.G in 180 deg Heading
Rotation RAO [deg/m]
0.9
0.8
0.7
0.6
0.5
0.4
0.3
0.2
0.1
0.0
4
6
8
10
12
14
16
18
20
22
24
Period [sec]
Pitch
Roll
Yaw

Appendix C

MOSES Crane Spreader Model File

```
$
$@@@@@@@@@@@@@@@@@@@@@@@@@@@@@@@@@@@@@@@@@@@@@@@@@@@@@@@@@@@@@@@@@@@@@@@@@@@@@@@@@@@@@@@@@@@@@@@@@@@@@@@@@@@@@@
$@@@@@@@@@@@@@@@@@@@@@@@@@@@@@@@@@@@@@@@@@@@@@@@@@@@@@@@@@@@@@@@@@@@@@@@@@@@@@@@@@@@@@@@@@@@@@@@@@@@@@@@@@@@@@@
$@@@@@@@@@@@@@@@@@@@@@@@@@@@@@@@@@@@@@@@@@@@@@@@@@@@@@@@@@@@@@@@@@@@@@@@@@@@@@@@@@@@@@@@@@@@@@@@@@@@@@@@@@@@@@@
$@@                                                                          @@
$@@                                                                          @@
$@@   ----  Crane Spreader for Lifting of Wind Turbine Foundation  ----   @@
$@@                                                                          @@
$@@                                                                          @@
$@@@@@@@@@@@@@@@@@@@@@@@@@@@@@@@@@@@@@@@@@@@@@@@@@@@@@@@@@@@@@@@@@@@@@@@@@@@@@@@@@@@@@@@@@@@@@@@@@@@@@@@@@@@@@@
$@@@@@@@@@@@@@@@@@@@@@@@@@@@@@@@@@@@@@@@@@@@@@@@@@@@@@@@@@@@@@@@@@@@@@@@@@@@@@@@@@@@@@@@@@@@@@@@@@@@@@@@@@@@@@@
$@@@@@@@@@@@@@@@@@@@@@@@@@@@@@@@@@@@@@@@@@@@@@@@@@@@@@@@@@@@@@@@@@@@@@@@@@@@@@@@@@@@@@@@@@@@@@@@@@@@@@@@@@@@@@@
$
$
$
$*******************            Points
$
&describe body spreader
$
*cr0     0.00000000      0.00000000     0.00000000
*cr1    -5.00000000     -5.00000000     0.00000000
*cr2     5.00000000     -5.00000000     0.00000000
*cr3     5.00000000      5.00000000     0.00000000
*cr4    -5.00000000      5.00000000     0.00000000
$
$
&describe piece spreader -diftype 3ddif
$
$***************                Element Properties
$
~boxcs  box     250     500     15      15
$
$
$***************                Crane Spreader Elements
$
beam    sp1     ~boxcs  *cr1    *cr2
beam    sp2     ~boxcs  *cr2    *cr3
beam    sp3     ~boxcs  *cr3    *cr4
beam    sp4     ~boxcs  *cr4    *cr1
```

Appendix D

MOSES Jacket Model File

```
$@@@@@@@@@@@@@@@@@@@@@@@@@@@@@@@@@@@@@@@@@@@@@@@@@@@@@@@@@@@@@@@@@@@@@@@@@@@
$@@@@@@@@@@@@@@@@@@@@@@@@@@@@@@@@@@@@@@@@@@@@@@@@@@@@@@@@@@@@@@@@@@@@@@@@@@@
$@@@@@@@@@@@@@@@@@@@@@@@@@@@@@@@@@@@@@@@@@@@@@@@@@@@@@@@@@@@@@@@@@@@@@@@@@@@
$@@                                                                        @@
$@@                                                                        @@
$@@     --------        Jacket Foundation for Wind Turbine      --------  @@
$@@                                                                        @@
$@@                                                                        @@
$@@@@@@@@@@@@@@@@@@@@@@@@@@@@@@@@@@@@@@@@@@@@@@@@@@@@@@@@@@@@@@@@@@@@@@@@@@@
$@@@@@@@@@@@@@@@@@@@@@@@@@@@@@@@@@@@@@@@@@@@@@@@@@@@@@@@@@@@@@@@@@@@@@@@@@@@
$@@@@@@@@@@@@@@@@@@@@@@@@@@@@@@@@@@@@@@@@@@@@@@@@@@@@@@@@@@@@@@@@@@@@@@@@@@@
$
$
$*******************            Points
$
&describe body jacket
$
*pt0      0.00000000      0.00000000      0.00000000
$
*pt1     -5.00000000     -5.00000000      0.00000000
*pt2      5.00000000     -5.00000000      0.00000000
*pt3      5.00000000      5.00000000      0.00000000
*pt4     -5.00000000      5.00000000      0.00000000
$
*pt5     -5.00000000     -5.00000000     -2.40000000
*pt6      5.00000000     -5.00000000     -2.40000000
*pt7      5.00000000      5.00000000     -2.40000000
*pt8     -5.00000000      5.00000000     -2.40000000
$
*pt9     -5.13524590     -5.13524590     -3.40000000
*pt10     5.13524590     -5.13524590     -3.40000000
*pt11     5.13524590      5.13524590     -3.40000000
*pt12    -5.13524590      5.13524590     -3.40000000
$
*pt13     0.00000000     -5.75903651     -8.01226994
*pt14     5.75903651      0.00000000     -8.01226994
*pt15     0.00000000      5.75903651     -8.01226994
*pt16    -5.75903651      0.00000000     -8.01226994
$
*pt17    -6.55532787     -6.55532787    -13.90000000
*pt18     6.55532787     -6.55532787    -13.90000000
*pt19     6.55532787      6.55532787    -13.90000000
*pt20    -6.55532787      6.55532787    -13.90000000
$
*pt21     0.00000000     -7.35664453    -19.82488682
*pt22     7.35664453      0.00000000    -19.82488682
*pt23     0.00000000      7.35664453    -19.82488682
*pt24    -7.35664453      0.00000000    -19.82488682
$
*pt25    -8.38114754     -8.38114754    -27.40000000
*pt26     8.38114754     -8.38114754    -27.40000000
*pt27     8.38114754      8.38114754    -27.40000000
*pt28    -8.38114754      8.38114754    -27.40000000
$
*pt29     0.00000000     -9.33940781    -34.48531832
*pt30     9.33940781      0.00000000    -34.48531832
*pt31     0.00000000      9.33940781    -34.48531832
*pt32    -9.33940781      0.00000000    -34.48531832
$
*pt33   -10.54508197    -10.54508197    -43.40000000
*pt34    10.54508197    -10.54508197    -43.40000000
*pt35    10.54508197     10.54508197    -43.40000000
*pt36   -10.54508197     10.54508197    -43.40000000
$
*pt37     0.00000000    -11.72848361    -52.15000000
*pt38    11.72848361      0.00000000    -52.15000000
*pt39     0.00000000     11.72848361    -52.15000000
*pt40   -11.72848361      0.00000000    -52.15000000
```

```
*pt41   -11.72848361    -11.72848361    -52.15000000
*pt42    11.72848361    -11.72848361    -52.15000000
*pt43    11.72848361     11.72848361    -52.15000000
*pt44   -11.72848361     11.72848361    -52.15000000
$
*pt45   -13.25000000    -13.25000000    -63.40000000
*pt46    13.25000000    -13.25000000    -63.40000000
*pt47    13.25000000     13.25000000    -63.40000000
*pt48   -13.25000000     13.25000000    -63.40000000
$
*pt49   -13.25000000    -13.25000000    -68.40000000
*pt50    13.25000000    -13.25000000    -68.40000000
*pt51    13.25000000     13.25000000    -68.40000000
*pt52   -13.25000000     13.25000000    -68.40000000
$
*top      0.00000000      0.00000000      0.00000000
$
&describe piece jacket -diftype 3ddif
$
$
$***************               Element Properties
$
~top    plate   135     135     2000    1000
$
~tube1  tube    508     15
~tube2  tube    610     15
~tube3  tube    711     15
~tube4  tube    813     30
~tube5  tube    960     35
~tube6  tube    1219    40
$
$
$***************               Jacket Elements
$
$
$
$***************               Top Box:
$
plate   top     ~top    *pt1    *pt2    *pt3    *pt4
$
$
$***************               Top:
$
beam beam1  ~tube5      *pt1    *pt5
beam beam2  ~tube5      *pt2    *pt6
beam beam3  ~tube5      *pt3    *pt7
beam beam4  ~tube5      *pt4    *pt8
$
beam beam5  ~tube5      *pt1    *pt2
beam beam6  ~tube5      *pt2    *pt3
beam beam7  ~tube5      *pt3    *pt4
beam beam8  ~tube5      *pt4    *pt1
$
$
$***************               Chords:
$
beam beam9  ~tube4      *pt5    *pt9
beam beam10 ~tube4      *pt9    *pt17
beam beam11 ~tube4      *pt17   *pt25
beam beam12 ~tube4      *pt25   *pt33
beam beam13 ~tube4      *pt33   *pt41
$
beam beam14 ~tube4      *pt6    *pt10
beam beam15 ~tube4      *pt10   *pt18
beam beam16 ~tube4      *pt18   *pt26
beam beam17 ~tube4      *pt26   *pt34
beam beam18 ~tube4      *pt34   *pt42
```

```
beam beam19 ~tube4      *pt7    *pt11
beam beam20 ~tube4      *pt11   *pt19
beam beam21 ~tube4      *pt19   *pt27
beam beam22 ~tube4      *pt27   *pt35
beam beam23 ~tube4      *pt35   *pt43
$
beam beam24 ~tube4      *pt8    *pt12
beam beam25 ~tube4      *pt12   *pt20
beam beam26 ~tube4      *pt20   *pt28
beam beam27 ~tube4      *pt28   *pt36
beam beam28 ~tube4      *pt36   *pt44
$
$
$***************               Piles & Bottom Chords:
$
beam beam29 ~tube6      *pt41   *pt45
beam beam30 ~tube6      *pt45   *pt49
beam beam31 ~tube6      *pt42   *pt46
beam beam32 ~tube6      *pt46   *pt50
beam beam33 ~tube6      *pt43   *pt47
beam beam34 ~tube6      *pt47   *pt51
beam beam35 ~tube6      *pt44   *pt48
beam beam36 ~tube6      *pt48   *pt52
$
$
$***************               Upper Diagonals:
$
beam beam37 ~tube1      *pt9    *pt13
beam beam38 ~tube1      *pt10   *pt13
beam beam39 ~tube1      *pt13   *pt17
beam beam40 ~tube1      *pt13   *pt18
beam beam41 ~tube1      *pt17   *pt21
beam beam42 ~tube1      *pt18   *pt21
beam beam43 ~tube1      *pt21   *pt25
beam beam44 ~tube1      *pt21   *pt26
$
beam beam45 ~tube1      *pt10   *pt14
beam beam46 ~tube1      *pt11   *pt14
beam beam47 ~tube1      *pt14   *pt18
beam beam48 ~tube1      *pt14   *pt19
beam beam49 ~tube1      *pt18   *pt22
beam beam50 ~tube1      *pt19   *pt22
beam beam51 ~tube1      *pt22   *pt26
beam beam52 ~tube1      *pt22   *pt27
$
beam beam53 ~tube1      *pt11   *pt15
beam beam54 ~tube1      *pt12   *pt15
beam beam55 ~tube1      *pt15   *pt19
beam beam56 ~tube1      *pt15   *pt20
beam beam57 ~tube1      *pt19   *pt23
beam beam58 ~tube1      *pt20   *pt23
beam beam59 ~tube1      *pt23   *pt27
beam beam60 ~tube1      *pt23   *pt28
$
beam beam61 ~tube1      *pt9    *pt16
beam beam62 ~tube1      *pt12   *pt16
beam beam63 ~tube1      *pt16   *pt17
beam beam64 ~tube1      *pt16   *pt20
beam beam65 ~tube1      *pt17   *pt24
beam beam66 ~tube1      *pt20   *pt24
beam beam67 ~tube1      *pt24   *pt25
beam beam68 ~tube1      *pt24   *pt28
```

```
$***************                Lower Diagonals:
$
beam beam69 ~tube2      *pt25   *pt29
beam beam70 ~tube2      *pt26   *pt29
beam beam71 ~tube2      *pt29   *pt33
beam beam72 ~tube2      *pt29   *pt34
beam beam73 ~tube2      *pt33   *pt37
beam beam74 ~tube2      *pt34   *pt37
beam beam75 ~tube2      *pt37   *pt45
beam beam76 ~tube2      *pt37   *pt46
$
beam beam77 ~tube2      *pt26   *pt30
beam beam78 ~tube2      *pt27   *pt30
beam beam79 ~tube2      *pt30   *pt34
beam beam80 ~tube2      *pt30   *pt35
beam beam81 ~tube2      *pt34   *pt38
beam beam82 ~tube2      *pt35   *pt38
beam beam83 ~tube2      *pt38   *pt46
beam beam84 ~tube2      *pt38   *pt47
$
beam beam85 ~tube2      *pt27   *pt31
beam beam86 ~tube2      *pt28   *pt31
beam beam87 ~tube2      *pt31   *pt35
beam beam88 ~tube2      *pt31   *pt36
beam beam89 ~tube2      *pt35   *pt39
beam beam90 ~tube2      *pt36   *pt39
beam beam91 ~tube2      *pt39   *pt47
beam beam92 ~tube2      *pt39   *pt48
$
beam beam93 ~tube2      *pt25   *pt32
beam beam94 ~tube2      *pt28   *pt32
beam beam95 ~tube2      *pt32   *pt33
beam beam96 ~tube2      *pt32   *pt36
beam beam97 ~tube2      *pt33   *pt40
beam beam98 ~tube2      *pt36   *pt40
beam beam99 ~tube2      *pt40   *pt45
beam beam100 ~tube2     *pt40   *pt48
$
$
$***************                Horizontal Braces:
$
beam beam101 ~tube3     *pt37   *pt41
beam beam102 ~tube3     *pt37   *pt42
$
beam beam103 ~tube3     *pt38   *pt42
beam beam104 ~tube3     *pt38   *pt43
$
beam beam105 ~tube3     *pt39   *pt43
beam beam106 ~tube3     *pt39   *pt44
$
beam beam107 ~tube3     *pt40   *pt41
beam beam108 ~tube3     *pt40   *pt44
```

Appendix E

Complete MOSES Simulation File

```
$
$@@@@@@@@@@@@@@@@@@@@@@@@@@@@@@@@@@@@@@@@@@@@@@@@@@@@@@@@@@@@@@@@@@@@@@@@@@@
$@@@@@@@@@@@@@@@@@@@@@@@@@@@@@@@@@@@@@@@@@@@@@@@@@@@@@@@@@@@@@@@@@@@@@@@@@@@
$@@@@@@@@@@@@@@@@@@@@@@@@@@@@@@@@@@@@@@@@@@@@@@@@@@@@@@@@@@@@@@@@@@@@@@@@@@@
$@@                                                                       @@
$@@                                                                       @@
$@@      -------   Installation of Wind Turbine Foundation   -------      @@
$@@                                                                       @@
$@@                                                                       @@
$@@@@@@@@@@@@@@@@@@@@@@@@@@@@@@@@@@@@@@@@@@@@@@@@@@@@@@@@@@@@@@@@@@@@@@@@@@@
$@@@@@@@@@@@@@@@@@@@@@@@@@@@@@@@@@@@@@@@@@@@@@@@@@@@@@@@@@@@@@@@@@@@@@@@@@@@
$@@@@@@@@@@@@@@@@@@@@@@@@@@@@@@@@@@@@@@@@@@@@@@@@@@@@@@@@@@@@@@@@@@@@@@@@@@@
$
$
$***************************************      SET BASIC PARAMETERS
$
&dimen -dimen meters m-tons
&TITLE Installation of Wind Turbine Foundation
&set diftyp = 3ddif
&set wdepth = 40
&set jackposx = 120
&set jackposy = -47
&set jackposz = 72
&set craneheight = 103
&set dweigth = 515
&default -depth %wdepth
&default -flood yes
&default -tanaka 1
$
$
$***************************************      Get Model
$
INMODEL
&env                                          $ make sure there is no
$                                             $ environment (flat seas)
$
$***************************************      Create Crane Boom Point
$                                             and Virtual Crane
$
MEDIT
   &describe body tanker
   *boompt %jackposx %jackposy %craneheight
   *c1 %jackposx-20 %jackposy+30 10
   *c2 %jackposx-20 %jackposy+30 %craneheight-10
   *c3 %jackposx %jackposy %craneheight+2
   *v1 %jackposx-13 20 21.6
   *v2 %jackposx-13 20 27
   *v3 %jackposx+13 20 21.6
   *v4 %jackposx+13 20 27
   &describe piece tanker -color green
   ~cr1 tube 5000 30
   ~cb1 box 1500 2500 30 30
   ~vt1 box 1500 1500 10 10
   beam crane1 ~cr1 *c1 *c2
   beam crane2 ~cb1 *c2 *c3
   beam tugbox1 ~vt1 *v1 *v2
   beam tugbox2 ~vt1 *v3 *v4
END_medit
$
$
$***************************************      Set Draft for Vessel to 13 m
$
&describe body tanker
&instate tanker -condition 13 0 0
$
$
```

```
                                    jacketinstall.cif
$************************************      Insert Dummy Weigth
$                                           to Account for Jacket Weigth
$                                           Before Ballasting the Vessel
$
MEDIT
   *dummy  %jackposx %jackposy %craneheight
   #weight *dummy %dweigth 10 10 10 -category dummy_w
END_medit
$
$
$************************************      Computing Vessel Weight
$
&weight -compute 14.95 14.7 60.7 60.7         $ ref Faltinsen p71
$
$
$************************************      Delete Dummy Weight
$
&apply -fraction -category dummy_w @ 0
$
$
$************************************      Instate Jacket
$
&describe body jacket
&instate -locate jacket %jackposx %jackposy %jackposz
$
$
$************************************      Instate Crane Spreader
$                                           above Jacket
$
&describe body spreader
&instate -locate spreader %jackposx %jackposy %jackposz+3
$
$
$************************************      Define Lifting Sling
$
MEDIT
   &set hooklen0 = &point(d_node *boompt *cr0)
   ~boom sling 80 -len %hooklen0-13 -emodulus 65000 -fyield 550
   ~cr-sli1 sling 80 -len 14.8 -emodulus 65000 -fyield 550
   ~cr-sli2 sling 80 -len 14.8 -emodulus 65000 -fyield 550
   ~cr-sli3 sling 80 -len 14.8 -emodulus 65000 -fyield 550
   ~cr-sli4 sling 80 -len 14.8 -emodulus 65000 -fyield 550
   CONNECTOR boom ~boom *boompt
   CONNECTOR cr-sli1 ~cr-sli1 *cr1
   CONNECTOR cr-sli2 ~cr-sli2 *cr2
   CONNECTOR cr-sli3 ~cr-sli3 *cr3
   CONNECTOR cr-sli4 ~cr-sli4 *cr4
   ASSEMBLY t-h_definition cr-boom boom \
   cr-sli1 cr-sli2 cr-sli3 cr-sli4 -initial
   ~cr-spr h_cat 80 -len 3 -emodulus 65000 -fyield 550
   CONNECTOR cr-spr1 ~cr-spr *cr1 *pt1
   CONNECTOR cr-spr2 ~cr-spr *cr2 *pt2
   CONNECTOR cr-spr3 ~cr-spr *cr3 *pt3
   CONNECTOR cr-spr4 ~cr-spr *cr4 *pt4
   ~m_line, b_cat, 82 -len 520 -depanchor %wdepth \
      -emod 2*5.6e4 -wtplen 0.131 -buoydia 0
   CONNECTOR MR-Line1 -anchor 45 400 ~m_line *p3015
   CONNECTOR MR-Line2 -anchor 135 400 ~m_line *p3624
   CONNECTOR MR-Line3 -anchor 225 400 ~m_line *p3624
   CONNECTOR MR-Line4 -anchor 315 400 ~m_line *p3015
END_medit
$
&select :mr-line -select mr-line@
&connector :mr-line -inactive
&instate -sl_set
&status body
$
$
```

```
$************************************      Move Jacket Into Equilibrium
$
&describe body tanker -ignore x y z rx ry rz
&equi
$
$
$************************************      Info
$
&status cl_flex
&status g_connector
&status tip-hook
&status b_w
$
$
$************************************      Pre-Tension Mooring Lines
$
&connector :mr-line -active
&connector MR-Line@ -l_tension 80
$
$
$************************************      Move Tanker Into Equilibrium
$
&describe body tanker -ignore
&equi
$
$
$************************************      Info
$
&status cl_flex
&status g_connector
&status tip-hook
&status b_w
$
$
$************************************      Define Tuggers
$
MEDIT
   &describe body tanker
   *tugb %jackposx+13 20 28
   *tugs %jackposx-13 20 28
   *pt47glob &point(coordinates *pt47 -global)
   *pt48glob &point(coordinates *pt48 -global)
   *tugbglob &point(coordinates *tugb -global)
   *tugsglob &point(coordinates *tugs -global)
   &set bleng = &point(d_node *tugbglob *pt47glob)
   &set sleng = &point(d_node *tugsglob *pt48glob)
   ~tugb h_cat 40 exact -len %bleng-4 -emodulus 50000 -fyield 550
   ~tugs h_cat 40 exact -len %sleng-4 -emodulus 50000 -fyield 550
   CONNECTOR tugb ~tugb *tugb *pt47
   CONNECTOR tugs ~tugs *tugs *pt48
END_medit
$
$
$************************************      System Equilibruim
$
&equi
$
$
$************************************      Run Pressure Database
$
&insert pressure13m.dat
$
$
```

```
$************************************      Info
$
&describe body tanker -pr_name tanker -md_name tanker
&status f_conn
&status b_w
&status body
&summary
   compart_sum
end
$
&describe body tanker
MEDIT
   *CG &body(CG tanker)
END_medit
$
$
$************************************      Run Time Domain Simulation with
$                                         JONSWAP Sea Spectrum w/looping
$
&loop h (0 22.5 45 67.5 90 112.5 135 157.5 180) $ environment heading
&loop p3.0 (4.9 6.3 7.3 8.3 9.3 10.3 11.3 12.3 13.3 14.2) $ mean periods hs 3.0
$&loop p3.5 (5.3 6.6 7.7 8.6 9.6 10.5 11.4 12.3 13.3 14.2) $ mean periods hs 3.5
&env sea -sea 2jonswap %h% 3 %p3.0% -time 1200 0.25 -spread 4 \
        -wind 24.5 0 -w_spectrum npd
tdom
prcpost
cf_mag
statistics 1 2 4 6 8 10 28 30 12 14 16 18 20 22 24 26 -hard -record 800 4800 \
        -heading 'heading %h%, wave period %p3.0%, significant wave height 3 m'
end
end
&endloop
&endloop
$
$
$************************************      Run Frequency Domain Simulation
$                                         for Hs = 3.0m
$
&env -sea 2JONSWAP 0 3 4  -spread 4 -wind 24.5 0 -w_spectrum npd
freq_resp
   rao
fp_std *boompt
   fr_point *boompt
   end
   matrices
   report
   end
&LOOP E (0 22.5 45 67.5 90 112.5 135 157.5 180)
&env sea -sea 2JONSWAP %E% 3 4 -spread 4 -wind 24.5 %E% -w_spectrum npd
st_point sea -E_PERIOD 4.9 6.3 7.3 8.3 9.3 10.3 11.3 12.3 13.3 14.2
report
end
fp_std *boompt
&loop r (BOOM tugs tugb)
st_cforce %r% -sea 2JONSWAP %E% 3 4 -spread 4 -wind 24.5 %E% -w_spectrum npd \
        -E_PERIOD 4.9 6.3 7.3 8.3 9.3 10.3 11.3 12.3 13.3 14.2
report
end
&endloop
&endloop
$
$
$************************************      All Done
$
&FINISH
```

```
&insert tanker.dat
&insert jacket.dat
&insert spreader.dat
```

Appendix F

Excel Jacket File

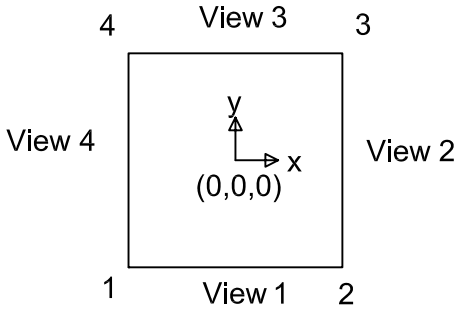
4
View 3
3
y
View 4
x
View 2
(0,0,0)
1
View 1
2

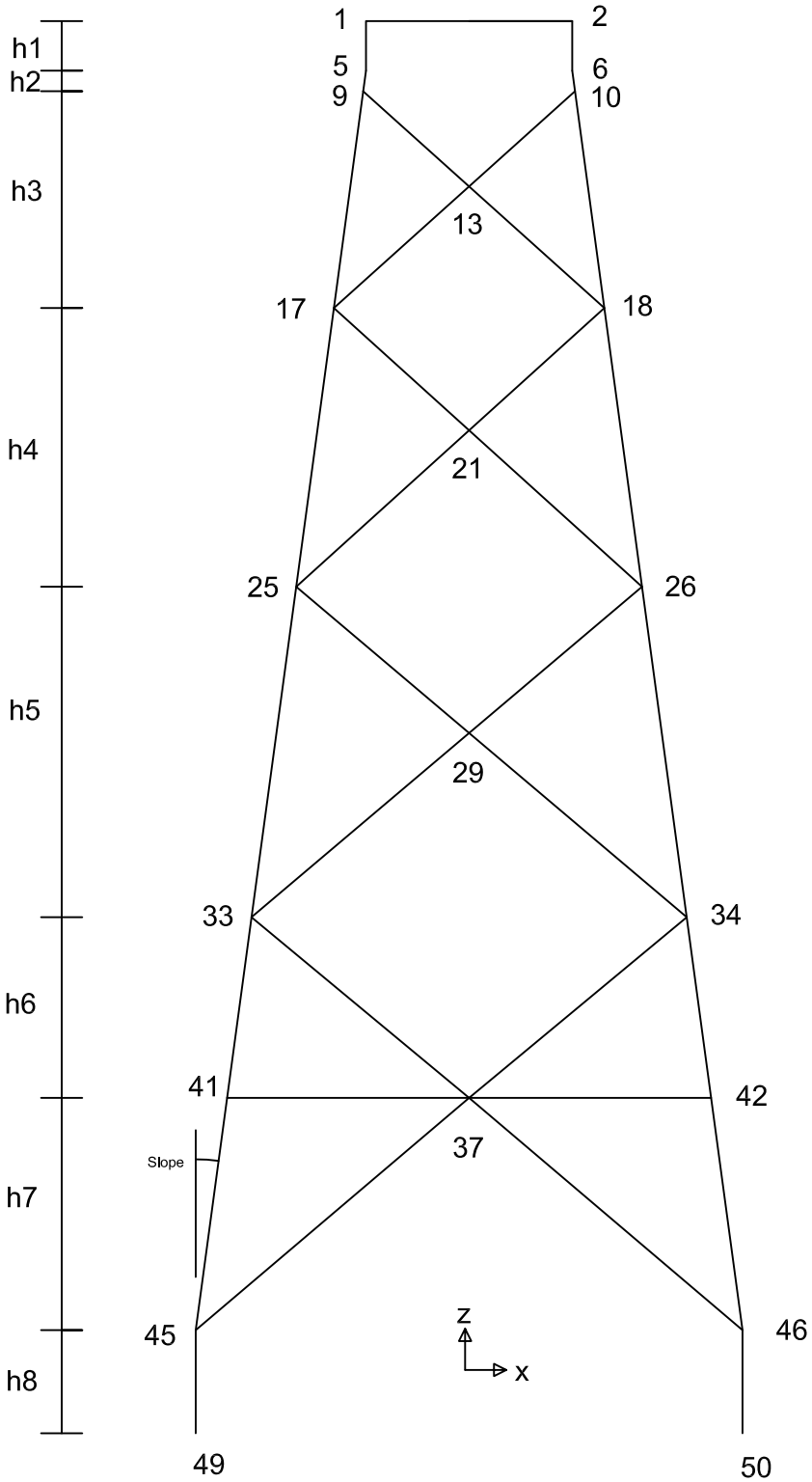
1
2
h1
5
6
h2
9
10
h3
13
17
18
h4
21
25
26
h5
29
33
34
h6
41
42
37
Slope
h7
z
45
46
h8
x
49
50

View 1

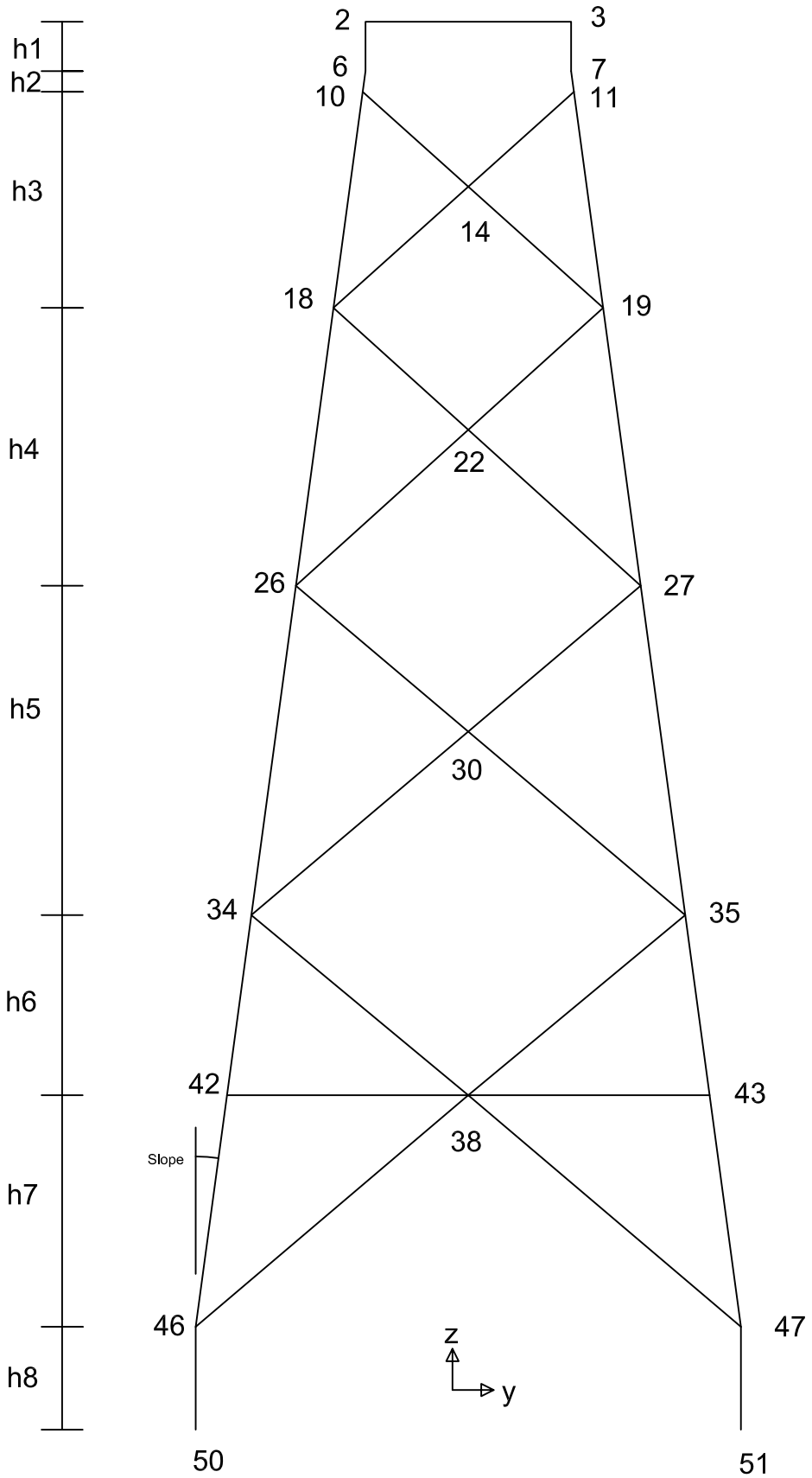
h1
h2
h3
h4
h5
h6
h7
h8
2
3
6
7
10
11
14
18
19
22
26
27
30
34
35
38
42
43
46
47
50
51
Slope
z
y

View 2

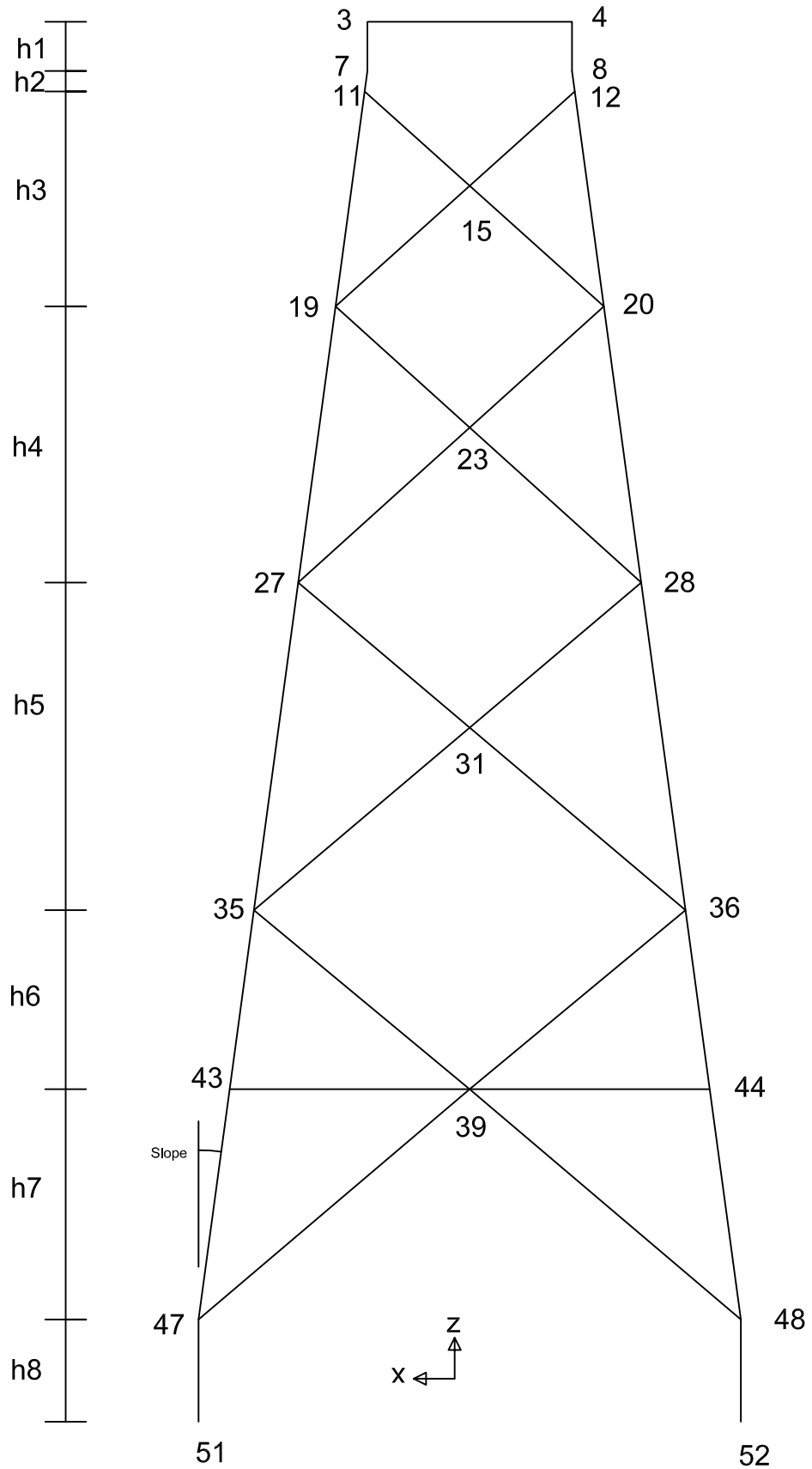
h1
h2
h3
h4
h5
h6
h7
h8
3
4
7
8
11
12
15
19
20
23
27
28
31
35
36
43
44
39
Slope
47
48
z
x
51
52

View 3

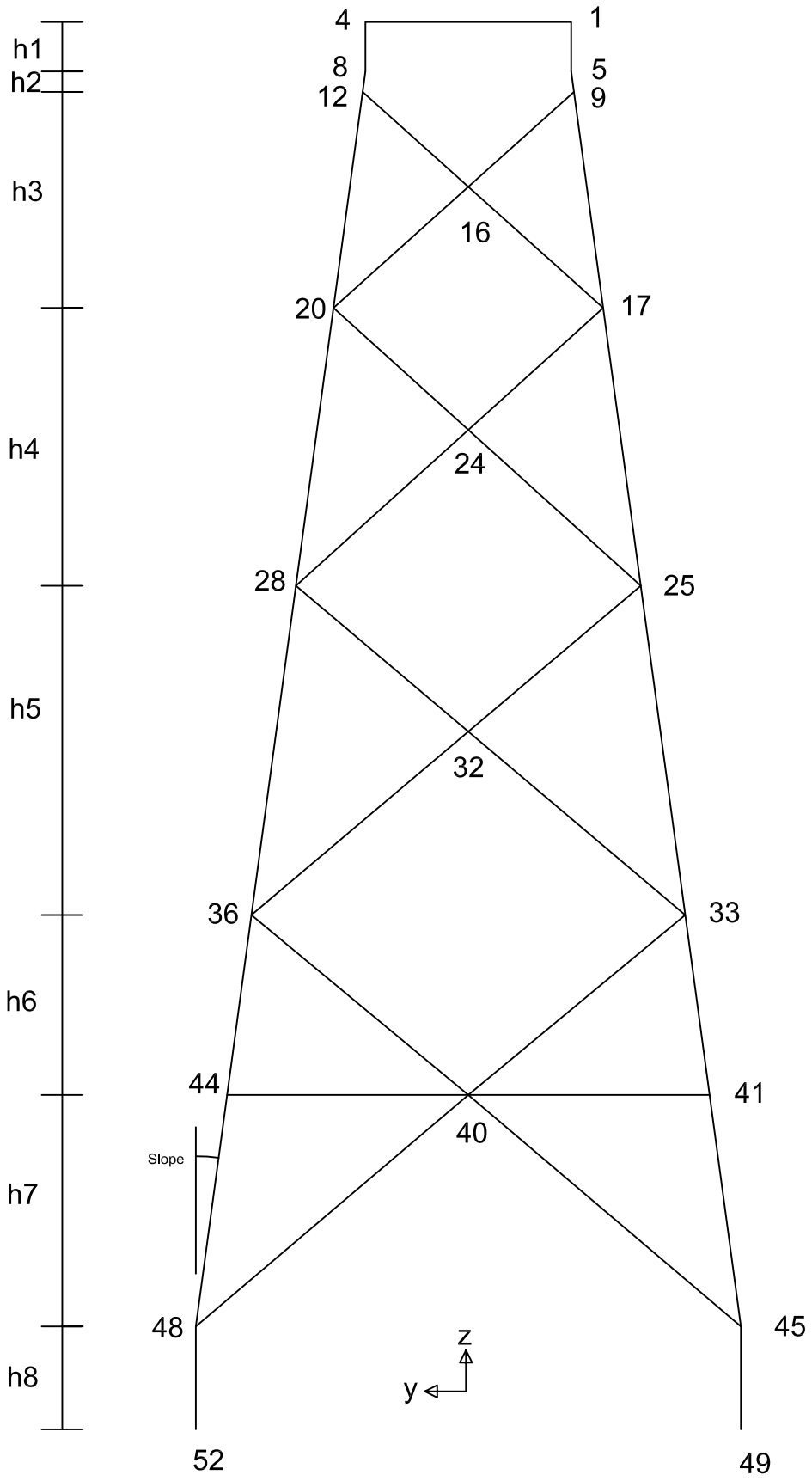
h1
h2
h3
h4
h5
h6
h7
h8
4
1
8
5
12
9
16
20
17
24
28
25
32
36
33
44
41
40
Slope
48
45
52
49
z
y

View 4

Jacket Coordinates

Input Dimensions: [m]

Top Width, Wt:	10.0
Bottom Width, Wb:	26.5
h1	2.40
h2	1.00
h3	10.50
h4	13.50
h5	16.00
h6	8.75
h7	11.25
h8	5.00
Total Height, H:	68.4
Pile Height, h8:	5.0
Jacket Height, Hj:	61.0
Slope:	0.135 rad
	7.749 deg

Input Top Nodes:

Node	x	y	z
1	-5	-5	0
2	5	-5	0
3	5	5	0
4	-5	5	0

Input Element Properties:

~top	plate	10000	135
~tube1	tube	508	15
~tube2	tube	610	15
~tube3	tube	711	15
~tube4	tube	813	30
~tube5	tube	960	35
~tube6	tube	1219	40

Point:	Moses Notation	x	y	z	
1	*pt1	-5.00000000	-5.00000000	0.00000000	
2	*pt2	5.00000000	-5.00000000	0.00000000	
3	*pt3	5.00000000	5.00000000	0.00000000	
4	*pt4	-5.00000000	5.00000000	0.00000000	
5	*pt5	-5.00000000	-5.00000000	-2.40000000	
6	*pt6	5.00000000	-5.00000000	-2.40000000	
7	*pt7	5.00000000	5.00000000	-2.40000000	
8	*pt8	-5.00000000	5.00000000	-2.40000000	
9	*pt9	-5.13524590	-5.13524590	-3.40000000	
10	*pt10	5.13524590	-5.13524590	-3.40000000	
11	*pt11	5.13524590	5.13524590	-3.40000000	
12	*pt12	-5.13524590	5.13524590	-3.40000000	
13	*pt13	0.00000000	-5.75903651	-8.01226994	(Mid-node)
14	*pt14	5.75903651	0.00000000	-8.01226994	(Mid-node)
15	*pt15	0.00000000	5.75903651	-8.01226994	(Mid-node)
16	*pt16	-5.75903651	0.00000000	-8.01226994	(Mid-node)
17	*pt17	-6.55532787	-6.55532787	-13.90000000	
18	*pt18	6.55532787	-6.55532787	-13.90000000	
19	*pt19	6.55532787	6.55532787	-13.90000000	
20	*pt20	-6.55532787	6.55532787	-13.90000000	
21	*pt21	0.00000000	-7.35664453	-19.82488682	(Mid-node)
22	*pt22	7.35664453	0.00000000	-19.82488682	(Mid-node)
23	*pt23	0.00000000	7.35664453	-19.82488682	(Mid-node)
24	*pt24	-7.35664453	0.00000000	-19.82488682	(Mid-node)
25	*pt25	-8.38114754	-8.38114754	-27.40000000	
26	*pt26	8.38114754	-8.38114754	-27.40000000	
27	*pt27	8.38114754	8.38114754	-27.40000000	
28	*pt28	-8.38114754	8.38114754	-27.40000000	
29	*pt29	0.00000000	-9.33940781	-34.48531832	(Mid-node)
30	*pt30	9.33940781	0.00000000	-34.48531832	(Mid-node)
31	*pt31	0.00000000	9.33940781	-34.48531832	(Mid-node)
32	*pt32	-9.33940781	0.00000000	-34.48531832	(Mid-node)
33	*pt33	-10.54508197	-10.54508197	-43.40000000	
34	*pt34	10.54508197	-10.54508197	-43.40000000	
35	*pt35	10.54508197	10.54508197	-43.40000000	
36	*pt36	-10.54508197	10.54508197	-43.40000000	
37	*pt37	0.00000000	-11.72848361	-52.15000000	(Mid-node)
38	*pt38	11.72848361	0.00000000	-52.15000000	(Mid-node)
39	*pt39	0.00000000	11.72848361	-52.15000000	(Mid-node)
40	*pt40	-11.72848361	0.00000000	-52.15000000	(Mid-node)

41	*pt41	-11.72848361	-11.72848361	-52.15000000
42	*pt42	11.72848361	-11.72848361	-52.15000000
43	*pt43	11.72848361	11.72848361	-52.15000000
44	*pt44	-11.72848361	11.72848361	-52.15000000
45	*pt45	-13.25000000	-13.25000000	-63.40000000
46	*pt46	13.25000000	-13.25000000	-63.40000000
47	*pt47	13.25000000	13.25000000	-63.40000000
48	*pt48	-13.25000000	13.25000000	-63.40000000
49	*pt49	-13.25000000	-13.25000000	-68.40000000
50	*pt50	13.25000000	-13.25000000	-68.40000000
51	*pt51	13.25000000	13.25000000	-68.40000000
52	*pt52	-13.25000000	13.25000000	-68.40000000

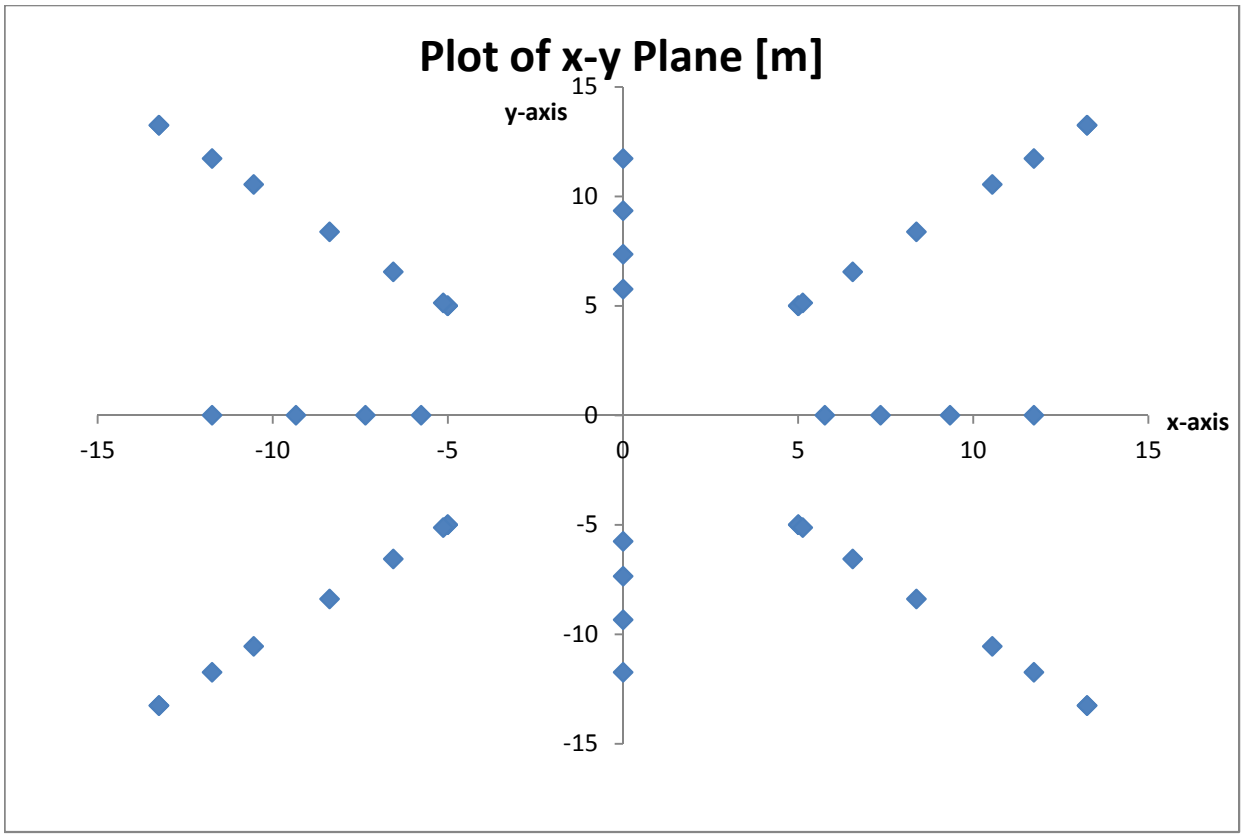

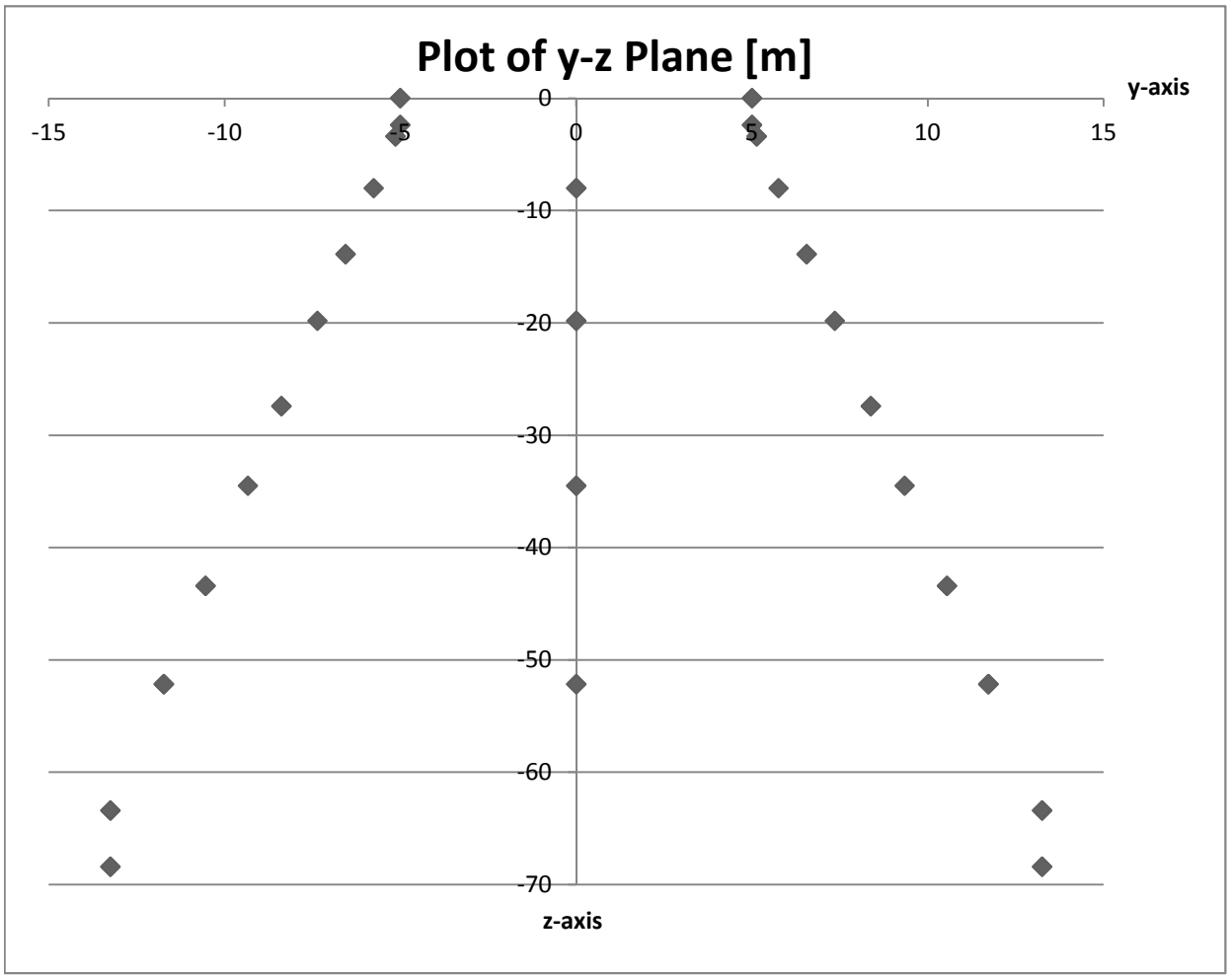

The plots are used to visually check if any of the points are misplaced

Jacket	Element Nr:	Connectivity:		Tube Nr:	Moses Notation:		
					$********** Jacket		
Top Box:					$********** Top Box:		
	1	1	2		plate top ~top	*pt1	*pt2
Top:					$********** Top:		
	1	1	5	5	beam beam1 ~tube5	*pt1	*pt5
	2	2	6	5	beam beam2 ~tube5	*pt2	*pt6
	3	3	7	5	beam beam3 ~tube5	*pt3	*pt7
	4	4	8	5	beam beam4 ~tube5	*pt4	*pt8
	1	5	2	5	beam beam5 ~tube5	*pt1	*pt2
	2	6	3	5	beam beam6 ~tube5	*pt2	*pt3
	3	7	4	5	beam beam7 ~tube5	*pt3	*pt4
	4	8	1	5	beam beam8 ~tube5	*pt4	*pt1
Chords:					$********** Chords:		
	1	9	5	9	4	beam beam9 ~tube4	*pt5	*pt9
	2	10	9	17	4	beam beam10 ~tube4	*pt9	*pt17
	3	11	17	25	4	beam beam11 ~tube4	*pt17	*pt25
	4	12	25	33	4	beam beam12 ~tube4	*pt25	*pt33
	5	13	33	41	4	beam beam13 ~tube4	*pt33	*pt41
	6	14	6	10	4	beam beam14 ~tube4	*pt6	*pt10
	7	15	10	18	4	beam beam15 ~tube4	*pt10	*pt18
	8	16	18	26	4	beam beam16 ~tube4	*pt18	*pt26
	9	17	26	34	4	beam beam17 ~tube4	*pt26	*pt34
	10	18	34	42	4	beam beam18 ~tube4	*pt34	*pt42
	11	19	7	11	4	beam beam19 ~tube4	*pt7	*pt11
	12	20	11	19	4	beam beam20 ~tube4	*pt11	*pt19
	13	21	19	27	4	beam beam21 ~tube4	*pt19	*pt27
	14	22	27	35	4	beam beam22 ~tube4	*pt27	*pt35
	15	23	35	43	4	beam beam23 ~tube4	*pt35	*pt43
	16	24	8	12	4	beam beam24 ~tube4	*pt8	*pt12
	17	25	12	20	4	beam beam25 ~tube4	*pt12	*pt20
	18	26	20	28	4	beam beam26 ~tube4	*pt20	*pt28
	19	27	28	36	4	beam beam27 ~tube4	*pt28	*pt36
	20	28	36	44	4	beam beam28 ~tube4	*pt36	*pt44

Piles & Bottom Chords: $********** Piles & Bottom Chords:

1	29	41	45	6	beam beam29 ~tube6	*pt41	*pt45
2	30	45	49	6	beam beam30 ~tube6	*pt45	*pt49
3	31	42	46	6	beam beam31 ~tube6	*pt42	*pt46
4	32	46	50	6	beam beam32 ~tube6	*pt46	*pt50
5	33	43	47	6	beam beam33 ~tube6	*pt43	*pt47
6	34	47	51	6	beam beam34 ~tube6	*pt47	*pt51
7	35	44	48	6	beam beam35 ~tube6	*pt44	*pt48
8	36	48	52	6	beam beam36 ~tube6	*pt48	*pt52

Upper Diagonals: $********** Upper Diagonals:

1	37	9	13	1	beam beam37 ~tube1	*pt9	*pt13
2	38	10	13	1	beam beam38 ~tube1	*pt10	*pt13
3	39	13	17	1	beam beam39 ~tube1	*pt13	*pt17
4	40	13	18	1	beam beam40 ~tube1	*pt13	*pt18
5	41	17	21	1	beam beam41 ~tube1	*pt17	*pt21
6	42	18	21	1	beam beam42 ~tube1	*pt18	*pt21
7	43	21	25	1	beam beam43 ~tube1	*pt21	*pt25
8	44	21	26	1	beam beam44 ~tube1	*pt21	*pt26
1	45	10	14	1	beam beam45 ~tube1	*pt10	*pt14
2	46	11	14	1	beam beam46 ~tube1	*pt11	*pt14
3	47	14	18	1	beam beam47 ~tube1	*pt14	*pt18
4	48	14	19	1	beam beam48 ~tube1	*pt14	*pt19
5	49	18	22	1	beam beam49 ~tube1	*pt18	*pt22
6	50	19	22	1	beam beam50 ~tube1	*pt19	*pt22
7	51	22	26	1	beam beam51 ~tube1	*pt22	*pt26
8	52	22	27	1	beam beam52 ~tube1	*pt22	*pt27
1	53	11	15	1	beam beam53 ~tube1	*pt11	*pt15
2	54	12	15	1	beam beam54 ~tube1	*pt12	*pt15
3	55	15	19	1	beam beam55 ~tube1	*pt15	*pt19
4	56	15	20	1	beam beam56 ~tube1	*pt15	*pt20
5	57	19	23	1	beam beam57 ~tube1	*pt19	*pt23
6	58	20	23	1	beam beam58 ~tube1	*pt20	*pt23
7	59	23	27	1	beam beam59 ~tube1	*pt23	*pt27
8	60	23	28	1	beam beam60 ~tube1	*pt23	*pt28
1	61	9	16	1	beam beam61 ~tube1	*pt9	*pt16
2	62	12	16	1	beam beam62 ~tube1	*pt12	*pt16
3	63	16	17	1	beam beam63 ~tube1	*pt16	*pt17
4	64	16	20	1	beam beam64 ~tube1	*pt16	*pt20
5	65	17	24	1	beam beam65 ~tube1	*pt17	*pt24
6	66	20	24	1	beam beam66 ~tube1	*pt20	*pt24
7	67	24	25	1	beam beam67 ~tube1	*pt24	*pt25
8	68	24	28	1	beam beam68 ~tube1	*pt24	*pt28

Lower Diagonals: $********** Lower Diagonals:

1	69	25	29	2	beam beam69 ~tube2	*pt25	*pt29
2	70	26	29	2	beam beam70 ~tube2	*pt26	*pt29
3	71	29	33	2	beam beam71 ~tube2	*pt29	*pt33
4	72	29	34	2	beam beam72 ~tube2	*pt29	*pt34
5	73	33	37	2	beam beam73 ~tube2	*pt33	*pt37
6	74	34	37	2	beam beam74 ~tube2	*pt34	*pt37
7	75	37	45	2	beam beam75 ~tube2	*pt37	*pt45
8	76	37	46	2	beam beam76 ~tube2	*pt37	*pt46
1	77	26	30	2	beam beam77 ~tube2	*pt26	*pt30
2	78	27	30	2	beam beam78 ~tube2	*pt27	*pt30
3	79	30	34	2	beam beam79 ~tube2	*pt30	*pt34
4	80	30	35	2	beam beam80 ~tube2	*pt30	*pt35
5	81	34	38	2	beam beam81 ~tube2	*pt34	*pt38
6	82	35	38	2	beam beam82 ~tube2	*pt35	*pt38
7	83	38	46	2	beam beam83 ~tube2	*pt38	*pt46
8	84	38	47	2	beam beam84 ~tube2	*pt38	*pt47
1	85	27	31	2	beam beam85 ~tube2	*pt27	*pt31
2	86	28	31	2	beam beam86 ~tube2	*pt28	*pt31
3	87	31	35	2	beam beam87 ~tube2	*pt31	*pt35
4	88	31	36	2	beam beam88 ~tube2	*pt31	*pt36
5	89	35	39	2	beam beam89 ~tube2	*pt35	*pt39
6	90	36	39	2	beam beam90 ~tube2	*pt36	*pt39
7	91	39	47	2	beam beam91 ~tube2	*pt39	*pt47
8	92	39	48	2	beam beam92 ~tube2	*pt39	*pt48
1	93	25	32	2	beam beam93 ~tube2	*pt25	*pt32
2	94	28	32	2	beam beam94 ~tube2	*pt28	*pt32
3	95	32	33	2	beam beam95 ~tube2	*pt32	*pt33
4	96	32	36	2	beam beam96 ~tube2	*pt32	*pt36
5	97	33	40	2	beam beam97 ~tube2	*pt33	*pt40
6	98	36	40	2	beam beam98 ~tube2	*pt36	*pt40
7	99	40	45	2	beam beam99 ~tube2	*pt40	*pt45
8	100	40	48	2	beam beam100 ~tube2	*pt40	*pt48

Horizontal Braces: $********** Horizontal Braces:

1	101	37	41	3	beam beam101 ~tube3	*pt37	*pt41
2	102	37	42	3	beam beam102 ~tube3	*pt37	*pt42
3	103	38	42	3	beam beam103 ~tube3	*pt38	*pt42
4	104	38	43	3	beam beam104 ~tube3	*pt38	*pt43
5	105	39	43	3	beam beam105 ~tube3	*pt39	*pt43
6	106	39	44	3	beam beam106 ~tube3	*pt39	*pt44
7	107	40	41	3	beam beam107 ~tube3	*pt40	*pt41
8	108	40	44	3	beam beam108 ~tube3	*pt40	*pt44

Appendix G

Calculations

Thickness of Top Plate to Account for Weight of Equipment:

Weight to be added, w_{eq}: $w_{eq} := 105.6\,\text{tonne}$ (Ref. DRW 3016-AJT-N-DR-1100)

Density of Steel, ρ: $\rho := 7850\,\frac{\text{kg}}{\text{m}^3}$

Width, b: $b := 10\,\text{m}$

Height, h: $h := 10\,\text{m}$

Required thickness, t: $t := \frac{w_{eq}}{\rho \cdot b \cdot h} = 135 \cdot \text{mm}$

Conclusion: *A steel plate with a thickness of **135 mm** needs to be added on the top of the jacket model to account for the weight of equipment.*

Wave Periods of Consideration for JONSWAP Analysis:

$g = 9.81 \cdot m \cdot s^{-2}$	Acceleration of gravity
H_s	Significant wave height
$H_{s.c} = H_s$	Characteristic significant wave height (Defined operational limitation, see DNV-OS-H101 Sec.3 C 803 Guidance note)
T_p	Wave spectrum peak period
T_m	Wave spectrum mean period
T_z	Mean zero up-crossing period
γ	JONSWAP Peak enhancement factor
ω_p	Angular spectral peak frequency

Wave periods to be considered:
(Ref. DNV-OS-H101, Sec.3 C 803)

$$8.9 \cdot \sqrt{\frac{H_{s.c}}{g}} \le T_z \le 13 \qquad \text{for} \qquad H_{s.c} \le 5.7m$$

For: $H_{s1} := 3.0m$ $\qquad 8.9 \cdot \sqrt{\frac{H_{s1}}{g}} = 4.9\,s$ to $13s$

For: $H_{s2} := 3.5m$ $\qquad 8.9 \cdot \sqrt{\frac{H_{s2}}{g}} = 5.3\,s$ to $13s$

Calculation of peak factor:
(Ref. DNV-RP-C205, 3.5.5.5)

$$\gamma = 5 \qquad \text{for} \qquad \frac{T_p}{\sqrt{H_{s.c}}} \le 3.6$$

$$\gamma = e^{5.75 - 1.15 \cdot \frac{T_p}{\sqrt{H_{s.c}}}} \qquad \text{for} \qquad 3.6 < \frac{T_p}{\sqrt{H_{s.c}}} \le 5$$

$$\gamma = 1 \qquad \text{for} \qquad 5 \le \frac{T_p}{\sqrt{H_{s.c}}}$$

Approximation of JONSWAP spectral moments:
(Ref. DNV-RP-C205, 3.5.5.6)

$$M_0 = \frac{1}{16}\cdot H_{s.c}^{\ 2}$$

$$M_2 = \frac{1}{16}\cdot H_{s.c}^{\ 2}\cdot \omega_p^{\ 2}\cdot \frac{11+\gamma}{5+\gamma}$$

$$\frac{M_0}{M_2} = \frac{1}{\omega_p^{\ 2}}\cdot \frac{5+\gamma}{11+\gamma}$$

Using zero-up-crossing period to find peak period, T_p:
(Ref. DNV-RP-C205, 3.5.3.2)

$$T_z = 2\pi\cdot\sqrt{\frac{M_0}{M_2}} = \frac{2\pi}{\omega_p}\cdot\sqrt{\frac{5+\gamma}{11+\gamma}}$$

$$\omega_p = \frac{2\pi}{T_z}\cdot\sqrt{\frac{5+\gamma}{11+\gamma}}$$

$$T_p = \frac{2\pi}{\omega_p}$$

$$\frac{2\pi}{T_p} = \frac{2\pi}{T_z}\cdot\sqrt{\frac{5+\gamma}{11+\gamma}}$$

$$T_p = T_z\cdot\sqrt{\frac{11+\gamma}{5+\gamma}}$$

The MOSES software uses the mean period in calculations and defines the relationship between mean period and peak period as:
(Ref. MOSES Reference Manual page 163)

$$T_p = 1.2958\cdot T_m$$

Calculating the periods of consideration by the use of the above fomulas and Microsoft Excel:
(Assuming 10 equally distributed periods are sufficient)

H_s [m]	T_z [s]	γ [-]	T_p [s]	T_m [s]
3.0	4.9	3.84	6.4	4.9
3.0	5.8	1.72	8.1	6.3
3.0	6.7	1.00	9.5	7.3
3.0	7.6	1.00	10.8	8.3
3.0	8.5	1.00	12.1	9.3
3.0	9.4	1.00	13.4	10.3
3.0	10.3	1.00	14.6	11.3
3.0	11.2	1.00	15.9	12.3
3.0	12.1	1.00	17.2	13.3
3.0	13.0	1.00	18.4	14.2

H_s [m]	T_z [s]	γ [-]	T_p [s]	T_m [s]
3.5	5.3	3.84	6.9	5.3
3.5	6.2	1.89	8.5	6.6
3.5	7.0	1.00	10.0	7.7
3.5	7.9	1.00	11.2	8.6
3.5	8.7	1.00	12.4	9.6
3.5	9.6	1.00	13.6	10.5
3.5	10.4	1.00	14.8	11.4
3.5	11.3	1.00	16.0	12.3
3.5	12.1	1.00	17.2	13.3
3.5	13.0	1.00	18.4	14.2

Simplified Splash Zone Analysis:

(DNV-RP-H103)

$g = 9.81 \cdot m \cdot s^{-2}$ Acceleration of gravity

$H_s := \begin{pmatrix} 3.0 \\ 3.5 \end{pmatrix} m$ Significant wave height

$H_{s.c} = H_s$ Characteristic significant wave height (Defined operational limitation, see DNV-OS-H101 Sec.3 C 803 Guidance note)

$H_j := 68.4m$ Height of jacket

$\rho_{sea} := 1025kg \cdot m^{-3}$ Density of sea water

$\rho_{steel} := 7850kg \cdot m^{-3}$ Density of steel

$W_{air} := 521tonne$ Jacket weight in air

$W_{sub} := 492tonne$ Jacket weight close to sea bed

$v_c := 0.25m \cdot s^{-1}$ Crane hoisting speed

Note: The significant wave height is defined as both 3.0 m and 3.5 m.
This results in two answers in most of the equations below.

Volume of Submerged Elements:

$$V := \frac{(W_{air} - W_{sub})}{\rho_{sea}} = 28.3 \cdot m^3$$

Hydrodynamic Parameters:
(Ref. DNV-RP-H103, 4.6)

Drag coefficient: The jacket is assumed to have a drag coefficient which is close to a typical subsea structure. Hence, the drag coefficient is taken as 2.5 according to DNV-RP-H103, 4.6.2

$C_D := 2.5$

$F_D = 0.5 \cdot \rho_{sea} \cdot C_D \cdot A \cdot u^2$

Added mass: The added mass is calculated according to DNV-RP-H103 4.6.3 and the jacket is assumed vertical.

$a_{leg} := 609.5mm$

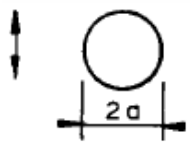

DNV-RP-H103 Appendix A

$$A_p := 4\pi \cdot a_{leg}^{\ 2}$$

$$\lambda := \frac{\sqrt{A_p}}{H_j + \sqrt{A_p}} = 0.031$$

$$C_{Ac} := \frac{2}{\pi} = 0.637$$

DNV-RP-H103 Appendix A

$$V_R := 4 \cdot \frac{4}{3} \cdot \pi \cdot a_{leg}^{\ 3}$$

$$A_{33o} := \rho_{sea} \cdot C_{Ac} \cdot V_R = 2.48 \cdot \text{tonne}$$

$$A_{33} := \left[1 + \sqrt{\frac{1 - \lambda^2}{2 \cdot \left(1 + \lambda^2\right)}}\right] \cdot A_{33o} = 4.22 \cdot \text{tonne}$$

$$C_A := \frac{A_{33}}{\rho_{sea} \cdot V_R} = 1.086$$

Vessel Response:

The vessel response in the crane tip is obtained from the frequency domain analysis in MOSES.

Charcteristic vertical single amplitude:

$$\eta_{ct} := \sqrt{\begin{pmatrix} 4.01\text{m} \\ 4.68\text{m} \end{pmatrix}^2 + (47\text{m} \cdot \sin(5.8\text{deg}))^2 + (1\text{m} \cdot \sin(2.06\text{deg}))^2} = \begin{pmatrix} 6.22 \\ 6.67 \end{pmatrix} \text{m}$$

Charcteristic vertical velocity:

$$v_{ct} := 2 \cdot \pi \sqrt{\left[\frac{\begin{pmatrix} 4.01\text{m} \\ 4.68\text{m} \end{pmatrix}}{10.5\text{s}}\right]^2 + \left(\frac{47\text{m} \cdot \sin(5.8\text{deg})}{19.5\text{s}}\right)^2 + \left(\frac{1\text{m} \cdot \sin(2.06\text{deg})}{11\text{s}}\right)^2} = \begin{pmatrix} 2.85 \\ 3.19 \end{pmatrix} \frac{\text{m}}{\text{s}}$$

Maximum vertical acceleration:

$$a_{ct} := 4\pi^2 \sqrt{\left[\frac{\begin{pmatrix} 4.01\text{m} \\ 4.68\text{m} \end{pmatrix}}{(10.5\text{s})^2}\right]^2 + \left[\frac{47\text{m} \cdot \sin(5.8\text{deg})}{(19.5\text{s})^2}\right]^2 + \left[\frac{1\text{m} \cdot \sin(2.06\text{deg})}{(11\text{s})^2}\right]^2} = \begin{pmatrix} 1.52 \\ 1.75 \end{pmatrix} \frac{\text{m}}{\text{s}^2}$$

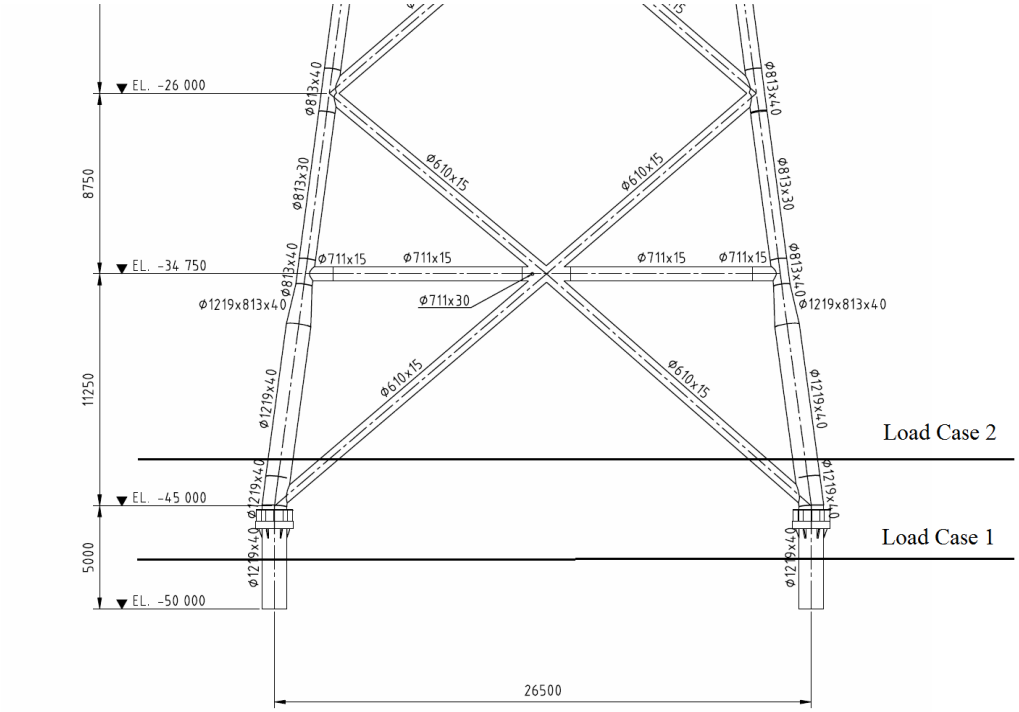

Load case 1 - Jacket Submerged 4m:

- Slamming impact force, F_{slam}, is zero
- Varying buoyancy force F_ρ, mass force F_M and drag force F_D are calculated
  The characteristic vertical relative velocity and acceleration are related to CoG of submerged part of structure (DNV-RP-H103, 4.5.2.3)

Distance from MWL to CoG of submerged part:

$$d := 2m$$

Characteristic wave amplitude:

$$\zeta_a := H_s \cdot 0.9 = \begin{pmatrix} 2.70 \\ 3.15 \end{pmatrix} m$$

Characteristic wave particle velocity and acceleration.

$$v_w := \overrightarrow{\left(0.3 \cdot \sqrt{\pi \cdot g \cdot H_s} \cdot e^{\frac{-0.35 \cdot d}{H_s}} \right)} = \begin{pmatrix} 2.28 \\ 2.55 \end{pmatrix} \frac{m}{s}$$

$$a_w := 0.1 \cdot \pi \cdot g \cdot e^{\frac{-0.35 \cdot d}{H_s}} = \begin{pmatrix} 2.44 \\ 2.52 \end{pmatrix} \frac{m}{s^2}$$

Characteristic slamming impact force:

Slamming coefficient smooth circular cylinder:

$$C_s := 3.0$$

Slamming impact velocity

$$v_s := v_c + \sqrt{v_w^2 + v_{ct}^2}$$

Characteristic slamming impact force

$$F_{slam} := 0kN$$

Varying buoyancy force:

$$A_w := \pi \cdot (1219mm)^2 - \pi \cdot [(1219 - 40)mm]^2$$

$$\delta V := A_w \cdot \sqrt{\zeta_a^2 + \eta_{ct}^2} = \begin{pmatrix} 2.0 \\ 2.2 \end{pmatrix} \cdot m^3$$

$$F_\rho := \rho_{sea} \cdot \delta V \cdot g = \begin{pmatrix} 21 \\ 22 \end{pmatrix} \cdot kN$$

Mass force:

$$F_M := \sqrt{\left[\left(W_{air} + A_{33}\right) \cdot a_{ct}\right]^2 + \left[\left(\rho_{sea} \cdot V + A_{33}\right) \cdot a_w\right]^2} = \begin{pmatrix} 802 \\ 921 \end{pmatrix} \cdot kN$$

Characteristic drag force:

Characteristic vertical relative velocity between object and water particles

$$v_{r.down} := v_c + \sqrt{v_{ct}^2 + v_w^2} = \begin{pmatrix} 3.9 \\ 4.34 \end{pmatrix} \frac{m}{s}$$

Lowering speed is conservatively set to 0 for calulation of hydrodynamic forces acting upwards.

$$v_{r.up} := 0 + \sqrt{v_{ct}^2 + v_w^2} = \begin{pmatrix} 3.65 \\ 4.09 \end{pmatrix} \frac{m}{s}$$

$$F_{D.down} := 0.5 \cdot C_D \cdot A_p \cdot v_{r.down}^2 \cdot \rho_{sea} = \begin{pmatrix} 90.9 \\ 112.4 \end{pmatrix} \cdot kN$$

$$F_{D.up} := 0.5 \cdot C_D \cdot A_p \cdot v_{r.up}^2 \cdot \rho_{sea} = \begin{pmatrix} 79.7 \\ 99.8 \end{pmatrix} \cdot kN$$

Characteristic total force:

$$F_{static} := \left(W_{sub}\right)\cdot g = 4825\cdot kN$$

$$F_{hyd.down} := \sqrt{\left(F_{D.down} + F_{slam}\right)^2 + \left(F_M - F_\rho\right)^2} = \begin{pmatrix} 786 \\ 906 \end{pmatrix}\cdot kN$$

$$F_{hyd.up} := \sqrt{\left(F_{D.up} + F_{slam}\right)^2 + \left(F_M - F_\rho\right)^2} = \begin{pmatrix} 785 \\ 905 \end{pmatrix}\cdot kN$$

$$F_{total} := F_{static} + F_{hyd.down} = \begin{pmatrix} 5611 \\ 5731 \end{pmatrix}\cdot kN$$

Convertet dynamic amplification factor:

$$DAF_{conv} := \frac{F_{total}}{W_{air}\cdot g} = \begin{pmatrix} 1.098 \\ 1.122 \end{pmatrix}$$

$$F_{min} := F_{static} - F_{hyd.up} = \begin{pmatrix} 4040 \\ 3920 \end{pmatrix}\cdot kN$$

Slack sling criterion:

$$\frac{F_{hyd.up}}{0.9F_{static}} = \begin{pmatrix} 0.181 \\ 0.208 \end{pmatrix}$$ = OK

Load case 2 - Jacket Submerged 6m:

- Slamming impact force, F_{slam}, is zero
- Varying buoyancy force F_ρ, mass force F_M and drag force F_D are calculated
  The characteristic vertical relative velocity and acceleration are related to CoG of submerged part of structure (DNV-RP-H103, 4.5.2.3)

Distance from MWL to CoG of submerged part:

$$d := 3m$$

Characteristic wave amplitude:

$$\zeta_a := H_s \cdot 0.9 = \begin{pmatrix} 2.70 \\ 3.15 \end{pmatrix} m$$

Characteristic wave particle velocity and acceleration.

$$v_w := \overrightarrow{\left(0.3 \cdot \sqrt{\pi \cdot g \cdot H_s} \cdot e^{\frac{-0.35 \cdot d}{H_s}} \right)} = \begin{pmatrix} 2.03 \\ 2.31 \end{pmatrix} \frac{m}{s}$$

$$a_w := 0.1 \cdot \pi \cdot g \cdot e^{\frac{-0.35 \cdot d}{H_s}} = \begin{pmatrix} 2.17 \\ 2.28 \end{pmatrix} \frac{m}{s^2}$$

Characteristic slamming impact force:

Slamming coefficient smooth circular cylinder:

$$C_s := 3.0$$

Slamming impact velocity

$$v_s := v_c + \sqrt{v_w^2 + v_{ct}^2}$$

Characteristic slamming impact force

$$F_{slam} := 0kN$$

Varying buoyancy force:

$$A_{w2} := A_w + 2 \cdot \left[\pi \cdot (610mm)^2 - \pi \cdot [(610 - 15)mm]^2 \right]$$

$$\delta V := A_{w2} \cdot \sqrt{\zeta_a^2 + \eta_{ct}^2} = \begin{pmatrix} 2.8 \\ 3.1 \end{pmatrix} \cdot m^3$$

$$F_\rho := \rho_{sea} \cdot \delta V \cdot g = \begin{pmatrix} 28 \\ 31 \end{pmatrix} \cdot kN$$

Mass force:

$$F_M := \sqrt{\left[\left(W_{air} + A_{33}\right) \cdot a_{ct}\right]^2 + \left[\left(\rho_{sea} \cdot V + A_{33}\right) \cdot a_w\right]^2} = \begin{pmatrix} 801 \\ 921 \end{pmatrix} \cdot kN$$

Characteristic drag force:

Characteristic vertical relative velocity between object and water particles

$$v_{r.down} := v_c + \sqrt{v_{ct}^2 + v_w^2} = \begin{pmatrix} 3.75 \\ 4.19 \end{pmatrix} \frac{m}{s}$$

Lowering speed is conservatively set to 0 for calulation of hydrodynamic forces acting upwards.

$$v_{r.up} := 0 + \sqrt{v_{ct}^2 + v_w^2} = \begin{pmatrix} 3.50 \\ 3.94 \end{pmatrix} \frac{m}{s}$$

$$F_{D.down} := 0.5 \cdot C_D \cdot A_p \cdot v_{r.down}^2 \cdot \rho_{sea} = \begin{pmatrix} 84 \\ 104.9 \end{pmatrix} \cdot kN$$

$$F_{D.up} := 0.5 \cdot C_D \cdot A_p \cdot v_{r.up}^2 \cdot \rho_{sea} = \begin{pmatrix} 73.2 \\ 92.8 \end{pmatrix} \cdot kN$$

Characteristic total force:

$$F_{static} := \left(W_{sub}\right) \cdot g = 4825 \cdot kN$$

$$F_{hyd.down} := \sqrt{\left(F_{D.down} + F_{slam}\right)^2 + \left(F_M - F_\rho\right)^2} = \begin{pmatrix} 777 \\ 896 \end{pmatrix} \cdot kN$$

$$F_{hyd.up} := \sqrt{\left(F_{D.up} + F_{slam}\right)^2 + \left(F_M - F_\rho\right)^2} = \begin{pmatrix} 776 \\ 895 \end{pmatrix} \cdot kN$$

$$F_{total} := F_{static} + F_{hyd.down} = \begin{pmatrix} 5602 \\ 5721 \end{pmatrix} \cdot kN$$

Convertet dynamic amplification factor:

$$DAF_{conv} := \frac{F_{total}}{W_{air} \cdot g} = \begin{pmatrix} 1.096 \\ 1.12 \end{pmatrix}$$

$$F_{min} := F_{static} - F_{hyd.up} = \begin{pmatrix} 4049 \\ 3930 \end{pmatrix} \cdot kN$$

Slack sling criterion:

$$\frac{F_{hyd.up}}{0.9F_{static}} = \begin{pmatrix} 0.179 \\ 0.206 \end{pmatrix}$$ = OK